

# **DESIGN, SYNTHESIS AND EVALUATION OF SGLT-2 INHIBITORS**

Thesis Submitted for the Award of the Degree of

**DOCTOR OF PHILOSOPHY**

in

**Pharmaceutical Chemistry**

By

**Shivani Sharma**

**Registration Number: 41700187**

**Supervised By**

**Dr. Navneet Khurana (18252)**

**Department of Pharmacology**

**(Professor)**

**School of Pharmaceutical Sciences**

**Co-Supervised by**

**Dr. Amit Mittal (31641)**

**Department of Pharmaceutical chemistry**

**(Professor)**

**School of Pharmaceutical Sciences**



**L** OVELY  
**P** ROFESSIONAL  
**U** NIVERSITY

*Transforming Education Transforming India*

**LOVELY PROFESSIONAL UNIVERSITY, PUNJAB  
2024**

## DECLARATION

I, hereby declared that the presented work in the thesis entitled “**Design, synthesis and evaluation of SGLT-2 Inhibitors.**” in fulfilment of degree of **Doctor of Philosophy (Ph. D.)** is outcome of research work carried out by me under the supervision Dr. Navneet Khurana, working as Professor, in the School of Pharmaceutical Sciences of Lovely Professional University, Punjab, India. In keeping with general practice of reporting scientific observations, due acknowledgements have been made whenever work described here has been based on findings of other investigator. This work has not been submitted in part or full to any other University or Institute for the award of any degree.

A handwritten signature in black ink, appearing to read 'Shivani', with a long horizontal stroke extending to the right.

**(Signature of Scholar)**

Name of the scholar: SHIVANI SHARMA

Registration No.: 41700187

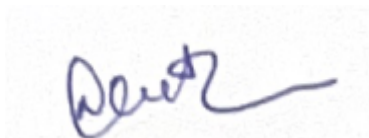
Department/school: School of Pharmaceutical Sciences

Lovely Professional University,

Punjab, India

## CERTIFICATE

This is to certify that the work reported in the Ph. D. thesis entitled “**Design, synthesis and evaluation of SGLT-2 Inhibitors**” submitted in fulfillment of the requirement for the reward of degree of **Doctor of Philosophy (Ph.D.)** in the School of Pharmaceutical Sciences, is a research work carried out by Shivani Sharma, 41700187 (Registration No.), is bonafide record of his/her original work carried out under my supervision and that no part of thesis has been submitted for any other degree, diploma or equivalent course.



**(Signature of Supervisor)**

Name of supervisor: Dr. Navneet Khurana

Designation: Professor

Department/school:

School of Pharmaceutical Sciences

University: Lovely Professional University



**(Signature of Co-Supervisor)**

Name of Co-Supervisor: Dr. Amit Mittal

Designation: Professor

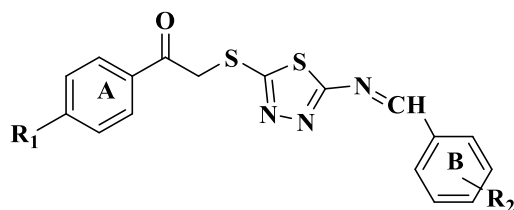
Department/school:

School of Pharmaceutical Sciences

University: Lovely Professional University

## ABSTRACT

Type-2 diabetes mellitus (T2DM) is the metabolic disorder that has the highest mortality rate and has a significant influence on contemporary society. T2DM prevalence was estimated at 537 million in 2021, and it is anticipated that this figure will increase to 643 million by 2030 and 783 million by 2045. Diabetes cannot be cured, and effectively treated with either insulin therapy or oral medications. Recently, Sodium-Glucose Cotransporter (SGLT) has been explored as a possible therapeutic target for diabetes. There are numerous SGLT isoforms, and SGLT2 principally accounts for 90% of the reabsorption of glucose in the kidney's proximal tube, whereas SGLT1 reabsorbs the remaining 10%. Due to their insulin-independent activities, which they trigger at various points during the development of T2DM, SGLT2 inhibitors are renowned for being potent.



The majority of SGLT2 inhibitors explored in the literature are glycosidal, in nature which are difficult to synthesize due to their bulky nature. The non-glucoside 1,3,4-thiadiazole pharmacophore is designed that have greater selectively for hSGLT2 over hSGLT1 by modifying their substitution at different positions to obtain a more efficacious anti-diabetic drug than the standard drug dapagliflozin. We have designed novel 1, 3, 4 thiadiazole compounds by introducing the electron donating groups such as methyl and methoxy at the para position of phenyl ring A designated as R<sub>1</sub>. Moreover, we have also substituted *ortho*, *meta* and *para* positions of the second phenyl ring B designated as R<sub>2</sub> with various electron donating groups and electron withdrawing groups. On the basis of above facts we have designed 102 compounds of Schiff base based 1, 3, 4 thiadiazole scaffold and performed docking studies with SGLT2 Protein (PDB ID: 3DH4) to calculate binding affinity scores using AutoDock vina 1.5.6. Among these, the 12 best Schiff base-derived 1,3,4-thiadiazole molecules that demonstrated the most favorable binding scores, ranging from -10.7 to -9.7 Kcal/mol were chosen and synthesized that were coded as **SSS 34**, **SSS 100**, **SSS 16**, **SSS**

**40, SSS 35, SSS 95, SSS 98, SSS 41, SSS 36, SSS 102, SSS 18 and SSS 96.** These selected compounds were synthesized with good % yield and validated through LCMS, <sup>1</sup>H NMR, and <sup>13</sup>C NMR analyses. *In-silico* toxicity profile of the synthesized compounds, reveals that they exhibit non-carcinogenic properties in rats and non-mutagenic characteristics. The results of *in-silico* ADME reveals that all the synthesized molecules are non-penetrating in the brain and have a low probability of GI absorption. Predicted lipophilicity (iLogP) of synthesized compounds were found to be 2.08-3.68. All the synthesized molecules predicted to have good oral bioavailability with a score of 0.55 and comply with druglikeness. Based on the MTT assay results, **SSS 35, SSSN 40, SSS 95, and SSS 100** exhibited higher IC<sub>50</sub> values i.e. 102.69, 89.77, 101.07 and 98.82, indicating low cytotoxicity for the synthesized compounds. Subsequently, these four compounds underwent further testing for their SGLT-2 inhibiting activity. The analysis of Human Sodium/glucose cotransporter 2 (SLC5A2) ELISA kit assay results revealed that compound **SSS 95** and **SSS 100** were more potent compounds compared with dapagliflozin values at low and high dose as standard control. SSS 95 exhibited high SGLT-2 inhibition activity at low dose (54.76±1.68) and high dose (78.57±2.8), while **SSS 100** exhibited significant SGLT2 inhibition at low dose (56.34±3.92) and high dose (74.60±1.12). Therefore for further *in vivo* evaluation of synthesized test compounds, we used **SSS 95** and **SSS 100**. *In vivo* results reveals that **SSS 100** significantly improved excretion of urinary glucose (854±46.51mg/body weight) as compared to positive control (775±32.68 mg/body weight) at the same dosage and duration. Treatment with **SSS 95** and **SSS 100** seemed to significantly reduce the urinary excretion of Na<sup>+</sup>, K<sup>+</sup>, and Cl<sup>-</sup> electrolytes, similar to the positive control. These findings imply that the correction of electrolyte imbalance by the test compounds in diabetic rats may not be solely attributed to a reduction in urinary electrolyte excretion. It is noteworthy that no instances of diarrhea were noted in the SD rats treated with **SSS 95** and **SSS 100** as compared to positive control, attributed to lack of selectivity for hSGLT1. However, **SSS 95** and **SSS 100** test compounds treated groups significantly decreased blood glucose levels relative to positive control indicates the anti-hyperglycemic effect of synthesized test compounds. These synthesized compounds has

shown positive results in histopathological analysis. The entire study suggests that synthesized compounds **SSS 95** and **SSS 100** having good potential as SGLT2 inhibitors for the treatment of type-II diabetes.

## ACKNOWLEDGEMENT

It is a moment of gratification and pride to look back with a sense of contentment at the long-travelled path, to be able to recapture some of the fine moments, to be able to think of the infinite number of people, some who were with me from the beginning, some who joined me at some stage during the journey, whose kindness, love and blessings has brought me to this day. I wish to thank each one of them from the bottom of my heart First and foremost, I would like to thanks the “almighty” for showering blessings of life and wisdom over me and for never forsaking me, even when I have forgotten, at too many occasions, to pray and thank him for all the blessings that he bestows on me. I would like to acknowledge my indebtedness and render my warmest thanks to, Dr. Amit Mittal and Dr. Navneet Khurana, for their valuable guidance and supervision for making this work possible. Their friendly guidance and expert advice have been invaluable throughout all stages of the work. I appreciate all his contributions of time, ideas, and efforts to make my Ph.D. experience productive and stimulating and imbibed the strength in me to work hard through this endeavour. Indeed, the words at my command are inadequate to express my gratifications to my esteemed teacher and guide who helped me in struggling this path of research. A journey is easier when you travel together. I would like to show my greatest appreciation to Dr. Subheet Kumar Jain for their valuable suggestions and approval of my research work and exemplary recognition. I would also like to thanks Ph.D. scholars and my friends Mr. Hardeep Singh, Dr. Palwinder Kaur, Dr. Deepshikha Patle, Dr. Divya Chauhan, Ms. Neha Srivastava, Ms. Priyanka, and Ms. Pooja for their time to time help, support, guidance. I feel highly obliged and have immense pleasure in expressing my heartfelt thanks to Dean Prof. Monica Gulati as well as HOD Dr. Sachin Kumar Singh, and other senior faculty members like Dr. Gurinder Singh, Dr. Rajesh Kumar, Dr. Pankaj Wadhwa, Dr. Sanjeev Kumar Sahu, Dr. Iqbal Singh, Dr. Sumant Saini, Dr. Charanjeet Kaur, Dr. Bhupinder Kapoor, Dr. Vikas Sharma, Dr. Gurdeep Singh, Dr. Mukta Gupta, Ms. Sharfuddin Mohammad, Dr. Ankit Yadav, Dr. Dileep Singh Bhagel, Dr. Rekha Sangwan, Ms. Archana. I express my thanks to the Chancellor Sir, Dr. Ashok Mittal and Pro-Chancellor Mam Dr. Rashmi Mittal for providing us supportive and friendly atmosphere, excellent research

facilities in and around the region, exposure to the scientific word and platform to rise. Special thanks to Dr. Jeena Gupta, School of Biotechnology and Biosciences, Lovely Professional University for framing and guiding the *in vitro* study plan and helping to complete the same. Also thanking Sourbh Garg for assisting me to carry out the *in vitro* studies.

I express my sincere thanks to my lovable friends who supported me in my tough times, and always cared for me in every situation, Soniya Singh, Munish Makkar, Pardeep Singh, Sandeep Singh Minhas, Shubham Kumar, Karun Kataria, Veena Bains, Jaya Minhas, Gurpreet Singh, Sneha Joshi. This work would not have been possible without their encouragement, love, kind support and believe. I acknowledge the help given by my juniors Debojyoti, Rohit, Chirag, Ankita, Ashutosh, Himal Deepali Dr. Priya Isha and Anuradha, all other who always support and helped me during the course. I personally express my thanks to my laboratory attendants Mr. Manoj Kumar and Vaibhav, Mr. Madan and all other non-teaching staff for their help and invaluable assistance. Last but not the least, this thesis would not have been possible without the confidence, endurance and support of my family. My family has always been a source of inspiration and encouragement. I wish to thanks my father Sh. Ashwani Kumar Sharma, mother Smt. Poonam Sharma. I would not be able to come to this position without the sacrifices made by my parents. A lot of support was provided by my younger brothers Ankur and Ankit. They believed in me, before I believe in myself. Thank you for always being with me. Above all I thank “My laddu Gopal ji ” Lord Shiva and Hanuman ji, heavily blessings from my grandparents and my parents for showering their infinite bounties, clemencies and graces upon me and for being my constants companions, the strongest source of motivation, inspiration and my ultimate Guardians; to them I owe a lifelong indebtedness.

**Shivani Sharma**



## TABLE OF CONTENTS

S. No.	Chapter Title	Page No.
<b>CHAPTER 1</b>	<b>INTRODUCTION</b>	<b>1-15</b>
<b>1</b>	Introduction	<b>1-7</b>
<b>1.1</b>	Role of Glucose Transporters in the kidney	<b>7</b>
<b>1.2</b>	The function of SGLT1 and SGLT2 in type-II diabetes	<b>8</b>
<b>1.3</b>	Sodium glucose cotransporter2 (SGLT2) inhibitors	<b>8-9</b>
<b>1.3.1</b>	Mode of action of SGLT2 inhibitors	<b>9-10</b>
<b>1.4</b>	The Benefits of SGLT2 Inhibitors for Diabetes Management	<b>10-12</b>
<b>1.4.1</b>	Glucose-lowering effects	<b>10-11</b>
<b>1.4.2</b>	Cardiovascular and Renal benefits	<b>11</b>
<b>1.4.3</b>	Weight loss	<b>11-12</b>
<b>1.4.4</b>	Lowering in Blood Pressure	<b>12</b>
<b>1.5</b>	Adverse effects of SGLT2 inhibitors	<b>12-15</b>
<b>1.5.1</b>	Genital and Urinary Tract Infections	<b>12-13</b>
<b>1.5.2</b>	Diabetic ketoacidosis (DKA)	<b>13</b>
<b>1.5.3</b>	Amputation	<b>14</b>
<b>1.5.4</b>	Cancer Risk	<b>14</b>
<b>1.5.5</b>	Skeletal fractures	<b>14-15</b>
<b>1.5.6</b>	Volume Depletion	<b>15</b>
<b>1.5.7</b>	Acute kidney injury (AKI)	<b>15</b>
<b>CHAPTER 2</b>	<b>LITERATURE REVIEW</b>	<b>15-42</b>
<b>2.1</b>	Historical Background	<b>16-17</b>
<b>2.2</b>	SGLT2 inhibitors discontinued from clinical trials	<b>16-18</b>

<b>2.2.1</b>	WAY-123783	<b>16-17</b>
<b>2.2.2</b>	T-1095	<b>17-18</b>
<b>2.2.3</b>	Sergliflozin	<b>18</b>
<b>2.2.4</b>	YM543	<b>18</b>
<b>2.3</b>	FDA & EMA approved SGLT2 inhibitors	<b>19-21</b>
<b>2.3.1</b>	Dapagliflozin	<b>19</b>
<b>2.3.2</b>	Canagliflozin	<b>19-20</b>
<b>2.3.3</b>	Ertugliflozin	<b>20</b>
<b>2.3.4</b>	Empagliflozin	<b>20-21</b>
<b>2.4</b>	SGLT2 inhibitors under investigation (not approved by the FDA and EMA)	<b>22-28</b>
<b>2.4.1</b>	Remogliflozin etabonate	<b>22-23</b>
<b>2.4.2</b>	Luseogliflozin (TS-071)	<b>23</b>
<b>2.4.3</b>	Ipragliflozin	<b>23-24</b>
<b>2.4.4</b>	Tofogliflozin	<b>24</b>
<b>2.4.5</b>	Sotagliflozin (LX4211)	<b>24</b>
<b>2.4.6</b>	Henagliflozin (SHR3824)	<b>25</b>
<b>2.4.7</b>	Bexagliflozin	<b>25</b>
<b>2.4.8</b>	Janagliflozin	<b>27</b>
<b>2.4.9</b>	Tianagliflozin	<b>27</b>
<b>2.4.10</b>	Licogliflozin	<b>27-28</b>
<b>2.5</b>	Advancement in profile of SGLT2 inhibitors	<b>28-44</b>
<b>2.5.1</b>	Glucose glucosides	<b>28-40</b>
<b>2.5.1.1</b>	Benzofuran Analogues	<b>28</b>
<b>2.5.1.2</b>	Indole- <i>O</i> -glucoside and benzimidazole- <i>O</i> -glucoside Analogues	<b>28-29</b>
<b>2.5.1.3</b>	Benzodioxane Analogues	<b>29</b>

<b>2.5.1.4</b>	Thiophene/Thiazole Analogs	<b>29-32</b>
<b>2.5.1.5</b>	Benzisothiazole and Indolizine Derivatives	<b>31-33</b>
<b>2.5.1.6</b>	Indole Derivatives	<b>31-33</b>
<b>2.5.1.7</b>	Chalcone Derivatives	<b>33-34</b>
<b>2.5.1.8</b>	Isoquinoline Derivatives	<b>34-35</b>
<b>2.5.1.9</b>	Pyridine Derivatives	<b>34-35</b>
<b>2.5.1.10</b>	Benzyltriazolopyridinone and Phenylhydantoin Derivatives	<b>35-36</b>
<b>2.5.1.11</b>	Biphenyl Derivatives	<b>36-39</b>
<b>2.5.1.12</b>	Oxime Analogues	<b>36-39</b>
<b>2.5.1.13</b>	Benzocyclobutane Analogues	<b>37-39</b>
<b>2.5.1.14</b>	Benzyl Analogues	<b>38-40</b>
<b>2.5.1.15</b>	Design and Exploration of 6-Deoxy O-Spiroketal Analogues	<b>38-40</b>
<b>2.5.1.16</b>	Exploration and Design of Analogues with 5-Fluoro-5-methyl-hexose Structure	<b>40</b>
<b>2.5.2</b>	Fructose glucosides	<b>41-42</b>
<b>2.5.3</b>	Xylose glycosides	<b>41-43</b>
<b>2.5.4</b>	Non-glucosidal Analogues	<b>43-44</b>
<b>2.5.4.1</b>	Exploration of Benzothiazinone and benzooxazinone Analogues	<b>43</b>
<b>2.5.4.2</b>	Triazole Analogues	<b>44</b>
<b>CHAPTER 3</b>	<b>RATIONALE, AIM AND OBJECTIVES</b>	<b>45-46</b>
<b>CHAPTER 4</b>	<b>WORK PLAN &amp; HYPOTHESIS</b>	<b>47-50</b>
<b>4.1</b>	Structural Modification	<b>47</b>
<b>4.2</b>	Molecular docking study	<b>47</b>

<b>4.3</b>	Synthesis and Characterization of feasible & most potent compounds	<b>47-48</b>
<b>4.4</b>	<i>In-Silico</i> prediction of ADMET studies of synthesized compounds	<b>48</b>
<b>4.5</b>	<i>In-vitro</i> evaluation of synthesized molecules by human SGLT2 inhibitory activity assay	<b>48</b>
<b>4.6</b>	<i>In-vivo</i> evaluation of Urinary Glucose Excretion & Streptozotocin-Induced Diabetes	<b>49</b>
<b>4.7</b>	Hypothesis	<b>49-50</b>
<b>CHAPTER 5</b>	<b>MATERIAL, METHODS AND EXPERIMENTAL</b>	<b>51-75</b>
<b>5.1</b>	Molecular Docking Studies	<b>51</b>
<b>5.1.1</b>	SGLT2 Protein Identification & Preparation	<b>51</b>
<b>5.1.2</b>	Validation of Protein for Docking	<b>51-52</b>
<b>5.1.3</b>	Molecular Docking Protocol	<b>52-53</b>
<b>5.1.4</b>	2D Interactions for Docking Results	<b>53-54</b>
<b>5.2</b>	Synthesis and Characterization	<b>54-67</b>
<b>5.2.1</b>	Synthesis of 2-amino-5-mercapto-1, 3, 4-thiadiazole (2)	<b>55-56</b>
<b>5.2.2</b>	Synthesis of 2-((5-amino-1, 3, 4-thiadiazol-2-yl)thio)-1-phenylethan-1-one (4a)	<b>56-57</b>
<b>5.2.3</b>	Synthesis of 2-((5-amino-1,3,4-thiadiazol-2-yl)thio)-1-(p-tolyl)ethan-1-one (4b)	<b>57</b>
<b>5.2.4</b>	2-((5-amino-1,3,4-thiadiazol-2-yl)thio)-1-(4-methoxyphenyl)ethan-1-one (4c)	<b>58</b>
<b>5.2.5</b>	Synthesis of 2-((5-((2-hydroxybenzylidene)amino)-1,3,4-thiadiazol-2-yl)thio)-1-phenylethan-1-one (SSS 34).	<b>58-59</b>
<b>5.2.6</b>	Synthesis of 2-((5-((2-hydroxy-4-methoxybenzylidene)amino)-1,3,4-thiadiazol-2-yl)thio)-	<b>59-60</b>

	1-phenylethan-1-one (SSS 100)	
<b>5.2.7</b>	Synthesis of 2-((5-((3,4-dimethoxybenzylidene)amino)-1,3,4-thiadiazol-2-yl)thio)-1-phenylethan-1-one (SSS 16)	<b>60-61</b>
<b>5.2.8</b>	Synthesis of 2-((5-((4-hydroxybenzylidene)amino)-1,3,4-thiadiazol-2-yl)thio)-1-phenylethan-1-one (SSS 40)	<b>61</b>
<b>5.2.9</b>	Synthesis of 2-((5-((2-hydroxybenzylidene)amino)-1,3,4-thiadiazol-2-yl)thio)-1-(p-tolyl)ethan-1-one (SSS 35)	<b>61-62</b>
<b>5.2.10</b>	Synthesis of 2-((5-((3,4-dihydroxy-5-nitrobenzylidene)amino)-1,3,4-thiadiazol-2-yl)thio)-1-(p-tolyl)ethan-1-one (SSS 95)	<b>62-63</b>
<b>5.2.11</b>	Synthesis of 2-((5-((3-hydroxy-4-methoxybenzylidene)amino)-1,3,4-thiadiazol-2-yl)thio)-1-(p-tolyl)ethan-1-one (SSS 98)	<b>63-64</b>
<b>5.2.12</b>	Synthesis of 2-((5-((4-hydroxybenzylidene)amino)-1,3,4-thiadiazol-2-yl)thio)-1-(p-tolyl)ethan-1-one (SSS 41)	<b>64</b>
<b>5.2.13</b>	Synthesis of 2-((5-((2-hydroxybenzylidene)amino)-1,3,4-thiadiazol-2-yl)thio)-1-(4-methoxyphenyl)ethan-1-one (SSS 36)	<b>64-65</b>
<b>5.2.14</b>	Synthesis of 2-((5-((2-hydroxy-4-methoxybenzylidene)amino)-1,3,4-thiadiazol-2-yl)thio)-1-(4-methoxyphenyl)ethan-1-one (SSS 102)	<b>65-66</b>
<b>5.2.15</b>	Synthesis of 2-((5-((3,4-dimethoxybenzylidene)amino)-1,3,4-thiadiazol-2-yl)thio)-1-(4-methoxyphenyl)ethan-1-one (SSS 18)	<b>66-67</b>

<b>5.2.16</b>	Synthesis of 2-((5-((3,4-dihydroxy-5-nitrobenzylidene)amino)-1,3,4-thiadiazol-2-yl)thio)-1-(4-methoxyphenyl)ethan-1-one (SSS 96)	<b>67</b>
<b>5.3</b>	<i>In-silico</i> toxicity Prediction	<b>68</b>
<b>5.4</b>	<i>In-silico</i> Pharmacokinetics Prediction	<b>68</b>
<b>5.5</b>	<i>In vitro</i> evaluation of synthesized compounds	<b>68-70</b>
<b>5.5.1</b>	MTT cell-viability assay	<b>68-69</b>
<b>5.5.2</b>	Human SGLT2 (SLC5A2) ELISA kit	<b>69-70</b>
<b>5.6</b>	<i>In vivo</i> evaluation of synthesized compounds	<b>70-75</b>
<b>5.6.1</b>	Experimental animals	<b>70-71</b>
<b>5.6.2</b>	Assessment of Urine Excretion of Glucose and other electrolytes	<b>71-72</b>
<b>5.6.3</b>	Diarrhea test	<b>73</b>
<b>5.6.4</b>	Effects of Blood Glucose Reduction in SD Rats with Diabetes Induced by Streptozotocin-Nicotinamide	<b>73-75</b>
<b>5.7</b>	Histopathological evaluation of SD rats Pancreas and Kidneys	<b>75</b>
<b>5.8</b>	Statistical Calculations	<b>75</b>
<b>CHAPTER 6</b>	<b>RESULTS AND DISCUSSION</b>	<b>76-110</b>
<b>6.1</b>	Molecular docking studies	<b>76-83</b>
<b>6.2</b>	Synthesis and Characterization of synthesized compounds	<b>83-86</b>
<b>6.3</b>	<i>In-silico</i> toxicity studies	<b>86-87</b>
<b>6.4</b>	<i>In-silico</i> ADME studies	<b>87-89</b>
<b>6.5</b>	<i>In-vitro</i> Evaluation	<b>89-98</b>
<b>6.5.1</b>	MTT Assay and Discussion	<b>89-96</b>
<b>6.5.2</b>	Human SGLT2 ELISA kit	<b>96-98</b>
<b>6.6</b>	<i>In-vivo</i> evaluation	<b>98-106</b>

<b>6.6.1</b>	Assessment of Urine Excretion of Glucose and other electrolytes	<b>99-102</b>
<b>6.6.2</b>	Diarrheogenic Activity Test	<b>102-103</b>
<b>6.6.3</b>	Effects of Blood Glucose Reduction in Rats with Diabetes Induced by Streptozotocin-Nicotinamide	<b>103-107</b>
<b>6.6.3.1</b>	Plasma Glucose estimation	<b>104-105</b>
<b>6.6.3.2</b>	Body weight (BW) assessment	<b>105-107</b>
<b>6.7</b>	Histopathological Estimation of SD rats kidney and Pancreas	<b>107-110</b>
<b>6.7.1</b>	Histopathology of Kidney	<b>107-108</b>
<b>6.7.2</b>	Histopathology of pancreas	<b>109-110</b>
<b>CHAPTER 7</b>	<b>CONCLUSION AND FUTURE PROSPECTIVES</b>	<b>111-113</b>
<b>CHAPTER 8</b>	<b>REFERENCES</b>	<b>114-128</b>

## LIST OF TABLES

S.NO.	Title of table	PAGE NO.
1	Anti-diabetic drugs and their side effects.	<b>2-5</b>
2	Approved treatment protocol for determining the Urinary Glucose Excretion model	<b>72</b>
3	Approved treatment protocol for type-II diabetes model	<b>74</b>
4	Structure and binding affinity of designed molecules from Schiff base of 1, 3, 4-thiadiazole derivatives.	<b>77-79</b>
5	The interactions of best designed molecules with nearby protein residues in 3DH4 active site.	<b>80-81</b>
6	Structural representation and percentage yield of potent synthesized compounds based on the highest binding affinity scores.	<b>83-85</b>
7	<i>In-silico</i> toxicity predictions.	<b>87</b>
8	Prediction of <i>in-silico</i> Physiochemical properties	<b>88</b>
9	Prediction of <i>in-silico</i> ADME properties	<b>89</b>
10	Relative % cell viability and IC <sub>50</sub> value of test compounds with reference of standard drug Dapagliflozin.	<b>90</b>
11	% SGLT2 inhibition of test compounds.	<b>96</b>
12	Effect on Urinary Glucose Excretion (mg/BW) after the treatment during 24h.	<b>99-100</b>
13	Effect on Urinary Excretion of electrolytes (mmol/L) after the treatment during 24h.	<b>101</b>
14	Effect on Diarrheogenic Activity after the treatment.	<b>102-103</b>



15	Effect on Plasma glucose level (mg/dL) before and after the treatment.	<b>104</b>
16	Change in mean body weight (g) before and after the treatment.	<b>106</b>

## LIST OF FIGURES

S.NO.	Title of figure	PAGE NO.
<b>1.</b>	Structures of Antidiabetic drugs.	<b>6-7</b>
<b>2.</b>	Mechanisms of Renal Glucose Reabsorption <i>via</i> SGLT2 and Its Inhibition	<b>10</b>
<b>3.</b>	Benefits/Risks of SGLT-2 inhibitors.	<b>12</b>
<b>4.</b>	Historical development of SGLT2 Inhibitors.	<b>17</b>
<b>5.</b>	Prototype (5A) and Approved SGLT2 Inhibitors (5B)	<b>22</b>
<b>6.</b>	Non approved SGLT-2 Inhibitors	<b>26</b>
<b>7.</b>	Design of O-spiroketal & 6'-O-spiro C-aryl glucosides SGLT2 inhibitors.	<b>29</b>
<b>8.</b>	Design of benzimidazole-O-glucoside, indole-O-glucoside and benzodioxane-O-glucoside SGLT2 inhibitor.	<b>30</b>
<b>9</b>	Exploration of C-glucoside bearing thiophene at the proximal ring (9A). Exploration of C-glucoside (7& 8) and (9) incorporating a thiazole at the distal ring (9B).	<b>32</b>
<b>10</b>	Design of benzisothiazole and indolizine- $\beta$ -D-glucopyranoside as SGLT2 inhibitors (10A). Design of novel N-indolyglycosides with C6-modification on the glucose moiety (10B). Design of C-glucosyl dihydrochalcone SGLT2 inhibitor (10C).	<b>33</b>
<b>11</b>	Design of novel tetrahydroisoquinoline-C-aryl glucoside SGLT2 inhibitor (11A). C-glucoside with thiophene ring as SGLT2 inhibitor (11B).	<b>35</b>
<b>12</b>	Benzyltriazolopyridinone and Phenylhydantoin SGLT2 inhibitors (12A). Design of biphenyl motif-containing C-arylglucoside SGLT2 inhibitors (12 B).	<b>37</b>

<b>13</b>	The hybrid design involves the creation of novel dioxabicyclo(3.2.1)octane derivatives. (13A). Design of oxime-containing C-glucosylarene SGLT2 inhibitor (13B). Design of Benzocyclobutane-C-glycosides (13C).	<b>39</b>
<b>14</b>	Design of C-benzyl glucosides as SGLT2 inhibitors (14 A). Designing 6-Deoxy O-Spiroketal C-Arylglucosides (14 B). Designing C-Aryl Glucosides with 5-Fluoro-5-methyl-hexose Structure (14 C).	<b>40</b>
<b>15</b>	Design of novel C-aryl D-glucofuranoside SGLT2 inhibitor (15A). Design of C-indolyxyloside SGLT2 inhibitors (15B).	<b>42</b>
<b>16</b>	Design of novel O-xyloside SGLT2 inhibitors (16A). Design of N-indolyxyloside SGLT2 inhibitors (16B).	<b>43</b>
<b>17</b>	Design of novel non-glucoside triazole benzothiazinone and benzooxazinone compounds (17A) and (17B).	<b>44</b>
<b>18</b>	Designing of non-glucoside thiadiazole based scaffold as SGLT2 Inhibitors.	<b>46</b>
<b>19</b>	Pharmacophore of non-glucoside 1,3,4 thiadiazole derivatives as SGLT2 Inhibitors.	<b>47</b>
<b>20</b>	Reaction scheme depicting the synthesis of potent compounds.	<b>48</b>
<b>21</b>	Research hypothesis for design, synthesis and evaluation of SGLT-2 inhibitors.	<b>50</b>
<b>22</b>	Protein validation for docking involved the Co-crystallized ligand (gal 701), depicted in stick model, and the re-docked ligand (gal 701), illustrated in line model.	<b>52</b>
<b>23</b>	Flow chart of the sequential steps involved in preparing the protein	<b>52</b>

<b>24</b>	Configuration File ("conf.txt") is displayed in Autodock	<b>53</b>
<b>25</b>	Reaction Scheme for most potent compounds	<b>55</b>
<b>26</b>	Designing of non-glucoside 1,3,4-thiadiazole based pharmacophore as SGLT2 Inhibitors.	<b>76</b>
<b>27</b>	2D Interactions of best designed compounds SSS 95 (A), SSS 100 (B), SSS 40 (C), SSS 35 (D) and dapagliflozin (E) on SGLT2 protein.	<b>82-83</b>
<b>28</b>	Effect of test compounds and Standard i.e. dapagliflozin at five different concentrations on % cell viability.	<b>91</b>
<b>29</b>	Effect of test compounds and Standard drug (dapagliflozin) on IC <sub>50</sub> .	<b>92</b>
<b>30</b>	% SGLT2 inhibition of test compounds.	<b>97</b>
<b>31</b>	Effect on Urinary excretion of Glucose (mg/bodyweight) after the treatment during 24h.	<b>100</b>
<b>32</b>	Effect on Urinary Excretion of electrolytes (mmol/L) after the treatment during 24h.	<b>102</b>
<b>33</b>	Impact on blood glucose levels (mg/dL) pre- and post-treatment	<b>105</b>
<b>34</b>	Impact on the body weight of rats (in grams) resulting from the treatment protocol.	<b>107</b>
<b>35</b>	Histopathology representation of rat's kidney tissue	<b>108</b>
<b>36</b>	Histopathological illustration of rat pancreatic tissue	<b>110</b>

## LIST OF ABBREVIATIONS

S.NO.	Abbreviations	Full forms
1.	2D	2-Dimensional
2.	3D	3-Dimensional
3.	ADME	Absorption, Distribution, Metabolism And Excretion`
4.	AKI	Acute Kidney Injury
5.	ANOVA	Analysis of Variance
6.	BW	Body weight
7.	CANVAS	Canagliflozin Cardiovascular Assessment Study
8.	CDH	Central Drug House
9.	CHO	Chinese Hamster Ovary
10.	CMC	Carboxy Methyl Cellulose
11.	CVD	Cardiovascular Disease
12.	CVOTs	Cardiovascular Outcome Trials
13.	DKA	Diabetic Ketoacidosis
14.	DMSO	Dimethylsulfoxide
15.	DPP-4	Dipeptidyl Peptidase-4
16.	EDG	Electron Donating Group
17.	EWG	Electron Withdrawing Group
18.	FBS	Fetal bovine serum
19.	FDA	Food And Drug Administration
20.	FTIR	Fourier Transform Infra Red Spectroscopy
21.	GFR	Glomerular Filtration Rate
22.	HbA1c	Glycated Haemoglobin
23.	HRP	Horseradish Peroxide

24.	<i>i.p.</i>	Intaperitoneal
25.	IC <sub>50</sub>	Half-Maximal Inhibitory Concentration
26.	IV	Intravenous
27.	MACE	Major Adverse Cardiovascular Events
28.	MI	Myocardial Infarction
29.	MS	Mass Spectroscopy
30.	MTT	3-[4,5-Dimethylthiazol-2-Yl]-2,5-Diphenyl Tetrazolium Bromide
31.	NAM	Nicotinamide
32.	NMR	Nuclear Magnetic Resonance
33.	OGTT	Oral Glucose Tolerance Test
34.	p.o	Per Oral
35.	PCT	Proximal Convoluted Tubule
36.	PGL	Plasma Glucose Level
37.	PKD	Peripheral Vascular Disease
38.	Rf	Retention Factor
39.	RMSD	Root Mean Square Deviation
40.	SD	Sprague-Dawley
41.	SD	Standard Deviation
42.	SGLT	Sodium Glucose Co-Transporter
43.	STZ	Streptozotocin
44.	T2DM	Type II Diabetes
45.	TLC	Thin Layer Chromatography
46.	UGE	Urinary Glucose Excretion
47.	USD	United State Dollars
48.	UTI	Urinary Tract Infection
49.	WHO	World Health Organization

## LISTS OF APPENDIXES

<b>Appendix Number</b>	<b>Title</b>	<b>Page No</b>
Appendix I	Letter of Candidacy For Ph.D	129
Appendix II	<sup>1</sup> H & <sup>13</sup> C NMR and Mass Spectra	130-147
Appendix III	Publication Details	148-150
Appendix IV	Allied Publication Details	151
Appendix V	Conference Attended Details	152-154
Appendix VI	Copyrights	155-156
Appendix VII	Animal House Certificate	157
Appendix VIII	Histopathology results	158-159

# *CHAPTER 1*



# INTRODUCTION

---

## 1. Introduction

The fact that type II diabetes is so prevalent and deadly has made it an issue of growing concern. The mortality rate climbed to roughly 6.7 million fatalities on a global scale in 2021 as a direct result of diabetes and the complications that are directly associated with it.<sup>1, 2</sup> Type II diabetes mellitus impacted 537 million people globally in 2021 and will reach 784 million by 2045 if the trend continues.<sup>3</sup> Type II diabetes is defined as persistently elevated glycemia, resistance of insulin, and abnormal functioning of  $\beta$  cell cause microvascular consequences such retinopathy, nephropathy, and neuropathy.<sup>4</sup> The World Health Organization (WHO) estimated that 9.3% of individuals between the ages of 20 and 79 years affected diabetes in 2021. Furthermore, approximately one half of incidences of type II diabetes, or 50.5%, were undiagnosed.<sup>5</sup> The incidence of type II diabetes in high income nations ranges from 87–91% of all diabetic individuals. It is estimated that 87.5% of individuals, mainly those residing in developing and middle-income nations, have type II diabetes.<sup>6-8</sup> It was predicted that 10.2% of women and 10.8% of men in the age range of 20-79 years have diabetes, with women having a slightly lower prevalence than men. The global health care costs attributable to diabetes are projected to reach USD 966 billion in 2021, representing a 316% rise over the previous 15 years.<sup>9, 10</sup> Obesity is a momentous factor in developing type II diabetes as accumulation of fatty tissues, which render cells unaffected by insulin in obese patients. Type II diabetes is on the rise, and while obesity is a major risk factor, it can still strike lean people. Abdominal fat storage increases the likelihood of developing type II diabetes more so than fat storage in the thighs and hips. Rise in blood sugar levels are a hallmark of progressing prediabetes to type II diabetes. Urban lifestyle factors like poor dietary habits and absence of physical activity lead to the advancement of type II diabetes mellitus (T2DM). Lifestyle choices like nutritional & physical activity therapies are routinely recommended to patients diagnosed with type II diabetes, however the vast majority of patients require medications in order to meet their glycemic targets. AACE recommends glycated haemoglobin (HbA1c) readings between 7.0% and 6.5%.<sup>11</sup> Achieving good glycemic control is the primary challenge

# INTRODUCTION

---

for preventing or halting the advancement of diabetes-related complications. Type II diabetes lead to risk of development of cardiovascular disorders and mortality. The different etiologic causes ultimately underlie the destructive cycle of diabetic vascular disease that are divided into two categories as conventional factors i.e. obesity, high blood pressure, abnormal cholesterol levels, and non-conventional factors such as insulin resistance, genetics, inflammation and many others.

**Table 1** displays the severe adverse effects i.e. hypoglycemia, pancreatitis, lactic acidosis, myocardial infarction, respiratory problems etc. of commonly used oral anti-diabetic medications such as thiazolidinediones, sulphonylureas, meglitinides, biguanides, and alpha-glucoside inhibitors and their structures depicted in **Figure 1**. The demand for a creative approach to mitigate the impact of insulin secretion is growing rapidly. A multitude of medicinal and targeted strategies are available for managing and maintaining diabetes.<sup>12</sup> Despite the fact that hyperglycemia may be harmful to the body as a whole, resulting in diabetes problems, the body perceives glucose as a crucial source of energy. Thus, its functioning requires several complex transport systems and metabolic processes. Renal gluconeogenesis, insulin usage in the blood, and glomerular filtrate glucose reabsorption are all demonstrated to play crucial roles in maintaining glucose homeostasis.<sup>13</sup> Impeding reabsorption of glucose in the kidney by Sodium Glucose Co-transporters is one of the emerging approaches for lowering blood sugar levels.

**Table 1.** Anti-diabetic drugs and their side effects.

Name of the target	Examples	Mechanism of action	Advantages	Side effects
Sulphonyl ureas	1 <sup>st</sup> Generation: Carbutamide Chlorpropamide Tolbutamide 2 <sup>nd</sup> generation: Glipizide 3rd Generation:	Binds to sulphonyl-ureas receptors in pancreatic beta cells leads to ATP-sensitive K <sup>+</sup> channel inhibition causes stimulation of	A1C reduction of 1–2%	Hypoglycemia and weight gain. <sup>14</sup>

## INTRODUCTION

---

	Glimepiride	release of insulin by $\text{Ca}^{+2}$ influx		
Biguanides	Metformin	Suppresses hepatic gluconeogenesis	Reduction in A1C levels (~ 1.5%)	Lactic acidosis & hypoglycemia. <sup>15</sup> -18
Amylin Agonists	Pramlintide	Causes a decrease in both postprandial glucose and glucagon	Reduction in A1C levels (~ 0.5%)	Nausea and hypoglycemia. <sup>19</sup>
Bile acid sequestrant	Colesevelam	Lowers LDL cholesterol levels and decreases load glucose levels	Reduction in A1C levels (~0.5%) and causes a reduction in LDL cholesterol of 13%.	Gastrointestinal (GI) side effects, cause a slight increase in triglyceride. <sup>19</sup>
$\alpha$ -glucosidase inhibitors	Miglitol Voglibose Acarbose	Decreases the rate of absorption of carbohydrates by inhibiting $\alpha$ -glucosidase enzymes	Reduction of A1C levels is 0.5–1.0%.	Gastrointestinal side effects. <sup>20</sup>

## INTRODUCTION

---

Thiazolidinediones (TZDs)	Pioglitazone Rosiglitazone Rivoglitazone	Activates PPAR- $\gamma$ , which causes a decrease in the generation of hepatic glucose.	Lower hypoglycemia incidence of and a longer-lasting effect than biguanides or sulphonylureas. A1C decrease of 0.5–1%	Fluid persistence, Higher risk of myocardial infarction, or heart obstruction. <sup>21</sup>
Meglitinides (Glinides)	Mitiglinide Nateglinide Repaglinide	Binds to sulphonylureas receptors in pancreatic beta cells leads to ATP-sensitive K <sup>+</sup> channel inhibition causes stimulation of release of insulin by Ca <sup>+2</sup> influx	A1C reduction is 1-1.5%. Quick onset and a shorter span of activity.	Headache, dizziness respiratory problems and Hypoglycemia. <sup>22</sup>
Incretin Mimetics	Liraglutide	Incretins are the secretagogues of insulin. Glucagon-like peptide-1 binding to the GLP receptor of the membrane.	A1C reduction is 0.5–1% and causes weight reduction.	Pancreatitis, allergic reactions and gastrointestinal (GI) side effects. <sup>23</sup>

## INTRODUCTION

---

Dipeptidyl peptidase-4 (DPP-4) Inhibitors	Alogliptin Gemigliptin	They increment the incretin levels which repress glucagon discharge.	Drop of ~0.8% in A1C reduction and devoid of hypoglycaemia risk.	GIT disturbances, CHF and hypersensitivity. <sup>24</sup>
Dopamine agonist	Bromocriptine	Boost brain dopamine production and contribute to the suppression of sympathetic tone.	Reduction in A1C levels (~ 0.7%)	Dizziness, drowsiness and lightheadedness. <sup>25</sup>
SGLT2 Inhibitors	Canagliflozin	Represses reabsorption of glucose in PCT and upgrades the discharge of glucose within the urine.	A1C rate reduction (0.5-0.7%)	Urinary or genital infections. <sup>26</sup>

# INTRODUCTION

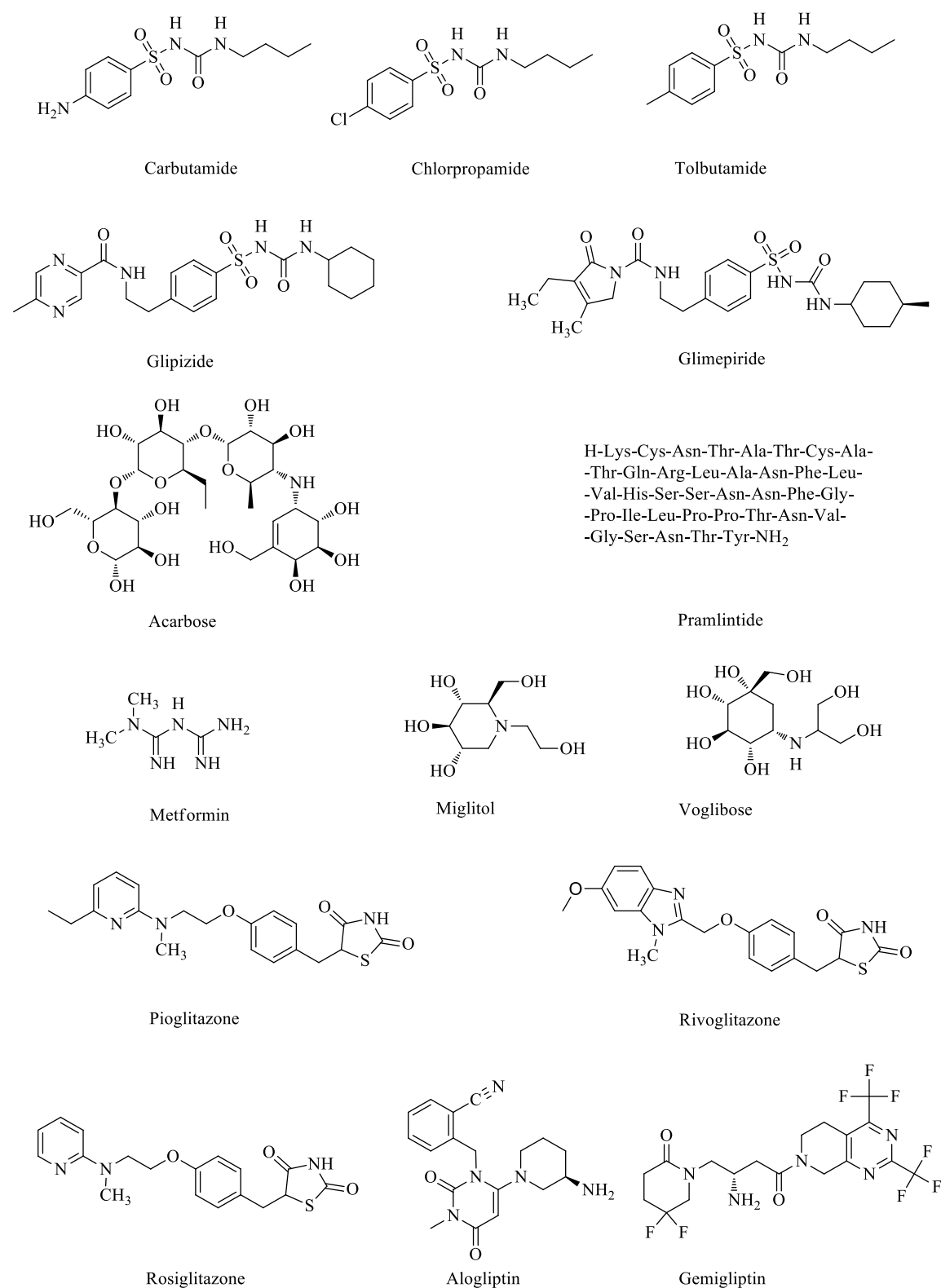


**Figure 1:** Structures of Antidiabetic drugs.

# INTRODUCTION

---

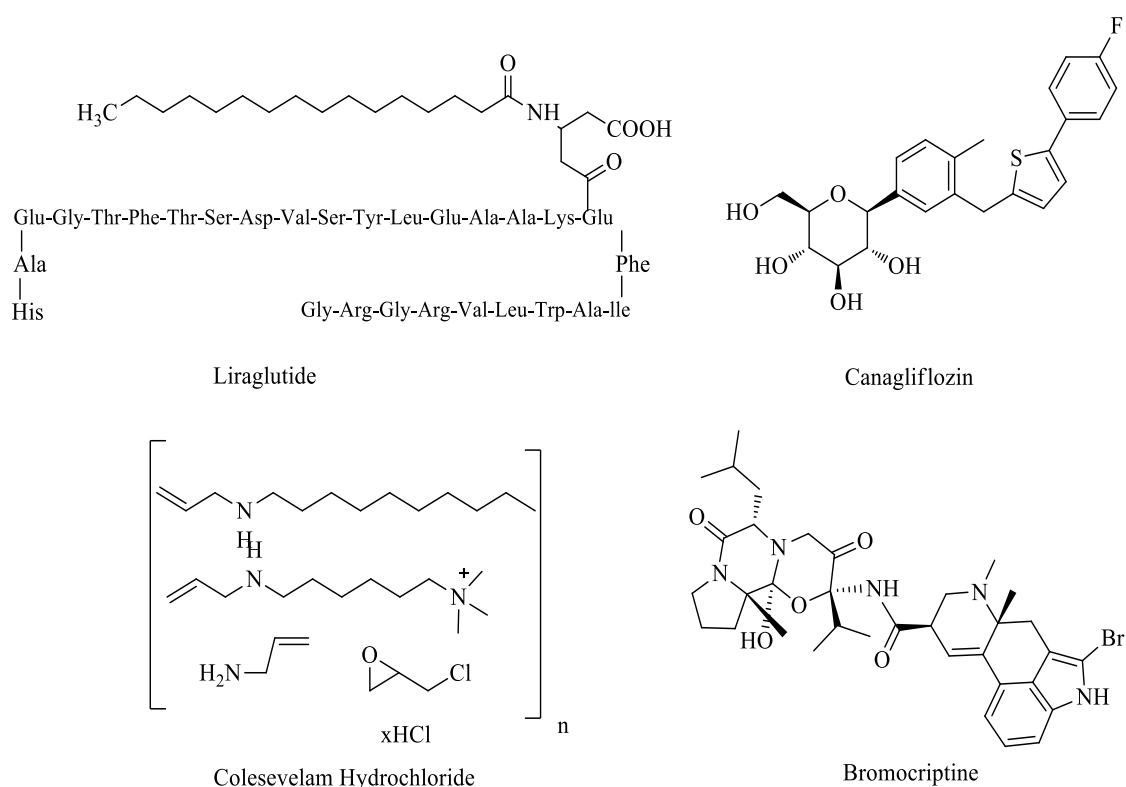


**Figure 1:** Structures of Antidiabetic drugs.

## 1.1 Role of Glucose Transporters in the kidney

The kidney reabsorbs significant amounts of glucose, playing a crucial role in maintaining the body's overall metabolic balance. In healthy humans, approximately 180 g of glucose are filtered daily through the renal glomerulus, with over 99% being reabsorbed along the tubular system. Glucose transport across cell membranes is carried out by two gene families: the facilitative glucose transporters (GLUTs) and the sodium-dependent glucose transporters (SGLTs), which use an active transport process. This latter process enables glucose to accumulate in cells against its concentration gradient. The SGLTs comprise a vast array of membrane proteins engaged in transporting glucose, amino acids, vitamins, osmolytes, and select ions. Two crucial sodium-coupled glucose transporters, namely SGLT1 and SGLT2, hold significance in the apical membrane of proximal tubular cells within the kidney.

# INTRODUCTION

---

## 1.2 The function of SGLT1 AND SGLT2 in type-II diabetes

Humans have six Sodium-Glucose Cotransporter isoforms. Among these, SGLT1 & SGLT2 transport glucose and Na<sup>+</sup> *via* cell membranes of intestine and kidney. Glifozins, known as cotransporters of sodium and glucose, represent a class of drugs that lower glucose levels by impeding its reabsorption through the kidneys and enhancing the excretion of glucose in urine. The SLC5A1 and SLC5A2 genes encode SGLT1 and SGLT2, respectively and cloned from the apical membrane of the PCT in the rat kidneys.<sup>27</sup> Despite sharing an identical amino acid sequence, SGLT1 and SGLT2 are not identical. In 1988, the protein SGLT2 was identified through homology screening. Kidney's proximal tubule has a film protein called SGLT2, which plays a vital role in the reabsorption of glucose.<sup>28</sup> SGLT2, a cotransporter with high capacity but low affinity, is responsible for absorbing 90% of glucose in the early proximal convoluted tubule (PCT) during stage one (S1).<sup>29, 30</sup> Cloning and expression studies led to the identification of SGLT1 in 1987. SGLT1 is localised to the PCT of kidney, enterocytes of the small intestine and heart.<sup>31</sup> The SGLT1 protein is a co-transporter that has a high affinity but a low capacity for the Na<sup>+</sup> and K<sup>+</sup> ions, which originate in the corresponding distal tubule that reabsorbs only 10%.<sup>32</sup>

## 1.3 SODIUM GLUCOSE COTRANSPORTER-2 (SGLT2) inhibitors

The SGLT2 inhibitors prevent the SGLT2 protein from functioning, increasing renal glucose excretion which in turn lowers hyperglycemia by preventing glucose from being reabsorbed in the PCT. The blockade of SGLT2 should result in a close correspondence between the amount of glucose filtered out and the amount excreted in urine. All SGLT2 inhibitors induce dose-dependent glucosuria and decrease glucose reabsorption by only 30–50% in healthy individuals.<sup>33</sup> In the glomeruli, it probably accounts somewhere around 50-90 g of the 180 g of daily filtered glucose. This discrepancy is intended to be explained by a variety of concepts. As SGLT2 proteins are thought to be continuously secreted into the PCT, it is possible that high dosages of SGLT2 inhibitors, which would completely saturate the transport mechanism, may restrict the quantity of SGLT2 proteins in the renal tubule. Unbound SGLT2 inhibitors could also be removed by the glomerulus.<sup>34</sup> Furthermore, the effectiveness of the



# INTRODUCTION

---

inhibitors in suppressing the production of SGLT2 proteins may depend on the site of secretion within the tubule. The SGLT2 inhibitors released at the PCT is responsible for the sustained response in urine glucose excretion seen with SGLT2 proteins. SGLT2 inhibitors may promote weight loss by increasing urine glucose excretion and calorie output.<sup>35</sup> Several SGLT2 inhibitors, which are medications used to lower glucose levels in type II diabetes patients, have been approved as a result of recent research.<sup>36</sup> However, SGLT1 inhibition may have unfavourable gastrointestinal side effects. Selective inhibition of the SGLT2 proteins, resulted in an enhanced glucose amount that was urinary excreted and had a glucose-lowering action.<sup>37</sup> Because SGLT2 inhibitors have a novel impact that is independent of insulin, they can be utilised at any stage of type II diabetes. SGLT2 inhibitors have become an intriguing molecular approach for diabetes medications to compensate for current therapies and avoid adverse effects.<sup>38</sup>

## 1.3.1 Mode of action of SGLT2 inhibitors

SGLTs actively transport  $\text{Na}^+$  down a gradient and glucose against its concentration gradient using energy from a sodium/potassium ATP pump.<sup>39</sup> SGLT2 inhibitors impair SGLT2 in the PCT to halt glucose reabsorption and enhance renal excretion in urine, which lowers plasma glucose levels as illustrated in **(Figure 2)**.<sup>40a</sup> SGLT2 acts in a manner that functions independently on insulin secretion results in low risk of hypoglycemia in contrast to conventional anti-diabetic agents. Thus, by blocking renal reabsorption of glucose and boosting urine glucose excretion, SGLT2 offers a new molecular strategy to reducing glucose plasma concentrations and complementing the actions of conventional type II diabetes medicines.

SGLT2 inhibitors reduce sodium and glucose reabsorption in the proximal tubule, diminishing the osmotic gradient and inducing osmotic diuresis. SGLT2 inhibitors primarily induce osmotic diuresis *via* glycosuria or natriuresis. The unique diuretic mechanism of SGLT2 inhibitors, distinguishing them from classical diuretics, has garnered attention. In early treatment, they bring benefits through hemodynamic changes, natriuresis, resulting in reduced weight, lower blood pressure, and increased hematocrit. However, these changes in weight, blood pressure, and hematocrit outlast the diuretic effect, suggesting that the influence of SGLT2 inhibitors on these

## INTRODUCTION

---

physiological parameters arises from their non-diuretic effects. Furthermore, SGLT2 inhibitors have minimal effects on prescribed diuretic doses, indicating that their induced diuresis does not predominantly drive physiological changes and clinical benefits in Heart Failure with Reduced Ejection Fraction (HFrEF).<sup>40b</sup> Hence, upcoming studies should prioritize investigating the effects of SGLT2 inhibitors beyond diuresis and plasma volume reduction. The benefits of SGLT2 inhibitors exceed its risks (**Figure 3**). When used orally, anti-diabetic drugs always have undesirable side effects and can be dangerous. There are more significant advantages to SGLT2 inhibitors than drawbacks

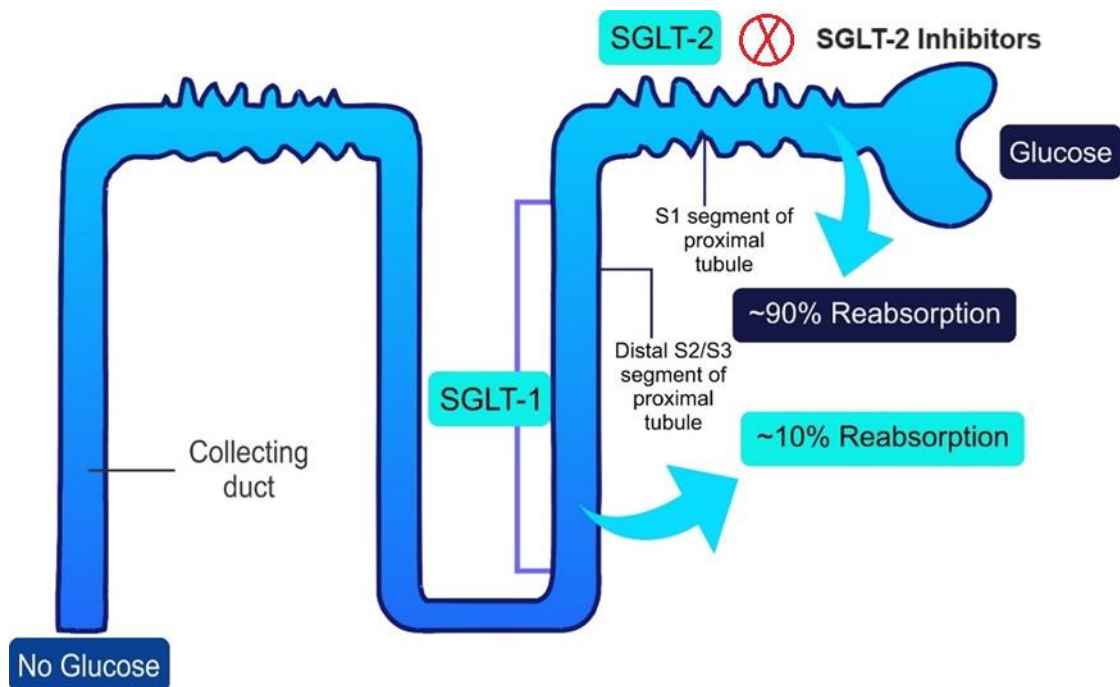


**Figure 2:** Mechanisms of Renal Glucose Reabsorption *via* SGLT2 and Its Inhibition

### 1.4 The Benefits of SGLT2 Inhibitors for Diabetes Management

#### 1.4.1 Glucose-lowering effects

SGLT2 inhibitors diminish HbA1c from 0.4% to 1.1%, depending on the starting HbA1c, drug and dosage utilised, and other factors.<sup>41</sup> Canagliflozin may have a slightly greater impact on HbA1c reduction compared to other SGLT2 inhibitors, particularly at higher doses, as it is thought to also inhibit SGLT1 in the gut. In head-to-head

## INTRODUCTION

---

comparisons, there is some indication that SGLT2 inhibitors might exhibit greater effectiveness than DPP-4 inhibitors but at small degree.<sup>42</sup> HbA1c is reduced more noticeably by sulfonylureas initially, but their effectiveness gradually diminishes over time, giving SGLT2 inhibitors a modest HbA1c edge after 2 years. The incidence of hypoglycemia among patients taking SGLT2 inhibitors is relatively modest.

### 1.4.2 Cardiovascular and Renal benefits

In individuals with T2DM, SGLT2 inhibitors reduce the occurrence of kidney and heart failure and maintain kidney function, as indicated in multiple clinical trial outcomes.<sup>43</sup> According to cardiovascular outcome trials (CVOTs), empagliflozin, canagliflozin, and dapagliflozin known as SGLT2 inhibitors have demonstrated a reduction in major adverse cardiovascular events (MACE).<sup>44</sup> The EMPA-REG OUTCOME study, which included 7020 patients with T2DM and diagnosed cardiovascular disease (CVD). Patients who received a dosage of 10 mg/25 mg of empagliflozin *versus* placebo had a lower risk of CVD compared to those who received a placebo. Stroke and myocardial infarction rates did not differ significantly. When compared to placebo, empagliflozin was associated with improved renal outcomes such as worsening nephropathy, serum creatinine doubling and reduced the rate of the main composite renal outcome by 39%.<sup>45</sup> Canagliflozin lowered the primary composite endpoint (MACE) by 14%. When compared to the placebo group, canagliflozin significantly reduced fatality from renal causes by 34%.<sup>46</sup>

In the DECLARE-TIMI 58 trial, a higher proportion of patients on primary prevention were enrolled, with 59.4% of the 17,160 participants having no documented CVD. In terms of MACE reduction, dapagliflozin failed to show a substantial effect. In comparison to the placebo group, treatment with dapagliflozin was found to be associated with a significantly reduced rate of renal composite outcome, according to the results of a clinical trial with > 40% reduction in eGFR, and fatality from renal causes.<sup>47</sup>

### 1.4.3 Weight loss

SGLT2 inhibitor-induced glucosuria causes weight reduction that tends to be persistent. The amount of weight loss experienced is somewhat varied based on the substance that is being used and the dose that is being administered. A comparison of individuals with

# INTRODUCTION

---

those who were given canagliflozin, empagliflozin, or dapagliflozin daily at doses i.e. 300 mg, 25 mg, and 10 mg give rise to a substantial weight loss in clinical trials.<sup>48</sup>

## 1.4.4 Lowering in Blood Pressure

By enhancing osmotic diuresis and decreasing intravascular volume, SGLT2 inhibitors reduce blood pressure. Moderately impaired renal function patients also show a reduction in BP despite a small decline in HbA1c, suggesting that this impact is independent of HbA1c reduction. Systolic BP reduces by 3.4 to 5.4 mm Hg & diastolic blood pressure is reduced by 1.5 to 2.2 mm Hg after using an SGLT2 inhibitor. The greatest decrease in systolic blood pressure with SGLT2 inhibitor medication is seen in type II diabetics with uncontrolled blood pressure at baseline.<sup>49</sup>

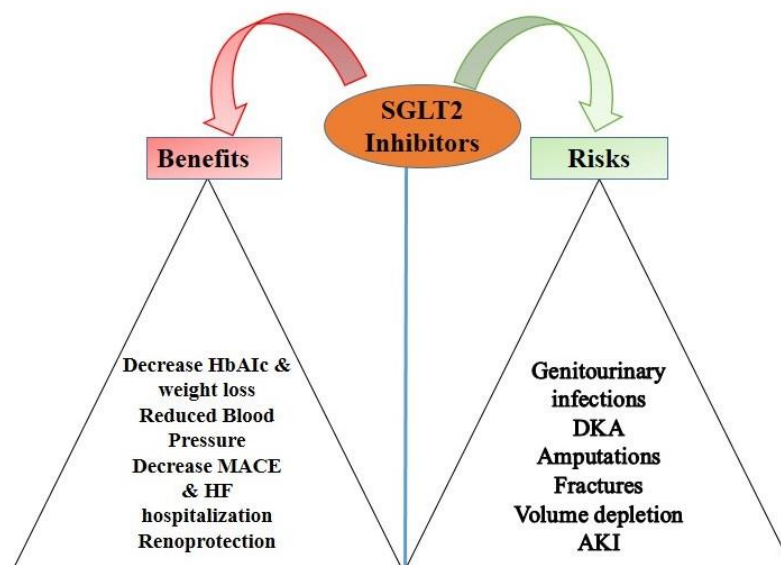


**Figure 3:** Benefits/Risks of SGLT2 inhibitors.

## 1.5 Adverse effects of SGLT2 inhibitors

### 1.5.1 Genital and Urinary Tract Infections

The prevalent adverse consequences associated with SGLT2 inhibitors are urinary and genital tract infections. SGLT2 inhibitor-induced glucosuria raises the incidence of genital and, to a lower extent, urinary tract infections (UTI).<sup>50</sup> The data that were available did not provide any clear evidence of a definitive dosage association between

## INTRODUCTION

---

the occurrence of these infections and the doses of SGLT2 inhibitors or the amount of UGE that was administered. The UTI level in dapagliflozin subjects has slightly increased in clinical studies. In most cases, it is notable that the dosage of dapagliflozin was not dependent on UTI or infections of the genital system and the same results were found in canagliflozin trials. Overall, women were twice as likely to get UTIs and genital infections as men. The type of SGLT2 inhibitor used may not entirely account for any observed heterogeneity in study results; rather, it is likely that the characteristics of the study population or the study's methodology are responsible for variation. In general, adverse effects are mild to moderate in intensity, but with a quick procedure, all cases of UTI and genital tract infections have been solved and do not need drug withdrawal. Pyelonephritis and urosepsis are relatively uncommon complications of SGLT2 inhibitors that can occur in the upper urinary tract. The odd ratio (OR) for incidence of genital fungal infections was increased fivefold i.e. 5.06 (95% CI 3.44, 7.45) and the incidence of UTIs was increased two fold i.e. 1.42 (95% CI 1.06, 1.90) in a clinical trials that compared SGLT2 inhibitors with either placebo or other anti-diabetic medications. Genital fungal infections are treatable with antifungal agents that can be administered either orally or topically. UTIs that are not complex typically respond well to standard treatment.

### **1.5.2 Diabetic ketoacidosis (DKA)**

This class of medication could significantly raise the risk of ketoacidosis with diabetes.<sup>51</sup> It has been occasionally correlated with serum glucose levels lower than 13.9 mmol/l. A recent study assessed a group of diabetic persons who had recently begun therapy with SGLT2 inhibitor versus a dipeptidyl peptitase-4 inhibitor. The study made use of a big database that had information on people living in the United States who had commercial health insurance. The empagliflozin and placebo groups had comparable DKA rates in the EMPA-REG OUTCOME study (4/4687 (0.09%) versus 1/2333 (0.04%), respectively) (8). In the CANVAS Program, canagliflozin caused 0.6 DKA episodes per 1000 patient-years, while placebo caused 0.3 (HR 2.33 (95% CI 0.76, 7.17)). If a diabetic patient has DKA while using an SGLT2 inhibitor, the drug shouldn't be continued, at least on the spot. This is due to the multiple instances of individuals experiencing DKA relapses when taking an SGLT2 inhibitor continuously.

# INTRODUCTION

---

## 1.5.3 Amputation

Canagliflozin increased the incidence of lower-extremity amputation in the CANVAS Study in comparison to placebo, the majority of those who experienced amputation severed at the toe or metatarsal level (71%). This agent enhances amputation risk for unknown reasons. Canagliflozin-induced amputations require further study.<sup>52</sup> The incidence of amputation was comparable in empagliflozin *versus* placebo group when the period to first incident was analysed. Statistically significant results were observed in all subgroups that were differentiated by well-known adverse outcomes for amputation. The incidence of lower-limb amputation was comparable following dapagliflozin (0.1%) and control (0.2%) therapy in randomised controlled studies.

## 1.5.4 Cancer Risk

Bladder cancers were prevalent in dapagliflozin-treated patients in comparison to placebo-treated patients during clinical trials. There was no discernible difference in bladder malignant development. Dapagliflozin is not recommended for patients who have a family history of bladder cancer. Cancer occurrences had reported in patients SGLT2 inhibitor-treated patients during randomised controlled trials. SGLT2 inhibitors were not markedly linked to a higher incidence of overall cancer with odd ratio 1.14 in comparison to placebo or other anti-diabetic agents.<sup>53</sup> Moreover, the EMPA-REG OUTCOME researchers noted that the authors omitted several bladder cancer occurrences from this massive and long-running empagliflozin trial.

## 1.5.5 Skeletal fractures

There is evidence that canagliflozin raises the incidence of bone fractures. There were more fractures among people using canagliflozin in the CANVAS study than those taking a placebo with a hazard ratio (HR) of 1.26. Canagliflozin's increased risk of fracture was evident within weeks of starting treatment and persisted at a steady rate thereafter.<sup>54</sup> Participants in the EMPA-REG OUTCOME study who received either empagliflozin or a placebo had a comparable incidence of fractures, with 3.8% of patients in the empagliflozin group experiencing fractures and 3.9% in the placebo group. No evidence was found to indicate SGLT2 inhibitors having a negative impact

## INTRODUCTION

---

on bone density in a clinical studies assessing the cumulative safety behaviour of SGLT2 inhibitors. The incidence of fracture events in the group treated with SGLT2 inhibitors was 1.59%, while in the placebo group it was 1.56%. Additionally, there was no discernible difference in the incidence of fracture occurrences amongst the above 3 SGLT2 inhibitors.

### 1.5.6 Volume Depletion

By stimulating osmotic diuresis, SGLT2 inhibitors reduce blood pressure. This effect is helpful for hypertension people but can cause light-headedness, hypotension, & loss of extracellular fluid volume, especially in the elderly and people with renal dysfunction. In clinical studies, there were few occurrences of side effects related to volume depletion in both the empagliflozin and placebo groups, with a slightly higher incidence in the empagliflozin group (5.1%) compared to the placebo group (4.9%). In CANVAS, canagliflozin caused volume depletion more often than placebo (26 versus 18.5 occurrences per 1000 person-years).<sup>55</sup>

### 1.5.7 Acute kidney injury (AKI)

Canagliflozin and dapagliflozin's elevated incidence of acute kidney injury (AKI) was warned by the USFDA after reports of a probable link between SGLT2 inhibitors and acute renal failure. The majority of documented instances happened within a month of initiating therapy and became better after it was stopped, while some people needed to be hospitalised and get dialysis. Among two groups of patients, those who used SGLT2 inhibitors did not have a higher incidence of acute kidney injury than those who did not. Empagliflozin and canagliflozin have been shown to slow the development of nephropathy and protect the kidneys, even if they cause a temporary drop in eGFR at first.<sup>45</sup>

Dehydration is included among the extra side effects of SGLT2. Mental disorder and arterial hypotension with syncopal risk are the most important consequences. Dapagliflozin and canagliflozin clinical trials were reported to reduce body weight. Empagliflozin causes unusual headaches. Ipragliflozin has been associated with polyuria, polydipsia, and constipation.

# *CHAPTER 2*



# LITERATURE REVIEW

---

## 2.1 HISTORICAL BACKGROUND

In 1836, phlorizin was isolated from apple tree bark. It comprised a moiety of glucose and two fragrant rings together with an alkyl spacer (Figure 3A).<sup>56</sup> Because of the bitter taste of phlorizin, antipyretic properties are expected and used for fever and malaria. In 1887, phlorizin was found to be a glycoside from apple bark. Aerobic metabolism is impaired by high concentrations of phlorizin ( $10^{-4}$ - $10^{-3}$  M) and actuates mitochondrial expansion. Ingestion of phlorizin at a dosage greater than 1g caused glycosuria and polyuria.<sup>57</sup>

Phlorizin is a non-specific dual SGLT1/SGLT2 phenolic O-glycosidic inhibitor that limits its utility. It is orally inactive due to  $\beta$ -glucosidase hydrolysis in the intestine. Hence, pharmaceutical research was carried out on phlorizin derivatives with SGLT2 selectivity, improved efficacy, and bio-availability. O-glucosides and C-glucosides evaluated and observed to have better behaviour in this regard. The progression of SGLT2 inhibitors, from the initial identification of phlorizin to the approval of selective SGLT2 inhibitors by the US FDA, has been extensively studied and undergone various phases of clinical trials as illustrated in **Figure 4**.

## 2.2 SGLT2 inhibitors discontinued from clinical trials

C-glucosides such as YM-543 and O-glucoside candidates, such as WAY-123783, T-1095, and sergliflozin, have been evaluated for use in preclinical trials, but have been abandoned in early clinical development.

### 2.2.1 WAY-123783

WAY-123783, an analog and non-glycosidal SGLT2 pyrazole inhibitor (**Figure 5A**) synthesized with an  $EC_{50} = 9.85$  mg/kg to improve hyperglycemia. WAY-123783 was considered to overcome the gastrointestinal tract instability of O-glycosides. It improved the excretion of glucose in healthy mice and decreased renal reabsorption of glucose by influencing SGLT2 activity. It corrects hyperglycemia not by blocking the absorption of intestinal glucose. Nevertheless, selective reabsorption inhibition of renal glucose promotes urinary excretion. It was given to healthy mice, generating a robust glucosuric effect ( $> 8$  g/dL) and inhibiting *in vitro* SGLT activity. WAY-123783 was transformed

## LITERATURE REVIEW

into its active metabolite, WAY-123783-glycoside, known for its ability to inhibit SGLT activity. Subsequently, further clinical development of WAY-123783 was halted.<sup>58</sup>

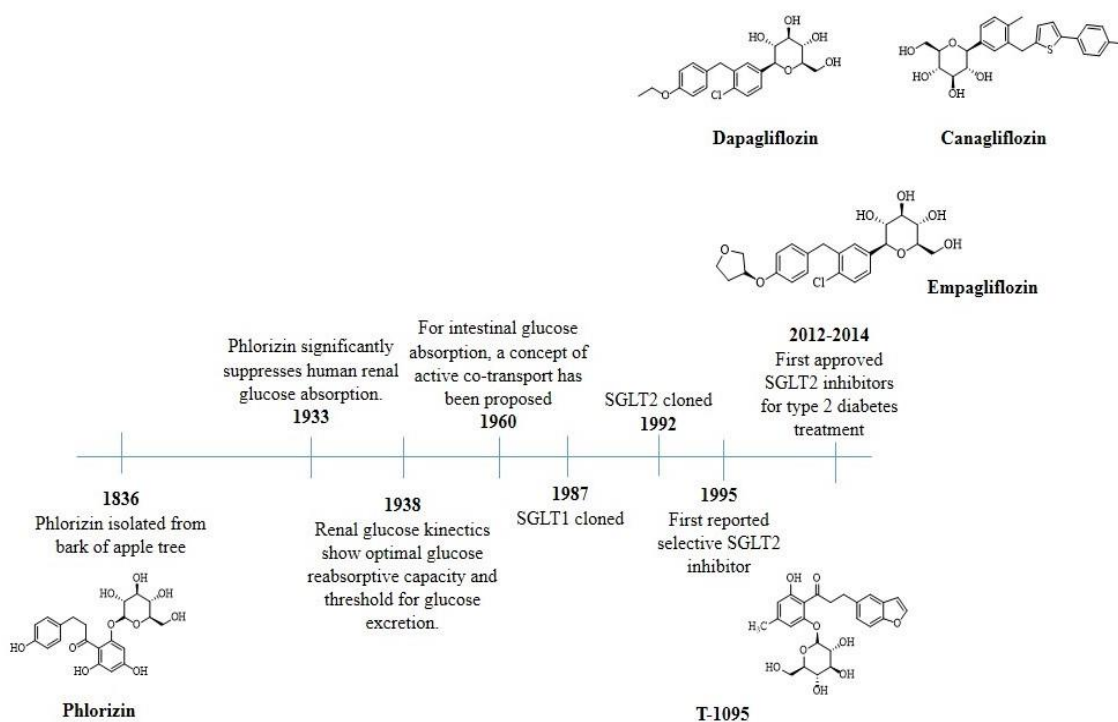


**Figure 4:** Historical development of SGLT2 Inhibitors.

### 2.2.2 T-1095

Structural modification of Phlorizin leads to the derivative of 4'-dehydroxyphlorizin, i.e. T-1095 and T-1095A (**Figure 5A**) were developed as non-selective SGLT inhibitors by Tanabe Seiyaku to overcome phlorizin's disadvantages. Oral T-1095, the glycone is absorbed into the bowels by metabolism that transforms the SGLT functioning within the kidney into the active form, T-1095A.<sup>59</sup> A 0.1% w/w dose of T-1095 decreased blood glucose elevation by 147 mg/dl and HbA1C (6.4%) by expanding urinary glucose disposal in KK-A<sup>y</sup> mice and preventing renal glucose reabsorption. This compound ameliorated insulin resistance that subsequently recovered hepatic glucose production

## LITERATURE REVIEW

---

and consumption rates.<sup>60</sup> Because of non-selectivity and safety issues, T-1095 did not pursue drug research after phase II. Long term administration of T-1095 restored the diminished secretion from  $\beta$ -cells and decreased diabetes-related complication. T-1095 suppressed dose-dependent hyperglycemia while increasing urinary glucose excretion (554 mg/day at a 0.1 % w/w dose) in KK-Ay mice.

### 2.2.3 Sergliflozin

In 2007, developed sergliflozin as a selective SGLT2 inhibitor and officially discontinued in 2008 after further clinical trials. Chemically, it is a benzylphenol O-glucoside prodrug and its active form, sergliflozin-A (**Figure 5A**) is about 296 times more selective for SGLT2 compared to phlorizin as a potent SGLT2 inhibitor.<sup>61</sup> It was found to lower the glucose level in post-prandial rats through improved glucose excretion during the clinical trial. Sergliflozin did not have a lowering effect on glucose and gastrointestinal adverse effects caused by SGLT-1 even when a 1000 mg dose was given 3 times per day, suggesting that SGLT-1 had significant enough selectivity to be a therapeutic candidate for diabetes. Sergliflozin therapy may have optimized SGLT1 activity without triggering a gastrointestinal disorder in clinical trials that raised the plasma levels of GLP-1.

### 2.2.4. YM543

The development of YM543, a SGLT2 inhibitor derived from azulene and C-glucoside, was terminated during Phase 2 clinical trials.<sup>62</sup> Orally administering YM543 at a dosage of 3mg/kg resulted in a notable 56% reduction in glucose AUC. (**Figure 5A**). *In vivo* studies of YM543 showed a dose-dependent increase in UGE, consistently observed and lasted for more than 12 hours. When given orally, it was found to be a consistently effective anti-hyperglycemic treatment for type II KK/Ay mice and type I STZ-induced diabetic rats.

# LITERATURE REVIEW

---

## 2.3 FDA & EMA APPROVED SGLT2 INHIBITORS

### 2.3.1 Dapagliflozin

In 2008, identified Dapagliflozin as a selective renal SGLT2 inhibitor with an  $EC_{50}$  = 1.12 nmol/l against hSGLT2, when compared to a 35.6 nmol/l  $EC_{50}$  for phlorizin. Dapagliflozin for hSGLT2 vs. hSGLT1 is highly selective and active (~1,200-fold). It is a C-aryl glycoside composed of a biaryl aglycone moiety linked to a glycone moiety. (**Figure 5B**).<sup>63</sup> Chemically, it is (2S,3R,4R,5S,6R)-2-[4-chloro-3-(4-ethoxybenzyl)phenyl]-6-(hydroxyl methyl)tetrahydro-2Hpyran 3,4, 5-triol. It was the European Union's first approved SGLT2 inhibitor in 2012. Dapagliflozin induces breast cancer, liver damage, and urinary bladder during clinical trials. Due to these risks, EMDAC of the FDA disapproved dapagliflozin. Following the resolution of the above concerns during clinical trials for hyperglycemic control in type II diabetes, the FDA approved it later in 2014 under the name "Farxiga." FDA approved the first combination of dapagliflozin-metformin hydrochloride, sold as Xigduo XR, in 2014. In healthy volunteers, it was observed during clinical studies that dapagliflozin at doses of 20-100 mg results in increased urinary excretion of about 50-60 g glucose over 24 h post-dose. The recommended tablet dosage for dapagliflozin includes 5 mg & 10 mg ensures both safety and effectiveness as a mono treatment. It also causes weight loss by excreting the body's glucose, which leads to a loss of calories. Renal function must be observed, particularly with impaired renal capacity and older patients, before starting dapagliflozin treatment as it will generally lead to lower glomerular filtration levels (GFR).

### 2.3.2 Canagliflozin

In 2013, the US FDA approved Canagliflozin, which is recognized as the first inhibitor SGLT2 with a C-aryl glycoside chemical structure and is marketed as "Invokana" by Janssen.<sup>64</sup> It consists of a sugar moiety attached to a thiophene-based aglycone (**Figure 5B**) and showed marked hypoglycemic effects in mice.<sup>65</sup> Chemically, canagliflozin is (2S,3R,4R,5S,6R)-2-(3-(5-(4fluoro-phenyl)thiophen-2-ylmethyl)-4-methyl-phenyl)-6-

## LITERATURE REVIEW

---

hydroxy-methyltetrahydropyran 3,4,5 triol. C-glucosides bearing a hetero-aromatic ring have greater gastrointestinal stability than the O-glucosides i.e. phlorizin and T-1095. During clinical studies, starting dose of 100 mg, followed by 300 mg two times daily doses, it has been observed that no remarkable glucose malabsorption was noticed. When 300 mg of canagliflozin was administered orally in healthy volunteers, it resulted in delayed post-prandial blood glucose as compared to the placebo with reductions in HbA1c i.e. 1.03%, BP (-3.7 to -5.4 mm Hg) and body weight (-3.6 kg). Administration of canagliflozin at a dose of 100-300 mg OD in patients with T2DM, steady-state concentration and the mean  $C_{max}$  were achieved after 4-5 days and 1-2 hrs post-dose.

### 2.3.3 Ertugliflozin

Ertugliflozin is an orally dynamic SGLT2 antagonist that has framed a novel dioxabicyclo ring framework (**Figure 5B**) for type II diabetes by Merck & Pfizer.<sup>66</sup> Ertugliflozin was endorsed in 2017 for treating type II diabetes under the brand name "Steglatro™" by the USFDA.<sup>67</sup> It is (1S,2S,3S,4R,5S)-5-[4-Chloro-3-(4-ethoxybenzyl) phenyl]-1-hydroxymethyl-6,8-dioxabicyclo[3.2.1]octane-2,3,4-triol. Ertugliflozin is a cocrystal labeled ertugliflozin LPGA in the drug known as L-pyroglutamic acid (L-PGA). Ertugliflozin is formulated for oral administration at 5 and 15 mg as an immediate-release tablet. The strength of the dose is expressed as a free form of ertugliflozin. This molecule was designed based on a model of the relationship between pharmacokinetics and pharmacodynamics (PKPD). The development approach aimed to reduce parameters like the human dose by expanding  $t_{1/2}$  and improving strength. On the other hand, the clearance and volume have been transformed into human  $t_{1/2}$ , 12 h.

### 2.3.4 Empagliflozin

Empagliflozin, SGLT2 inhibitor approved by the USFDA in 2014 (**Figure 5B**). In clinical trials, glycemic control was found to be boosted by 10 mg and 25 mg of the medication per day.<sup>68</sup> It is a C-glucoside analogue, chemically known as (2S,3R,4R,5S,6R)-2-(4-chloro-3-(4-(((R)-tetrahydrofuran-3-yl)oxy)benzyl)phenyl)-6-(hydroxymethyl)tetrahydro-2H-pyran-3,4,5-triol. The Clearance (CL) and Steady-state

## LITERATURE REVIEW

---

volume of distribution ( $V_{dss}$ ) of Empagliflozin were stated to be 10.6 L/h, 73.8 L, and 12.4 h  $t_{1/2}$ . On oral administration once a day, empagliflozin is readily absorbed ( $t_{max}$  attained < 2h post- dose). Empagliflozin exposure, which is not affected by food, rises in proportion to dose (in the therapeutic dose range i.e. 10-100 mg) and shows linear time pharmacokinetics. The metabolism of the drug was mainly by glucuronide formation and primarily unchanged in the urine and fecal. Empagliflozin inhibited the reabsorption of glucose and significantly increased UGE by 74, 90, and 81 g at therapeutic doses in comparison with placebo and lowered blood glucose from day 1. The peak antihyperglycemic efficacy of empagliflozin at a dose of 10 and 25 mg/day was demonstrated. Glycaemic findings such as decreases in HbA1c (0.66-0.78 %), reduced body weight (2.26-2.48 kg) and BP, cardiac workload, serum uric acid and preserved renal function from phase III studies of 10-104 weeks' duration. Empagliflozin exposure, which is not affected by food, rises in proportion to dose (in the therapeutic dose range i.e. 10-100 mg) and shows linear time pharmacokinetics. The metabolism of the drug was mainly by glucuronide formation and primarily unchanged in the urine and fecal. Empagliflozin inhibited the reabsorption of glucose and significantly increased UGE by 74, 90, and 81 g at therapeutic doses in comparison with placebo and lowered blood glucose from day 1. The peak antihyperglycemic efficacy of empagliflozin at a dose of 10 and 25 mg/day was demonstrated. Glycaemic findings such as decreases in HbA1c (0.66-0.78 %), reduced body weight (2.26-2.48 kg) and BP, cardiac workload, serum uric acid and preserved renal function from phase III studies of 10-104 weeks' duration.

## LITERATURE REVIEW

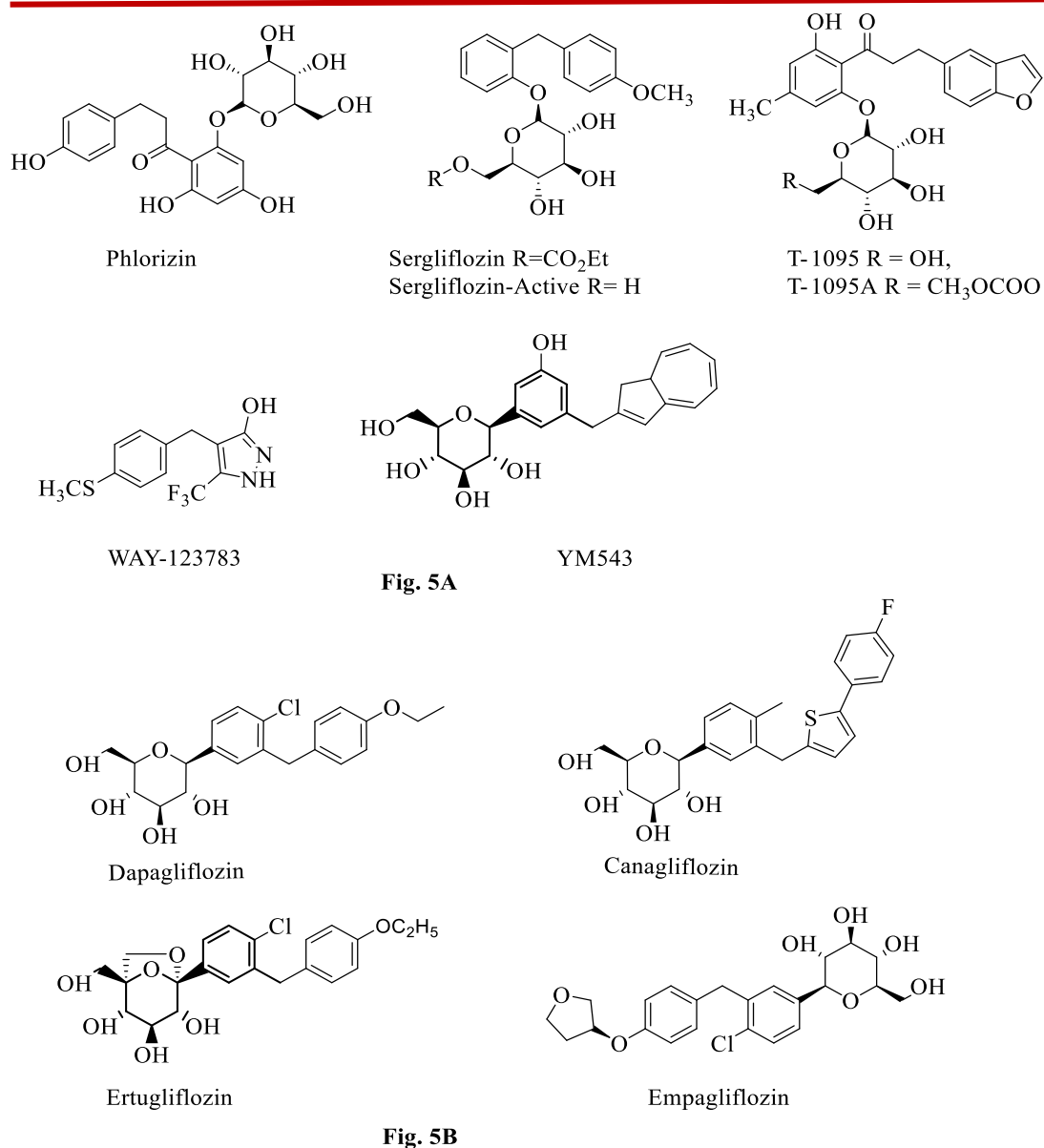


**Figure 5:** Prototype (5A) and Approved SGLT2 Inhibitors (5B)

### 2.4 SGLT2 inhibitors under investigation (not approved by the FDA and EMA)

#### 2.4.1 Remogliflozin etabonate

Remogliflozin etabonate is an oral selective antagonist of SGLT2 that was gained access as a remedy for type II diabetes in India in 2019.<sup>69</sup> Chemically, it is methyl (2S,3S,4S,5R,6R)-3,4,5-trihydroxy-6-((4-(4-isopropoxybenzyl)-1-isopropyl-5-methyl-1H-pyrazol-3-yl)oxy)tetrahydro-2H-pyran-2-carboperoxoate. Remogliflozin etabonate

## LITERATURE REVIEW

---

is a benzylpyrazole O-glycoside and is biotransformed into its active form, i.e. remogliflozin, which is metabolized into GSK27982, which also displays inhibitory effects on SGLT2.<sup>70</sup> Remogliflozin showed (K<sub>i</sub>) values for hSGLT2/hSGLT1 were 12.4 and 4520 nmol/l respectively. Its inhibitory impact on rodents becomes two-fold for SGLT2 and 1/7th for SGLT-1. Remogliflozin is more active than Phlorizin, T-1095, and sergliflozin *in vivo* SGLT2 inhibition (**Figure 6**).

### 2.4.2 Luseogliflozin (TS-071)

Luseogliflozin is an orally active SGLT2 antagonist that was firstly approved for usage in Japan in 2014 and is sold as "Lusefi" for T2DM care for adults.<sup>71</sup> Luseogliflozin is currently under investigation in phase III for clinical development by Taisho Pharmaceuticals. Luseogliflozin's recommended OD dose is 2.5 mg, which might be raised to 5.0 mg once daily if the initial dose doesn't correct hyperglycemia. The hSGLT2 IC<sub>50</sub> value of Luseogliflozin was 2.26 nM (**Figure 6**). Luseogliflozin is (1S)-1,5-anhydro-1-[5-(4-ethoxybenzyl)-2-methoxy-4-methyl phenyl]-1-thio-D-glucitol (TS-071) and derivatives of phenyl-ether sulphide.<sup>72</sup> When administered as a single oral dose at a concentration of 1 mg/kg, luseogliflozin was observed to cause a 300-fold increase in urinary glucose excretion and decreased hyperglycemia following the oral ingestion of glucose in Zucker fatty rats. When administered orally to Beagle dogs at a dosage of 1mg/kg, luseogliflozin demonstrated more than 2600-fold increased urinary glucose excretion (UGE), leading to increased bioavailability (92.7%) of TS-071 in animals. During the pharmacokinetics studies, Luseogliflozin demonstrated dose-proportional pharmacokinetics without any cumulative ability. The drug's mean t<sub>max</sub> ranged from 0.67 hours to 2.25 hours.

### 2.4.3 Ipragliflozin

Ipragliflozin (ASP1941) is the first SGLT2 antagonist to be licensed in 2014 in Japan and is not approved in the EU and USA (**Figure 6**). It is (1S)-1, 5-anhydro-1-[3-(1-benzothiophen-2-yl methyl)-4-fluorophenyl]-D-glucitol. Ipragliflozin has been sold under the brand name "Suglat," an effective SGLT2 antagonist in the care of T2DM patients.<sup>73</sup> *In vitro* inhibition activity in CHO cells expressing hSGLT2 and hSGLT1,



## LITERATURE REVIEW

---

showing substantial IC<sub>50</sub> of 7.38 nM and 1880 nM, and inhibitors of <sup>14</sup>C-methyl- $\alpha$ -D-glucopyranoside. Ipragliflozin induced a marked advancement in the UGE and reduction in hyperglycemia *in vivo* studies. The recommended initial dosage of ipragliflozin in adults is 50-100 mg once daily may be increased if hyperglycemia is not adequately controlled.

### 2.4.4 Tofogliflozin

Tofogliflozin is an O-spiroketal C-aryl glucoside SGLT2 inhibitor that was approved in 2012 in Japan and is in clinical trials in Phase III.<sup>74</sup> Chemically, it is (1S,3'R,4'S,5'S,6'R)-6-[(4-ethylphenyl)methyl]-6'-(hydroxymethyl)-3',4',5,6' tetra hydro-3H-spiro[2-benzofuran-1,2'-pyran]-3',4',5'-triol. <sup>14</sup>C-AMG inhibition in CHO cells that express hSGLT2 and hSGLT1 was examined for *in vitro* tofogliflozin-inhibitory activity.<sup>75</sup> After IV administration of tofogliflozin, steady-state volume of distribution (V<sub>ss</sub>) and clearance (CL) were reported as 10.0 L/h and 50.6 L. The IC<sub>50</sub> value for tofogliflozin against human SGLT2 was determined to be 2.9 nmol/L. This indicates that tofogliflozin has a strong affinity for inhibiting SGLT2 (**Figure 6**).

### 2.4.5 Sotagliflozin (LX4211)

Sotagliflozin, or LX4211, functions as a dual inhibitor, targeting both SGLT1 and SGLT2 that was developed by Lexicon Pharmaceuticals.<sup>76</sup> It is a molecule based on L-xyloside and is being investigated for its potential use in both type I and type II diabetes (**Figure 6**). Chemically, it is (2S,3R,4R,5S,6R)-2-(4-chloro-3-(4-ethoxybenzyl)phenyl)-6-(methylthio)tetrahydro-2H-pyran-3,4,5-triol. *In vivo* results showed that limited SGLT1 inhibition is a complementary objective to reducing blood glucose and SGLT2 inhibition. *In vitro* cell line studies of human SGLT2 and SGLT1, the investigation into sotagliflozin demonstrating a selectivity approximately 20 times greater for SGLT2. In the KKAY mice model, sotagliflozin has been reported to improve glucose homeostasis by decreasing fasting plasma glucose at a dose of 150-300 mg, i.e. 52-60 mg/dL.

## LITERATURE REVIEW

---

### 2.4.6 Henagliflozin (SHR3824)

Henagliflozin Proline is currently under investigation in phase II for clinical development. Henagliflozin is (1R,2S,3S,4R,5R)-5-(4-Chloro-3-(4-ethoxy-3-fluorobenzyl) phenyl)-1-(hydroxymethyl)-6,8-dioxabicyclo[3.2.1]octane-2,3,4-triol. Henagliflozin has IC<sub>50</sub> of 2.38 nM (**Figure 6**) and > 800-fold SGLT2 selectivity versus SGLT1.<sup>77, 78</sup> *In vivo*, pharmacological research affirmed that on day 1 of treatment, it lowered blood glucose AUC<sub>0-24 h</sub> values by 23.7%, 32.7%, and 36.5% at doses ranging from 0.3-3.0 mg/kg. Chronic SHR3824 therapy significantly improved glycemic control in db/db mice's soleus muscles.

### 2.4.7 Bexagliflozin

Bexagliflozin, also known as EGT1442, is a novel candidate in the class of SGLT2 inhibitors is a phenolic C-glucoside analogue which is approved by USFDA in 2023 for treating the type-2 diabetes under the brand name “brenzavvy” (**Figure 6**).<sup>79a, 79b</sup> It is a phenolic C-glucoside analogue and chemically (2S,3R,4R,5S,6R)-2-[4-chloro-3-[[4-(2-cyclopropyloxyethoxy)phenyl]methyl]phenyl]-6-(hydroxymethyl)oxane-3,4,5-triol. Bexagliflozin blocked dose-dependent uptake of SGLT1 and SGLT2-mediated Na<sup>+</sup>-dependent AMG. The IC<sub>50</sub> value of Bexagliflozin was found to be 2 nM with a selectivity level of 2435-fold against human SGLT2 relative to human SGLT1. In phase III clinical studies of 24 weeks' duration, glycemic control was found to be boosted by 20 mg of bexagliflozin once a day. A reduction in HbA1c levels by 0.37%, a decrease in body weight by 1.61 kg, and a decrease in fasting plasma glucose levels by 0.76 mmol/L were observed in comparison to the placebo group. These findings suggest an improvement in glycemic control in the treated group.

## LITERATURE REVIEW

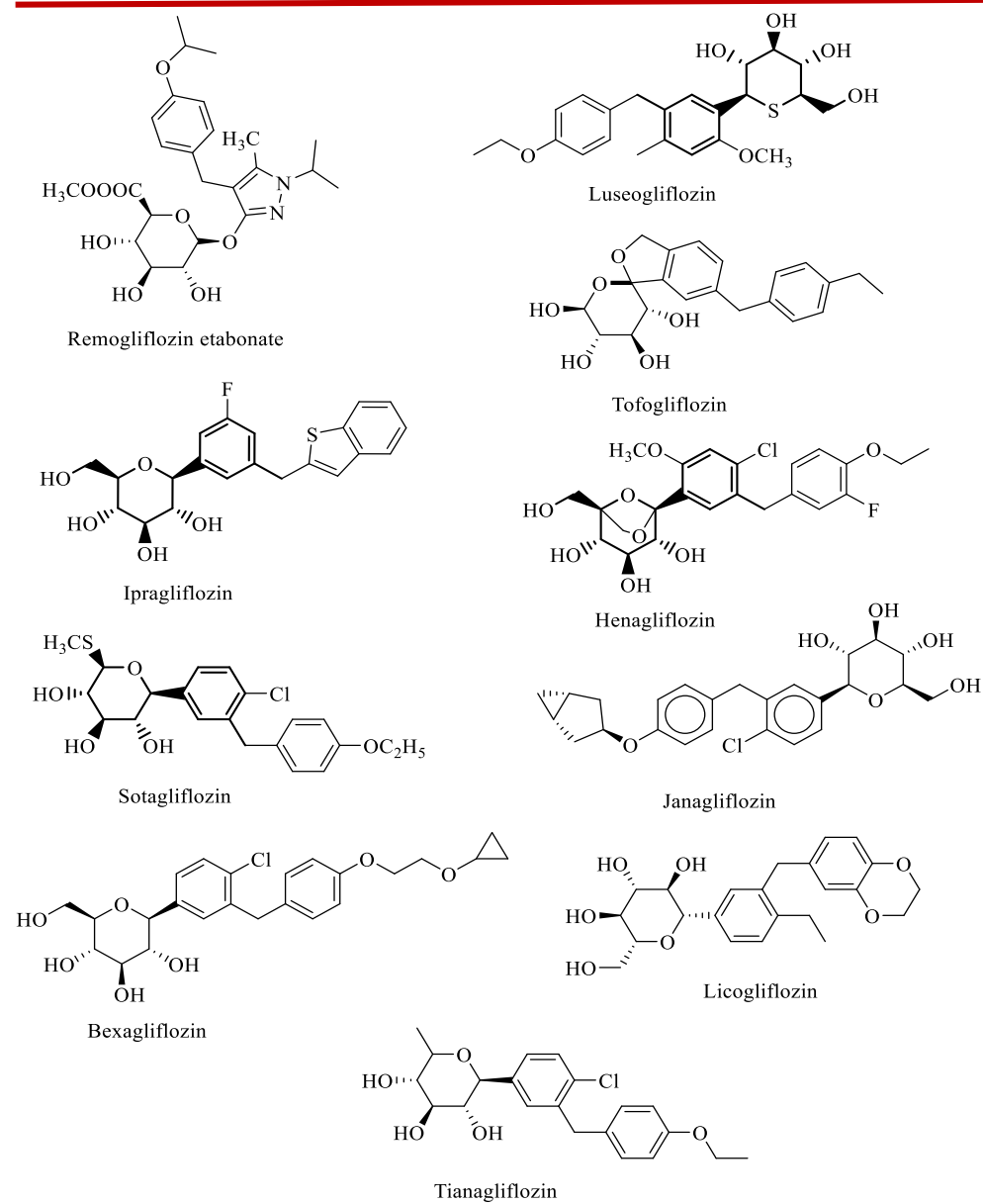


**Figure 6:** Non approved SGLT2 Inhibitors

## LITERATURE REVIEW

---

### 2.4.8 Janagliflozin

Janagliflozin is an orally effective inhibitor of SGLT2 that Xuanzhu Pharma Co., Ltd and Sihuan Pharma Co., Ltd have created and patented worldwide. In China, Janagliflozin is currently undergoing Phase 3 clinical trials for treating T2DM. Chemically, it is (2S,3R,4R,5S,6R)-2-(3-(4-(((1R,3s,5S)-bicyclo[3.1.0]hexan-3-yl)oxy)benzyl)-4-chlorophenyl)-6-(hydroxymethyl)tetrahydro-2H-pyran-3,4,5-triol. The IC<sub>50</sub> value of janagliflozin was found to be 0.51 μg/ml for hSGLT2 compared to hSGLT1.<sup>80</sup> As suggested, the ideal initial dose and a pharmacologically active dose of janagliflozin were 10 mg and 50 mg (**Figure 6**).

### 2.4.9 Tianagliflozin

Tianagliflozin, also known as 6-deoxy dapagliflozin, is currently in the first phase of clinical trials for the management of type II diabetes by the Tianjin Institute of Pharmaceutical Research (TIPR).<sup>81</sup> Chemically, it is (2S,3R,4S,5S)-2-(4-chloro-3-(4-ethoxybenzyl)phenyl)-6-methyltetrahydro-2H-pyran-3,4,5-triol. Tianagliflozin is created by removing the 6-hydroxyl moiety from the glucose moiety of dapagliflozin (**Figure 6**). It is more potent with an IC<sub>50</sub> = 0.67 nM against human SGLT2 versus the 1.1 nM IC<sub>50</sub> value of dapagliflozin. Tianagliflozin maintains a lower selectivity level of 823-fold than dapagliflozin against human SGLT2 compared to human SGLT1. Urinary glucose excretion (UGE) for tianagliflozin at doses of 1, 5, and 10 mg/kg was higher (513, 1108, and 1599 mg/kg) than for dapagliflozin at equivalent doses. There was statistical significance at 5 and 10 mg/kg, implying that tianagliflozin would potentially induce even more urinary glucose excretion than dapagliflozin at those doses.

### 2.4.10 Licogliflozin

Licogliflozin (LIK066), currently being studied, is a type of inhibitor that affects both SGLT1 and SGLT2, making it a dual inhibitor and was developed by Novartis Pharmaceuticals (**Figure 6**).<sup>82</sup> It is (2S,3R,4R,5S,6R)-2-{3-[(2,3-dihydro-1,4-benzodioxin-6-yl)methyl]-4-ethylphenyl}-6(hydroxyl methyl) oxane-3,4,5-triol. The IC<sub>50</sub> value of licogliflozin was found to be 20.6 nM against hSGLT1 and 0.58 nM against hSGLT2 with > 30 fold selectivity for SGLT2. In phase IIa clinical studies of

## LITERATURE REVIEW

---

12 weeks' duration, glycemic control was found to be boosted by 50 mg of licogliflozin once a day. Glycaemic findings such as a drop in HbA1c (0.58 %), reduced body weight (-2.15), and systolic BP (-9.5 mm Hg) and diastolic BP (-4.45) were predicted and compared to empagliflozin and placebo. Further studies on Licogliflozin for type-2 diabetes mellitus were prematurely terminated due to weak enrolment.

### 2.5 Advancement in profile of SGLT2 inhibitors

#### 2.5.1 Glucose glucosides

##### 2.5.1.1 Benzofuran Analogues

**B. Lv *et al.* (2009)** developed a new series of *O*-spiroketal C-aryl glucosides and assessed for activity against (hSGLT 1 and 2) using cell-based assays.<sup>83</sup> The fundamental spiro(isobenzofuran-1,2-pyran) skeleton has proven to be a key framework for modification (**Figure 7**). Compound **1** had the IC<sub>50</sub> value for human SGLT2 was 3.8 nM, and a selectivity of 184 times that of human SGLT1. Single oral dosing at 1.0 mg/kg to typical SD Rats caused a glucose loss of 1220 mg/200 g body weight for 24 hours that appeared to be approximate ~ 120 times greater than vehicle controls.

**B. Xu *et al.* (2009)** identified 6'-*O*-spiro C-aryl glucoside showed great potential as a lead compound due to its strong ability to inhibit hSGLT2, with an IC<sub>50</sub> = 71 nM.<sup>84</sup> Compound **2** exhibited 10-fold higher inhibitory activity against hSGLT2 with an IC<sub>50</sub> = 6.6 nM, which is similar to dapagliflozin's (6.7 nM) inhibitory activity. By introducing a chloro group at the 4' position of the neighboring phenyl ring, the activity was increased (**Figure 7**). However, despite its strong inhibitory activity on hSGLT2, for hSGLT-1, dapagliflozin demonstrated higher potency than 6'-*O*-spiro C-aryl glucoside.

##### 2.5.1.2 Indole-*O*-glucoside and benzimidazole-*O*-glucoside Analogues

**X. Zhang *et al.* (2005)** revealed a progression of benzo-intertwined heteroaryl-*O*-glucosides was developed and assessed for activity against (hSGLT 1 and 2) using cell-based assays.<sup>85</sup> Substitution of the ketone/phenol part of (T-1095A) with a benzo-fused heterocycle while persisting SGLT2 inhibitory action (**Figure 8**). Benzimidazole-*O*-

## LITERATURE REVIEW

---

glucoside **3** and indole-O-glucoside **4** were shown strong SGLT2 *in vitro* inhibitory action with IC<sub>50</sub> of 3.9 nM and 2.4 nM.

### 2.5.1.3 Benzodioxane Analogues

**J. Dudash *et al.* (2004)** incorporated a set of glucose conjugates and tested them for SGLT-1 and SGLT2 inhibition.<sup>86</sup> Compound T-1095 gave the core structure of these glucose conjugates (**Figure 8**). Changes in benzofuran moiety and 4'-phenyl ring replacement in T-1095 compound increased selectivity at SGLT2. Benzodioxane analog **5** has shown the best results with IC<sub>50</sub> = 10 nM against hSGLT2 and 162-overlay selectivity for SGLT2 over SGLT-1. Compound **5** was assessed to actuate urinary glucose discharge in male Zucker Diabetic Fatty (ZDF) rodents. At the point when a 3mg/kg dose was administered intravenously, compound **5** actuated discharge of 608 mg of glucose in the urine and had inhibitory action on SGLT2 *in vivo*.

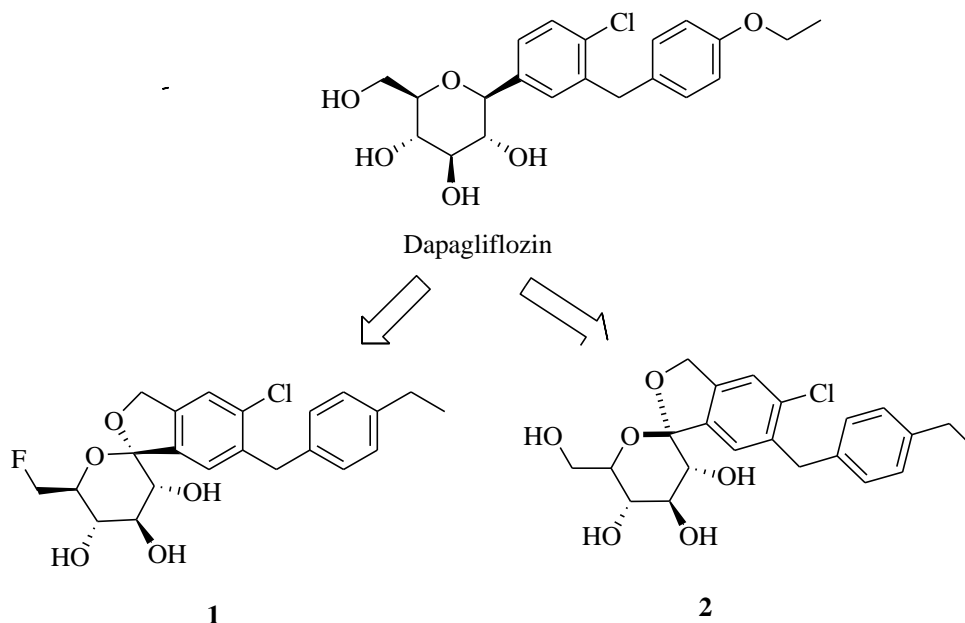


**Figure 7:** Design of O-spiroketal & 6'-O-spiro C-aryl glucosides SGLT2 inhibitors.

### 2.5.1.4 Thiophene/Thiazole Analogs

**S. H. Lee *et al* (2011)** revealed a set of new SGLT2 inhibitors made from thiophene C-aryl glucoside. To establish novel SGLT2 targeting antidiabetic agents, C-glucosides carrying thiophene rings at the proximal ring were utilized.<sup>86</sup> Opting to replace the

## LITERATURE REVIEW

---

proximal ring of dapagliflozin with a phenyl ring could be a favorable strategy for altering the compound's physicochemical characteristics, perhaps to improve biological action (**Figure 9A**). Among the analogs, compound **6** bearing ethylphenyl at the distal ring demonstrated *in vitro* SGLT2 inhibitory action with an  $IC_{50} = 4.47$  nM. Novel inhibitors of the thiazole motif C-aryl glucoside SGLT2 have been developed, synthesized, and biologically assessed (**Figure 9B**) by **Song K.S. et al.**<sup>87</sup> The best SGLT2 *in vitro* inhibitory effect was shown ( $IC_{50} \geq 0.772$  nM) for thiophenyl compound **7** and ( $IC_{50} = 0.720$  nM) for furanyl compound **8**.

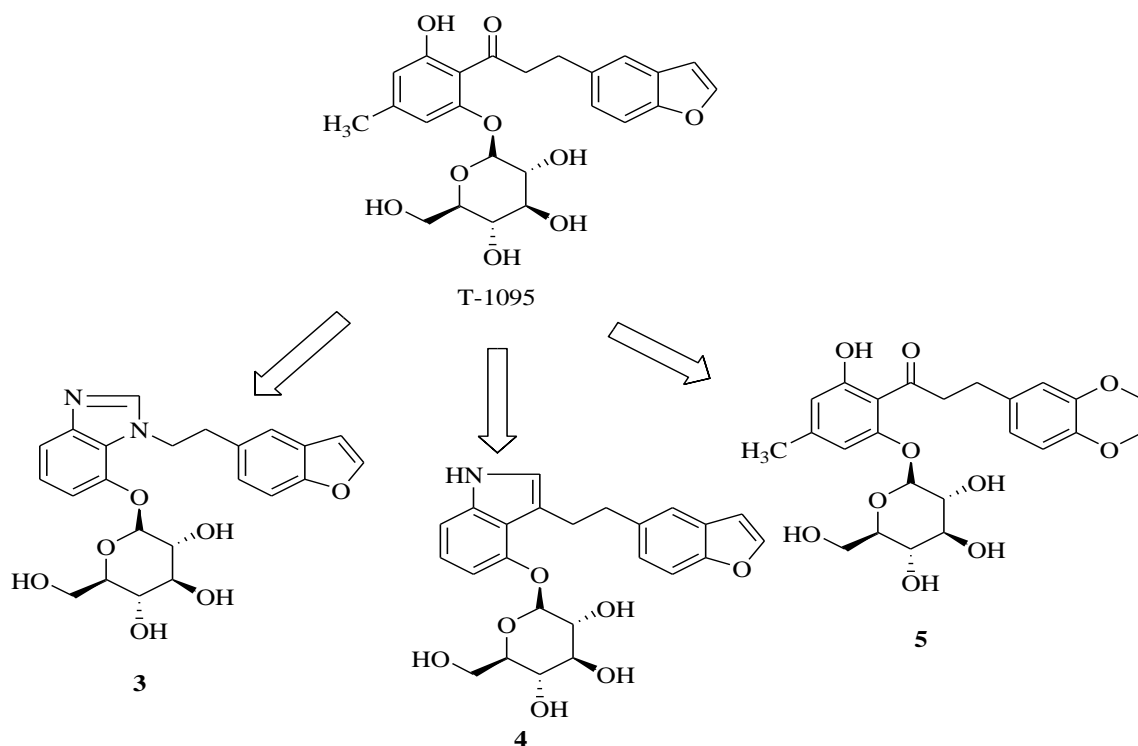


**Figure 8:** Design of benzimidazole-O-glucoside, indole-O-glucoside and benzodioxane-O-glucoside SGLT2 inhibitor.

**E.J. Park et al. (2011)** revealed C-glucosides having a heterocyclic ring were improvised to establish peculiar SGLT2 focusing on anti-diabetic activity by evacuating the -OH group at the C-6 position of compound **8** with methyl moiety.<sup>88</sup> A sequences

## LITERATURE REVIEW

---

of chemical glucose modifications were shown to discover their probable effectiveness as an appropriate glucose replacement per se (**Figure 9B**). Among the analogs, compound **9** had the outstanding SGLT2 *in vitro* inhibitory effect with an IC<sub>50</sub> of 7.01 nM.

### 2.5.1.5 Benzisothiazole and Indolizine Derivatives

H. Zhou *et al.* (2010) disclosed the advancement of benzisothiazole and indolizine-β-D-glucopyranoside (**Figure 10A**) as hSGLT2 inhibitors.<sup>89</sup> The compound **10**, which is a C-glucoside of benzisothiazole, exhibited an IC<sub>50</sub> value of 10 nM as an inhibitor of SGLT2.

### 2.5.1.6 Indole Derivatives

Chu *et al.* (2016) produced N-indolyl-glycoside as SGLT2 inhibitors by reforming the C-6 position on the sugar moiety, and studied the effects of SGLT2 inhibition (**Figure 10B**).<sup>90</sup> These derivatives were synthesized *via* modifying N-indolylglycoside as the fundamental scaffold with 6-amide/triazole/urea/thiourea and examining the SAR which resulted in the 6-amide derivatives **11** and **12** as potent compounds. Compounds **11** and **12** with an EC<sub>50</sub> value i.e. 42nM and 39 nM against hSGLT2.



## LITERATURE REVIEW

---

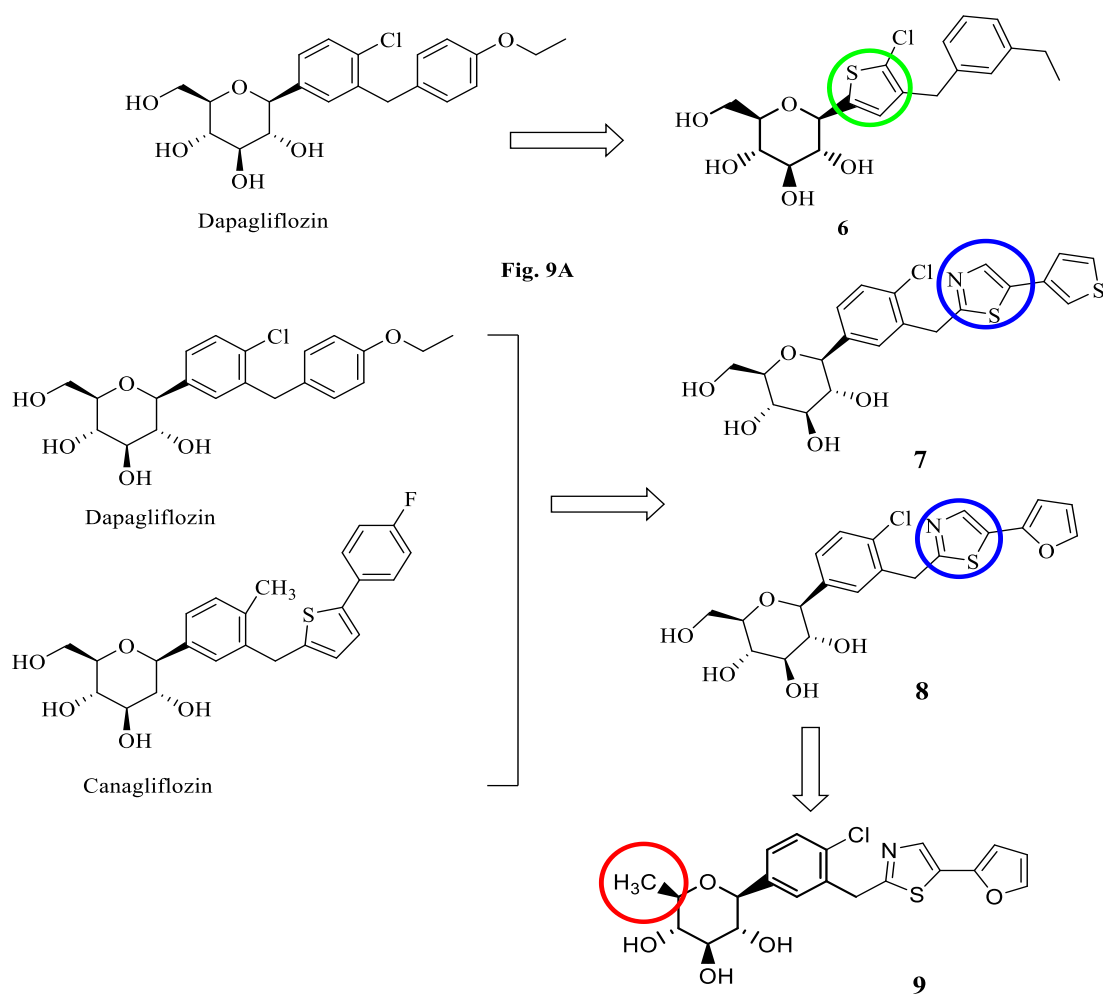
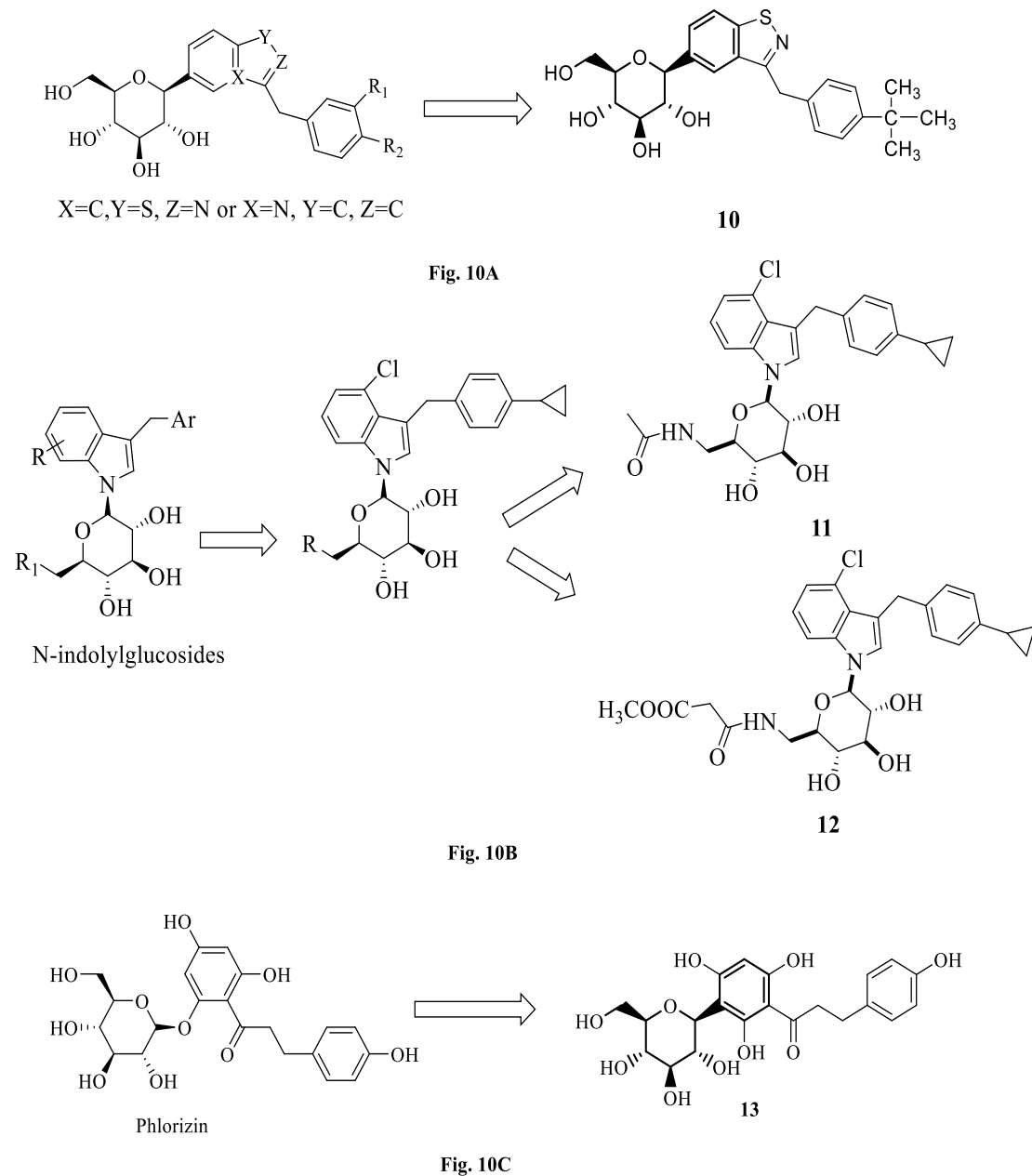


Fig. 9A

Fig. 9B

**Figure 9.** Exploration of C-glycoside bearing thiophene at the proximal ring (9A). Exploration of C-glycoside (7 & 8) and (9) incorporating a thiazole at the distal ring. (9B).

## LITERATURE REVIEW



**Figure 10.** Design of benzisothiazole and indolizine- $\beta$ -D-glucopyranoside as SGLT2 inhibitors (10A). Design of novel *N*-indolylglycosides with C6-modification on the glucose moiety (10B). Design of C-glucosyl dihydrochalcone SGLT2 inhibitor (10C).

## LITERATURE REVIEW

---

### 2.5.1.7 Chalcone Derivatives

J Ana R. and associates (2017) synthesized and assessed a range of C-glucosyl dihydrochalcones, along with their chalcone precursors as SGLT1/SGLT2 inhibitors.<sup>91</sup> In green rooibos (*Aspalathus linearis*) extracts, Nothofagin, (compound **13**) with an  $IC_{50}$  = 11.9 nM was the most intense and dynamic C-glucosyl dihydrochalcones against SGLT2 (**Figure 10C**). The results of a computer docking analysis based on an SGLT2 homology model showed a 40-fold decline in SGLT1 action and almost 6-fold surge in SGLT2 action.

### 2.5.1.8 Isoquinoline Derivatives

In 2016, tetrahydroisoquinoline-C-aryl glycosides were produced by X. Pan *et al.* through changes in the proximal dapagliflozin ring to the tetrahydroisoquinoline ring (**Figure 11A**) and evaluated them as the SGLT2 inhibitor.<sup>92</sup> Out of these synthesized compounds, compound **14** contains a naphthalene moiety at 1-position and a Cl-moiety at 4'-position displayed the strongest SGLT2 inhibition action (81.7%), which was slightly comparable to dapagliflozin (85.4%).

### 2.5.1.9 Pyridine Derivatives

In 2013, the consequences of substituting the phenyl ring of canagliflozin for heteroaromatics were investigated and evaluated by Koga *et al.*<sup>93</sup> Among those derivatives that have been substituted with 3-pyridyl, 2-pyrimidyl, and 5-member heteroaryl indicated very strong inhibition activities towards SGLT2 (**Figure 11B**) and a slightly reduced activation with 5-pyrimidyl substitution. The UGE was caused by 2666 mg/200 g body weight when compound **15** was administered orally SD rats over a period of 24 hours. The  $IC_{50}$  value of compound **15** for hSGLT1 was 750 nM and hSGLT2 was 2.0 nM in CHOK cells.

## LITERATURE REVIEW

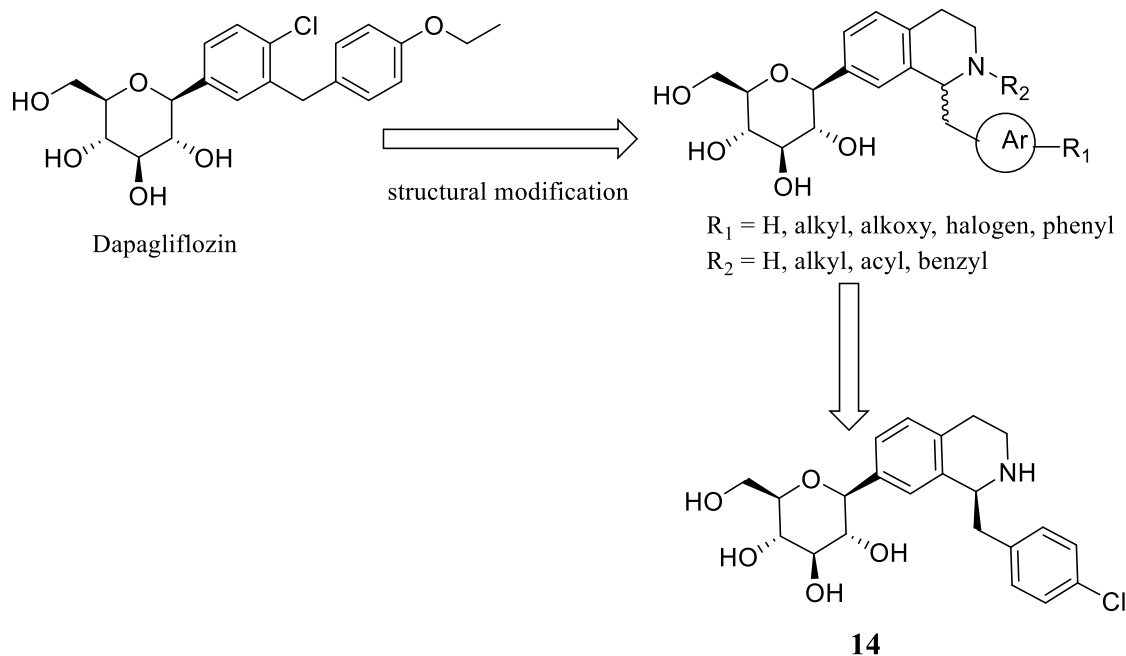


Fig. 11A

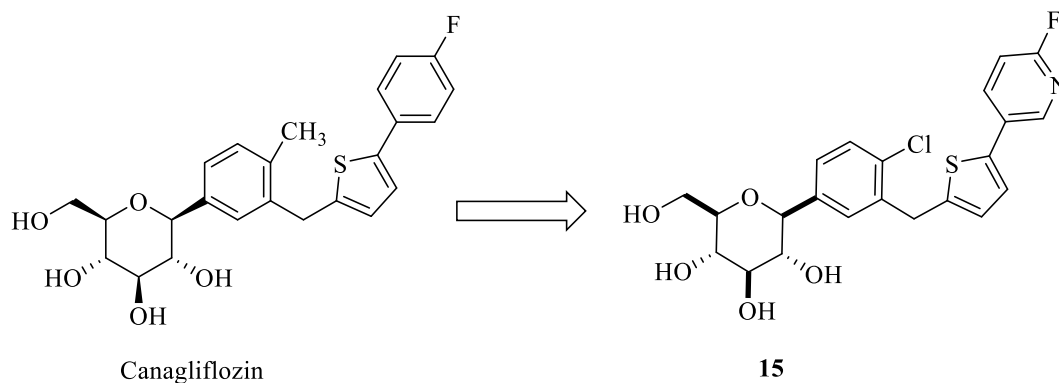


Fig. 11B

**Figure 11.** Design of novel tetrahydroisoquinoline-C-aryl glucoside SGLT2 inhibitor (11A). C-glycoside with pyridine ring as SGLT2 inhibitor (11B).

### 2.5.1.10 Benzyltriazolopyridinone and Phenylhydantoin Derivatives

Guo *et al.* (2014) shows the development, synthesis, and SAR of benzyltriazolopyridinone and phenyl hydantoin for C-glycosides, which were discovered to be novel aglycone moieties for SGLT2 inhibitors (Figure 12A).<sup>94</sup> Out of the benzyltriazolopyridinone arrangement, compound 16 not only indicate high

## LITERATURE REVIEW

---

inhibitory action toward SGLT2, but it also displayed extremely high selectivity over SGLT-1 with  $IC_{50} = 33$  nM and confirmed excellent metabolic stability in a liver microsomal assay. The Phenylhydantoin series showed robust metabolic endurance of the liver microsomas and reduced blocking of CYP P450 function ( $IC_{50} = 10.9$  nM), with compound **17**.

### 2.5.1.11 Biphenyl Derivatives

**Y. Ding *et al.* (2015)** developed and produced a sequence of C-aryl glucosides with a biphenyl moiety (**Figure 12B**) for evaluation as SGLT2 inhibitors.<sup>95</sup> Out of the screened substances, compound **18** showcased the most formidable SGLT2 inhibition, boasting an  $IC_{50}$  value = 1.9 nM. At a dosage of 3 mg/kg, the urinary glucose discharge of compound **18** and canagliflozin was found to be 180 mg and 200 mg, respectively, when compared to the control vehicle. Rodents treated with a single oral dose of 5.0 mg/kg of compound **18** displayed a decrease in plasma glucose levels.

In 2017, a compound (**HSK0935**) was found by **Yao Li and colleagues** with a remarkable 1.3 nM hindrance and a high 843 overlap in the hSGLT2 selectivity.<sup>96</sup> Among Sprague-Dawley (SD) rats, it has been shown to have strong urinary glucose excretion and has affected further rhesus monkeys. HSK0935 is derived from the hybrid of ertugliflozin and sotagliflozin (**Figure 13A**).

### 2.5.1.12 Oxime Analogues

**M.C. Yuan *et al.* (2018)** discovered an aryl C-glycoside having C = N/C–N at the C-6 glucose site, resulting in the discovery of oxime compound **19** (**Figure 13B**) as a promising SGLT2 inhibitor.<sup>97</sup> Compound **19** indicated high hSGLT2 inhibitory activity with an  $EC_{50}$  value = 46 nM. Besides, *in vivo* experiments in healthy SD rats reveal that compound **19** (0.1 or 10 mg/kg) could cause glucosuria and lower plasma levels of glucose (> 450 mg/dL) in STZ-induced rats to a comparable level.

## LITERATURE REVIEW

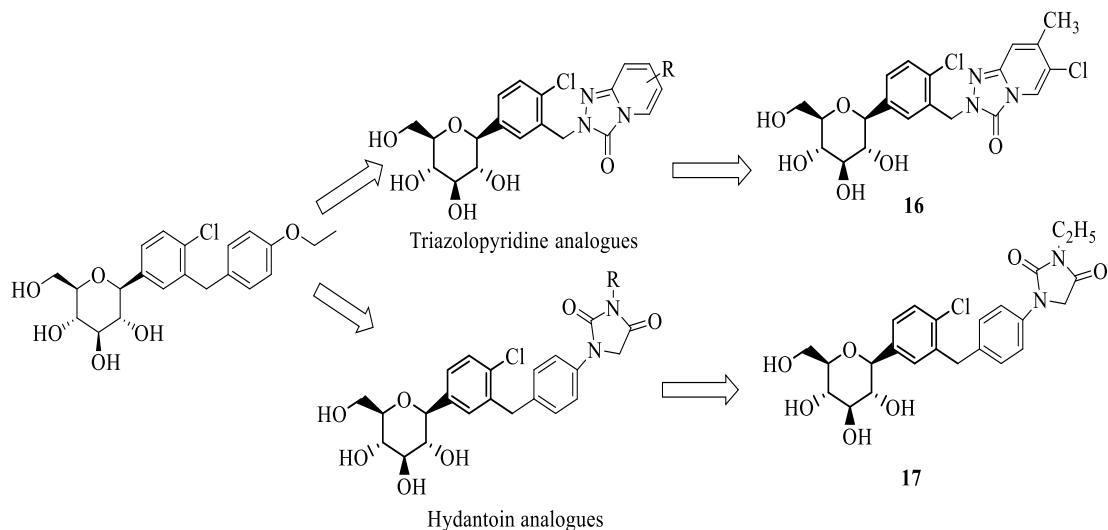


Fig. 12 A

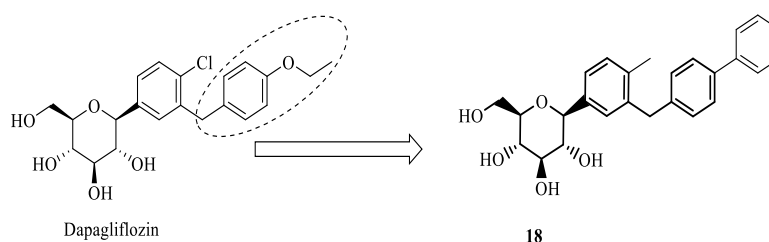


Fig. 12 B

**Figure 12.** Benzyltriazolopyridinone and Phenylhydantoin SGLT2 inhibitors (12A).

Design of biphenyl motif-containing C-arylglucoside SGLT2 inhibitors (12 B).

### 2.5.1.13 Benzocyclobutane Analogues

**In 2018, Kuo and colleagues** synthesized and assessed a range of benzocyclobutane C-glucosides for their efficacy as dual inhibitors of SGLT1/SGLT2 that can be administered orally (**Figure 13C**).<sup>98</sup> Compound **20** has a substantial  $IC_{50}$  for SGLT1 and SGLT2 inhibition, or 45 nM and 1 nM, respectively. It exhibited outstanding PK (pharmacokinetic) profiles (with bioavailability ranging from 78% to 107%) across multiple animal models, including mice, rats, dogs, and monkeys. In SD rats, compound **20** considerably decreased dose-dependent plasma glucose rates. In ZDF rats, compound **20** showed anti-hyperglycemic benefit up to 24 h.

## LITERATURE REVIEW

---

### 2.5.1.14 Benzyl Analogues

**Mukkamala *et al.* (2020)** developed previously undisclosed novel dapagliflozin aglycon based C-benzyl glucoside derivatives.<sup>99</sup> Modifications to the distal ring of the biarylmethane aglycon utilizing Weinreb-amide (WA) functionality could provide access to additional analogs. The nonradioactive fluorescence glucose uptake assay was implemented to evaluate all novel compounds for their effectiveness in inhibiting SGLT1 and SGLT2. Among the investigated compounds, Compound **21** exhibited the highest inhibitory activity against both SGLT2 and SGLT1, with IC<sub>50</sub> values = 0.64 nM and 500 nM. This inhibitory activity was compared to that of dapagliflozin (**Figure 14C**).

### 2.5.1.15 Design and Exploration of 6-Deoxy O-Spiroketal Analogues

In 2019, novel 6-deoxy O-spiroketal C-arylglucosides have been developed and evaluated as SGLT2 inhibitors by **Wang *et al.***<sup>100</sup> The SAR investigation conducted on biological studies suggested that the alteration of fluoro and methyl moieties are necessary for the efficient SGLT2 inhibition. Compound **22** bearing methyl group shows excellent hSGLT2 inhibitory activity i.e. IC<sub>50</sub> = 4.5 nM in comparison to tofogliflozin with IC<sub>50</sub> value of 2.5nM (**Figure 14B**).

## LITERATURE REVIEW

---

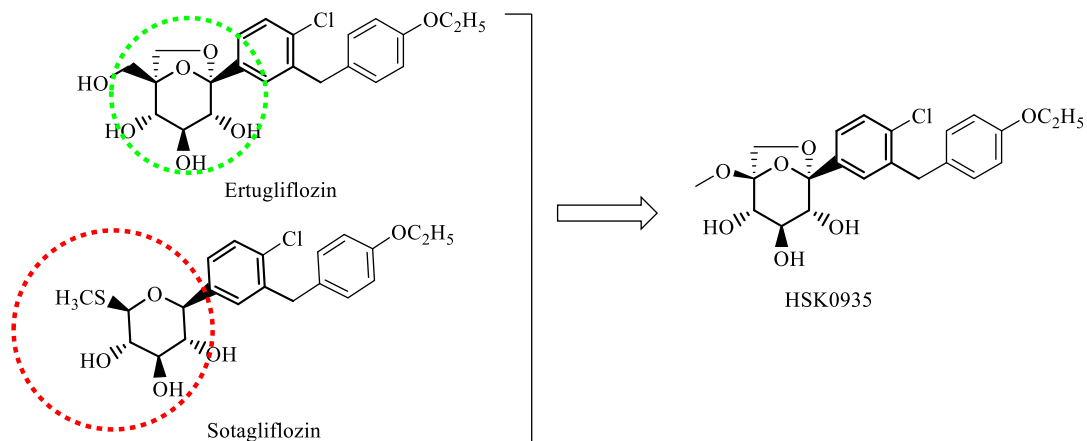


Fig. 13 A

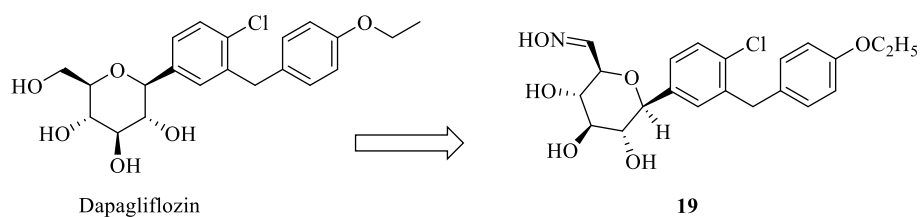


Fig. 13 B

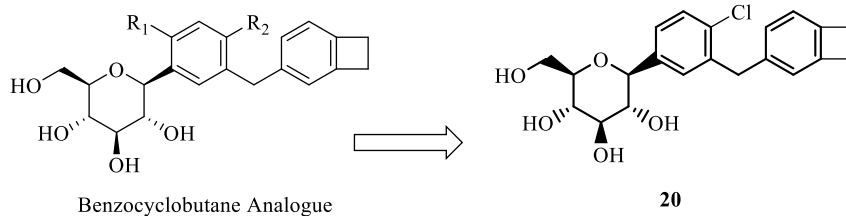
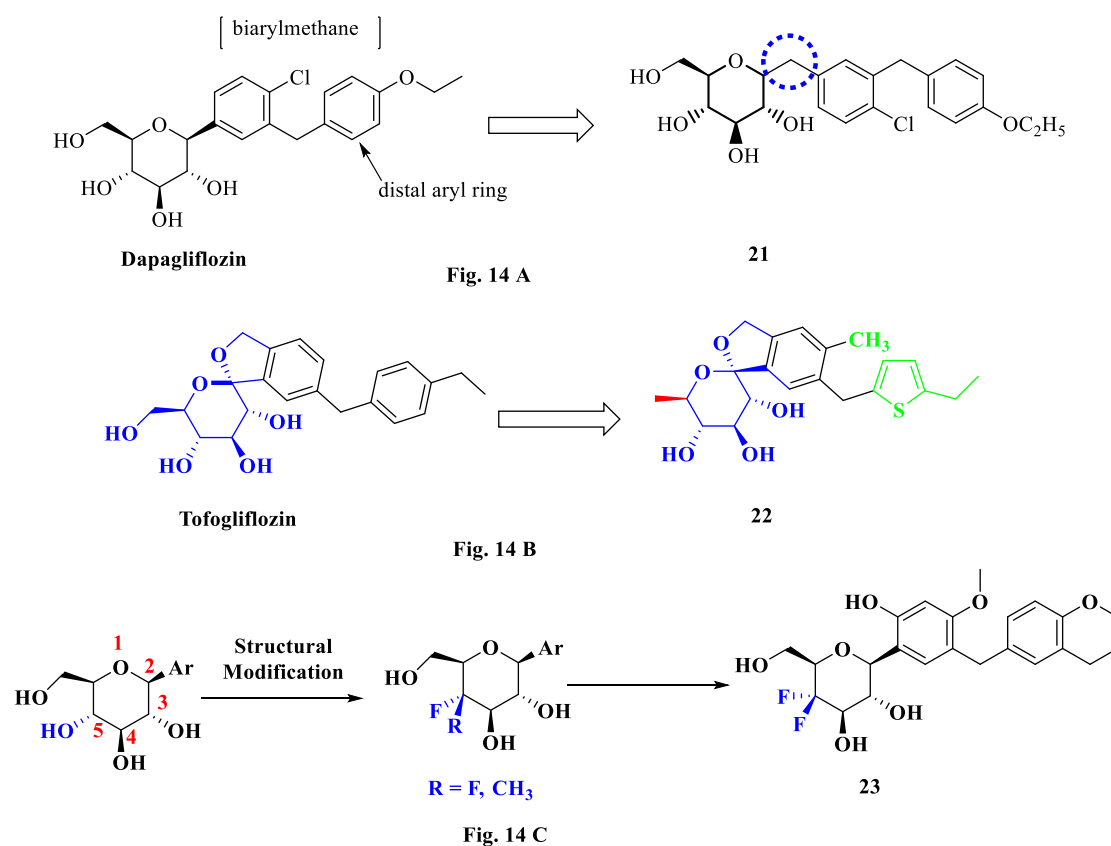


Fig. 13 C

**Figure 13.** The hybrid design involves the creation of novel dioxabicyclo(3.2.1)octane derivatives. (13A). Design of oxime-containing C-glycosylarene SGLT2 inhibitor (13B). Design of Benzocyclobutane-C-glycosides (13C).



## LITERATURE REVIEW



**Figure 14.** Design of C-benzyl glucosides as SGLT2 inhibitors (14 A). Designing 6-Deoxy O-Spiroketal C-Arylglucosides (14 B). Designing C-Aryl Glucosides with 5-Fluoro-5-methyl-hexose Structure (14 C).

### 2.5.1.16 Exploration and Design of Analogues with 5-Fluoro-5-methyl-hexose Structure

Novel C-aryl glucosides, which act as dual inhibitors of SGLT1/SGLT2 and contain a 5-fluoro-5-methyl-hexose and 5, 5-Difluoro-hexose, was created and assessed by **Xu and colleagues** in 2020.<sup>101</sup>

Compound **23**, which is a 5,5-di-fluoro-aryl glucoside, demonstrated remarkable inhibitory effects on SGLT1 and SGLT2, with  $IC_{50}$  values of 96 nM and 1.3 nM, respectively, among the tested compounds. Compound **23**, when administered orally to SD rats at doses of 1 mg/kg and 10 mg/kg, inhibited blood glucose surge significantly in an OGTT (**Figure 14C**).

## LITERATURE REVIEW

---

### 2.5.2 Fructose glucosides

**Lin et al. (2013)** Novel C-aryl-D-glucofuranosides have been developed and assessed for inhibitory action on hSGLT2 and hSGLT1.<sup>102</sup> SAR experiments related to the aromatic ring replacement of different groups and their effect on SGLT inhibition have been performed (**Figure 15A**). Among the compounds evaluated, compound **24**, exhibited the strongest *in vitro* SGLT2 inhibitory action,  $EC_{50} = 0.62 \mu\text{M}$  and a 47-fold overlap selectivity against SGLT1.

### 2.5.3 Xylose glycosides

**Yao et al. (2012)** discovered a new class of SGLT2 inhibitors based on C connected indolyl xyloside.<sup>103</sup> C-indolyl xylosides were found to be stronger inhibitors of hSGLT2 than their recently discovered N-indolylxylosides. Compound **25** is the most active SGLT2 inhibitor of C-indolyl xylosides, with an  $EC_{50}$  of 47 nM. The distal p-cyclopropylphenyl and 7th position substituents of the indole motif were needed for optimal SGLT2 inhibitory activity, according to SAR studies (**Figure 15B**). Regardless of the fact that D-xyloside is coupled with 1- or 3-substituted indoles, none of the synthesized compounds demonstrated noteworthy selectivity toward hSGLT2 when compared to hSGLT-1.

**Goodwin et al. (2009)** announced the discovery of a novel SGLT2 inhibitors class that specifically target L-xylose (**Figure 16A**).<sup>104</sup> O-xyloside (compound **26**) indicated excellent inhibitory activity against SGLT2 with an  $IC_{50} = 14 \text{ nM}$  and a 134 fold selectivity for SGLT2, corresponding to the 169-fold selectivity observed for dapagliflozin. The single-dose ingestion of 75mg/kg Compound **26** by oral gavage or in the form of a diet admixture led to persisting glucosuria for 24 hours. The extended pharmacodynamic influence indicates that continuous administration would be adequate to administer once a day.

The research on N-glycosides as SGLT2 inhibitors, in which D-xylose was used as the sugar unit instead of D-glucose and the aglycone was a 3-substituted indole, was initiated by **Yao et al.** in 2011<sup>105</sup> that has been synthesized and evaluated in a SGLT2 inhibitory activity assay for (**Figure 16B**). One of the best compounds was the

## LITERATURE REVIEW

---

compound **27** with an  $EC_{50}$  of 161 nM when compared with phlorizin (108 nM). In Sprague-Dawley rats, compound **27** reported an increase in urinary glucose discharge from 12 to 783 fold when given orally.

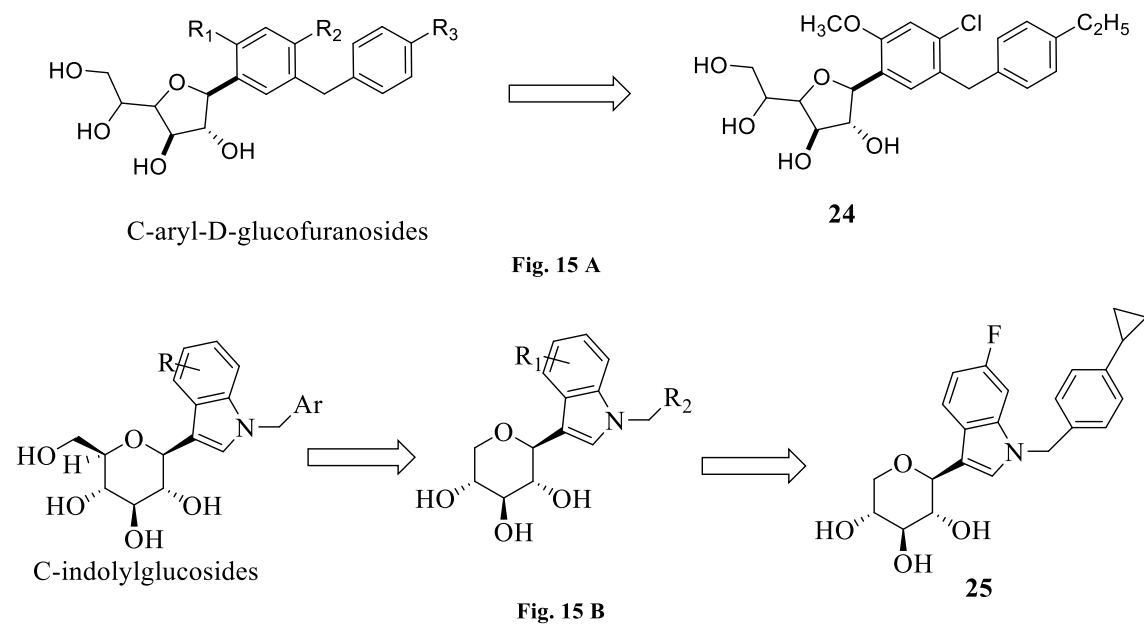


**Figure 15.** Design of novel C-aryl D-glucofuranoside SGLT2 inhibitor (15A). Design of C-indolylxyloside SGLT2 inhibitors (15B).

## LITERATURE REVIEW

---

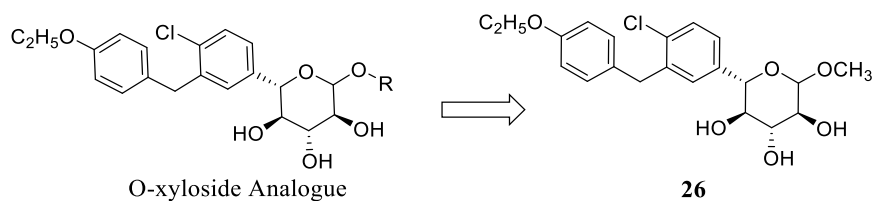


Fig. 16A

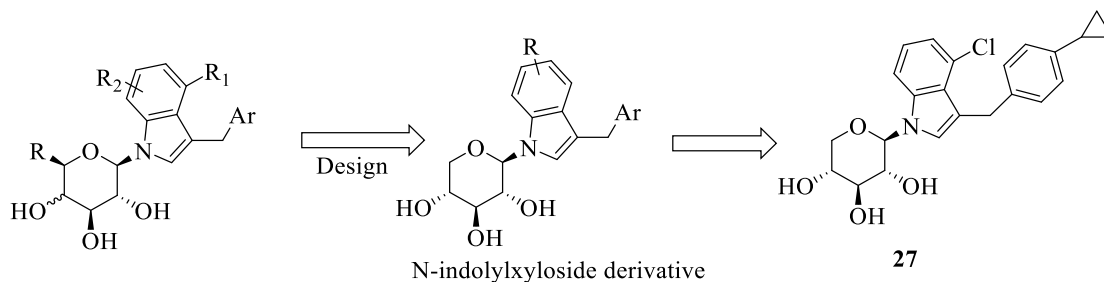


Fig. 16B

**Figure 16.** Design of novel O-xyloside SGLT2 inhibitors (16A). Design of N-indolylyxoside SGLT2 inhibitors (16B).

### 2.5.4 Non-glucosidal Analogues

#### 2.5.4.1 Exploration of Benzothiazinone and benzoxazinone Analogues

**A.-R. Li *et al.* (2011)** identified a variety of novel non-glucoside benzothiazinone and benzoxazinone compounds as SGLT2 inhibitors with outstanding potency and SGLT2 selectivity.<sup>106</sup> N-substituents of triazole and 6-chloro, 8-chloro, 6, 8-dichloro substituents of benzoxazinone compounds were synthesized and evaluated. 6, 8-dichlorosubstituted compounds **28** and **29** and have shown the best results, IC<sub>50</sub> values = 0.009  $\mu$ M & 0.010  $\mu$ M against hSGLT2 and exhibited a SGLT2 selectivity that was greater than 1000 times that of SGLT-1 and SGLT6, rendering them superior to dapagliflozin (**Figure 17A**).

## LITERATURE REVIEW

---

### 2.5.4.2 Triazole Analogues

In their study, **Du et al. (2011)** improved a group of triazole derivatives that featured an aromatic tail and a benzoxazinone ring at the head, and then assessed their inhibitory activity in an SGLT2 assay.<sup>107</sup> Incorporating polar groups into several triazole derivatives led to the creation of compound **30**, which exhibited a substantial increase in solubility (64  $\mu\text{g/mL}$ ) while sustaining an effective inhibition of 12 nM and compound **31** shows outstanding *in vitro* inhibitory activity with  $\text{IC}_{50} = 5$  nM against hSGLT2 (**Figure 17B**).

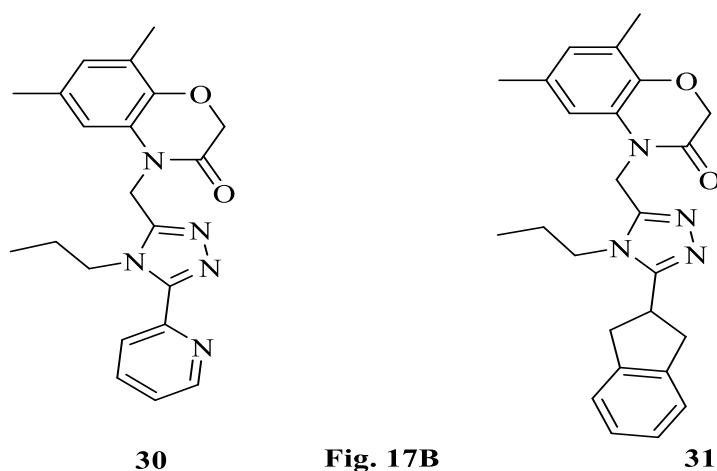
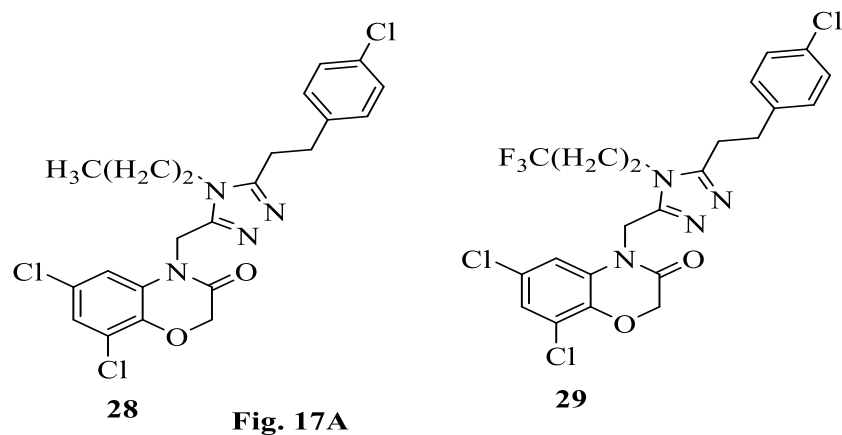


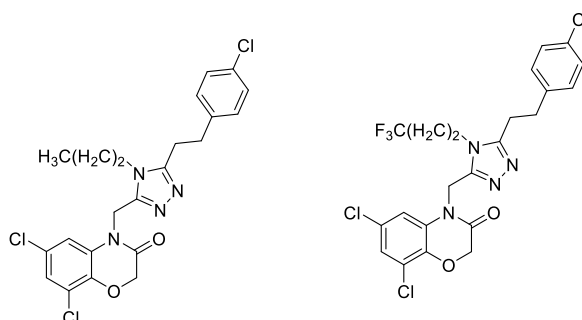
**Figure 17.** Design of novel non-glucoside triazole benzothiazinone and benzoxazinone compounds (17A) and (17B).

# *CHAPTER 3*

## RATIONALE, AIM AND OBJECTIVES

---

**Recent literature Work on Non-glucoside thiazole derivatives as SGLT2 inhibitors:** From a literature survey conducted by **A.-R. Li *et al.***, it was found that no previous work has been reported on the non-glucoside thiazole derivatives synthesized in this research project. The majority of SGLT2 inhibitors explored in the literature are glycosidal, which are difficult to synthesize due to their bulky nature. However, **A.-R. Li *et al.*** identified a variety of novel non-glucoside benzothiazinone and benzoxazinone triazole compounds as SGLT2 inhibitors with exceptional potency and SGLT2 selectivity. They synthesized and evaluated N-substituents of triazole and 6-chloro, 8-chloro, 6, 8-dichloro substituents of benzoxazinone compounds, and found that compounds with 6,8-dichloro substituents exhibited the best results with  $IC_{50}$  values = 0.009  $\mu$ M & 0.010  $\mu$ M against hSGLT2, and exhibited a SGLT2 selectivity that was greater than 1000 times that of SGLT1 and SGLT6, making them superior to dapagliflozin.



### Rationale for design of 1, 3, 4-thiadiazole derivatives:

In the presented research project, after taking the basic non-glucoside triazole scaffold into the consideration from literature. We have designed novel 1,3,4 thiadiazoles that have greater selectivity for hSGLT2 over hSGLT1 by modifying their substitution at different positions to obtain a more efficacious anti-diabetic drug than the standard drug dapagliflozin.

## RATIONALE, AIM AND OBJECTIVES

---

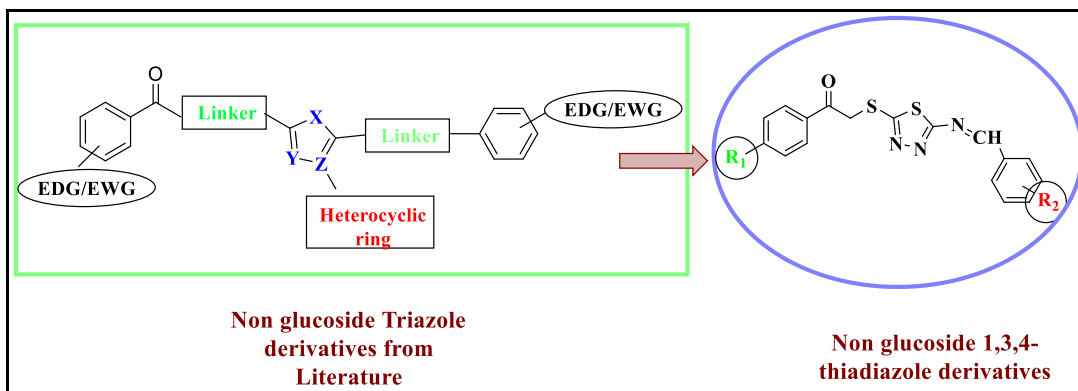


**Figure 18:** Designing of non-glucoside thiadiazole based scaffold as SGLT2 Inhibitors.

### **Aim and objectives of the proposed research work:**

The research project aimed to design, synthesize and evaluate SGLT2 inhibitors. To achieve this aim following objectives have been proposed:

1. Design of novel substituted 1, 3, 4-thiadiazole derivatives
2. *In silico* studies using Molecular docking approaches.
3. Synthesis and characterization of substituted 1, 3, 4-thiadiazole derivatives.
4. *In vitro* evaluation of synthesized molecules.
5. *In vivo* evaluation of synthesized molecules.



# *CHAPTER 4*

## WORK PLAN AND HYPOTHESIS

### 4.1 Structural Modification:

In order to create a new anti-diabetic agent using a non-glycoside heterocyclic moiety, it is important to understand the binding interactions between emerging drugs and SGLT2 receptors. A proposal for a pharmacophore of non-glycoside SGLT2 inhibitors has been put forth using a comprehensive review of the literature review. This proposal incorporates structural modifications illustrated in the **Figure 19** and research plan.

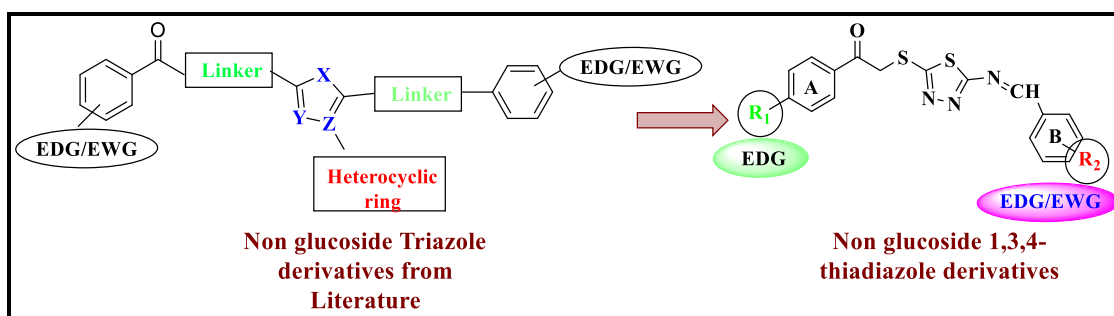
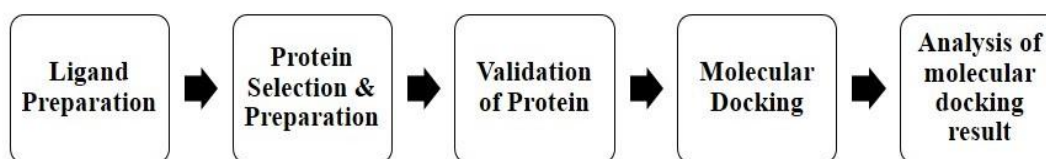


**Figure 19:** Pharmacophore of non-glycoside 1,3,4 thiadiazole derivatives as SGLT2 Inhibitors.

### 4.2 Molecular docking study:

The protein data bank was accessed to download the SGLT2 protein (PDB ID: 3DH4) that was chosen. The protein was subsequently loaded into Autodock Vina 1.5.6 software to separate it from the ligand. This software was employed to evaluate the ligand's affinity and enhance its effectiveness as the primary lead molecule for an SGLT2 inhibitor. The process involved the following steps:



**4.3 Synthesis and characterization of feasible & most potent compounds:** The reaction scheme was executed to synthesize the most potent and synthetically feasible compounds by modifying the R<sub>1</sub> position with electron releasing groups and R<sub>2</sub> position with electron donating/attracting groups to analyze the effects of different substituents on binding affinity energy and SGLT2 inhibitory activity. Characterization of synthesized compounds will be done by R<sub>f</sub> value, FTIR, <sup>1</sup>H NMR and <sup>13</sup>C NMR.

## WORK PLAN AND HYPOTHESIS

### Proposed Reaction scheme:

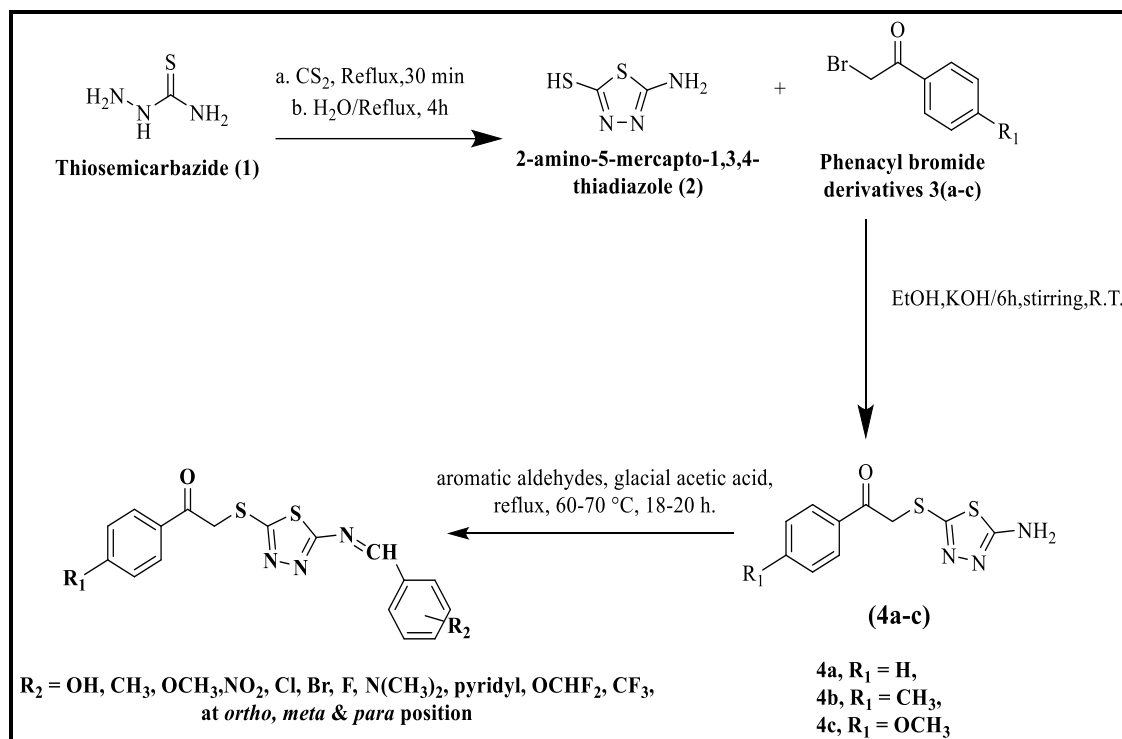


**Figure 20:** Reaction scheme depicting the synthesis of potent compounds.

#### 4.4 *In-Silico* prediction of ADMET studies of synthesized compounds

The synthesized compounds underwent toxicity assessment to examine potential risks, including carcinogenicity and mutagenicity, utilizing the Lazar toxicity predictor. Furthermore, the pharmacokinetics of the compounds was analyzed online, encompassing the computation of pharmacokinetic properties, drug-likeness, and physicochemical characteristics, with the assistance of SWISS ADME software.

#### 4.5 *In-vitro* evaluation of synthesized molecules by human SGLT2 inhibitory activity assay:

For *in vitro* investigations, the utilization of an hSGLT2 ELISA Kit is chosen for its heightened sensitivity and enhanced specificity in detecting Human SLC5A2 within Chinese Hamster Ovary (CHO) cells expressing hSGLT2 in a stable manner.<sup>72</sup>

## WORK PLAN AND HYPOTHESIS

---

### 4.6 *In-vivo* evaluation of Urinary Glucose Excretion & Streptozotocin-Induced Diabetes:

The goal of this research endeavor is to design an evaluation for non-glucoside thiadiazole derivatives that were synthesized as SGLT2 inhibitors. The evaluation will be performed by observing an increase in excreted glucose in urine and a decrease in PGL in a streptozotocin-induced Sprague-Dawley rat model.<sup>63, 105</sup>

### 4.7 HYPOTHESIS

This research work focuses on the design of novel 2-((5-(benzylideneamino)-1,3,4-thiadiazol-2-yl)thio)-1-phenylethan-1-one derivatives by incorporating the fundamental non-glucoside triazole scaffold described in the literature. The objective was to enhance the selectivity of these compounds for human sodium-glucose cotransporter 2 (hSGLT-2) while minimizing their affinity for human sodium-glucose cotransporter 1 (hSGLT-1). This was achieved by modifying the substitution patterns at various positions. The aim of this work was to develop an anti-diabetic drug with improved efficacy compared to the standard drug dapagliflozin. After taking into account the fundamental non-glucoside triazole scaffold from literature, we have designed novel 1, 3, 4 thiadiazole compounds by introducing the electron releasing groups i.e. methyl and methoxy, located at the para position of phenyl ring A designated as R<sub>1</sub>. Moreover, we have also substituted *ortho*, *meta* and *para* positions of the phenyl ring B next to imine bond designated as R<sub>2</sub> with various EDGs/EWGs viz methyl, methoxy, hydroxyl, nitro, chloro, bromo, fluoro, trifluoromethyl, dimethylamino, pyridyl, difluoromethoxy. On the basis of above facts we have designed 102 compounds Schiff base of 1, 3, 4 thiadiazole scaffold and performed docking studies to calculate binding affinity scores using AutoDock vina 1.5.6. On the basis of docking scores, compounds were selected for the synthesis and characterization. Synthesized compound underwent MTT assay to evaluate their cytotoxicity and further less cytotoxic compounds, SGLT2 enzyme inhibition assays were conducted using SLC5A2 ELISA kit assay. Compounds with higher SGLT-2 inhibitory activity further underwent *in-vivo* evaluation for assessing urinary glucose excretion and its anti-diabetic activity.

## WORK PLAN AND HYPOTHESIS

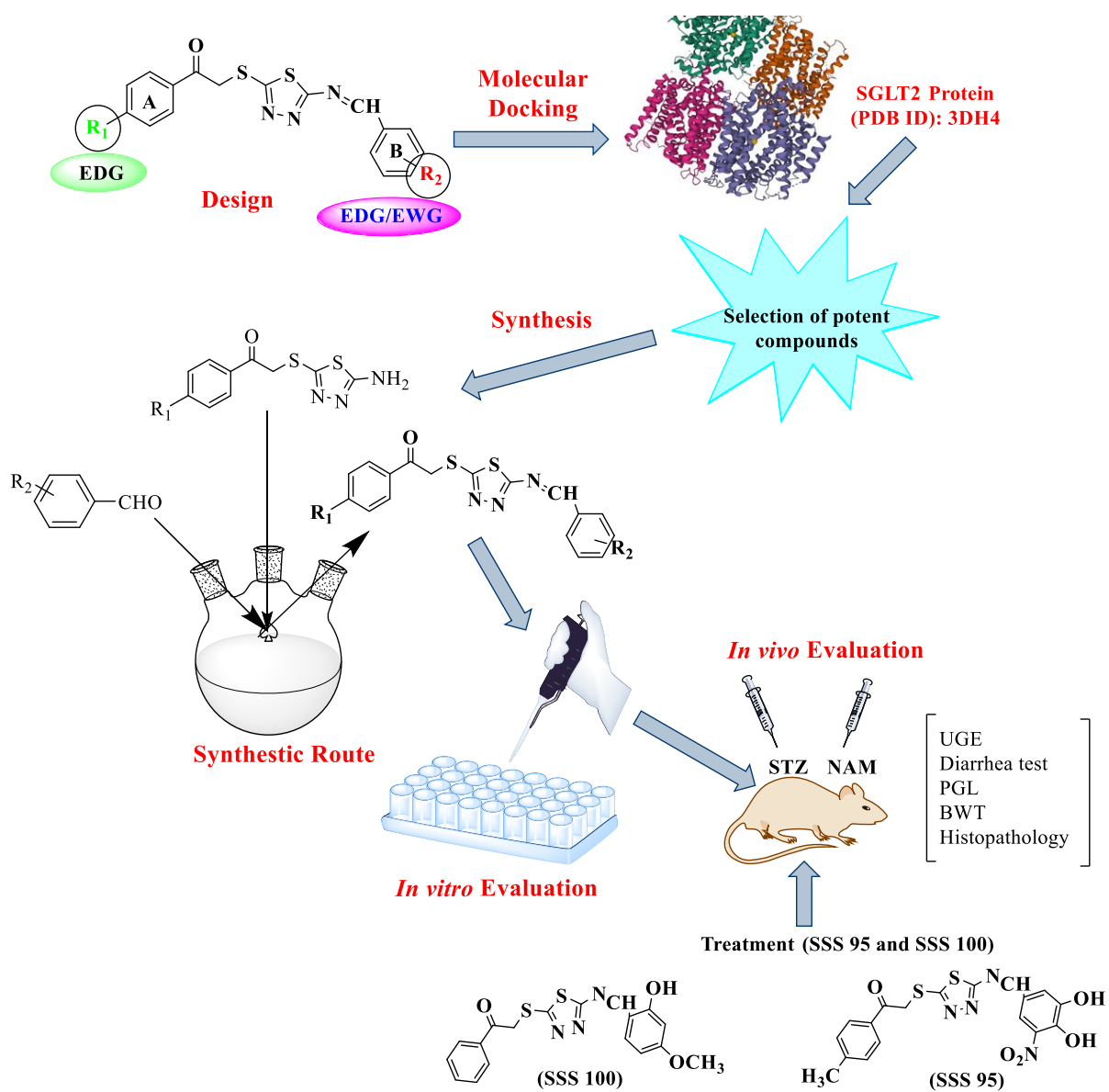


**Figure 21:** Research hypothesis for design, synthesis and evaluation of SGLT-2 inhibitors.

# *CHAPTER 5*

## MATERIAL, METHODS AND EXPERIMENTAL

---

### 5.1 Molecular Docking Studies

Molecular modelling is a well-researched tool for recognizing potent compounds without committing so much time and resources to research.<sup>108-110</sup> Auto Dock Device Vina 1.5.6 software was used to analyze the behaviour with respect to binding affinity (kcal/mol), and observations were evaluated for better docked conformation in the binding affinity ranking score. With the help of Chemdraw Ultra 16.0, newly designed 1, 3, 4 thiadiazole ligands were drawn and translated into a 3D structure using Chemdraw Ultra 3D. The Semiempirical MM2 system optimized the geometry of all designed ligands and saved to pdb files.<sup>111</sup> SGLT2 Protein (PDB ID: 3DH4) i.e. was collected and downloaded from the protein database to obtain the leading SGLT2 inhibitor.<sup>112</sup> The results of Auto Dock Vina (ADT) analysis included an evaluation of various interactions such as close contact, hydrogen bond, hydrophilic and hydrophobic interactions, as outcome measures.

#### 5.1.1 SGLT2 Protein Identification & Preparation

Once SGLT2 protein was identified, afterward, Autodock Vina is used to load the desired protein for extracting ligands. The software is employed to assess the performance of the ligand as a lead SGLT2 inhibitor and investigate its affinity

#### 5.1.2 Validation of Protein for Docking

The SGLT2 protein is validated by extracting and docking the co-crystallized ligand (gal 701) in the same manner as the actual ligand.<sup>113-115</sup> The method's validity was assessed by comparing redocked and crystallographic conformations, revealing an RMSD of less than 1 for the ligand atoms, as illustrated in **Figure 22**. The binding affinity was -7.3 kcal/mol, accompanied by an R value of = 0. The main residues at the binding site are: Asn 267, Asn 142, Tyr 263, Gln 428, Tyr 269, Ile 270, Leu 137, Met 369, Tyr 138, and Tyr 269.

## MATERIAL, METHODS AND EXPERIMENTAL

---

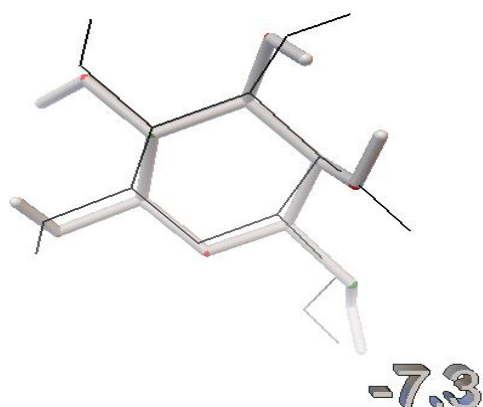


**Figure 22:** Protein validation for docking involved the Co-crystallized ligand (gal 701), depicted in stick model, and the re-docked ligand (gal 701), illustrated in line model.

### 5.1.3 Molecular Docking Protocol

To identify the most potent SGLT2 inhibitors, the designed molecules were evaluated using a molecular modelling approach. In *Vibrio parahaemolyticus*, the 3DH4 protein was developed by locating the active binding site. First, a ligand was extracted from the protein for protein validation. The protein was then ready for docking analysis, sequential steps are illustrated in **Figure 23**.

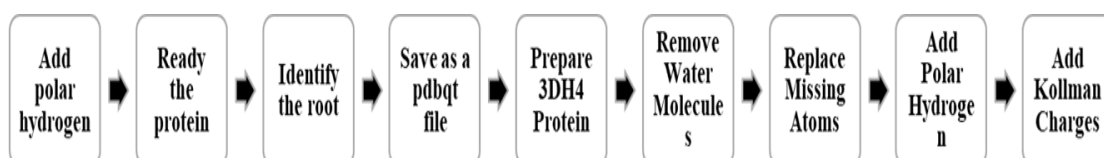


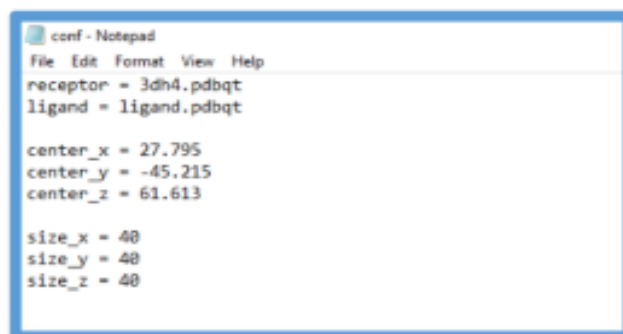
**Figure 23:** Flow chart of the sequential steps involved in preparing the protein

Following this, a grid box is created, utilizing the ligand as the center, and subsequently saved by closing the current configuration. The search space volume is constrained to be less than  $27000 \text{ \AA}^3$ . The "conf.txt" configuration file is then generated from the grid output file, incorporating variables for the x, y, & z coordinates, along with the size. Configuration file is as illustrated in **Figure 24**.



## MATERIAL, METHODS AND EXPERIMENTAL

---



```
conf - Notepad
File Edit Format View Help
receptor = 3dh4.pdbqt
ligand = ligand.pdbqt

center_x = 27.795
center_y = -45.215
center_z = 61.613

size_x = 40
size_y = 40
size_z = 40
```

**Figure 24:** Configuration File ("conf.txt") is displayed in Autodock

Additionally, the command “program files\the scripps research institute\vina\vina.exe - config conf.txt-log log.txt” was used to dock Schiff base based 1, 3, 4 thiadiazoles *via* the command prompt. The automatically generated output file includes the binding affinity (Kcal/mol), accordingly, all designed molecules have been examined, and their binding affinities are displayed. Designed molecules with best binding affinity were subjected to ADME and toxicity analysis.

### 5.1.4 2D Interactions for Docking Results

The AutoDock Tool and command prompt were used to determine the binding affinity of all compounds. After analysing the docking results, 12 newly designed molecules were found to be more potent in comparison to the standard drug, dapagliflozin with binding affinity score of -8.9 Kcal/mol. The optimal binding scores within the range of -10.7 to -9.7 Kcal/mol were observed for these 12 Schiff base-based 1,3,4-thiadiazoles. and selected to investigate the interactions with the SGLT2 protein (PDB ID:3DH4). Pymol software was used to convert the ligand output pdbqt and protein pdbqt into a single pdb format<sup>116</sup>, which was then loaded into the Discovery Studio Visualizer to generate the 2D interaction file.<sup>117, 118</sup>

Considering the basic non-glucoside triazole framework, we have formulated diverse novel 1, 3, 4-thiadiazoles using Schiff base as a foundation to create SGLT2 inhibitors. This involved modifying their substitutions at different locations to enhance lead

## MATERIAL, METHODS AND EXPERIMENTAL

---

molecule properties, followed by docking simulations using AutoDock Vina software. From the potential derivatives, we chose and synthesized 12 the most effective ligands based on their binding affinity scores, comparing them to the standard SGLT2 inhibitor, dapagliflozin.

### 5.2 Synthesis and Characterization:

Chemicals and solvents, all of analytical grade, were procured from Loba Chemie, Spectrochem, and CDH. They were utilized without the need for any further purification. For determination of melting point, a Tempo capillary melting point apparatus was utilized after calibration of the thermometer in ice-cold water at 0°C. The progress of reactions was tracked using pre-coated TLC plates from Merck, and development was achieved through exposure to iodine vapor. Subsequently, the plates were examined under a UV chamber for verification. Nuclear magnetic resonance spectra for proton ( $^1\text{H}$ ) and carbon ( $^{13}\text{C}$ ) were obtained using a 500 MHz Bruker AC-400 F spectrometer and the results were reported in ppm relative to TMS as an internal standard. DMSO was used as the solvent. A Perkin Elmer 10.6.1 FT-IR spectrophotometer was used to record infrared (IR) spectra, which were obtained using a potassium bromide pellet. To record Mass spectra, a Shimadzu 000018 mass spectrometer (GCMS-TQ8040 NX) was utilized. The synthetic scheme for most potent compounds is shown in **Figure 25**.

## MATERIAL, METHODS AND EXPERIMENTAL

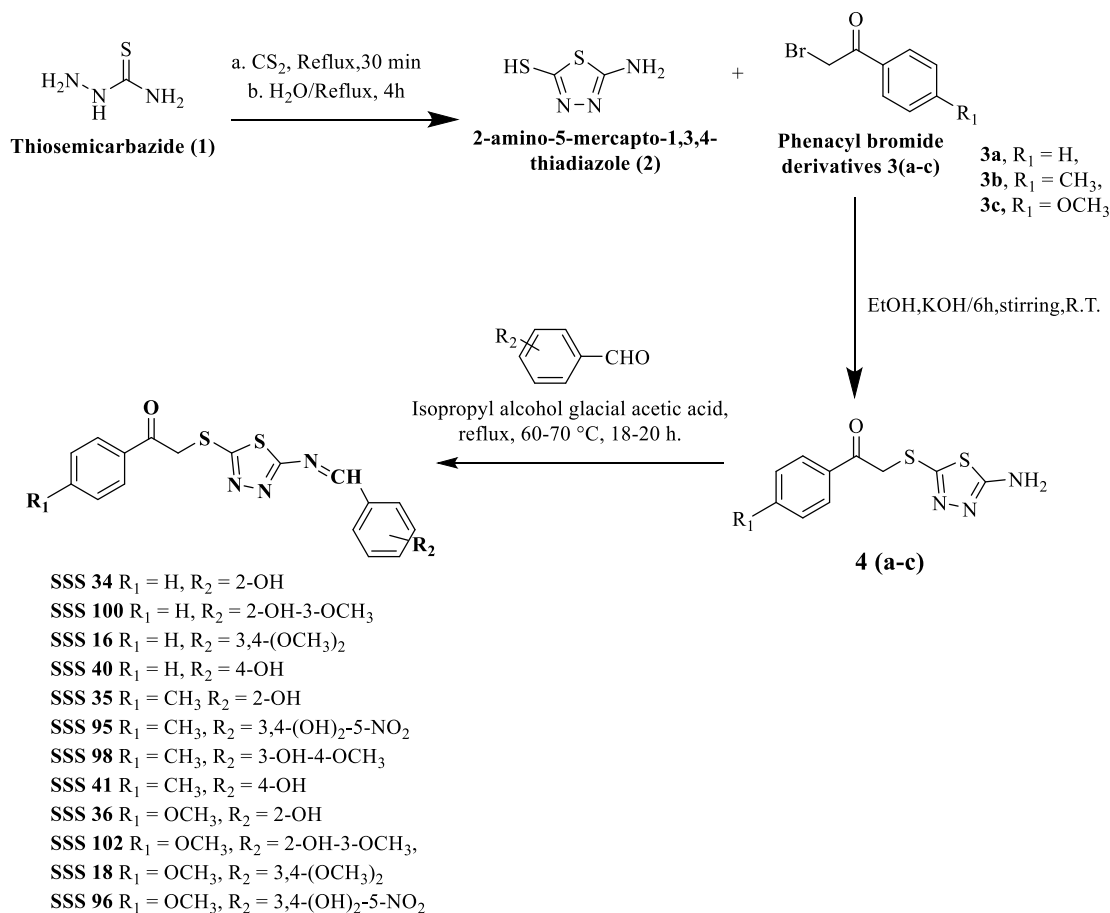


**Figure 25:** Reaction Scheme for most potent compounds

### 5.2.1 Synthesis of 2-amino-5-mercapto-1, 3, 4-thiadiazole (2)

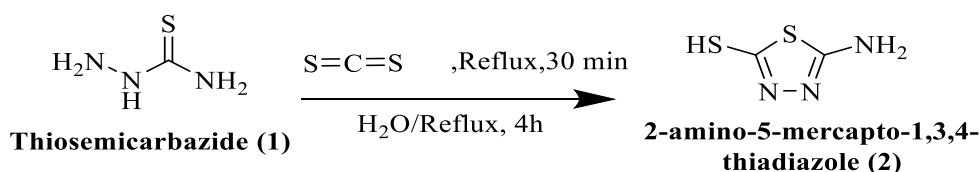
Thiosemicarbazide 1 (10 mmol, 1 equivalent) underwent reflux with carbon disulfide (10 mmol, 1 equivalent) for about thirty minutes. The reaction was then cooled, and 10 ml of water was added. Following the initial reflux, the reaction mixture was subjected to an additional 4 hours of reflux, neutralized with potassium hydroxide, and monitored for the desired product using TLC with Methanol: Chloroform (1:9) as the eluent. The resulting precipitate was filtered and recrystallized from ethanol to yield 2-amino-5-mercapto-1, 3, 4-thiadiazole.

## MATERIAL, METHODS AND EXPERIMENTAL

---

### “2-amino-5-mercapto-1, 3, 4-thiadiazole (2)

Yield: 84%, white powder, M.P. 232-234 °C, FTIR ( $\nu$  max  $\text{cm}^{-1}$ ): 3326, 3242 (-NH<sub>2</sub>), 2553 (S-H<sub>str</sub>, thiol), 1549 (C=N), MS: m/z: 133 [M<sup>+</sup>], <sup>1</sup>H NMR (500 MHz, DMSO-d<sub>6</sub>)  $\delta$  ppm: 7.07 (s, 2H, NH<sub>2</sub>), 13.1 (s, 1H, SH).”



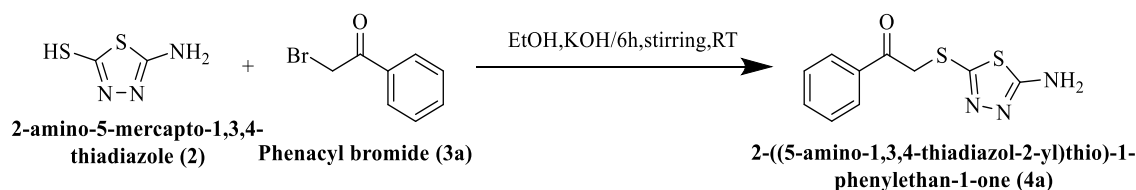
### 5.2.2 Synthesis of 2-((5-amino-1, 3, 4-thiadiazol-2-yl)thio)-1-phenylethan-1-one (4a)

Compound **2** (1.33g, 0.01 mole) was mixed with potassium hydroxide (0.01 mole) in 10 ml of water under stirring, resulting in a colorless mixture. This mixture was then left at RT. Subsequently, phenacylbromide (**3a**) (1.99g, 0.01 mole) was promptly added to the reaction mixture while stirring, and it was dissolved in 10 ml of ethanol. The reaction mixture underwent a thickening process and was stirred at room temperature for 6 hours. Subsequently, it was allowed to cool for half an hour and monitored by TLC with Methanol: Chloroform (1:9) as the eluent. After the reaction concluded, the resulting mixture was transferred to ice-chilled water, leading to the separation of the solid product through filtration. The product obtained from filtration underwent multiple washes with water and ether, followed by drying. Subsequently, the dried product underwent purification through recrystallization using ethanol.

### “2-((5-amino-1, 3, 4-thiadiazol-2-yl)thio)-1-phenylethan-1-one (4a)

Yield: 85%, yellow solid crystals, M.P.: 176-177 °C, R<sub>f</sub>: 0.64 (Methanol: Chloroform (1:9), FTIR ( $\nu$  max  $\text{cm}^{-1}$ ): 3378, 3254 (-NH<sub>2</sub>), 3109 (Ar-CH), 2900 (Aliph. CH), 1691 (C=O), 1588 (C=N); LCMS: m/z: 252 (M+1, 100); <sup>1</sup>H NMR (500 MHz, DMSO-d<sub>6</sub>)  $\delta$  ppm: 4.81 (s, 2H, -CH<sub>2</sub>), Phenyl-H [7.54-7.57 (t, 2H), 7.67-7.70 (t, 1H), 8.00-8.02 (d, 2H)], 7.27 (s, 2H, -NH<sub>2</sub>).”

## MATERIAL, METHODS AND EXPERIMENTAL

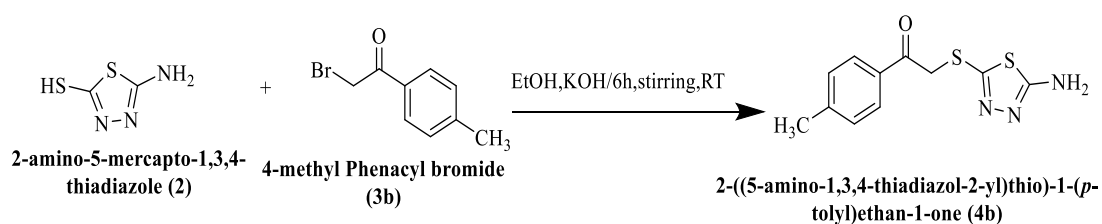


### 5.2.3. Synthesis of 2-((5-amino-1,3,4-thiadiazol-2-yl)thio)-1-(p-tolyl)ethan-1-one (4b)

Under continuous stirring, compound **2** (1.33g, 0.01 mole) was combined with potassium hydroxide (0.01 mole) in 10 ml of water, producing a colorless mixture. The resultant mixture was then allowed to stand at RT. Subsequently, 4-methylphenacylbromide (**3b**) (2.13 g, 0.01 mole) was promptly added to the reaction mixture while stirring, and it was dissolved in 10 ml of ethanol. The reaction mixture underwent a thickening process and was stirred at room temperature for 6 hours. Subsequently, it was allowed to cool for half an hour and monitored by TLC with Methanol: Chloroform (1:9) as the eluent. After the reaction concluded, the resulting mixture was transferred to ice-chilled water, leading to the separation of the solid product through filtration. The product obtained from filtration underwent multiple washes with water and ether, followed by drying. Subsequently, the dried product underwent purification through recrystallization using ethanol.

#### “2-((5-amino-1,3,4-thiadiazol-2-yl)thio)-1-(p-tolyl)ethan-1-one (4b)

Yield: 80%, yellow solid crystals, M.P.: 166–168 °C, R<sub>f</sub>: 0.70 (Methanol: Chloroform (1:9), FTIR (ν max cm<sup>-1</sup>): 3395, 3259 (-NH<sub>2</sub>), 3116 (Ar-CH), 2902 (Aliph. CH), 1686 (C=O), 1591 (C=N); MS: m/z: 266 [M<sup>+</sup>]; <sup>1</sup>H NMR (500 MHz, DMSO-d<sub>6</sub>) δ ppm: 2.39 (s, 3H, -CH<sub>3</sub>), 4.76 (s, 2H, -CH<sub>2</sub>), Phenyl-H [7.35-7.36 (d, 2H), 7.90-7.92 (d, 2H)], 7.27 (s, 2H, -NH<sub>2</sub>).”



## MATERIAL, METHODS AND EXPERIMENTAL

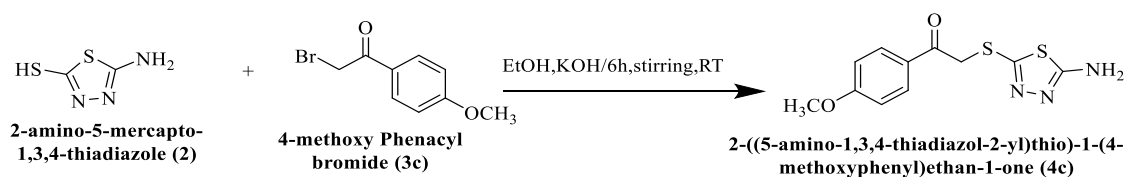
---

### 5.2.4 2-((5-amino-1,3,4-thiadiazol-2-yl)thio)-1-(4-methoxyphenyl)ethan-1-one (4c)

Under stirring conditions, compound **2** (1.33g, 0.01 mole) was combined with potassium hydroxide (0.01 mole) in 10 ml of water, producing a colorless mixture. This mixture was then left at RT. Following that, 4-methoxyphenacylbromide (**3c**) (2.29 g, 0.01 mole) was promptly added to the reaction mixture while stirring, and it was dissolved in 10 ml of ethanol. The reaction mixture underwent a thickening process and was stirred at room temperature for 6 hours. Subsequently, it was allowed to cool for half an hour and monitored by TLC with Methanol: Chloroform (1:9) as the eluent. After the reaction concluded, the resulting mixture was transferred to ice-chilled water, leading to the separation of the solid product through filtration. The product obtained from filtration underwent multiple washes with water and ether, followed by drying. Subsequently, the dried product underwent purification through recrystallization using ethanol.

### “2-((5-amino-1,3,4-thiadiazol-2-yl)thio)-1-(4-methoxyphenyl)ethan-1-one (4c)

Yield: 79%, white solid crystals, M.P.: 187–189 °C, R<sub>f</sub>: 0.75 (Methanol: Chloroform (1:9), FTIR (ν max cm<sup>-1</sup>): 3277 (-NH<sub>2</sub>), 3082 (Ar-CH), 2839 (Aliph. CH), 1665 (C=O), 1595 (C=N); MS: m/z: 281 [M<sup>+</sup>]; <sup>1</sup>H NMR (500 MHz, DMSO-d<sub>6</sub>) δ ppm: 3.86 (s, 3H, -OCH<sub>3</sub>), 4.74 (s, 2H, -CH<sub>2</sub>), Phenyl-H [7.79-8.00 (d, 2H), 7.06-7.07 (d, 2H)], 7.26 (s, 2H, -NH<sub>2</sub>).”

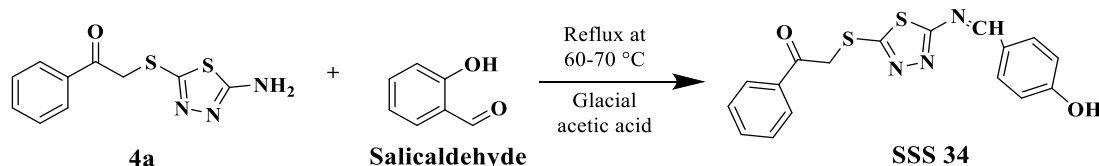


### 5.2.5 Synthesis of 2-((5-((2-hydroxybenzylidene)amino)-1,3,4-thiadiazol-2-yl)thio)-1-phenylethan-1-one (SSS 34)

Dissolve 2.51 g (0.01 mol) of **4a** in 25 ml of isopropyl alcohol and reflux it with salicylaldehyde (1.59 g, 0.015 mol) for 18 hours at temperatures ranging from 60 to 70°C. Subsequently, 2-3 drops of glacial acetic acid were introduced into the reaction mixture. The advancement of the reaction was tracked using TLC with an eluent mixture

## MATERIAL, METHODS AND EXPERIMENTAL

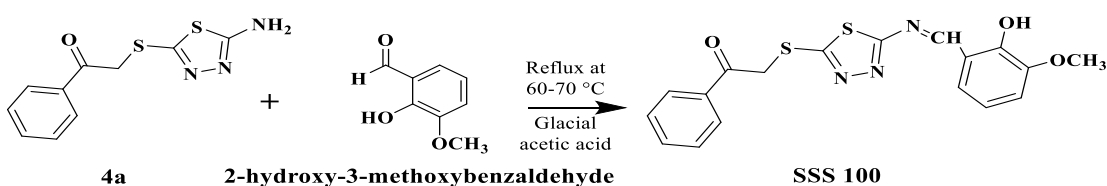
consisting of 80% EA and 20% hexane. Upon completion of the reaction, the product was cooled to RT, and distillation was carried out under vacuum pressure utilizing a rotavapor. The resulting crude product underwent recrystallization using methanol, with the process being repeated 2-3 times to yield a pure and dried final product.



**“2-((5-((2-hydroxybenzylidene)amino)-1,3,4-thiadiazol-2-yl)thio)-1-phenylethan-1-one (SSS 34):** Yield: 90%, yellow solid crystals, M.P.: 187–189 °C, R<sub>f</sub>: 0.75 (Ethylacetate: Hexane (8:2), LC-MS (ESI) m/z: 356 (M+H)<sup>+</sup>, <sup>1</sup>H NMR (400 MHz, DMSO-d<sub>6</sub>) δ ppm: 5.17 (s, 2H, -CH<sub>2</sub>), 6.96 (m, 2H, Ar-H), 7.29 (m, 1H, Ar-H), 7.49 (m, 2H, Ar-H), 7.57 (m, 1H, Ar-H), 7.60 (d, 1H, Ar-H), 8.09 (m, 2H, Ar-H), 9.11 (s, 1H, Imine), 11.22 (s, 1H, -OH), <sup>13</sup>C NMR (100 MHz, DMSO-d<sub>6</sub>) δ ppm: 41.86, 117.43, 120.24, 128.98, 129.37, 130.82, 134.38, 135.68, 136.22, 160.70, 163.26, 167.44, 173.80, 193.23.”

### 5.2.6 Synthesis of 2-((5-((2-hydroxy-4-methoxybenzylidene)amino)-1,3,4-thiadiazol-2-yl)thio)-1-phenylethan-1-one (SSS 100)

Dissolve 2.51 g (0.01 mol) of **4a** in 25 ml of isopropyl alcohol and reflux it with 2-hydroxy-3-methoxybenzaldehyde (2.28 g, 0.015 mol) for 19 hours at temperatures ranging from 60 to 70°C. Subsequently, 2-3 drops of glacial acetic acid were introduced into the reaction mixture. The advancement of the reaction was tracked using TLC with an eluent mixture consisting of 80% EA and 20% hexane. Upon completion of the reaction, the product was cooled to RT, and distillation was carried out under vacuum pressure utilizing a rotavapor. The resulting crude product underwent recrystallization using methanol, with the process being repeated 2-3 times to yield a pure and dried final product.



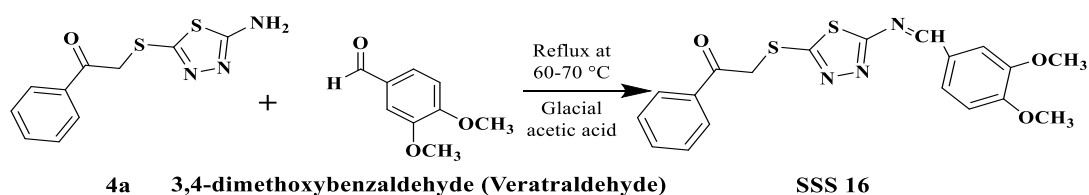
## MATERIAL, METHODS AND EXPERIMENTAL

---

“2-((5-((2-hydroxy-4-methoxybenzylidene)amino)-1,3,4-thiadiazol-2-yl)thio)-1-phenylethan-1-one (SSS 100): Yield: 90%, yellow solid crystals, M.P.: 180–182 °C, R<sub>f</sub>: 0.62 (Ethylacetate: Hexane (8:2), LC-MS (ESI) m/z: 386 (M+H)<sup>+</sup>, <sup>1</sup>H NMR (400 MHz, DMSO-d<sub>6</sub>) δ ppm: 3.86 (s, 3H, OCH<sub>3</sub>), 5.16 (s, 2H, -CH<sub>2</sub>), 6.94 (d, 1H, Ar-H), 7.25 (d, 1H, Ar-H), 7.47 (d, 1H, Ar-H), 7.74 (m, 3H, Ar-H), 8.10 (m, 2H, Ar-H), 9.11 (s, 1H, Imine), 10.86 (s, 1H, -OH). <sup>13</sup>C NMR (100 MHz, DMSO-d<sub>6</sub>) δ ppm: 41.70, 56.15, 114.58, 117.42, 120.33, 128.50, 130.81, 131.42, 136.21, 160.89, 163.47, 164.18, 167.41, 173.75, 191.52.”

### 5.2.7 Synthesis of 2-((5-((3,4-dimethoxybenzylidene)amino)-1,3,4-thiadiazol-2-yl)thio)-1-phenylethan-1-one (SSS 16)

Dissolve 2.51 g (0.01 mol) of **4a** in 25 ml of isopropyl alcohol and reflux it with 3,4-dimethoxybenzaldehyde (2.49 g, 0.015 mol) for 20 hours at temperatures ranging from 60 to 70°C. Subsequently, 2-3 drops of glacial acetic acid were introduced into the reaction mixture. The advancement of the reaction was tracked using TLC with an eluent mixture consisting of 80% EA and 20% hexane. Upon completion of the reaction, the product was cooled to RT, and distillation was carried out under vacuum pressure utilizing a rotavapor. The resulting crude product underwent recrystallization using methanol, with the process being repeated 2-3 times to yield a pure and dried final product.



“2-((5-((3,4-dimethoxybenzylidene)amino)-1,3,4-thiadiazol-2-yl)thio)-1-phenylethan-1-one (SSS 16): Yield: 95%, yellow solid crystals, M.P.: 189–191 °C, R<sub>f</sub>: 0.73 (Ethylacetate: Hexane (8:2), LC-MS (ESI) m/z: 400 (M+H)<sup>+</sup>, <sup>1</sup>H NMR (400 MHz, DMSO-d<sub>6</sub>) δ ppm: 3.83 (s, 6H, OCH<sub>3</sub>), 4.85 (s, 2H, -CH<sub>2</sub>), 7.16 (m, 1H, Ar-H), 7.29-7.40 (m, 2H, Ar-H), 7.55 (m, 4H, Ar-H), 8.09 (m, 1H, Ar-H), 9.85 (s, 1H, Imine).



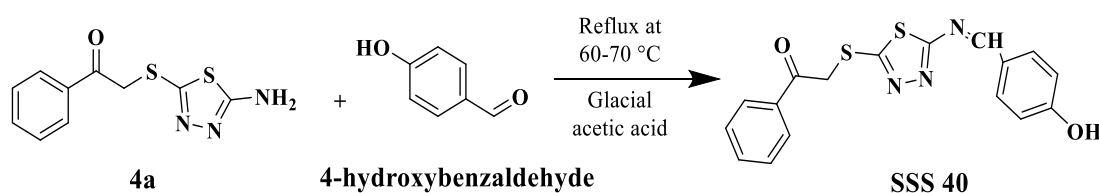
## MATERIAL, METHODS AND EXPERIMENTAL

---

$^{13}\text{C}$  NMR (100 MHz, DMSO- $d_6$ )  $\delta$  ppm: 42.05, 56.36, 109.88, 111.76, 111.99, 126.62, 127.20, 128.97, 129.37, 130.11, 134.38, 135.64, 149.65, 154.67, 169.41, 170.27, 193.87.”

### 5.2.8 Synthesis of 2-((5-((4-hydroxybenzylidene)amino)-1,3,4-thiadiazol-2-yl)thio)-1-phenylethan-1-one (SSS 40)

Dissolve 2.51 g (0.01 mol) of **4a** in 25 ml of isopropyl alcohol and reflux it with 4-hydroxyaldehyde (1.59 g, 0.015 mol) for 18 hours at temperatures ranging from 60 to 70°C. Subsequently, 2-3 drops of glacial acetic acid were introduced into the reaction mixture. The advancement of the reaction was tracked using TLC with an eluent mixture consisting of 80% EA and 20% hexane. Upon completion of the reaction, the product was cooled to RT, and distillation was carried out under vacuum pressure utilizing a rotavapor. The resulting crude product underwent recrystallization using methanol, with the process being repeated 2-3 times to yield a pure and dried final product.



**“2-((5-((4-hydroxybenzylidene)amino)-1,3,4-thiadiazol-2-yl)thio)-1-phenylethan-1-one (SSS 40):** Yield: 92%, yellow solid crystals, M.P.: 178–179 °C, R<sub>f</sub>: 0.66 (Ethylacetate: Hexane (8:2), LC-MS (ESI) m/z: 356 (M+H)<sup>+</sup>,  $^1\text{H}$  NMR (400 MHz, DMSO- $d_6$ )  $\delta$  ppm: 5.13 (s, 2H, -CH<sub>2</sub>), 6.94 (d, 2H, Ar-H), 7.52 (m, 2H, Ar-H), 7.70 (m, 1H, Ar-H), 7.84 (m, 2H, Ar-H), 8.15 (m, 2H, Ar-H), 8.74 (s, 1H, Imine), 10.61 (s, 1H, -OH).  $^{13}\text{C}$  NMR (100 MHz, DMSO- $d_6$ )  $\delta$  ppm: 41.74, 116.63, 126.19, 128.96, 129.36, 133.12, 134.36, 135.70, 162.11, 163.40, 169.02, 174.90, 193.24.”

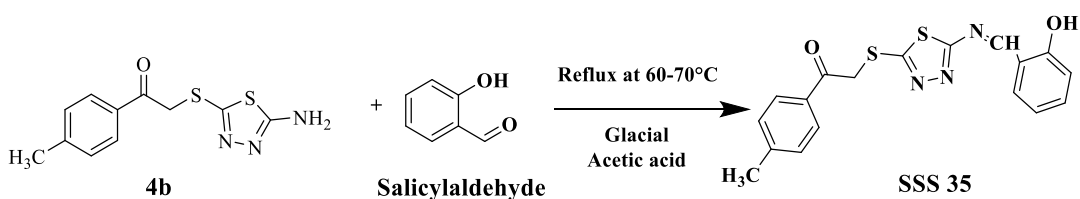
### 5.2.9 Synthesis of 2-((5-((2-hydroxybenzylidene)amino)-1,3,4-thiadiazol-2-yl)thio)-1-(p-tolyl)ethan-1-one (SSS 35)

Dissolve 2.66 g (0.01 mol) of **4b** in 25 ml of isopropyl alcohol and reflux it with salicylaldehyde (1.59 g, 0.015 mol) for 18 hours at temperatures ranging from 60 to 70°C. Subsequently, 2-3 drops of glacial acetic acid were introduced into the reaction

## MATERIAL, METHODS AND EXPERIMENTAL

---

mixture. The advancement of the reaction was tracked using TLC with an eluent mixture consisting of 80% EA and 20% hexane. Upon completion of the reaction, the product was cooled to RT, and distillation was carried out under vacuum pressure utilizing a rotavapor. The resulting crude product underwent recrystallization using methanol, with the process being repeated 2-3 times to yield a pure and dried final product.

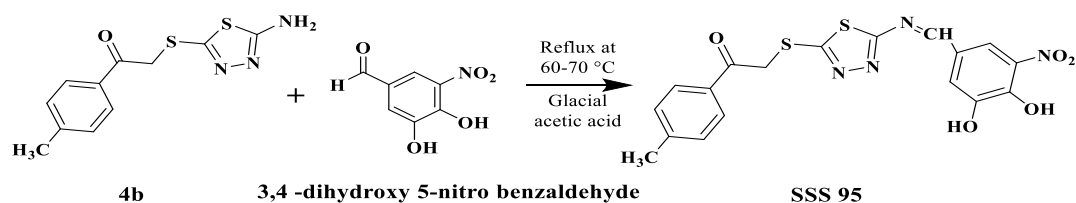


**“2-((5-((2-hydroxybenzylidene)amino)-1,3,4-thiadiazol-2-yl)thio)-1-(p-tolyl)ethan-1-one (SSS 35):** Yield: 80%, rust colored solid crystals, M.P.: 160–162 °C, R<sub>f</sub>: 0.77 (Ethylacetate: Hexane (8:2), **LC-MS (ESI) m/z:** 370 (M+H)<sup>+</sup>, **<sup>1</sup>H NMR (400 MHz, DMSO-d<sub>6</sub>) δ ppm:** 2.41 (s, 3H, -CH<sub>3</sub>), 4.77 (s, 2H, -CH<sub>2</sub>), 6.92 (m, 2H, Ar-H), 6.92 (m, 2H, Ar-H), 7.28 (d, 2H, Ar-H), 7.40 (m, 1H, Ar-H), 7.98 (m, 3H, Ar-H), 9.79 (s, 1H, Imine), 10.64 (s, 1H, -OH). **<sup>13</sup>C NMR (100 MHz, DMSO-d<sub>6</sub>) δ ppm:** 21.68, 42.0, 117.70, 119.95, 122.76, 129.64, 136.89, 161.19, 192.15.”

### 5.2.10 Synthesis of 2-((5-((3,4-dihydroxy-5-nitrobenzylidene)amino)-1,3,4-thiadiazol-2-yl)thio)-1-(p-tolyl)ethan-1-one (SSS 95)

Dissolve 2.66 g (0.01 mol) of **4b** in 25 ml of isopropyl alcohol and reflux it with 3,4-dihydroxy-5-nitro benzaldehyde (2.74 g, 0.015 mol) for 20 hours at temperatures ranging from 60 to 70°C. Subsequently, 2-3 drops of glacial acetic acid were introduced into the reaction mixture. The advancement of the reaction was tracked using TLC with an eluent mixture consisting of 80% EA and 20% hexane. Upon completion of the reaction, the product was cooled to RT, and distillation was carried out under vacuum pressure utilizing a rotavapor. The resulting crude product underwent recrystallization using methanol, with the process being repeated 2-3 times to yield a pure and dried final product.

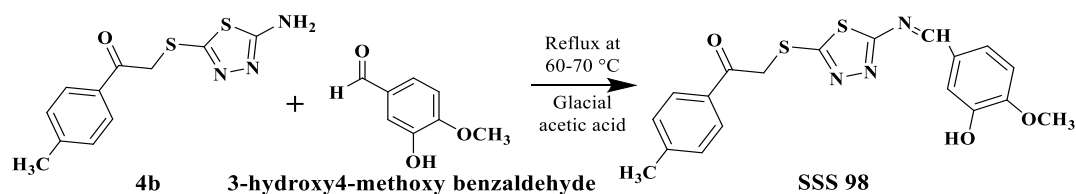
## MATERIAL, METHODS AND EXPERIMENTAL



**“2-((5-((3,4-dihydroxy-5-nitrobenzylidene)amino)-1,3,4-thiadiazol-2-yl)thio)-1-(p-tolyl)ethan-1-one (SSS 95):** Yield: 90%, yellow solid crystals, M.P.: 192–194 °C, Rf: 0.68 (Ethylacetate: Hexane (8:2), LC-MS (ESI) m/z: 431 (M+H)<sup>+</sup>, <sup>1</sup>H NMR (400 MHz, DMSO-d<sub>6</sub>) δ ppm: 2.41 (s, 3H, -CH<sub>3</sub>), 4.77 (s, 2H, -CH<sub>2</sub>), 7.37 (m, 3H, Ar-H), 8.04 (m, 3H, Ar-H), 8.80 (s, 1H, Imine), 9.81 (s, 2H, -OH). <sup>13</sup>C NMR (100 MHz, DMSO-d<sub>6</sub>) δ ppm: 21.72, 41.86, 117.43, 120.33, 128.98, 129.37, 130.82, 134.38, 135.68, 136.22, 160.70, 163.26, 167.44, 173.80, 193.23.”

### 5.2.11 Synthesis of 2-((5-((3-hydroxy-4-methoxybenzylidene)amino)-1,3,4-thiadiazol-2-yl)thio)-1-(p-tolyl)ethan-1-one (SSS 98)

Dissolve 2.66 g (0.01 mol) of **4b** in 25 ml of isopropyl alcohol and reflux it with 3-hydroxy-4-methoxybenzaldehyde (2.28 g, 0.015 mol) for 20 hours at temperatures ranging from 60 to 70°C. Subsequently, 2-3 drops of glacial acetic acid were introduced into the reaction mixture. The advancement of the reaction was tracked using TLC with an eluent mixture consisting of 80% EA and 20% hexane. Upon completion of the reaction, the product was cooled to RT, and distillation was carried out under vacuum pressure utilizing a rotavapor. The resulting crude product underwent recrystallization using methanol, with the process being repeated 2-3 times to yield a pure and dried final product.



**“2-((5-((3-hydroxy-4-methoxybenzylidene)amino)-1,3,4-thiadiazol-2-yl)thio)-1-(p-tolyl)ethan-1-one (SSS 98):** Yield: 70%, greyish colored solid crystals, M.P.: 157–159 °C, Rf: 0.65 (Ethylacetate: Hexane (8:2), LC-MS (ESI) m/z: 400 (M+H)<sup>+</sup>, <sup>1</sup>H NMR (400 MHz, DMSO-d<sub>6</sub>) δ ppm: 2.41 (s, 3H, -CH<sub>3</sub>), 3.88 (s, 3H, -OCH<sub>3</sub>), 5.13 (s, 2H, -CH<sub>2</sub>),

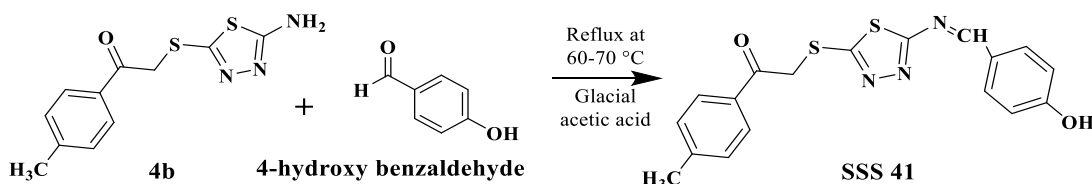
## MATERIAL, METHODS AND EXPERIMENTAL

---

6.96 (m, 2H, Ar-H), 7.45 (m, 3H, Ar-H), 7.99 (m, 2H, Ar-H), 9.10 (s, 1H, Imine), 10.28 (s, 1H, -OH).  $^{13}\text{C}$  NMR (100 MHz, DMSO- $d_6$ )  $\delta$  ppm: 21.72, 41.86, 56.49, 117.42, 120.51, 122.97, 129.89, 133.16, 144.95, 148.83, 151.18, 163.39, 167.60, 173.70, 192.71.”

### 5.2.12 Synthesis of 2-((5-((4-hydroxybenzylidene)amino)-1,3,4-thiadiazol-2-yl)thio)-1-(p-tolyl)ethan-1-one (SSS 41)

Dissolve 2.66 g (0.01 mole) of **4b** in 25 ml of isopropyl alcohol and reflux it with 4-hydroxyaldehyde (1.59 g, 0.015 mole) for 18 hours at temperatures ranging from 60 to 70°C. Subsequently, 2-3 drops of glacial acetic acid were introduced into the reaction mixture. The advancement of the reaction was tracked using TLC with an eluent mixture consisting of 80% EA and 20% hexane. Upon completion of the reaction, the product was cooled to RT, and distillation was carried out under vacuum pressure utilizing a rotavapor. The resulting crude product underwent recrystallization using methanol, with the process being repeated 2-3 times to yield a pure and dried final product.



“2-((5-((4-hydroxybenzylidene)amino)-1,3,4-thiadiazol-2-yl)thio)-1-(p-tolyl)ethan-1-one (SSS 41): Yield: 77%, yellow solid crystals, M.P.: 187–189 °C, R<sub>f</sub>: 0.71 (Ethylacetate: Hexane (8:2), LC-MS (ESI) m/z: 370 (M+H)<sup>+</sup>,  $^1\text{H}$  NMR (400 MHz, DMSO- $d_6$ )  $\delta$  ppm: 2.41 (s, 3H, -CH<sub>3</sub>), 4.77 (s, 2H, -CH<sub>2</sub>), 6.95 (d, 2H, Ar-H), 7.28 (s, 2H, Ar-H), 7.40 (d, 1H, Ar-H), 7.75 (d, 2H, Ar-H), 7.98 (d, 1H, Ar-H), 9.79 (s, 1H, Imine), 10.64 (s, 1H, -OH).  $^{13}\text{C}$  NMR (100 MHz, DMSO- $d_6$ )  $\delta$  ppm: 21.68, 42.0, 116.67, 128.06, 129.10, 129.89, 132.58, 133.15, 144.73, 149.72, 163.85, 170.27, 193.40.”

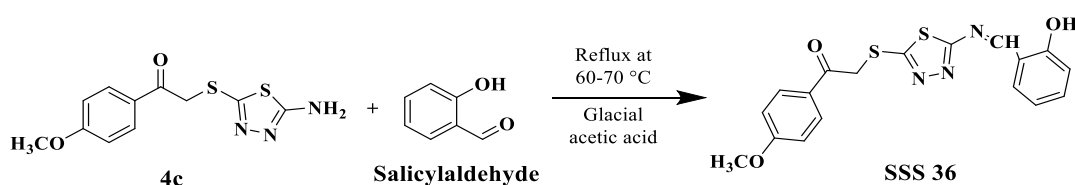
### 5.2.13 Synthesis of 2-((5-((2-hydroxybenzylidene)amino)-1,3,4-thiadiazol-2-yl)thio)-1-(4-methoxyphenyl)ethan-1-one (SSS 36)

Dissolve 2.81 g (0.01 mol) of **4c** in 25 ml of isopropyl alcohol and reflux it with

## MATERIAL, METHODS AND EXPERIMENTAL

---

salicylaldehyde (1.59 g, 0.015 mole) for 18 hours at temperatures ranging from 60 to 70°C. Subsequently, 2-3 drops of glacial acetic acid were introduced into the reaction mixture. The advancement of the reaction was tracked using TLC with an eluent mixture consisting of 80% EA and 20% hexane. Upon completion of the reaction, the product was cooled to RT, and distillation was carried out under vacuum pressure utilizing a rotavapor. The resulting crude product underwent recrystallization using methanol, with the process being repeated 2-3 times to yield a pure and dried final product.

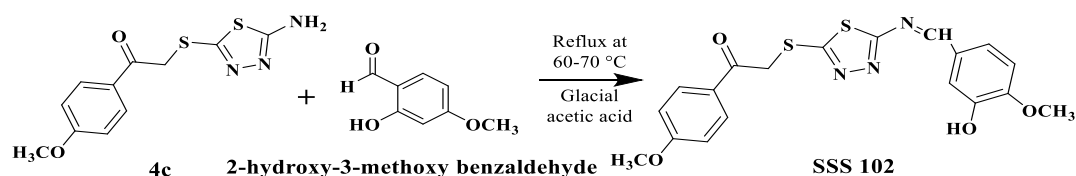


**“2-((5-((2-hydroxybenzylidene)amino)-1,3,4-thiadiazol-2-yl)thio)-1-(4-methoxyphenyl)ethan-1-one (SSS 36):** Yield: 90%, yellow solid crystals, M.P.: 190–192 °C, R<sub>f</sub>: 0.74 (Ethylacetate: Hexane (8:2), **LC-MS (ESI) m/z:** 386 (M+H)<sup>+</sup>, **<sup>1</sup>H NMR (400 MHz, DMSO-d<sub>6</sub>) δ ppm:** 3.87 (s, 3H, -OCH<sub>3</sub>), 5.07 (s, 2H, -CH<sub>2</sub>), 6.91 (m, 2H, Ar-H), 7.11 (m, 2H, Ar-H), 7.51 (m, 1H, Ar-H), 7.87 (d, 1H, Ar-H), 8.02 (d, 2H, Ar-H), 9.09 (s, 1H, Imine), 11.22 (s, 1H, -OH). **<sup>13</sup>C NMR (100 MHz, DMSO-d<sub>6</sub>) δ ppm:** 41.70, 56.15, 114.58, 117.42, 120.33, 128.50, 130.81, 131.42, 136.21, 160.89, 163.47, 164.18, 167.41, 173.75, 191.52.”

### 5.2.14 Synthesis of 2-((5-((2-hydroxy-4-methoxybenzylidene)amino)-1,3,4-thiadiazol-2-yl)thio)-1-(4-methoxyphenyl)ethan-1-one (SSS 102)

Dissolve 2.81 g (0.01 mole) of 4c in 25 ml of isopropyl alcohol and reflux it with 2-hydroxy-4-methoxybenzaldehyde (2.28 g, 0.015 mole) for 19 hours at temperatures ranging from 60 to 70°C. Subsequently, 2-3 drops of glacial acetic acid were introduced into the reaction mixture. The advancement of the reaction was tracked using TLC with an eluent mixture consisting of 80% EA and 20% hexane. Upon completion of the reaction, the product was cooled to RT, and distillation was carried out under vacuum pressure utilizing a rotavapor. The resulting crude product underwent recrystallization with methanol, a process repeated 2-3 times to obtain a pure and dried final product.

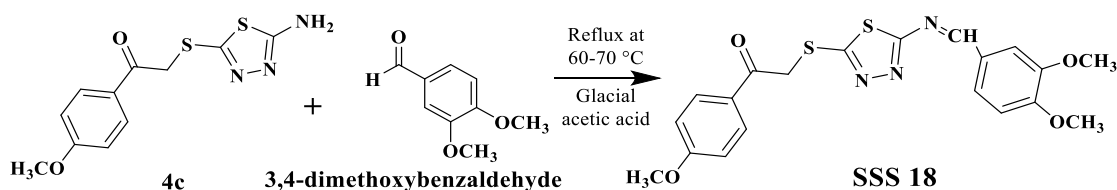
## MATERIAL, METHODS AND EXPERIMENTAL



“2-((5-((2-hydroxy-4-methoxybenzylidene)amino)-1,3,4-thiadiazol-2-yl)thio)-1-(4-methoxyphenyl)ethan-1-one (SSS 102): Yield: 95%, mustard yellow solid crystals, M.P.: 187–189 °C, R<sub>f</sub>: 0.66 (Ethylacetate: Hexane (8:2), LC-MS (ESI) m/z: 414 (M+H)<sup>+</sup>, <sup>1</sup>H NMR (400 MHz, DMSO-d<sub>6</sub>) δ ppm: 3.87 (s, 6H, -OCH<sub>3</sub>), 5.11 (s, 2H, -CH<sub>2</sub>), 6.91 (m, 1H, Ar-H), 7.11 (m, 2H, Ar-H), 7.24 (d, 1H, Ar-H), 8.05 (d, 3H, Ar-H), 9.12 (s, 1H, Imine), 10.86 (s, 1H, -OH). <sup>13</sup>C NMR (100 MHz, DMSO-d<sub>6</sub>) δ ppm: 42.05, 56.36, 109.88, 111.99, 117.41, 126.62, 129.37, 130.11, 135.64, 149.55, 154.67, 170.27, 193.89.”

### 5.2.15 Synthesis of 2-((5-((3,4-dimethoxybenzylidene)amino)-1,3,4-thiadiazol-2-yl)thio)-1-(4-methoxyphenyl)ethan-1-one (SSS 18)

Dissolve 2.81 g (0.01 mole) of **4c** in 25 ml of isopropyl alcohol and reflux it with 3,4-dimethoxybenzaldehyde (2.49 g, 0.015 mole) for 19 hours at temperatures ranging from 60 to 70°C. Subsequently, 2-3 drops of glacial acetic acid were introduced into the reaction mixture. The advancement of the reaction was tracked using TLC with an eluent mixture consisting of 80% EA and 20% hexane. Upon completion of the reaction, the product was cooled to RT, and distillation was carried out under vacuum pressure utilizing a rotavapor. The resulting crude product underwent recrystallization using methanol, with the process being repeated 2-3 times to yield a pure and dried final product.



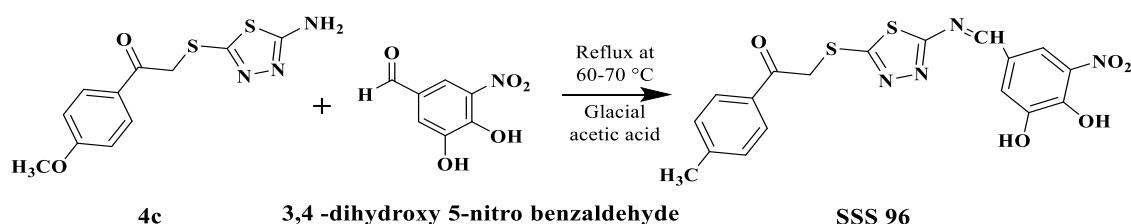
## MATERIAL, METHODS AND EXPERIMENTAL

---

“2-((5-((3,4-dimethoxybenzylidene)amino)-1,3,4-thiadiazol-2-yl)thio)-1-(4-methoxyphenyl)ethan-1-one (SSS 18): Yield; 70%, yellow solid crystals, M.P.: 164–166 °C, R<sub>f</sub>: 0.75 (Ethylacetate: Hexane (8:2), LC-MS (ESI) m/z: 430 (M+H)<sup>+</sup>, <sup>1</sup>H NMR (400 MHz, DMSO-d<sub>6</sub>) δ ppm: 3.87 (s, 9H, -OCH<sub>3</sub>), 4.76 (s, 2H, -CH<sub>2</sub>), 7.29 (m, 3H, Ar-H), 7.61 (m, 2H, Ar-H), 8.07 (m, 2H, Ar-H), 8.79 (s, 1H, Imine). <sup>13</sup>C NMR (100 MHz, DMSO-d<sub>6</sub>) δ ppm: 41.74, 56.35, 114.43, 131.40, 160.70, 163.26, 167.44, 173.80, 193.23.”

### 5.2.16 Synthesis of 2-((5-((3,4-dihydroxy-5-nitrobenzylidene)amino)-1,3,4-thiadiazol-2-yl)thio)-1-(4-methoxyphenyl)ethan-1-one (SSS 96)

Dissolve 2.81 g (0.01 mole) of **4c** in 25 ml of isopropyl alcohol and reflux it with 3,4-dihydroxy-5-nitrobenzaldehyde (2.74 g, 0.015 mole) for 20 hours at temperatures ranging from 60 to 70°C. Subsequently, 2-3 drops of glacial acetic acid were introduced into the reaction mixture. The advancement of the reaction was tracked using TLC with an eluent mixture consisting of 80% EA and 20% hexane. Upon completion of the reaction, the product was cooled to RT, and distillation was carried out under vacuum pressure utilizing a rotavapor. The resulting crude product underwent recrystallization using methanol, with the process being repeated 2-3 times to yield a pure and dried final product.



“2-((5-((3,4-dihydroxy-5-nitrobenzylidene)amino)-1,3,4-thiadiazol-2-yl)thio)-1-(4-methoxyphenyl)ethan-1-one (SSS 96): Yield: 90%, greyish colored solid crystals, M.P.: 177–179 °C, R<sub>f</sub>: 0.75 (Ethylacetate: Hexane (8:2), LC-MS (ESI) m/z: 447 (M+H)<sup>+</sup>, <sup>1</sup>H NMR (400 MHz, DMSO-d<sub>6</sub>) δ ppm: 3.89 (s, 3H, -OCH<sub>3</sub>), 4.80 (s, 2H, -CH<sub>2</sub>), 7.07 (d, 2H, Ar-H), 7.47 (s, 1H, Ar-H), 8.01 (m, 3H, Ar-H), 8.80 (s, 1H, Imine), 9.81 (s, 2H, -OH). <sup>13</sup>C NMR (100 MHz, DMSO-d<sub>6</sub>) δ ppm: 41.73, 56.49, 114.48, 117.41, 120.41, 128.49, 131.42, 147.80, 164.01, 167.58, 173.68, 191.52.”

## MATERIAL, METHODS AND EXPERIMENTAL

---

**5.3 *In-silico* toxicity prediction:** The toxicity of the synthesized compounds was evaluated to determine any associated risks, such as carcinogenicity and mutagenicity. The compounds were converted to SMILES format using ChemDraw Professional 16 software and analyzed for toxicity using the Lazar toxicity predictor.<sup>119</sup>

**5.4 *In-silico* pharmacokinetics prediction:** The SWISS ADME software, accessible at <http://www.swissadme.ch/index.php>, was employed for the online computation of pharmacokinetic properties, drug-likeness, and physicochemical characteristics of the synthesized compounds.<sup>120</sup>

### 5.5 *In vitro* evaluation of synthesized compounds

#### 5.5.1 MTT cell-viability assay

The recently synthesized compounds underwent a cell viability assessment through the MTT assay, conducted on the Chinese Hamster Ovary cell line (CHO) at the School of Bioengineering and Biosciences, LPU, India. The compounds were evaluated at five distinct concentrations, with Dapagliflozin serving as the control in this assay measuring growth inhibitory activity. The DMEM medium, FBS, trypsin, DMSO, and MTT utilized in the assay were obtained from Sigma Aldrich Chemicals. Dapagliflozin was graciously supplied as a complimentary sample by Enrico Pharmaceuticals, India. The CHO cell line was obtained from the National Centre for Cell Science, Pune, India. All synthesized compounds were dissolved in DMSO (mg/ml).

The evaluation of the newly synthesized compounds' effect on cell growth inhibition was conducted through the MTT assay, employing a tetrazolium. The assay gauges viable cells by monitoring the reduction of the tetrazolium salt, MTT, leading to the formation of purple formazan crystals in live cells. Cell viability is subsequently determined by analyzing the absorbance of the cell sample post-assay.

At a concentration of  $1 \times 10^8$  cells per well, cells were cultivated in 96-well plates, left to adhere for 24 hours, and maintained at 37°C in an atmosphere with 5.0% CO<sub>2</sub>. Subsequently, the cells were subjected to triplicate treatments with varying concentrations of the test samples and the reference drug, dapagliflozin, at 6.25 µg/ml,



## MATERIAL, METHODS AND EXPERIMENTAL

---

12.5 µg/ml, 25 µg/ml, 50 µg/ml, and 100 µg/ml, maintained at 37°C overnight. A 20 µl aliquot of MTT solution was directly introduced into all the relevant wells. Following a 4-hour incubation period at 37°C, the media was extracted, and the formazan crystals, formed through the reduction of MTT by active cells, were dissolved in 80 µl of DMSO. The mixture was then incubated for half an hour to facilitate the dissolution of the formazan crystals. The absorbance of each well was measured using an ELISA plate reader at 540 nm. All experiments were performed in triplicate and replicated twice for statistical analysis. Results were presented as mean ± SEM. The IC<sub>50</sub>, indicating the concentration of a drug necessary for 50% inhibition of CHO cell proliferation *in vitro*, was calculated using Microsoft Excel, and the values were reported in µg/ml.

### 5.5.2 Human SGLT2 (SLC5A2) ELISA kit

Prior to the experiment, we selected high and low doses of standard and test compounds with the best IC<sub>50</sub> values and prepared the plates using low (5mM +20 mM mannitol for osmotic balance) and high glucose media (30 mM). For instance, the high and low doses for the treatment are as: standard (110 & 55 µL), SSS100 (90 & 45 µL), SSS35 (100 & 50 µL), SSS95 (100 & 50 µL), and SSS40 (90 & 45 µL). After treatment with the above doses, cell lysate was prepared using a homogenizing buffer including protease inhibitors to avoid protein degradation. Afterward, the cells were scraped using a cell scraper, followed by centrifugation to obtain a good amount of protein. After centrifugation to process the sample, we remove the pellet and consider the supernatant for further assessment.

**Reagent Preparation:** All reagents were kept at room temperature. In the event of crystal formation in buffer concentrates, warming was allowed until complete dissolution was achieved. The wash buffer was prepared by diluting distilled water in a 5:15 fold ratio.

**Standard:** Into each tube, 150 µL of standard diluent was added. A series of 2-fold dilutions was then created using the stock solution. Thorough mixing of each tube was ensured before advancing to the next transfer, with the undiluted standard serving as the high standard.

## MATERIAL, METHODS AND EXPERIMENTAL

---

**Assay procedure:** began by introducing diluted standards, which were maintained at varying concentrations (i.e., 20, 40, 80, 160, 320, and 640 pg/ml), into separate wells. One well was designated as the set standard well, while the others were designated as testing sample wells. In the well designated for standards, 50  $\mu$ L of diluents were added. Likewise, in the wells designated for testing samples, 40  $\mu$ L of diluents were added. Subsequently, 10  $\mu$ L of four distinct test compounds were introduced at both low and high concentrations into the testing sample wells, each in triplicate, except for the blank well, which received no sample. Every well was covered using the plate cover supplied with the kit and subsequently incubated at 37°C for about 45 minutes. After the incubation period, each well was aspirated, and a four-time wash was performed for 1–3 minutes with the wash buffer (250  $\mu$ L each time) supplied with the kit. Following this, any remaining wash buffer was aspirated to ensure its complete removal. Subsequently, 50  $\mu$ L of HRP-conjugated detection antibody was introduced into each well, excluding the blank. The wells were then covered once more and incubated at 37°C for half an hour. Following that, each plate was aspirated and underwent a minimum of five washes with wash buffer. Subsequently, 50  $\mu$ L of Chromogen solution-B was added to each well, gently mixed, and allowed to re-incubate at 37°C for 15 minutes, shielded from light. In the last step, 50  $\mu$ L of stop solution was introduced into each well, leading to a color change from blue to yellow. Once the color transitioned to yellow, the optical absorbance at a wavelength of 450 nm was immediately measured using a microplate ELISA reader, and the results were recorded.

### 5.6. *In vivo* evaluation of synthesized compounds

The evaluation of synthesized compounds *in vivo* was conducted with the approval of the Institutional Animal Ethics Committee (IAEC) under the corresponding approval number: LPU/IAEC/2023/24

**5.6.1 Experimental animals:** *in vivo* investigation comprised male Sprague Dawley rats weighing between 350-380 grams. The rats were housed in a controlled conditions with a 12-hour light/dark cycles and a temperature of  $25 \pm 5^\circ$  C, and kept in paddy husk beds. During the study, the rats were given a standard laboratory pellet diet and had

## **MATERIAL, METHODS AND EXPERIMENTAL**

---

unrestricted access to water, aiming to maintain consistency in diet and hydration, control for potential confounding variables, and ensure the animals' overall health and well-being. The study incorporated nine treatment groups, as outlined in the table. The identical treatment protocol was administered to all groups after the two-week period of dietary manipulation, commencing on day 15.

### **5.6.2 Assessment of Urine Excretion of Glucose and other electrolytes**

Glucosuria was measured in normal SD rats as part of a glucose tolerance test protocol. SD rats were further divided into vehicle control, synthesized compound-SSS 95 per se, synthesized compound-SSS 100 per se, Glucose, Glucose + Dapagliflozin, Glucose + synthesized compound-SSS 95 (low & high dose: 5 mg/kg & 10 mg/kg), Glucose + synthesized compound-SSS 100 (low & high dose: 5 mg/kg & 10 mg/kg).

In preparation for baseline urine collection, Sprague-Dawley rats were subjected to an 18-hour overnight fast and were placed in metabolism cages with unrestricted access to water. The subsequent day, the rats were weighed and randomly grouped in sets of eight (n=8), ensuring minimal variance in body weight among the groups. Fifteen minutes following the oral administration of a control substance and test compounds (low and high doses of SSS 95 and SSS 100), the rats received a glucose solution (2 grams per kilogram). They were then promptly returned to the metabolism cages to ensure complete urine collection over a 24-hour period post-dose. Food access was permitted one hour after glucose administration, & in tubes, urine samples were gathered, and their volumes were measured and documented. Glucose concentration in the urine samples was determined using the glucose oxidase-peroxidase method. Additionally, urine samples were analyzed for sodium, potassium, and chloride using the ion-selective electrode method at Sant Path Laboratory, Ludhiana. The effects of the compounds were assessed relative to the vehicle group using Microsoft Excel. Means  $\pm$  SD were utilized to present all results.

## MATERIAL, METHODS AND EXPERIMENTAL

---

**Table 2:** Approved treatment protocol for determining the Urinary Glucose Excretion model:

<b>Group Number</b>	<b>Name of the Group</b>	<b>Treatment dosage and administration route</b>	<b>Animals number</b>
<b>Group-1</b>	Vehicle	0.5% CMC, per oral	8
<b>Group-2</b>	Synthesized molecule-SSS 95 <i>per se</i>	10 mg/kg, per oral	8
<b>Group-3</b>	Synthesized molecule-SSS 100 <i>per se</i>	10 mg/kg, per oral	8
<b>Group-4</b>	Diabetic control	2 g/kg of Glucose (single dose, per oral)	8
<b>Group-5</b>	Standard control	2 g/kg of Glucose single dose, per oral) + 10 mg/kg Dapagliflozin (per oral)	8
<b>Group-6</b>	Synthesized molecule-SSS 95 low dose	2 g/kg of Glucose (single dose, p.o.) + 5 mg/kg (p.o.)	8
<b>Group-7</b>	Synthesized molecule- SSS 95 high dose	2 g/kg of Glucose (single dose, p.o.) + 10 mg/kg (p.o.)	8
<b>Group-8</b>	Synthesized molecule- SSS 100 low dose	2 g/kg of Glucose (single dose, p.o.) + 5 mg/kg (p.o.)	8
<b>Group-9</b>	Synthesized molecule- SSS 100 high dose	2 g/kg of Glucose (single dose, p.o.) + 10 mg/kg (p.o.)	8
		Total	72

## MATERIAL, METHODS AND EXPERIMENTAL

---

### Diarrhea test

The Sprague-Dawley (SD) rats received a single dosage of the test compounds at low & high doses (5mg/kg & 10mg/kg). After administration, all animals were individually housed in metabolism cages and provided with food & water ad libitum for the duration of the experiment. The SD rats were closely monitored on an hourly basis for the first 8 hours post-dosing. The bottoms of the cages were lined with white paper for easy observation of fecal consistency. Diarrhea presence was documented and evaluated based on the subsequent criteria: (-) normal feces (black color, well-formed, firm), (+) soft feces (light color, well-formed, but soft), (++) loose stools (light color, not well-formed, soft), (+++) watery diarrhea.

### 5.6.4 Effects of blood glucose reduction in SD rats with diabetes induced by Streptozotocin-Nicotinamide

Male SD rats underwent a period of 2-week acclimatization before the induction of diabetes through the administration of Streptozotocin (STZ) and Nicotinamide (NAM). The SD rats were subsequently categorized into various groups: vehicle control, synthesized compound-SSS 95 alone, synthesized compound-SSS 100 alone, STZ + NAM, STZ + NAM + Dapagliflozin, STZ + NAM + synthesized compound-SSS 95 (at low & high doses: 5 mg/kg & 10 mg/kg), and STZ + NAM + synthesized compound-SSS 100 (at low & high doses: 5 mg/kg & 10 mg/kg). On the 15th day, diabetes was induced in the SD rats by administering a single intraperitoneal STZ injection at a dosage of 60 mg/kg. This was freshly prepared in 0.1 M citrate buffer (pH 4.5), following the intraperitoneal administration of nicotinamide (NAM) at 120 mg/kg, which was prepared in a saline solution, with an interval of 15 minutes. Following 7 days of STZ-NAM injection administration, the rats' body weight and blood glucose levels were evaluated using an Accu-Chek Active Glucometer through tail pricking to confirm disease induction. Random groups of eight rats were assigned, ensuring their average blood glucose levels fell within 250-450 mg/dL. On the 22nd day, the disease-induced rats were orally administered a solution containing test compounds (at low dose: 5 mg/kg and high dose: 10 mg/kg) dissolved in a vehicle, along with the vehicle alone, as per the treatment protocol. Following the commencement of treatment, PGL

## MATERIAL, METHODS AND EXPERIMENTAL

and body weight indices were re-evaluated at 30, 60, 90, and 120-minute time points after the administration of test compounds to observe their immediate effects. The treatment regimen continued for 7 days. Subsequently, on the 28th day, BW and PGL were examined to evaluate the treatment's impact on the diseased rats. The rats maintained their normal pellet diet throughout the study. Finally, the rats were sacrificed for histopathological examination of the pancreas and kidneys.

**Table 3:** Approved treatment protocol for type-II diabetes model:

Group Number	Name of the Group	Treatment dosage and administration route	Animals number
Group-1	Vehicle control	0.5% CMC (per oral)	8
Group-2	Synthesized molecule-SSS 95 <i>per se</i>	10 mg/kg (per oral)	8
Group-3	Synthesized molecule-SSS 100 <i>per se</i>	10 mg/kg (per oral)	8
Group-4	Diabetes control	STZ (60 mg/kg, single dose, i.p.) + NAM (120 mg/kg, single dose, i.p.)	8
Group-5	Standard control	STZ (60 mg/kg, single dose, i.p.) + NAM (120 mg/kg, single dose, i.p.) + 10 mg/kg of Dapagliflozin (per oral)	8
Group-6	Synthesized molecule-SSS 95 low dose	STZ (60 mg/kg, single dose, i.p.) + NAM (120 mg/kg, single dose, i.p.) + 5 mg/kg (per oral)	8
Group-7	Synthesized molecule-SSS 95 high dose	STZ (60 mg/kg, single dose, i.p.) + NAM (120 mg/kg, single dose, i.p.) + 10 mg/kg (per oral)	8
Group-8	Synthesized molecule-SSS 100 low dose	STZ (60 mg/kg, single dose, i.p.) + NAM (120 mg/kg, single dose, i.p.) + 5 mg/kg (per oral)	8
Group-9	Synthesized molecule-SSS 100 high dose	STZ (60 mg/kg, single dose, i.p.) + NAM (120 mg/kg, single dose, i.p.) + 10 mg/kg (per oral)	8
		Total	72

## MATERIAL, METHODS AND EXPERIMENTAL

---

### **Parameters of evaluation:**

**PGL:** was evaluated before treatment commencement on day 22 and on the 28th day post-treatment, in accordance with the protocol, to monitor the impact of the synthesized test compounds and the response of rats with type-II diabetes and insulin resistance.

**Body weight assessment:** On days 15, 22, and 28 of the protocol, respectively, the animal's body weights of the animals were assessed.

### **5.7 Histopathological evaluation of SD rats Pancreas and Kidneys**

Upon the sacrifice of rats in each group, the SD rats' kidneys and pancreas were collected and promptly placed in a 10% formalin solution to prevent tissue desiccation or damage during dissection. Subsequently, tissue slides were readied and underwent eosin & haematoxylin staining.<sup>121</sup> A pathologist at Synergy Laboratory in Jalandhar conducted the histopathological evaluation.

### **5.8 Statistical calculations**

The mean $\pm$ SD was used to analyze the results from both *in vitro* and *in vivo* assessments. Statistical analysis for the diabetic studies and urinary glucose excretion data employed the one way ANOVA approach implemented with Sigma Plot Software version 11.0 (Tukey-test). The significance thresholds were established at 5%, 1%, and 0.1% with corresponding p-values of < 0.05, < 0.01, and < 0.001, respectively.

# *CHAPTER 6*



## RESULTS AND DISCUSSION

### 6.1 Molecular docking studies

After taking into account the fundamental non-glucoside triazole scaffold from literature,<sup>106</sup> we have designed novel 1, 3, 4 thiadiazole compounds by introducing the electron releasing groups i.e. methyl and methoxy, located at the para position of phenyl ring A designated as R<sub>1</sub>. Moreover, we have also substituted 2, 3, 4, 5 or 6 positions of the phenyl ring B next to imine bond designated as R<sub>2</sub> with various EDGs/EWGs viz methyl, methoxy, hydroxyl, nitro, chloro, bromo, fluoro, trifluoromethyl, dimethylamino, pyridyl, difluoromethoxy (**Figure 26**). On the basis of above facts we have designed 102 compounds Schiff base of 1, 3, 4 thiadiazole scaffold and performed docking studies to calculate binding affinity scores using AutoDock vina 1.5.6. To perform the docking analysis, the 3DH4 protein was initially validated by extracting a ligand from it, and then polar hydrogen was added to it. The root was detected and the resulting structure was saved as pdbqt file. The SGLT2 protein is validated by extracting and docking the co-crystallized ligand (gal 701) in the same manner as the actual ligand.<sup>113-115</sup> The AutoDock Tool and command prompt were used to determine the binding affinity (Kcal/mol) of all designed compounds. **Table 4** displays the binding affinities of 102 meticulously designed molecules, showcasing scores ranging from -10.7 to -7.7 Kcal/mol, in direct comparison to the established standard drug, dapagliflozin.

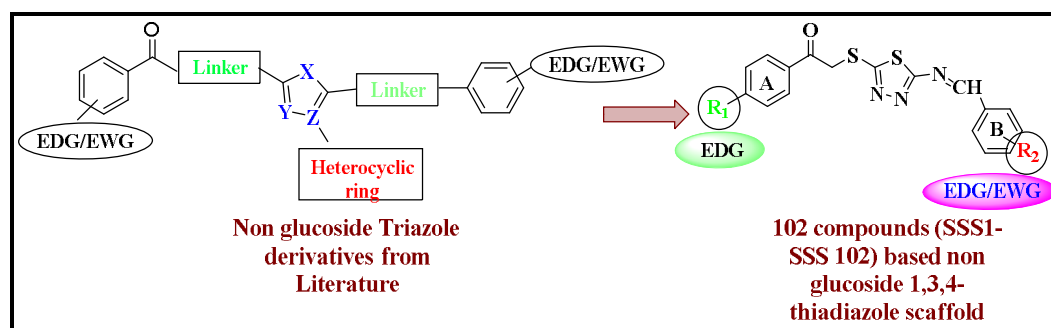
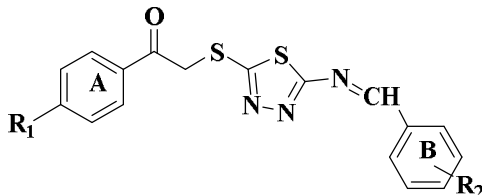


**Figure 26:** Designing of non-glucoside 1,3,4-thiadiazole based pharmacophore as SGLT2 Inhibitors.

## RESULTS AND DISCUSSION

**Table 4. Structure and binding affinity of designed molecules from Schiff base of 1, 3, 4-thiadiazole derivatives.**



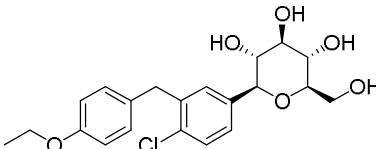
Molecule	R <sub>1</sub>	R <sub>2</sub>	Binding Affinity (Kcal/mol)
SSS 35	CH <sub>3</sub>	2-OH	-10.7
SSS 95	CH <sub>3</sub>	3,4-dihydroxy-5-nitro	-10.6
SSS 40	H	4-OH	-10.4
SSS 100	H	2-OH-3-OCH <sub>3</sub>	-10.3
SSS 36	OCH <sub>3</sub>	2-OH	-10.2
SSS 102	OCH <sub>3</sub>	2-OH-3-OCH <sub>3</sub>	-10.1
SSS 18	OCH <sub>3</sub>	3,4-(OCH <sub>3</sub> ) <sub>2</sub>	-10
SSS 98	CH <sub>3</sub>	3-hydroxy-4-methoxy	-10
SSS 96	OCH <sub>3</sub>	3,4-dihydroxy-5-nitro	-9.9
SSS 34	H	2-OH	-9.8
SSS 41	CH <sub>3</sub>	4-OH	-9.8
SSS 16	H	3,4-(OCH <sub>3</sub> ) <sub>2</sub>	-9.7
SSS 62	CH <sub>3</sub>	2-Cl-3-CF <sub>3</sub>	-9.4
SSS 23	CH <sub>3</sub>	3,4,5-(OCH <sub>3</sub> ) <sub>3</sub>	-9.4
SSS 79	H	2,4-Dihydroxy	-9.4
SSS 55	H	4-(2-pyridyl)	-9.3
SSS 37	H	3-OH	-9.3
SSS 38	CH <sub>3</sub>	3-OH	-9.3
SSS 51	OCH <sub>3</sub>	4-NO <sub>2</sub>	-9.3
SSS 63	OCH <sub>3</sub>	2-Cl-3-CF <sub>3</sub>	-9.3
SSS 56	CH <sub>3</sub>	4-(2-pyridyl)	-9.3
SSS 50	CH <sub>3</sub>	4-NO <sub>2</sub>	-9.2
SSS 49	H	4-NO <sub>2</sub>	-9.2
SSS 57	OCH <sub>3</sub>	4-(2-pyridyl)	-9.2
SSS 2	CH <sub>3</sub>	H	-9.2
SSS 5	CH <sub>3</sub>	4-Cl	-9.2
SSS 8	CH <sub>3</sub>	2-Cl	-9.2
SSS 47	CH <sub>3</sub>	3-NO <sub>2</sub>	-9.2
SSS 48	OCH <sub>3</sub>	3-NO <sub>2</sub>	-9.2
SSS 59	CH <sub>3</sub>	4-OCHF <sub>2</sub>	-9.2
SSS 61	H	2-Cl-3-CF <sub>3</sub>	-9.2
SSS 68	CH <sub>3</sub>	2,3-Dichloro	-9.2
SSS 69	OCH <sub>3</sub>	2,3-Dichloro	-9.2

## RESULTS AND DISCUSSION

---

SSS 71	CH <sub>3</sub>	3,4-Dichloro	-9.2
SSS 77	CH <sub>3</sub>	2,6-Dichloro	-9.2
SSS 80	CH <sub>3</sub>	2,4-Dihydroxy	-9.2
SSS 83	CH <sub>3</sub>	4-F	-9.2
SSS 86	CH <sub>3</sub>	4-CH <sub>3</sub>	-9.2
SSS 89	CH <sub>3</sub>	2,4,6-(OCH <sub>3</sub> ) <sub>3</sub>	-9.2
SSS 17	CH <sub>3</sub>	3,4-(OCH <sub>3</sub> ) <sub>2</sub>	-9.1
SSS 42	OCH <sub>3</sub>	4-OH	-9.1
SSS 10	H	3-Cl	-9.1
SSS 19	H	4-OH-3-OCH <sub>3</sub>	-9.1
SSS 25	H	3-Br	-9.1
SSS 32	CH <sub>3</sub>	5-Br	-9.1
SSS 66	OCH <sub>3</sub>	3-OC <sub>2</sub> H <sub>5</sub> -4-OH	-9.1
SSS 78	OCH <sub>3</sub>	2,6-Dichloro	-9.1
SSS 81	OCH <sub>3</sub>	2,4-Dihydroxy	-9.1
SSS 84	OCH <sub>3</sub>	4-F	-9.1
SSS 87	OCH <sub>3</sub>	4-CH <sub>3</sub>	-9.1
SSS 101	CH <sub>3</sub>	2-OH-3-OCH <sub>3</sub>	-9
SSS 94	H	3,4-dihydroxy-5-nitro	-9
SSS 1	H	H	-9
SSS 9	OCH <sub>3</sub>	2-Cl	-9
SSS 20	CH <sub>3</sub>	4-OH-3-OCH <sub>3</sub>	-9
SSS 39	OCH <sub>3</sub>	3-OH	-9
SSS 58	H	4-OCHF <sub>2</sub>	-9
SSS 72	OCH <sub>3</sub>	3,4-Dichloro	-9
SSS 75	OCH <sub>3</sub>	2,4-Dichloro	-9
SSS 76	H	2,6-Dichloro	-9
SSS 90	OCH <sub>3</sub>	2,4,6-(OCH <sub>3</sub> ) <sub>3</sub>	-9
SSS 3	OCH <sub>3</sub>	H	-8.9
SSS 4	H	4-Cl	-8.9
SSS 11	CH <sub>3</sub>	3-Cl	-8.9
SSS 12	OCH <sub>3</sub>	3-Cl	-8.9
SSS 13	H	4- OCH <sub>3</sub>	-8.9
SSS 26	CH <sub>3</sub>	3-Br	-8.9
SSS 27	OCH <sub>3</sub>	3-Br	-8.9
SSS 43	H	2-NO <sub>2</sub>	-8.9
SSS 53	CH <sub>3</sub>	4-N(CH <sub>3</sub> ) <sub>2</sub>	-8.9
SSS 65	CH <sub>3</sub>	3-OC <sub>2</sub> H <sub>5</sub> -4-OH	-8.9
SSS 67	H	2,3-Dichloro	-8.9
SSS 70	H	3,4-Dichloro	-8.9
SSS 88	H	2,4,6-(OCH <sub>3</sub> ) <sub>3</sub>	-8.9
SSS 91	H	2-CH <sub>3</sub>	-8.9
SSS 99	OCH <sub>3</sub>	3-hydroxy-4-methoxy	-8.9
SSS 6	OCH <sub>3</sub>	4-Cl	-8.8
SSS 7	H	2-Cl	-8.8
SSS 14	CH <sub>3</sub>	4- OCH <sub>3</sub>	-8.8

## RESULTS AND DISCUSSION

SSS 21	OCH <sub>3</sub>	4-OH-3-OCH <sub>3</sub>	-8.8
SSS 44	CH <sub>3</sub>	2-NO <sub>2</sub>	-8.8
SSS 46	H	3-NO <sub>2</sub>	-8.8
SSS 60	OCH <sub>3</sub>	4-OCHF <sub>2</sub>	-8.8
SSS 64	H	3-OC <sub>2</sub> H <sub>5</sub> -4-OH	-8.8
SSS 82	H	4-F	-8.8
SSS 15	OCH <sub>3</sub>	4- OCH <sub>3</sub>	-8.7
SSS 24	OCH <sub>3</sub>	3,4,5-(OCH <sub>3</sub> ) <sub>3</sub>	-8.7
SSS 30	OCH <sub>3</sub>	4-Br	-8.7
SSS 45	OCH <sub>3</sub>	2-NO <sub>2</sub>	-8.7
SSS 54	OCH <sub>3</sub>	4-N(CH <sub>3</sub> ) <sub>2</sub>	-8.7
SSS 73	H	2,4-Dichloro	-8.7
SSS 97	H	3-hydroxy-4-methoxy	-8.7
SSS 33	OCH <sub>3</sub>	5-Br	-8.6
SSS 29	CH <sub>3</sub>	4-Br	-8.5
SSS 22	H	3,4,5-(OCH <sub>3</sub> ) <sub>3</sub>	-8.4
SSS 28	H	4-Br	-8.4
SSS 52	H	4-N(CH <sub>3</sub> ) <sub>2</sub>	-8.2
SSS 92	CH <sub>3</sub>	2-CH <sub>3</sub>	-8.2
SSS 31	H	5-Br	-8
SSS 74	CH <sub>3</sub>	2,4-Dichloro	-7.9
SSS 93	OCH <sub>3</sub>	2-CH <sub>3</sub>	-7.9
SSS 85	H	4-CH <sub>3</sub>	-7.7
Dapagliflozin (Standard SGLT2 Inhibitor)			-8.9

Upon analysis of the docking results, it was observed that 12 newly developed molecules exhibited higher potency compared to the standard drug, dapagliflozin, with a binding affinity score of -8.9 Kcal/mol. Among these, the 12 Schiff base-derived 1,3,4-thiadiazoles demonstrated the most favorable binding affinity scores, ranging from -10.7 to -9.7 Kcal/mol, featuring EDGs at the second phenyl B as shown in Table 5. Furthermore, Pymol software was used to convert the ligand output pdbqt and SGLT2 protein pdbqt into a single pdb format,<sup>116</sup> which was then loaded into the Discovery Studio Visualizer to generate the 2D interaction file.<sup>117, 118</sup> All 12 of the best molecules were chosen to study their 2D interactions with the SGLT2 protein residues in 3DH4 active site as shown in Table 5. The glucosidal hydroxyl group of the dapagliflozin molecule demonstrated a hydrogen bond interaction with Asn 267, Asn 260 & Asn 147. Best designed molecules showed hydrogen bond interactions with Asn 267, Asn 260 &

## RESULTS AND DISCUSSION

Asn 147 amino acid residues of active site of 3DH4 similar to standard drug dapagliflozin. Additionally, these molecules also showed hydrophobic pie-pie T shaped & pie-pie stacking interactions with Tyr 263,  $\pi$ -sulphur Interactions with Tyr 263 and Tyr 262,  $\pi$ -alkyl/alkyl interactions with Ile 270 & Ala 259 amino acids residue of protein. The **Figure 27** illustrates the 2D interactions of select optimally designed molecules with 3DH4 active site.<sup>122</sup>

**Table 5:** The interactions of best designed molecules with nearby protein residues in 3DH4 active site.

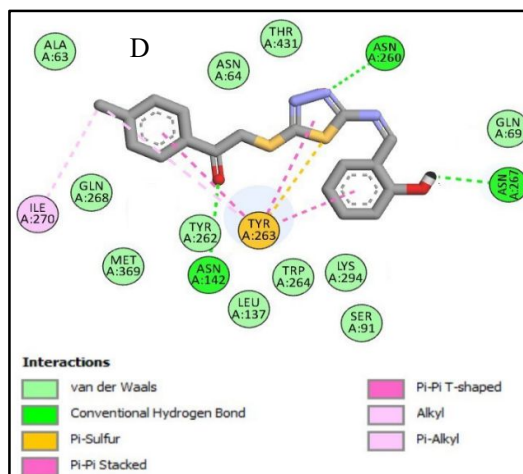
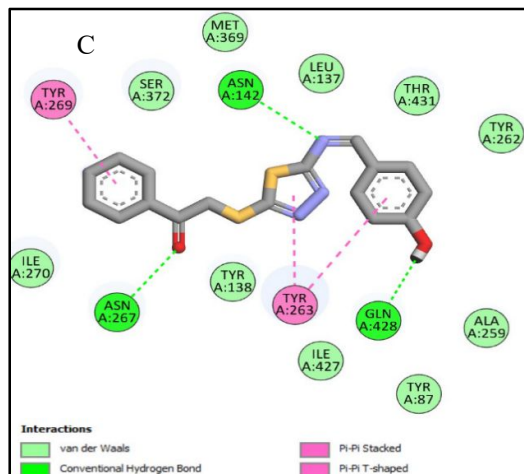
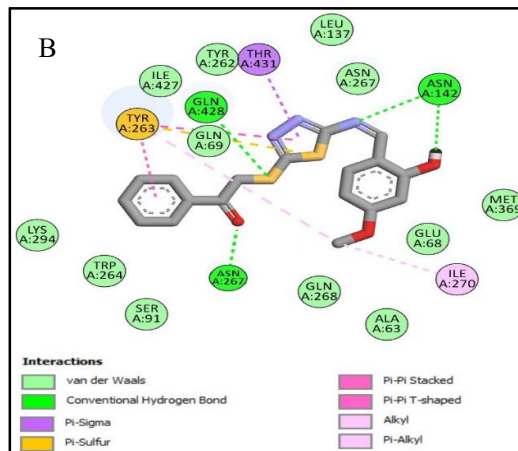
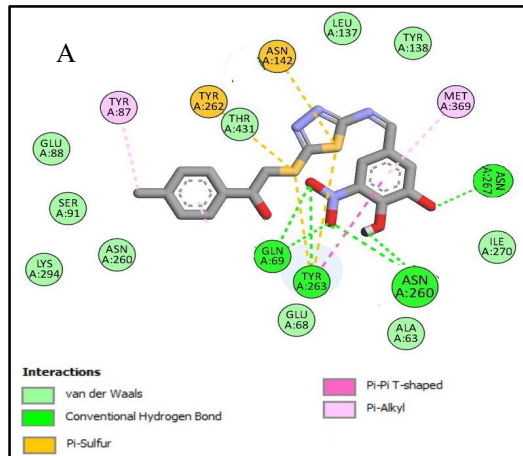
S.N O.	Molecules	Binding affinity score (Kcal/mol)	Hydrogen Bond Interactions	pie-pie T shaped & pie-pie stacking Interactions	pie - sulphur Interactions	$\pi$ - $\sigma$ Interactions	$\pi$ -alkyl/alkyl Interactions
1.	SSS 35	-10.7	Asn 142 Asn 267 Asn 260	Tyr 263	Tyr 263		Tyr 263 Ile 270
2.	SSS 95	-10.6	Asn 260 Tyr 263 Gln 69 Asn 267	Tyr 263	Tyr 262 Asn 142	-	Tyr 87 Met 369
3.	SSS 40	-10.4	Asn 142 Asn 267 Gln 428	Tyr 263 Tyr 269	-	-	-
4.	SSS 100	-10.3	Asn 142 Asn 267	Tyr 263	Tyr 263 tyr 262	Thr 431	Ile 270
5.	SSS 36	-10.2	Asn 267 Asn 260 Ser 91	Tyr 263	Tyr 262 Tyr 263	-	Met 359

## RESULTS AND DISCUSSION

---

6.	SSS 102	-10.1	Asn 267 Asn 142	Tyr 263	-	Ile 270	Tyr 263 Ile 270 Ala 259
7.	SSS 18	-10.0	Asn 267 Asn 142 Asn 260	Tyr 263	Tyr 262 Tyr 263	-	Leu 137 Trp 264 Ala 259 Ala 63 Ile 270
8.	SSS 98	-10.0	Asn 142 Asn 267 Ala 259	Tyr 263	-	Ile 270	Tyr 263 Ile 270
9.	SSS 96	-9.9	Asn 260 Asn 267 Asn 64	-	Tyr 262 Tyr 263	-	Trp 264 Ala 259 Leu 137
10	SSS 34	-9.8	Asn 142 Gln 428 Trp 264	Tyr 263	Tyr 263 tyr 262	-	-
11	SSS 41	-9.8	Asn 267 Lys 294 Gln 69	Tyr 263	Tyr 262 Tyr 263	-	Tyr 263 Ile 270
12	SSS 16	-9.7	Asn 260 Gln 428	Tyr 263	Tyr 262 Tyr 263	Thr 431	Ile 270
13	Dapaglif lozin (001)	-8.9	Asn 267 Asn 142 Asn 260	Tyr 269	-	Ile 270	Tyr 269 Ile 270 Ala 63

# RESULTS AND DISCUSSION



## RESULTS AND DISCUSSION

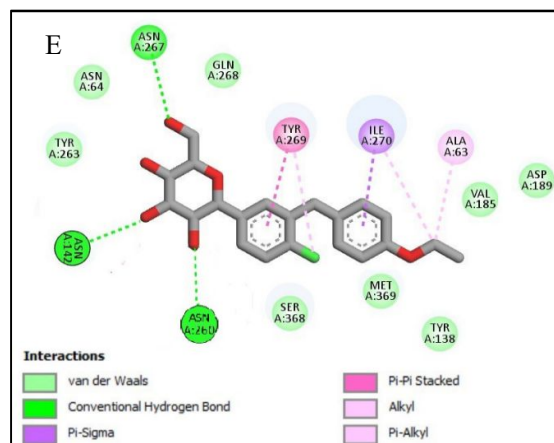


**Figure 27:** 2D Interactions of few best designed compounds SSS 95 (A), SSS 100 (B), SSS 40 (C), SSS 35 (D) and dapagliflozin (E) on SGLT2 protein.

### 6.2 Synthesis and Characterization of synthesized compounds

Compounds were synthesized based on the highest binding affinity scores exhibiting optimal binding affinities ranging from -9.7 to -10.7 kcal/mol within the active site of SGLT2 protein (PDB ID: 3DH4) as shown in **Table 6**. The synthesis of novel non-glucoside Schiff bases of 1, 3, 4-thiadiazole derivatives was validated through LCMS, Proton NMR ( $^1\text{H}$  &  $^{13}\text{C}$ ). Furthermore, synthesized compounds underwent comprehensive evaluation, including *in-silico* toxicity and ADME studies, as well as *in vitro* and *in vivo* activity assessments.

**Table 6:** Structural representation and percentage yield of potent synthesized compounds based on the highest binding affinity scores.

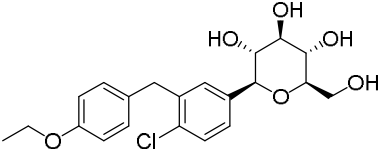
S. No.	Compound Code	Structure of Compounds	Binding Affinity (Kcal/mol)	% Yield
1.	SSS 34		-9.8	90



## RESULTS AND DISCUSSION

2.	SSS 100		-10.3	90
3.	SSS 16		-9.7	95
4.	SSS 40		-10.4	92
5.	SSS 35		-10.7	80
6.	SSS 95		-10.6	90
7.	SSS 98		-10.0	70
8.	SSS 41		-9.8	77
9.	SSS 36		-10.3	90
10	SSS 102		-10.1	95

## RESULTS AND DISCUSSION

11	SSS 18		-10.0	70
12	SSS 96		-9.9	90
13	Dapaglifloz -in		-8.9	

### 6.2.1 Synthesis procedure of 2-amino-5-mercapto-1,3,4-thiadiazole (2)

Thiosemicarbazide 1 (10 mmol) and carbon disulfide (10 mmol) were gently refluxed for 30 minutes. Following the cooling process, water was introduced, and the mixture underwent reflux for a duration of 4 hours, followed by filtration. The resultant solution was neutralized using potassium hydroxide. Subsequently, the precipitate was filtered, and recrystallization was carried out from ethanol, yielding 84%.

### 6.2.2 Synthetic discussion on 2-amino-5-benzoylmethylenethio-1,3,4-thiadiazole derivatives 4(a-c).

Upon stirring, potassium hydroxide (10 mmol) was added to a slurry of compound 2 (10 mmol) in water, a colourless solution was formed under stirring at room temperature. Subsequently, 10 mmol of various substituted  $\alpha$ -bromoketones 3(a-c) in ethanol were swiftly introduced with stirring, resulting in the formation of a thick reaction mixture. The mixture was stirred vigorously for 6 hours at room temperature, followed by a 30-minute cooling period and dilution with cold water. The solid was filtered, washed with water and ether, and subsequently recrystallized from ethanol, yielding 80-85%.

## RESULTS AND DISCUSSION

---

### 6.2.3 Synthetic discussion on Schiff bases of 2-amino-5-benzoylmethylenethio-1,3,4-thiadiazole derivatives.

To obtain the final product, 1 equivalent of **4(a-c)** was reacted with 1.5 equivalents of various substituted aromatic aldehydes in isopropyl alcohol at a volume ratio of 5:1. The reaction mixture underwent reflux at a temperature 60-70°C for 18-20 hours, with the inclusion of 2-3 drops of acetic acid. Upon completion, the product was cooled to room temperature, and distillation was conducted using a vacuum pressure rotavapor to obtain a pure and dried product. The resulting crude product was then subjected to recrystallization using methanol to obtain a pure and dried product with the yield of 70-95%. Purity and structural confirmations of all the synthesized compounds has been determine using the spectral analysis *viz* NMR and Mass spectrometry.

### 6.3 *In-silico* toxicity studies

At present, the concern over the toxicity of synthesized compounds is substantial. To address this, a thorough examination was conducted on all synthesized molecules to assess any potential toxicity issues impeding their further development. A study was carried out on 12 synthesized compounds, and *in-silico* toxicity predictions were executed using the online software available at <https://lazar.in-silico.ch/predict>.

The process for predicting the toxicity of synthesized compounds involves the following steps:

1. Generate or sketch the 2D structure of the designed compound using Chem Bio Draw software.
2. Duplicate the SMILES notation for each structure from Chem Bio Draw.
3. Transfer the SMILES data to a web page.
4. Subsequently, conduct predictions for all types of toxicity.

The **Table 7** displays the *in-silico* profile of the synthesized compounds, revealing that all the synthetic compounds exhibit non-carcinogenic properties in rats similar to standard dapagliflozin. Furthermore, all the synthesized molecules exhibit non-mutagenic characteristics, in contrast to dapagliflozin, which possesses mutagenic properties.

## RESULTS AND DISCUSSION

---

**Table 7:** *In-silico* toxicity predictions.

<b>Molecule Code</b>	<b>Carcinogenicity (mouse)</b>	<b>Carcinogenicity (Rat)</b>	<b>Mutagenicity (Salmonella typhimurium)</b>
SSS 34	NF*	Non-carcinogen	Non-mutagen
SSS 100	NF*	Non-carcinogen	Non-mutagen
SSS 16	Non-carcinogen	Non-carcinogen	Non-mutagen
SSS 40	Non-carcinogen	Non-carcinogen	Non-mutagen
SSS 35	Non-carcinogen	Non-carcinogen	Non-mutagen
SSS 95	Non-carcinogen	Non-carcinogen	Non-mutagen
SSS 98	NF*	NF*	Non-mutagen
SSS 41	NF*	Non-carcinogen	Non-mutagen
SSS 36	Non-carcinogen	Non-carcinogen	Non-Mutagen
SSS 102	Non-carcinogen	Non-carcinogen	Non-Mutagen
SSS 18	Non-carcinogen	Non-carcinogen	Non-mutagen
SSS 96	Non-carcinogen	Non-carcinogen	Non-mutagen
<b>Dapagliflozin</b>	NF*	Non-carcinogen	Mutagen

\*NF = Not found

### 6.4 *In-silico* ADME studies

The ADMET methodology holds paramount importance in drug discovery and production projects, as it strives to attain the optimal combination of properties essential for lead and hits development. Given that toxicity is linked to the pharmacokinetic profile of compounds, we conducted an *in-silico* analysis of ADME properties for all the synthesized compounds. This analysis aimed to estimate their water solubility and lipophilicity, alongside assessing their toxicity. The *in-silico* ADME properties were quantified to predict physicochemical attributes, lipophilicity, pharmacokinetic profile, and drug likeness, adhering to the Lipinski rule of five. Lipinski's law of five is obeyed by all of the synthesized molecules (**Table 8**). Predicted lipophilicity (iLogP) of synthesized compounds were found to be 2.08-3.68. The hallmarks of drug-like behavior are enhanced by blood-brain barrier penetration (BBB) and GI absorption.

## RESULTS AND DISCUSSION

---

**Table 9** suggests that all the synthesized molecules are non-penetrating in the brain similar to standard drug dapagliflozin and have a low probability of GI absorption while dapagliflozin has high GI absorption. All of the synthesized molecules were predicted to be CYP3A4 inhibitors, but none were predicted to be CYP2D6 inhibitors. All the synthesized molecules predicted to have good oral bioavailability with a score of 0.55 and comply with druglikeness same as that of standard drug dapagliflozin. All the synthesized molecules are expected to exhibit a Topological Polar Surface Area (TPSA) falling between 75 and 150 Å<sup>2</sup>, with a corresponding 55% bioavailability.

**Table 8:** Prediction of *in-silico* Physiochemical properties

Molecule code	Log P	MW	H-bond donors	H-bond acceptors	No. of rotatable bonds	TPSA (Å <sup>2</sup> )
<b>SSS 34</b>	2.44	355.43	1	5	6	128.98
<b>SSS 100</b>	3.01	385.46	1	6	7	138.21
<b>SSS 16</b>	3.37	399.49	0	6	8	127.21
<b>SSS 40</b>	2.69	355.43	1	5	6	128.98
<b>SSS 35</b>	3.12	369.46	1	5	6	128.98
<b>SSS 95</b>	2.22	430.46	1	6	7	130.03
<b>SSS 98</b>	3.41	399.49	1	6	7	138.21
<b>SSS 41</b>	2.68	369.46	1	5	6	128.98
<b>SSS 36</b>	3.16	385.46	1	6	7	138.21
<b>SSS 102</b>	3.53	415.49	1	7	8	147.44
<b>SSS 18</b>	3.68	429.51	0	7	9	136.44
<b>SSS 96</b>	2.08	429.51	2	9	8	140.26
<b>Dapagliflozin</b>	3.12	408.87	4	6	6	99.38

## RESULTS AND DISCUSSION

**Table 9:** Prediction of *in-silico* ADME properties

Molecule code	GI Absorption	BBB permeant	CYP2D6 inhibitor	CYP3A4 inhibitor	Bioavailability score	% Bioavailability	Druglikeness
SSS 34	Low	No	No	Yes	0.55	55	Yes
SSS 100	Low	No	No	Yes	0.55	55	Yes
SSS 16	Low	No	No	Yes	0.55	55	Yes
SSS 40	Low	No	No	Yes	0.55	55	Yes
SSS 35	Low	No	No	Yes	0.55	55	Yes
SSS 95	Low	No	No	Yes	0.55	55	Yes
SSS 98	Low	No	No	Yes	0.55	55	Yes
SSS 41	Low	No	No	Yes	0.55	55	Yes
SSS 36	Low	No	No	Yes	0.55	55	Yes
SSS 102	Low	No	No	Yes	0.55	55	Yes
SSS 18	Low	No	No	Yes	0.55	55	Yes
SSS 96	Low	No	No	Yes	0.55	55	Yes
Dapagliflozin	High	No	No	Yes	0.55	55	Yes

### 6.5 *In-vitro* Evaluation

#### 6.5.1 MTT Assay

Cytotoxicity of all synthesized compounds were evaluated by MTT assay. *In vitro* MTT assay of a series of Schiff bases of 2-amino-5-benzoylmethylenethio-1,3,4-thiadiazole derivatives displayed IC<sub>50</sub> values range i.e. 50.55-102.69 µg/ml against CHO cell line, respectively. Relative % cell viability of synthesized compounds at different five concentration and IC<sub>50</sub> values of synthesized compounds were reported in **Table 10** and visually represented in **Figure 28 & 29**.

## RESULTS AND DISCUSSION

**Table 10:** Relative % cell viability and IC<sub>50</sub> value of test compounds with reference of standard drug Dapagliflozin.

S. No.	Test Compound	% Viability (Concentration µg/ml)*					IC <sub>50</sub>
		6.25	12.5	25	50	100	
1.	SSS 34	84.60±0.42	72.42±0.20	62.22±0.30	44.09±0.20	36.63±0.27	59.76
2.	SSS 100	93.38±1.61	84.13±1.60	75.35±0.58	64.11±1.66	52.88±1.79	<b>98.82</b>
3.	SSS 16	78.37±0.22	69.40±0.35	57.22±0.26	45.04±0.26	29.08±0.27	50.55
4.	SSS 40	84.51±0.46	75.82±0.40	67.04±0.27	58.07±0.13	49.95±0.20	<b>89.77</b>
5.	SSS 35	93.38±1.71	84.23±1.50	75.16±1.31	64.11±1.28	54.67±1.89	<b>102.69</b>
6.	SSS 95	93.38±1.74	84.13±1.27	75.07±1.27	63.92±0.78	54.01±2.39	<b>101.07</b>
7.	SSS 98	78.09±0.94	70.82±0.35	64.30±0.48	50.42±0.23	42.11±0.46	69.12
8.	SSS 41	81.09±0.74	71.29±0.53	58.82±0.50	46.17±0.61	33.33±0.27	55.92
9.	SSS 36	86.68±0.74	73.74±0.53	68.46±0.63	61.66±0.33	45.70±0.88	84.28
10.	SSS 102	84.79±0.38	75.92±0.13	66.57±0.61	54.29±0.27	44.75±0.23	77.14
11.	SSS 18	78.09±0.38	71.01±0.20	64.58±0.35	50.51±0.50	42.20±0.40	69.44
12.	SSS 96	78.09±0.80	71.01±0.20	64.49±1.13	50.14±0.40	42.02±0.42	68.87
13.	Dapagliflozin	80.78±0.34	75.69±0.43	68.87±0.23	60.42±0.28	57.34±0.23	117.95

\*All values are expressed as the mean± SEM and determinations were carried out in triplicate.

## RESULTS AND DISCUSSION

---

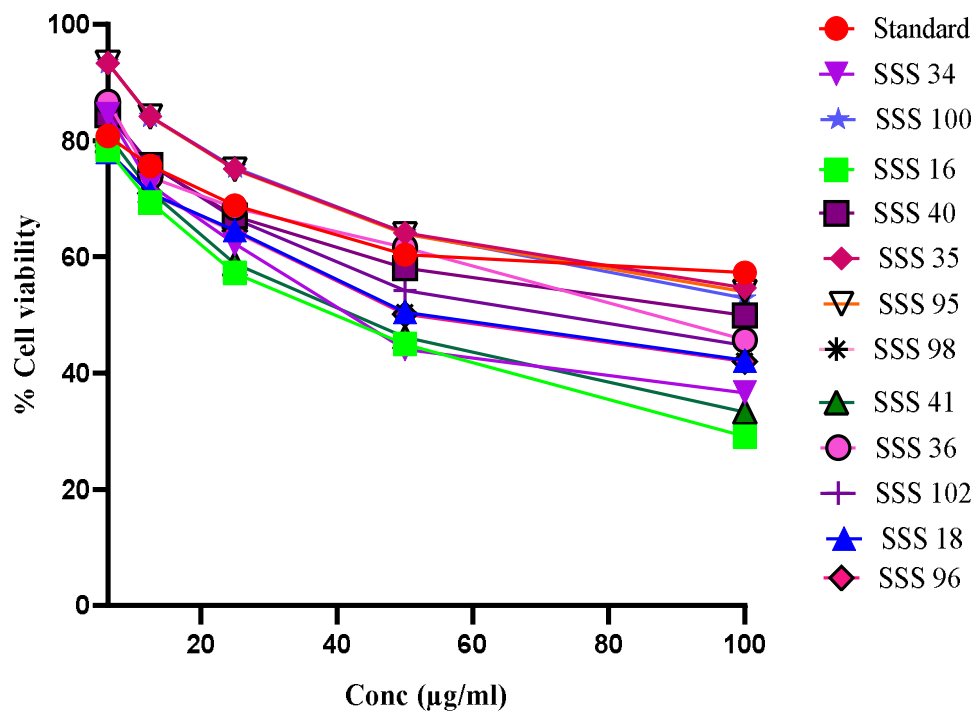


**Figure 28:** Effect of test compounds and Standard i.e. dapagliflozin at five different concentrations on % cell viability.



## RESULTS AND DISCUSSION

---

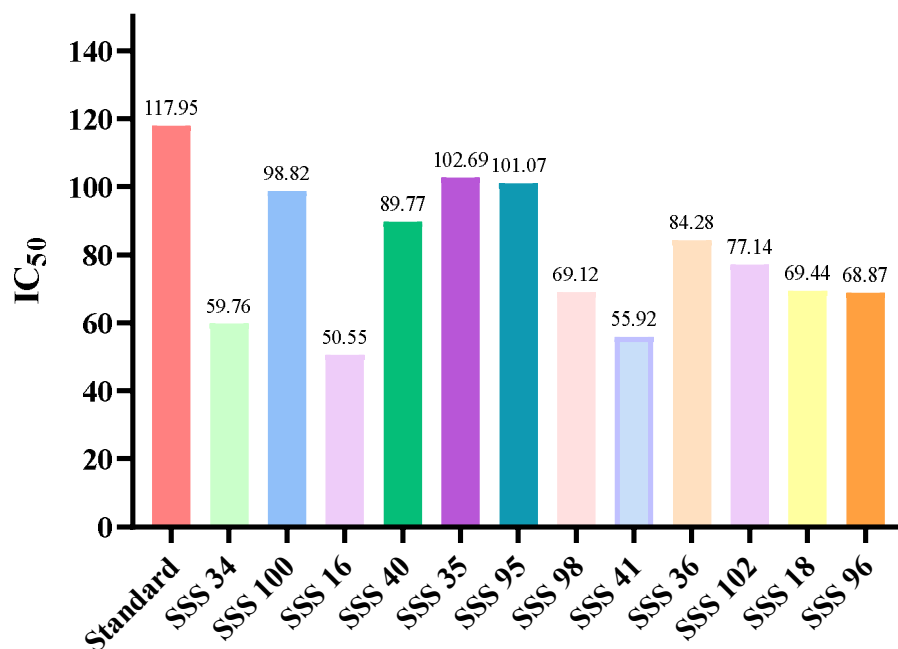


**Figure 29:** Effect of test compounds and Standard drug (dapagliflozin) on IC<sub>50</sub>.

### DISCUSSION

The initial synthesized compound, **SSS 34**, is characterized by an unsubstituted phenyl ring A and a phenyl ring B substituted with an electron-donating group, namely a hydroxyl group, at the *ortho* position. These two rings are connected by a sulfur bridge and an imine bond. The MTT assay results suggest that **SSS 34** exhibits a moderate cytotoxic impact on cell viability, possessing an IC<sub>50</sub> value of 59.76 μg/ml, in comparison to the reference drug with IC<sub>50</sub> values of 117.95 μg/ml. *In-vitro* results further validated by docking study. **SSS 34** demonstrated a dock score of -9.8 kcal/mol. Notably, there are two hydrogen bond interactions observed: one between the carbonyl group and Asn 142, and another between the thiadiazole ring and Gln 428. Additionally, the hydroxyl group of phenyl ring B exhibits one hydrogen bond interactions with amino acid residues such as Trp 264. The sulfur bridge and the thiadiazole ring in **SSS 34** exhibit π-sulfur interactions with Tyr 262 and Tyr 263. Furthermore, the phenyl ring B demonstrates a π-π T-shaped interaction with Tyr 263.

## RESULTS AND DISCUSSION

---

**SSS 40** was designed by incorporating an electron-donating group (-OH) moiety at the *para* position. The outcomes of the MTT assay show that **SSS 40** exhibits a reduced cytotoxic impact on cell viability, as evidenced by an  $IC_{50}$  value of 89.77  $\mu\text{g/ml}$ , in comparison to the reference drug with  $IC_{50}$  values of 117.95  $\mu\text{g/ml}$ . **SSS 40** has showed the docking score -10.4 kcal/mol. Three hydrogen bond interactions were observed: one between the carbonyl group and Asn 267, another between the imine and Asn 142, and a third between the -OH moiety of phenyl ring B and Gln 428. The phenyl ring B and thiadiazole ring demonstrates a  $\pi$ - $\pi$  T-shaped interaction with Tyr 263. The phenyl ring A shows  $\pi$ - $\pi$  stacking with Tyr 269. **SSS 40** demonstrates a superior  $IC_{50}$  value and enhanced cell viability compared to **SSS 34**. It is suggested that the electron-releasing behaviour of the hydroxyl moiety, located at the *para* position has a more pronounced effect on enhancing cell viability compared to its presence at the *ortho* position.

**SSS 100** was synthesized by introducing a -OH moiety at the second position and a -CH<sub>3</sub>O moiety at the fourth position of phenyl ring B, while phenyl ring A remained unaltered. The MTT assay results reveal that **SSS 100** exhibits a reduced cytotoxic effect on cell viability, as indicated by an  $IC_{50}$  value of 98.82  $\mu\text{g/ml}$ , in comparison to the standard drug with  $IC_{50}$  values of 117.95  $\mu\text{g/ml}$ . Docking score of **SSS 100** was found to be -10.3 kcal/mol. The *in-vitro* results are further corroborated by the docking study. Similar to the standard drug, the hydroxyl group and imine in the compound demonstrated hydrogen bond interactions with Asn 142, and another interaction was observed between the carbonyl group and Asn 267. The methoxy group of phenyl ring B is involved in alkyl and pie-alkyl interactions with Ile 270. Additionally, the thiadiazole ring demonstrates  $\pi$ - $\sigma$  interaction &  $\pi$ -sulfur interactions with Thr 431 and Tyr 263. The observation suggests that the presence of a -OH & -CH<sub>3</sub>O moiety, located at the 2<sup>nd</sup> & 4<sup>th</sup> position of phenyl ring B contributes to an improvement in both the docking score and cell viability.

**SSS 16** was crafted by introducing two methoxy groups at the *meta* and *para* positions of phenyl ring B, while phenyl ring A remained unaltered, resulting in a docking score of -9.7 kcal/mol. This alteration resulted in decreased cell viability in CHO cells, as evidenced by an  $IC_{50} = 50.55 \mu\text{g/ml}$ , compared to the standard drug ( $IC_{50} = 117.95 \mu\text{g/ml}$ ). It shows only one hydrogen bonding interaction with Asn 260 amino acid

## RESULTS AND DISCUSSION

---

residues similar to dapagliflozin. This effect is attributed to the electron-donating nature of the methoxy moiety at the *3rd* and *4th* positions causing steric hindrance on ring B, ultimately lower IC<sub>50</sub> value and has highest cytotoxic effect.

**SSS 35** was created through the addition of a –CH<sub>3</sub> moiety at the fourth position of phenyl ring A and a hydroxyl group at the *ortho* position of phenyl ring B. **SSS 35** demonstrated notable cell viability in CHO cells, presenting highest IC<sub>50</sub> = 102.69 μg/ml, in contrast to the dapagliflozin (IC<sub>50</sub> = 117.95 μg/ml). The binding affinity of **SSS 35** was determined to be -10.7 kcal/mol. Three hydrogen bond interaction is observed with between the carbonyl group & Asn 142, thiadiazole ring & Asn 260 and hydroxyl group of phenyl ring B & Asn 267 similarly shown by reference drug. Phenyl ring A and B, as well as the thiadiazole ring, demonstrate a pie-pie T-shaped & pie-pie stacking, interactions respectively, with Tyr 263 amino acid residues of the protein. The methyl group of phenyl ring A participates in alkyl and pie-alkyl interactions with the Ile 270 and Tyr 263 like amino acid residues. Furthermore, the sulfur of the thiadiazole ring engages in a π-sulfur interaction with Tyr 263. This can be attributed to the electron-donating nature of both the methyl and hydroxyl groups of phenyl rings A and B, contributing to the stronger binding affinity, higher IC<sub>50</sub> value and are less cytotoxic.

**SSS 41** were produced by adding a –CH<sub>3</sub> moiety to the fourth position of phenyl ring A and introducing a hydroxyl moiety to the 4<sup>th</sup> position of phenyl ring B. Binding affinity of **SSS 41** was determined to be -9.8 kcal/mol, demonstrating three H-bonding interactions with the amino acids Asn 267, Gln 69, and Lys 294. The results reveals that the electron-releasing groups, namely methyl & hydroxyl moieties both located at the 4<sup>th</sup> position of phenyl rings A and B, resulted in a decrease in cell viability. This effect is further highlighted by a lower IC<sub>50</sub> = 55.92 μg/ml and more cytotoxic compared to **SSS 35**.

**SSS 95** was synthesized by introducing a –CH<sub>3</sub> moiety at the 4<sup>th</sup> position of phenyl ring A and a 3,4-dihydroxy-5-nitro group at phenyl ring B, exhibiting strong binding affinity with a docking score of -10.6 kcal/mol. The nitro & hydroxyl group oxygen atoms engage in four hydrogen bond interactions with Gln 69, Tyr 263, Asn 260 and Asn 267. The sulfur bridge and thiadiazole ring exhibit π-sulfur interactions with Tyr 262 and Asn 142. Phenyl ring B demonstrates a pie-pie T-shaped interaction with Tyr 263. Both

## RESULTS AND DISCUSSION

---

phenyl rings A and B exhibit pi-alkyl interactions with Tyr 87, Met 369, & Ala 259 like amino acid residues. Notably, SSS 95 displayed substantial cell viability on CHO cells, boasting an IC<sub>50</sub> value of 101.07 µg/ml in comparison to the standard drug with IC<sub>50</sub> values of 117.95 µg/ml. Our conjecture is that the electron-withdrawing characteristic of the nitro group predominates over the electron-donating attributes of the methyl and hydroxyl groups in phenyl rings A and B, leading to a favorable docking score and IC<sub>50</sub> value, suggesting lower cytotoxicity.

**SSS 98** was produced by adding a -CH<sub>3</sub> moiety to the 4<sup>th</sup> position of phenyl ring A and introducing 3-hydroxy-4-methoxy moiety on the phenyl ring B. **SSS 98** exhibits H-bonding interactions with Asn 142 amino acid residue of protein, yielding a docking score of -10.0 kcal/mol. It has moderate cytotoxic effect on CHO cells (IC<sub>50</sub> = 69.12 µg/ml)

Following that, we synthesized and assessed two compounds, **SSS 36** and **SSS 102**, incorporating a methoxy group at the para position of phenyl ring A. Additionally, a hydroxyl group was introduced at the ortho position of phenyl ring B in both **SSS 36** and **SSS 102**, with **SSS 102** featuring an extra methoxy group at the para position. **SSS 36** displays three H-bonding with amino acid residues like Asn 267, Asn 260 and Ser 91 residue of the protein, resulting in a binding affinity-10.2 kcal/mol. It demonstrates a moderate cell viability IC<sub>50</sub> value of 84.28 µg/ml. **SSS 102** has a binding affinity of -10.1 kcal/mol and exhibits two H-bonding with Asn 267 & Asn 142. Despite the slightly lower docking score, it shows a lower IC<sub>50</sub> value of 77.14 µg/ml. This deduction indicates that an additional methoxy moiety on the phenyl ring B at fourth position led to a decrease in both the docking score and cell viability in **SSS 102** compared to **SSS 36**.

**SSS 18** was synthesized by introducing three methoxy groups: one on the phenyl ring A at 4<sup>th</sup> position and another two on the phenyl ring B at the 3<sup>rd</sup> and 4<sup>th</sup> positions. The resulting docking score and IC<sub>50</sub> value were determined to be -10.0 kcal/mol and 69.44 µg/ml, respectively. This indicates that incorporation of three EDGs contributes to a decrease in both the docking score and IC<sub>50</sub> value.

## RESULTS AND DISCUSSION

SSS 96 was produced by introducing a  $-\text{CH}_3\text{O}$  moiety on the phenyl ring B at the 4<sup>th</sup> position and a 3,4-dihydroxy-5-nitro group at phenyl ring B, displaying robust binding affinity with a docking score of  $-9.9$  kcal/mol. It establishes three hydrogen bond interactions with amino acid residues Asn 260, Asn 267, and Asn 64. Despite its elevated binding affinity score, it exhibited a lower  $\text{IC}_{50}$  value, specifically  $68.87$   $\mu\text{g/ml}$  and has moderate cytotoxic effect on CHO cells.

### 6.5.2 SGLT2 Inhibition activity using hSGLT2 (SLC5A2) ELISA kit

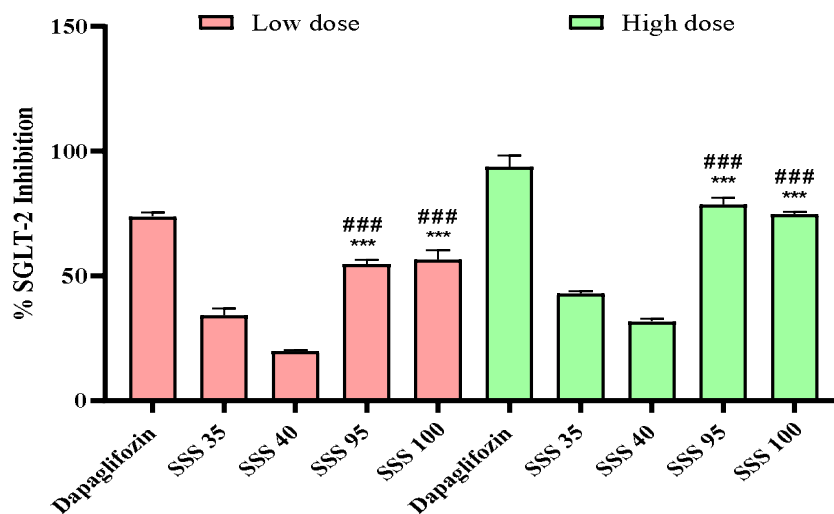
Based on the MTT assay results, SSS 35, SSS 40, SSS 95, and SSS 100 exhibited higher  $\text{IC}_{50}$  values, indicating low cytotoxicity for the synthesized compounds. Subsequently, these four compounds underwent further testing for their SGLT2 inhibiting activity. We selected high and low doses of standard and test compounds and prepared the plates using low (5mM +20 mM mannitol for osmotic balance) and high glucose media (30 mM). For instance, the high and low doses for the treatment are as: standard (110 & 55  $\mu\text{L}$ ), SSS100 (90 & 45  $\mu\text{L}$ ), SSS35 (100 & 50  $\mu\text{L}$ ), SSS95 (100 & 50  $\mu\text{L}$ ), and SSS40 (90 & 45  $\mu\text{L}$ ) and the results were recorded in Table 11 and represented as shown in Figure 30.

Table 11: % SGLT2 inhibition of test compounds

S. No.	Test Compounds	% SGLT2 Inhibition
1.	Dapaglifozin (LD)	73.8 $\pm$ 1.68
2.	SSS 35 (LD)	34.12 $\pm$ 2.80
3.	SSS 40 (LD)	19.84 $\pm$ 0.56
4.	SSS 95 (LD)	54.76 $\pm$ 1.68 <sup>***,###</sup>
5.	SSS 100 (LD)	56.34 $\pm$ 3.92 <sup>***,###</sup>
6.	Dapaglifozin (HD)	93.65 $\pm$ 4.48
7.	SSS 35 (HD)	42.85 $\pm$ 1.12
8.	SSS 40 (HD)	31.74 $\pm$ 1.12
9.	SSS 95 (HD)	78.57 $\pm$ 2.80 <sup>***,###</sup>
10.	SSS 100 (HD)	74.60 $\pm$ 1.12 <sup>***,###</sup>

## RESULTS AND DISCUSSION

Mean values are presented with their standard error (n=2), \*\*\*p<0.001, \*\*p<0.01, \*p<0.05, compared to SSS 35 and ### p<0.001, ##p<0.01, #p<0.05, compared to SSS 40. LD = Low Dose and HD = High dose



**Figure 30:** % SGLT2 inhibition of test compounds. Mean values are presented with their standard error (n=2), \*\*\*p<0.001, \*\*p<0.01, \*p<0.05, compared to SSS 35 and ### p<0.001, ##p<0.01, #p<0.05, compared to SSS 40. LD = Low Dose and HD = High dose

**SSS 95:** Methyl at R<sub>1</sub>, 3,4-dihydroxy-5-nitro at R<sub>2</sub> has binding affinity score -10.6 Kcal/mol and showed high SGLT2 inhibition activity at low dose (54.76±1.68) and high dose (78.57±2.80).

**SSS 100:** Hydrogen at R<sub>1</sub>, 2-hydroxy-4-methyl at R<sub>2</sub> has binding affinity score -10.3 Kcal/mol and exhibited high SGLT2 inhibition activity at low dose (56.34±3.92) and high dose (74.60±1.12).

**SSS 35:** Methyl at R<sub>1</sub>, 2-hydroxy at R<sub>2</sub> has binding affinity score -10.7 Kcal/mol and exhibited low SGLT2 inhibition activity at low dose (34.12±2.80) and high dose (42.85±1.12).

**SSS 40:** Hydrogen at R<sub>1</sub>, 4-hydroxy at R<sub>2</sub> has binding affinity score -10.4 Kcal/mol and exhibited least SGLT2 inhibition activity at low dose (19.84±0.56) and high dose (31.74±1.12).

## RESULTS AND DISCUSSION

---

**SSS 95** and **SSS 100** are more active compounds as compared to **SSS 35** and **SSS 40** in SGLT2 inhibition assay at both high and low doses using SLC5A2 ELISA kit. Despite having high docking score **SSS 35** and **SSS 40**, shown least SGLT2 inhibition activity. It seems that di-substitution and tri-substitution with bulkier moieties of at R<sub>2</sub> position exhibited more SGLT2 inhibition activity than mono-substitution. Favourable substitution for SGLT2 inhibition at R<sub>1</sub> position seems to be hydrogen or methyl group rather than methoxy group. Therefore for further *in vivo* evaluation of synthesized test compounds, we used **SSS 95** and **SSS 100** in spite of better binding affinity of other molecules than **SSS 100**.

**6.6 In-vivo evaluation:** Glucosuria of synthesized test compounds was measured in normal SD rats as part of a glucose tolerance test protocol. SD rats were further divided into vehicle control, synthesized compound-SSS 95 per se, synthesized compound-100 per se, Glucose, Glucose + Dapagliflozin, Glucose + synthesized compound-SSS 95 (low and high dose: 5 mg/kg and 10 mg/kg), Glucose + synthesized compound-100 (low and high dose: 5 mg/kg and 10 mg/kg). After 15 days of acclimatization, in preparation for baseline urine collection, Sprague-Dawley rats were subjected to an 18-hour overnight fast and were placed in metabolism cages with unrestricted access to water. The subsequent day, the rats were weighed and randomly grouped in sets of eight (n=8), ensuring minimal variance in body weight among the groups. Fifteen minutes following the oral administration of a control substance dapagliflozin, standard drug i.e. and test compounds (low and high doses of **SSS 95** and **SSS 100**), the rats received glucose solution (2 grams per kilogram). They were then promptly returned to the metabolism cages to ensure complete urine collection over a 24-hour period post-dose. Food access was permitted one hour after glucose administration, and in tubes, urine samples were gathered, and their volumes were measured and documented. The concentration of glucose in the urine samples was determined using the glucose oxidase-peroxidase method. Additionally, urine samples were analyzed for sodium, potassium, and chloride ions using the ion-selective electrode method at Sant Path Laboratory, Ludhiana.

## RESULTS AND DISCUSSION

### 6.6.1 Assessment of Urine Excretion of Glucose and other electrolytes

Urinary glucose excretion (UGE) of Groups 2 to 4 significantly increased as compared to vehicle control (Group 1). There is significant difference in UGE between Groups 5 to 9 relative to negative control (Group 4). The quantities of 24-hour urinary glucose excretion induced by SSS 95, SSS 100, and dapagliflozin (positive control) were presented in **Figure 31** and **Table 12**. Groups 6 to 9 significantly enhanced the UGE compared with positive control (Group 5). However, SSS 100 significantly improved excretion of urinary glucose ( $854 \pm 46.51$  mg/body weight) as compared to positive control ( $775 \pm 32.68$  mg/body weight) at the same dosage and duration.

**Table 12:** Effect on Urinary Glucose Excretion (mg/BW) after the treatment during 24h.

Group No.	Group Name	Body weight (gm)	Urine glucose Concentration (mg/dl)	Urine Volume (ml)	Urine glucose Excretion (mg/BW)
<b>Group 1</b>	Vehicle control	360±9.51	991±7.78	24±1.67	65±4.56
<b>Group 2</b>	Synthesized molecule-SSS 95 <i>per se</i>	341±14.42	5186±5.19	24±2.07	406±77.2***
<b>Group 3</b>	Synthesized molecule-SSS 100 <i>per se</i>	347±14.7	5385±9.96	24±2.07	366.±39.93***
<b>Group 4</b>	Negative control	372±16.09	5731±20.02	30±1.06	454±23.03***
<b>Group 5</b>	Positive control	378±9.11	9922±16.56	30±1.09	775±32.68 ###
<b>Group 6</b>	Synthesized molecule-SSS 95 low dose	355±16.06	7009±18.53	25±2.77	495±59.70###
<b>Group 7</b>	Synthesized molecule- SSS 95 high dose	351±15.49	8403±39.44	25±2.13	600±62.55 ###



## RESULTS AND DISCUSSION

<b>Group 8</b>	Synthesized molecule- SSS 100 low dose	351±14.45	7290±11.92	26±1.92	527±45.08 ##
<b>Group 9</b>	Synthesized molecule- SSS 100 high dose	350±12.16	10038±39.55	30±0.88	854±46.51### ^^

The data is expressed as mean ± SD. \*\*\* denotes  $p < 0.001$ , compared to the vehicle group, while ## and ### represent  $p < 0.01$  and  $p < 0.001$ , respectively, compared to the diabetic control group. ^^ represents  $p < 0.01$  compared to standard control group.

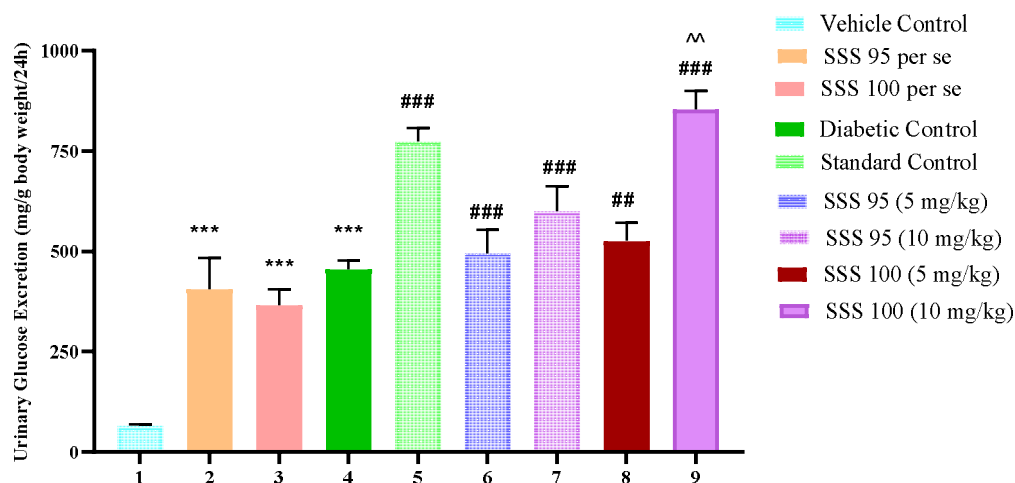


**Figure 31:** Effect on Urinary excretion of Glucose (mg/bodyweight) after the treatment during 24h. The data is expressed as mean ± SD. \*\*\* denotes  $p < 0.001$ , compared to the vehicle group, while ## and ### represent  $p < 0.01$  and  $p < 0.001$ , respectively, compared to the diabetic control group. ^^ represents  $p < 0.01$  compared to standard control group.

Comparatively, diabetic rats (Group 4) demonstrated a significant rise in the urinary excretion levels of  $\text{Na}^+$ ,  $\text{K}^+$ , and  $\text{Cl}^-$  in contrast to the rats in the vehicle control group (Group 1). Treatment with SSS 95 and SSS 100 (Groups 6-9) seemed to significantly reduce the urinary excretion of these electrolytes compared to the untreated diabetic group (Group 4) and significantly decreased the similar to the positive control (Group 5) are represented in Figure 32 and Table 13. These findings imply that the correction

## RESULTS AND DISCUSSION

of electrolyte imbalance by the test compounds in diabetic rats may not be solely attributed to a reduction in urinary electrolyte excretion.

**Table 13:** Effect on Urinary Excretion of electrolytes (mmol/L) after the treatment during 24h.

Group No.	Group Name	Body weight (g)	Urinary Na <sup>+</sup> Excretion Concentration (mmol/L/24 h)	Urinary K <sup>+</sup> Excretion Concentration (mmol/L/24 h)	Urinary Cl <sup>-</sup> Excretion Concentration (mmol/L/24 h)
Group 1	Vehicle	360±9.51	130±5.89	175±8.56	212±13.1
Group 2	Synthesized molecule-SSS 95 <i>per se</i>	341±14.42	134±5.35	180±6.16	229±5.71
Group 3	Synthesized molecule-SSS 100 <i>per se</i>	347±14.7	138±6.61	185±2.90	224±2.50
Group 4	Diabetic control	372±16.09	205±4.47** *	252±3.54 ***	308±6.18 ***
Group 5	Standard control	378±9.11	148±2.79###	212±7.40 ###	272±4.16 ###
Group 6	Synthesized molecule-SSS 95 low dose	355±16.06	150±2.16###	204±3.35###	240±4.26 ###
Group 7	Synthesized molecule- SSS 95 high dose	351±15.49	152±5.18 ###	201±5.87###	261±6.71 ###
Group 8	Synthesized molecule- SSS 100 low dose	351±14.45	156±5.57###	193±6.64###	237±5.73###
Group 9	Synthesized molecule- SSS 100 high dose	350±12.16	132±6.97### ^^	179±4.83### ^^	222±9.36### ^^

Mean values are presented as mean ± SD. \*\*\* indicates p < 0.001, respectively, in contrast to the vehicle group. ### signifies p < 0.01 and p < 0.001, respectively, in comparison to the diabetic control group. ^^ indicates p < 0.001, compared to the standard control group.

## RESULTS AND DISCUSSION

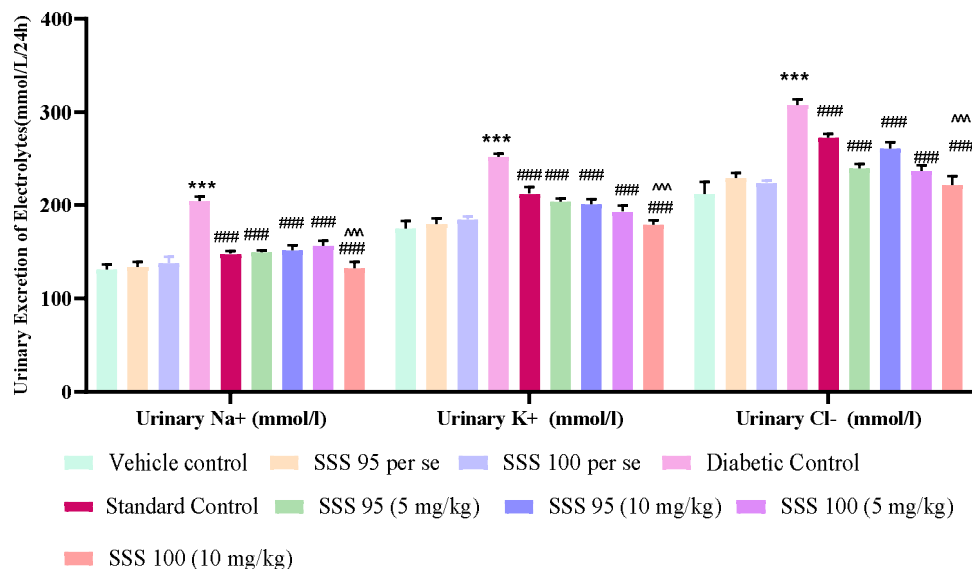


**Figure 32:** Effect on Urinary Excretion of electrolytes (mmol/L) after the treatment during 24h. Mean values are presented as mean  $\pm$  SD. \*\*\* indicates  $p < 0.001$ , respectively, in contrast to the vehicle group. ### signifies  $p < 0.01$  and  $p < 0.001$ , respectively, in comparison to the diabetic control group. ^^ indicates  $p < 0.001$ , compared to the standard control group.

**6.6.2 Diarrheogenic activity test:** The diarrheogenic activity test was conducted for SSS 95 and SSS 100 to investigate potential adverse effects arising from the absence of selectivity for hSGLT2 versus hSGLT1. It is noteworthy that no instances of diarrhea were noted in the SD rats treated with SSS 95 and SSS 100 (Group 6-9) as compared to positive control group 5 within 8 hours following oral administration of a single dose, ranging from 5 to 10 mg/kg as illustrated in **Table 14**.

**Table 14:** Effect on Diarrheogenic Activity after the treatment.

Group No.	Group Name	Status of Diarrhea
Group 1	Vehicle control	(-)
Group 2	Synthesized molecule-SSS 95 <i>per se</i>	(-)
Group 3	Synthesized molecule-SSS 100 <i>per se</i>	(-)
Group 4	Negative control	(-)

## RESULTS AND DISCUSSION

---

<b>Group 5</b>	Positive control	(-)
<b>Group 6</b>	Synthesized molecule-SSS 95 low dose	(-)
<b>Group 7</b>	Synthesized molecule- SSS 95 high dose	(-)
<b>Group 8</b>	Synthesized molecule- SSS 100 low dose	(-)
<b>Group 9</b>	Synthesized molecule- SSS 100 high dose	(-)

(-) normal feces (black color, well-formed, firm)

### 6.6.3 Effects of blood glucose reduction in rats with diabetes induced by Streptozotocin-Nicotamide

For the *in vivo* assessment of synthesized test compounds, a type-II diabetic model was meticulously established in male SD rats. The SD rats were subsequently categorized into various groups: vehicle control, synthesized compound-SSS 95 alone, synthesized compound-SSS 100 alone, STZ + NAM, STZ + NAM + Dapagliflozin, STZ + NAM + synthesized compound-SSS 95 (at 5 mg/kg & 10 mg/kg dose), and STZ + NAM + synthesized compound-SSS 100 (5 mg/kg & 10 mg/kg dose). On the 15<sup>th</sup> day of protocol, diabetes was initiated in SD rats with a single i.p. injection of STZ (60 mg/kg) and NAM (120 mg/kg). Following 7 days of STZ-NAM injection administration, the rats' BW & PGL were evaluated to confirm disease induction. On the 22<sup>nd</sup> day, diabetic rats commenced a 7-day treatment regimen. Following this, on the 28<sup>th</sup> day, both body weight and blood glucose levels were assessed to gauge the treatment's effect on the afflicted rats. The *in vivo* study's findings demonstrate that **SSS 95** and **SSS 100** significantly reduced PGL in diabetic animals. On the 30<sup>th</sup> day, the animals were euthanized, and the pancreas and kidneys from each euthanized animal were preserved in a 10% formalin solution for histopathological evaluation. The histopathological results validated that the pancreatic cells and kidneys of animals treated with **SSS 95** and **SSS 100** had nearly reverted to their normal histology after 7 days of treatment, which was comparable to the normal control and positive control groups.

## RESULTS AND DISCUSSION

### 6.6.3.1 Plasma Glucose estimation

On the 22nd and 28th days, glucose levels (measured in mg/dl) were assessed using the GOD-POD kit. The blood glucose levels were examined on the 22nd day (pre-treatment) and the 28th day (post-treatment). The results indicated that by the 22nd day, the levels of blood glucose in groups 4-9 (administered with STZ-NAM) were significantly elevated compared to vehicle group-1. Nevertheless, by the 28th day, subsequent to a 7-day treatment period, there was a significant reduction in PGLs in the STZ-NAM administered groups (5 to 9) compared to the diabetic control group-4. However, test compounds treated groups i.e. Group 6 to 9 significantly decreased blood glucose levels relative to standard control (Group 5). The influence of various treatments on the PGLs of the rats is elaborated in **Table 15** and **Figure 33**.

**Table 15:** Impact on blood glucose levels (mg/dL) pre- and post-treatment.

Group No.	Group Name	Day 22 (Pre-treatment)	Day 28 (Post treatment)
Group 1	Vehicle Group	117±9.66	110±11.5
Group 2	Synthesized molecule-SSS 95 <i>per se</i>	120±12.24	114±7.54
Group 3	Synthesized molecule-SSS 100 <i>per se</i>	125±3.33	120±5.54
Group 4	Diabetic control	314±9.36***	323±10.22** *
Group 5	Standard control	307±14.89***	158±15.9###
Group 6	Synthesized molecule-SSS 95 low dose	316±11.83***	200±7.59###
Group 7	Synthesized molecule-SSS 95 high dose	318±11.54***	183±15.07###
Group 8	Synthesized molecule-SSS 100 low dose	310±14.63***	179±12.5###
Group 9	Synthesized molecule-SSS 100 high dose	316±11.58***	137±4.89### ^^

## RESULTS AND DISCUSSION

The data is presented as mean  $\pm$  SD. \*\*\* denotes  $p < 0.001$ , respectively, compared to the vehicle group, while ### signifies  $p < 0.001$  compared to the diabetic control group. ^^ represents  $p < 0.001$  compared to the standard control group.

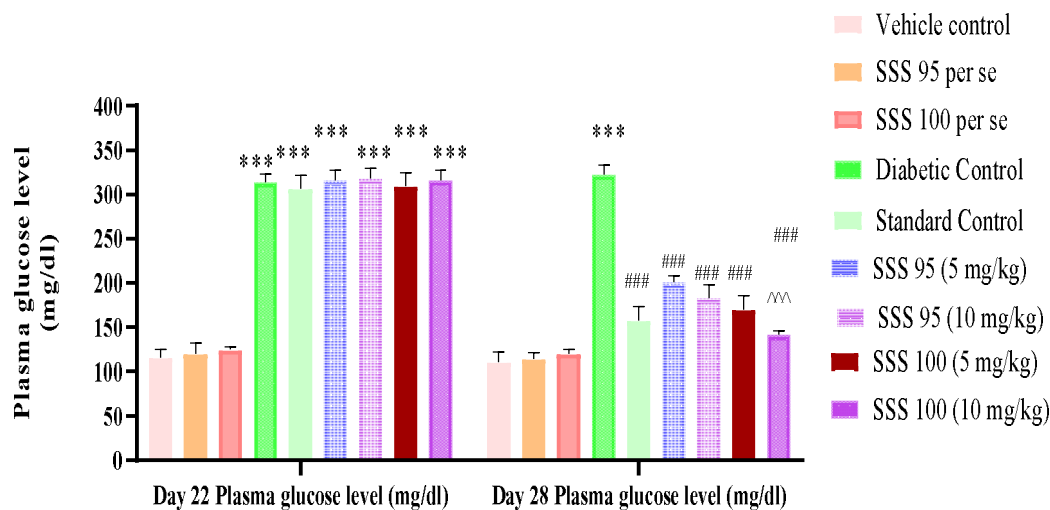


**Figure 33:** Impact on blood glucose levels (mg/dL) pre- and post-treatment. The data is presented as mean  $\pm$  SD. \*\*\* denotes  $p < 0.001$ , respectively, compared to the vehicle group, while ### signifies  $p < 0.001$  compared to the diabetic control group. ^^ represents  $p < 0.001$  compared to the standard control group.

**6.6.3.2 Body weight (BW) assessment:** Male SD rats used in the experiment were assessed for their body weight on Days 15, 22, and 28 of the study. There was no notable variance in the mean BW of the rats by the Day 15 across the various groups, all of which were on a standard pellet diet. Similarly, on the 22nd day, the diabetic control (4 to 9 groups) exhibited a notable reduction in BW compared to rats in groups 1 to 3, which did not receive STZ-NAM. On the 28th day, corresponding to 7 days after treatment, the mean body weight of Groups 5 to 9 were not significantly different in comparison to negative control (Group 4). But mean body weight of Groups 6 to 9, were significantly different relative to positive Control (Group 5). From the state of diabetes to the phase of recovery, the alteration in body weight is outlined in Table 16 & Figure 34.

**Table 16:** Change in mean body weight (g) before and after the treatment.

## RESULTS AND DISCUSSION

Group No.	Group Name	Day 15 of Protocol	Day 22 of Protocol	Day 28 of Protocol
Group 1	Vehicle	360±9.51	368±9.50	373±10.1
Group 2	Synthesized molecule-SSS 95 <i>per se</i>	341±14.43	351±14.3	358±13.9
Group 3	Synthesized molecule-SSS 100 <i>per se</i>	347±14.7	356±14.04	361±14.19
Group 4	Diabetic control	372±16.09	334±15.0*	328±21.57* **
Group 5	Standard control	378±9.11	340±16.1*	325±22.8 <sup>#</sup>
Group 6	Synthesized molecule-SSS 95 low dose	355±16.06	342±17.18 **	331±19.5
Group 7	Synthesized molecule- SSS 95 high dose	351±15.4	338±14.2* **	328±20.4 <sup>#</sup>
Group 8	Synthesized molecule- SSS 100 low dose	355±14.4	333±17.5* **	321±17.8 <sup>#</sup>
Group 9	Synthesized molecule- SSS 100 high dose	350±12.1	329±16.5* **	319±13.9 <sup>##</sup>

The data is presented as mean ± SD. \*, \*\*, \*\*\* represents  $p < 0.05$ ,  $p < 0.01$ ,  $p < 0.001$  respectively, compared to the vehicle group, while #, ## represents  $p < 0.05$ ,  $p < 0.01$  compared to the diabetic control group.

## RESULTS AND DISCUSSION

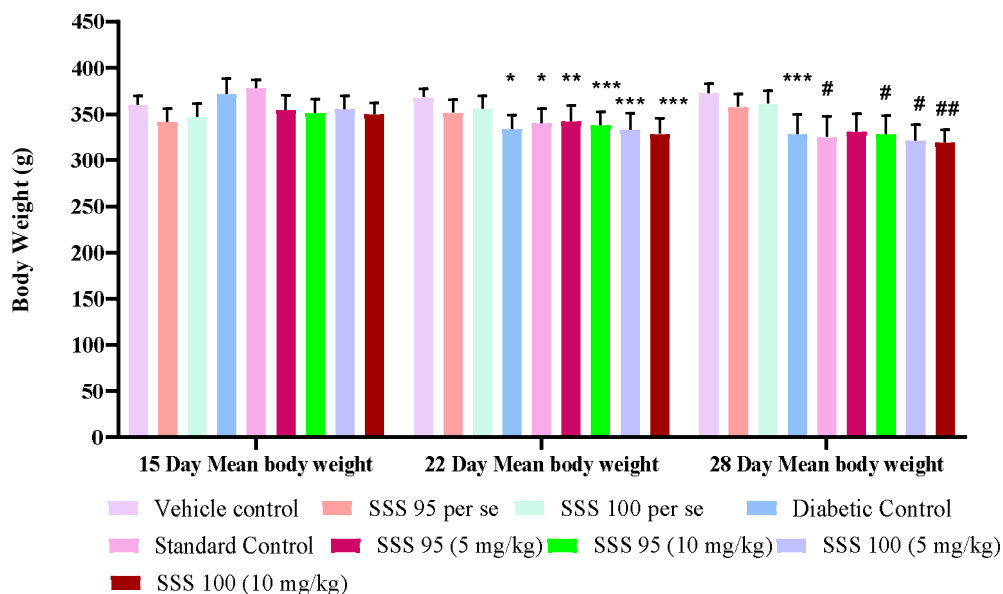


**Figure 34:** Impact on the body weight of rats (in grams) resulting from the treatment protocol. The data is presented as mean  $\pm$  SD. \*, \*\*, \*\*\* represents  $p < 0.05$ ,  $p < 0.01$ ,  $p < 0.001$  respectively, compared to the vehicle group, while #, ## represents  $p < 0.05$ ,  $p < 0.01$  compared to the diabetic control group.

### 6.7 Histopathological Estimation of SD rats kidney and Pancreas

#### 6.7.1 Histopathology of Kidney

Following the sacrifice of rats in each group, the kidney and pancreas of SD rats were harvested and promptly preserved in a 10% formalin solution to prevent tissue desiccation or damage during dissection. Subsequently, tissue slides were readied and underwent eosin & haematoxylin staining and magnified at 40X. The examination of kidney tissue is depicted in the **Figure 35**. Image (A) illustrates the kidney of a control rat from Group 1 treated with vehicle only, while Image (B) and Image (C) show the kidney of Group 2 and Group 3, respectively, treated with Test compound SSS 95 per se (10 mg/kg) and Test compound SSS 100 per se (10 mg/kg) alone, both displaying notable kidney histology. Image (D) represents the kidney of a rat from Group 4 with STZ-NAM induced diabetes, exhibiting thickening of basement membrane, mesangial



## RESULTS AND DISCUSSION

---

expansion, and tubular atrophy in sections from both kidney, along with vessel hyalinization. Image (E) showcases the kidney of a diabetic rat treated with Dapagliflozin in Group 5, displaying normal kidney histology. Images (F & G) exhibit the kidney of Group 6 and Group 7, treated with Test compound SSS 95 at 5 and 10 mg/kg, respectively, revealing focal sclerosis of glomeruli, focal tubular atrophy, and otherwise unremarkable renal parenchyma. Finally, Images (H & I) present the kidney of Group 8 and Group 9, treated with Test compound SSS 100 at 5 and 10 mg/kg, respectively, displaying unremarkable histology.

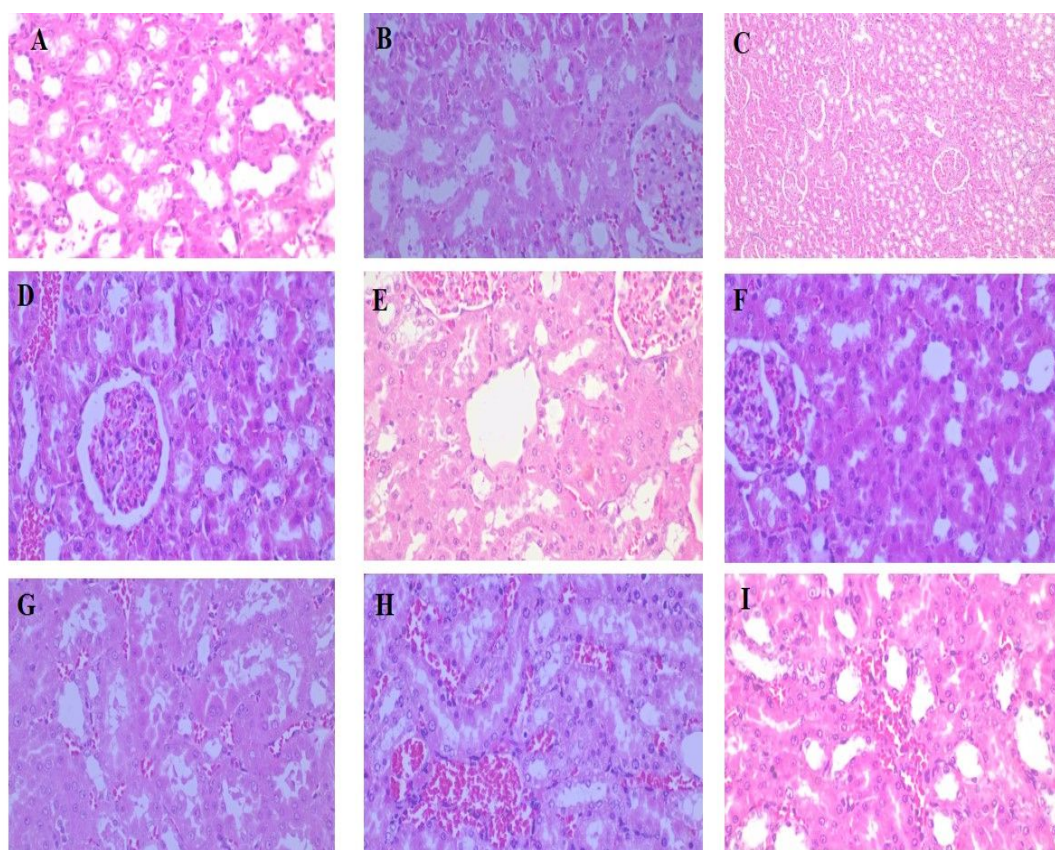


**Figure 35:** Histopathology representation of rat's kidney tissue, Image A: Vehicle (Group-1), Image B: SSS 95 per se (Group-2), Image C: SSS 100 per se (Group-3), Image D: Negative control (Group-4), Image E: Positive control (Group-5), Image F: SSS 95 (Group-6; low dose 5 mg/kg), Image G: (Group-7; high dose 10 mg/kg), Image

## RESULTS AND DISCUSSION

---

H: SSS 100 (Group-8; low dose 5 mg/kg), Image I: SSS 100 (Group-9; high dose 10 mg/kg).

### 6.7.2 Histopathology of pancreas

The examination of pancreas tissue is depicted in the **Figure 36**. Image (J-L) illustrates the pancreas of a control rat from Group 1 treated with the vehicle only, the pancreas of Group 2 and Group 3, treated with Test compound SSS 95 per se (10 mg/kg) and test compound SSS 100 per se (10 mg/kg) revealed normal acinar parenchyma of pancreas along with ducts and islets of Langerhans. Image (M) displays the pancreas of a rat from Group 4 with induced diabetes, exhibiting swollen and degenerated acinar cells, a reduction in islets of Langerhans. Image (N) presents the pancreas of a rat treated with Dapagliflozin in Group 5, exhibiting a normal pancreas histology. Images (O) show the pancreas of Group 6 treated with Test compound SSS 95 at a low dose (5 mg/kg), revealing acinar cells with a normal appearance along with a slight reduction of beta cells in the Islets of Langerhan. Finally, Images (P, Q & R) display the pancreas of Groups 7, 8, and 9, treated with Test compound SSS 95 (high dose: 10mg/kg), SSS 100 (low and high dose: 5 and 10mg/kg), respectively, showing a normal acinar parenchyma of the pancreas, along with intact ducts and islets of Langerhans.

## RESULTS AND DISCUSSION

---

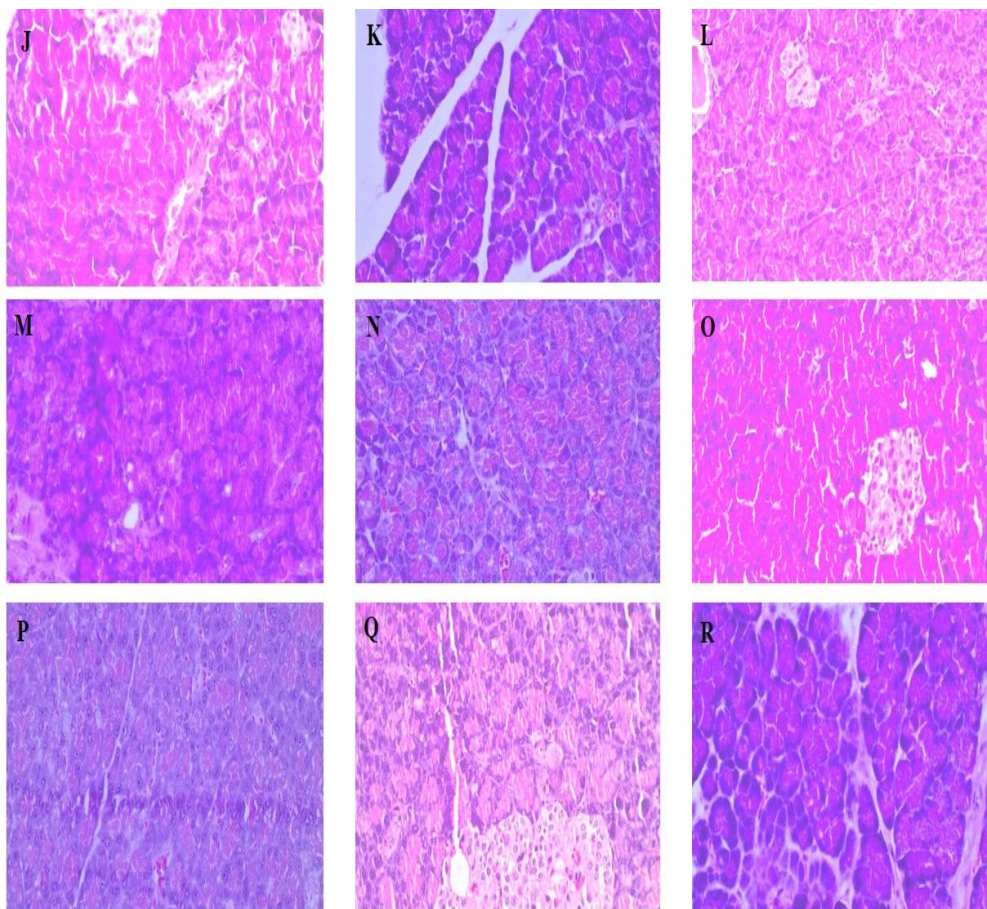


**Figure 36:** Histopathological illustration of rat pancreatic tissue, Image J: Vehicle (Group 1), Image K: SSS 95 per se (Group 2), Image L: SSS 100 per se (Group 3), Image M: Negative control (Group 4), Image N: Positive control (Group 5), Image O: SSS 95 (Group 6; low dose 5 mg/kg), Image P: (Group 7; high dose 10 mg/kg), Image Q: SSS 100 (Group 8; low dose 5 mg/kg), Image R: SSS 100 (Group 9; high dose 10 mg/kg).

# *CHAPTER 7*

## CONCLUSION AND FUTURE PROSPECTIVES

---

Type-II diabetes mellitus stands as the metabolic disorder with the highest mortality rate, exerting a substantial impact on modern society. Lately, researchers have delved into the potential of SGLT as a viable therapeutic target for diabetes. Most SGLT2 inhibitors investigated in literature are glycosidal, presenting challenges in synthesis due to their bulky nature. The design involves a non-glucoside 1,3,4-thiadiazole pharmacophore with enhanced selectivity for hSGLT2 over hSGLT-1. This is achieved through strategic modifications in substitution positions, aiming for a more effective anti-diabetic drug compared to the standard dapagliflozin. We formulated innovative compounds featuring 1,3,4-thiadiazole by incorporating electron-releasing groups i.e. methyl and methoxy on the phenyl ring A at the fourth position, denoted as R<sub>1</sub>. Additionally, we introduced diverse electron-donating groups/electron withdrawing groups at the 2, 4, 5 and 6 positions, located on the second phenyl ring B, designated as R<sub>2</sub>. Using the information provided, we developed 102 compounds of Schiff base with a foundation in the 1,3,4-thiadiazole scaffold. Subsequently, we conducted docking studies with the SGLT2 protein (PDB ID: 3DH4) to assess binding affinity scores, utilizing AutoDock Vina 1.5.6. Out of these, we selected the top 12 Schiff base-derived 1,3,4-thiadiazole molecules, exhibiting the most advantageous binding affinity scores ranging from -10.7 to -9.7 Kcal/mol featuring electron-donating groups (EDGs). These selected compounds were synthesized and assigned the codes **SSS 34, SSS 100, SSS 16, SSS 40, SSS 35, SSS 95, SSS 98, SSS 41, SSS 36, SSS 102, SSS 18, and SSS 96**. The chosen compounds were successfully synthesized with high percentage yields and subjected to validation through LCMS, <sup>1</sup>H NMR, and <sup>13</sup>C NMR analyses. The *in-silico* toxicity profiling of the synthesized compounds indicated that demonstrated non-carcinogenic properties in rats and non-mutagenic characteristics. The *in-silico* ADME results indicate that all the synthesized molecules do not penetrate the brain and exhibit a low likelihood of gastrointestinal absorption. The predicted lipophilicity (iLogP) of the synthesized compounds ranges from 2.08 to 3.68. Moreover, all the synthesized molecules are anticipated to have favorable oral bioavailability, scoring 0.55, and are in accordance with drug-likeness criteria. According to the MTT assay results, SSS 35, SSS 40, SSS 95, and SSS 100 demonstrated elevated IC<sub>50</sub> values, specifically 102.69,

## CONCLUSION AND FUTURE PROSPECTIVES

---

89.77, 101.07, and 98.82, respectively. These findings suggest low cytotoxicity for the synthesized compounds. Following this, the four compounds underwent additional testing for their SGLT2 inhibiting activity. The analysis of the Human SGLT2 (SLC5A2) ELISA kit assay results indicated that compounds **SSS 95** and **SSS 100** exhibited greater potency. **SSS 95** demonstrated substantial SGLT2 inhibition activity at both low dose ( $54.76 \pm 1.68$ ) and high dose ( $78.57 \pm 2.8$ ), while **SSS 100** exhibited significant SGLT2 inhibition at low dose ( $56.34 \pm 3.92$ ) and high dose ( $74.60 \pm 1.12$ ). Hence, for subsequent *in vivo* assessments of the synthesized test compounds, **SSS 95** and **SSS 100** were selected. *In vivo* findings indicate that **SSS 100** notably enhanced the excretion of urinary glucose ( $854 \pm 46.51$  mg/body weight) in comparison to the positive control ( $775 \pm 32.68$  mg/body weight) at the same dosage and duration. The heightened urinary glucose excretion observed with the test compounds is likely attributed to the inhibition of the SGLT2 enzyme. This enzyme is accountable for around 90% glucose reabsorption in the kidney's proximal tubule, consequently contributing to lower glucose levels. Administration of **SSS 95** and **SSS 100** appeared to markedly decrease the urinary excretion of  $\text{Na}^+$ ,  $\text{K}^+$ , and  $\text{Cl}^-$  electrolytes, akin to the positive control. These results suggest that the correction of electrolyte imbalance by the test compounds in diabetic rats may not be solely linked to a reduction in urinary electrolyte excretion. It is worth noting that no occurrences of diarrhea were observed in the SD rats treated with **SSS 95** and **SSS 100**, in comparison to the positive control. This lack of side effect is likely attributed to the compounds' lack of selectivity for hSGLT1. Nevertheless, the groups treated with the test compounds **SSS 95** and **SSS 100** exhibited a notable decrease in PGLs compared to the standard control. This suggests the anti-hyperglycemic effect of the synthesized test compounds. Histopathological examination of the pancreas and kidney from the animal groups treated with test compounds **SSS 95** and **SSS 100**, respectively, indicated normal islets of Langerhans and unremarkable histology of the kidney. In summary, the overall results indicate that the presence of two phenyl rings, A and B, linked by sulfur and connected by an imine bridge, with substitutions at  $\text{R}_1$  and  $\text{R}_2$  positions involving electron-donating groups, is crucial for enhancing the potency of the compounds.

## CONCLUSION AND FUTURE PROSPECTIVES

---

### FUTURE PROSPECTIVES

The comprehensive study suggests that **SSS 95** and **SSS 100** exhibit a significant impact on increasing urinary glucose and electrolyte excretion while lowering blood glucose levels. This positions them as potential SGLT2 inhibitors for treating T2DM. The future development of substituted non-glucosidal SGLT2 inhibitors with a thiadiazole nucleus holds promise for advancing T2DM treatment. Given the importance of this research, its implications extend to both social realms. The identified potent molecules, particularly **SSS 95** and **SSS 100**, hold promise for formulation as SGLT2 inhibitors.

# *CHAPTER 8*



## REFERENCES

---

1. Sun, H.; Saeedi, P.; Karuranga, S.; Pinkepank, M.; Ogurtsova, K.; Duncan, B. B.; Stein, C.; Basit, A.; Chan, J. C. N.; Mbanya, J. C.; Pavkov, M. E.; Ramachandaran, A.; Wild, S. H.; James, S.; Herman, W. H.; Zhang, P.; Bommer, C.; Kuo, S.; Boyko, E. J.; Magliano, D. J. IDF Diabetes Atlas: Global, Regional and Country-Level Diabetes Prevalence Estimates for 2021 and Projections for 2045. *Diabetes Res. Clin. Pract.* **2022**, *183*, 109119. DOI: [10.1016/j.diabres.2021.109119](https://doi.org/10.1016/j.diabres.2021.109119)
2. Maliwal, D.; Pissurlenkar, R. R. S.; Telvekar, V. Identification of Novel Potential Anti-diabetic Candidates Targeting Human Pancreatic  $\alpha$ -Amylase and Human  $\alpha$ -Glycosidase: An Exhaustive Structure-Based Screening. *Can. J. Chem.* **2022**, *100* (5), 338–352. DOI: [10.1139/cjc-2021-0238](https://doi.org/10.1139/cjc-2021-0238)
3. Saeedi, P.; Petersohn, I.; Salpea, P.; Malanda, B.; Karuranga, S.; Unwin, N.; Colagiuri, S.; Guariguata, L.; Motala, A. A.; Ogurtsova, K.; Shaw, J. E.; Bright, D.; Williams, R.; IDF Diabetes Atlas Committee. Global and Regional Diabetes Prevalence Estimates for 2019 and Projections for 2030 and 2045: Results from the International Diabetes Federation Diabetes Atlas, 9th Edition. *Diabetes Res. Clin. Pract.*, 9th ed. **2019**, *157*, 107843. DOI: [10.1016/j.diabres.2019.107843](https://doi.org/10.1016/j.diabres.2019.107843)
4. Stratton, I. M.; Adler, A. I.; Neil, H. A. W.; Matthews, D. R.; Manley, S. E.; Cull, C. A.; Hadden, D.; Turner, R. C.; Holman, R. R. Association of Glycaemia with Macrovascular and Microvascular Complications of Type 2 Diabetes (UKPDS 35): Prospective Observational Study. *B.M.J.* **2000**, *321* (7258), 405–412. DOI: [10.1136/bmj.321.7258.405](https://doi.org/10.1136/bmj.321.7258.405)
5. Ogurtsova, K.; Guariguata, L.; Barengo, N. C.; Ruiz, P. L.-D.; Sacre, J. W.; Karuranga, S.; Sun, H.; Boyko, E. J.; Magliano, D. J. IDF Diabetes Atlas: Global Estimates of Undiagnosed Diabetes in Adults for 2021. *Diabetes Res. Clin. Pract.* **2022**, *183*, 109118. DOI: [10.1016/j.diabres.2021.109118](https://doi.org/10.1016/j.diabres.2021.109118)
6. Smokovski, I. *Managing Diabetes in Low Income Countries*; Springer, 2021.
7. Lloyd, H. Perioperative Care of the Adult Diabetic Patient. *J. Perioper. Pract.* **2020**, *30* (12), 372–377. DOI: [10.1177/1750458920915660](https://doi.org/10.1177/1750458920915660)
8. Adler, A.; Bennett, P. *Chair*; Gregg, E.; Narayan, K. V.; Schmidt, M. I.; Sobngwi, E.; Tajima, N.; Tandon, N.; Unwin, N. Reprint of: classification of diabetes mellitus. *Diabetes Res. Clin. Pract.* **2021**, 108972.
9. Federation, I. IDF Diabetes Atlas, Tenth. *Int. Diabetes* **2021**.

## REFERENCES

---

10. Williams, R.; Karuranga, S.; Malanda, B.; Saeedi, P.; Basit, A.; Besançon, S.; Bommer, C.; Esteghamati, A.; Ogurtsova, K.; Zhang, P.; Colagiuri, S.. Global and Regional Estimates and Projections of Diabetes-Related Health Expenditure: Results from the International Diabetes Federation Diabetes Atlas, 9th Edition. *Diabetes Res. Clin. Pract.*, 9th ed. **2020**, *162*, 108072. DOI: [10.1016/j.diabres.2020.108072](https://doi.org/10.1016/j.diabres.2020.108072)
11. Care, D. Care in Diabetesd2018. *Diabetes Care* **2018**, *41* (1), S137–S143.
12. Nauck, M. A.; Wefers, J.; Meier, J. J. Treatment of Type 2 Diabetes: Challenges, Hopes, and Anticipated Successes. *Lancet Diabetes Endocrinol.* **2021**, *9* (8), 525–544. DOI: [10.1016/S2213-8587\(21\)00113-3](https://doi.org/10.1016/S2213-8587(21)00113-3)
13. Gerich, J. E. Role of the Kidney in Normal Glucose Homeostasis and in the Hyperglycaemia of Diabetes Mellitus: Therapeutic Implications. *Diabet. Med.* **2010**, *27* (2), 136–142. DOI: [10.1111/j.1464-5491.2009.02894.x](https://doi.org/10.1111/j.1464-5491.2009.02894.x)
14. Panten, U.; Schwanstecher, M.; Schwanstecher, C. Sulfonylurea Receptors and Mechanism of Sulfonylurea Action. *Exp. Clin. Endocrinol. Diabetes* **1996**, *104* (1), 1–9. DOI: [10.1055/s-0029-1211414](https://doi.org/10.1055/s-0029-1211414)
15. Bailey, C. J. Biguanides and NIDDM. *Diabetes Care* **1992**, *15* (6), 755–772. DOI: [10.2337/diacare.15.6.755](https://doi.org/10.2337/diacare.15.6.755)
16. Owen, M. R.; Doran, E.; Halestrap, A. P. Evidence That Metformin Exerts Its Anti-diabetic Effects Through Inhibition of Complex 1 of the Mitochondrial Respiratory Chain. *Biochem. J.* **2000**, *348* (3), 607–614. DOI: [10.1042/bj3480607](https://doi.org/10.1042/bj3480607)
17. Musi, N.; Hirshman, M. F.; Nygren, J.; Svanfeldt, M.; Bavenholm, P.; Rooyackers, O.; Zhou, G.; Williamson, J. M.; Ljunqvist, O.; Efendic, S.; Moller, D. E.; Thorell, A.; Goodyear, L. J. Metformin Increases AMP-Activated Protein Kinase Activity in Skeletal Muscle of Subjects with Type 2 Diabetes. *Diabetes* **2002**, *51* (7), 2074–2081. DOI: [10.2337/diabetes.51.7.2074](https://doi.org/10.2337/diabetes.51.7.2074)
18. SISowers JR, K.D. Metformin: An Update. *Ann. Intern. Med.* **2002**, *137*, 2533.
19. Quianzon, C. C.; Cheikh, I. E. History of Current Non-insulin Medications for Diabetes Mellitus. *J. Community Hosp. Intern. Med. Perspect.* **2012**, *2* (3), 19081. DOI: [10.3402/jchimp.v2i3.19081](https://doi.org/10.3402/jchimp.v2i3.19081)
20. Van de Laar, F. A. Alpha-Glucosidase Inhibitors in the Early Treatment of Type 2 Diabetes. *Vasc. Health Risk Manag.* **2008**, *4* (6), 1189–1195. DOI: [10.2147/vhrm.s3119](https://doi.org/10.2147/vhrm.s3119)

## REFERENCES

---

21. Nesto, R. W.; Bell, D.; Bonow, R. O.; Fonseca, V.; Grundy, S. M.; Horton, E. S.; Le Winter, M.; Porte, D.; Semenkovich, C. F.; Smith, S.; Young, L. H.; Kahn, R.; American Heart Association; American Diabetes Association. Thiazolidinedione Use, Fluid Retention, and Congestive Heart Failure: A Consensus Statement from the American Heart Association and American Diabetes Association. October 7, 2003. *Circulation* **2003**, *108* (23), 2941–2948. DOI: [10.1161/01.CIR.0000103683.99399.7E](https://doi.org/10.1161/01.CIR.0000103683.99399.7E)
22. Melander, A. Kinetics-Effect Relations of Insulin-Releasing Drugs in Patients with Type 2 Diabetes: Brief Overview. *Diabetes* **2004**, *53* (Suppl. 3) (suppl\_3), S151–S155. DOI: [10.2337/diabetes.53.suppl\\_3.s151](https://doi.org/10.2337/diabetes.53.suppl_3.s151)
23. Hansen, K. B.; Vilsbøll, T.; Knop, F. K. Incretin Mimetics: A Novel Therapeutic Option for Patients with Type 2 Diabetes—A Review. *Diabetes Metab. Syndr. Obes.* **2010**, *3*, 155–163.
24. Drucker, D.; Nauck, M. GLP-1R Agonists (Incretin Mimetics) and DPP-4 Inhibitors (Incretin Enhancers) for the Treatment of Type 2 Diabetes. *Lancet* **2006**, *368* (3), 1696–1705.
25. Inzucchi, S. E.; Bergenstal, R. M.; Buse, J. B.; Diamant, M.; Ferrannini, E.; Nauck, M.; Peters, A. L.; Tsapas, A.; Wender, R.; Matthews, D. R. Management of Hyperglycaemia in Type 2 Diabetes: A Patient-Centered Approach. Position Statement of the American Diabetes Association (ADA) and the European Association for the Study of Diabetes (EASD). *Diabetologia* **2012**, *55* (6), 1577–1596. DOI: [10.1007/s00125-012-2534-0](https://doi.org/10.1007/s00125-012-2534-0)
26. Tahrani, A. A.; Barnett, A. H.; Bailey, C. J. SGLT Inhibitors in Management of Diabetes. *Lancet Diabetes Endocrinol.* **2013**, *1* (2), 140–151. DOI: [10.1016/S2213-8587\(13\)70050-0](https://doi.org/10.1016/S2213-8587(13)70050-0)
27. Lee, Y. J.; Lee, Y. J.; Han, H. J. Regulatory Mechanisms of Na<sup>+</sup>/Glucose cotransporters in Renal Proximal Tubule Cells. *Kidney Int. Suppl.* **2007**, *72* (106), S27–S35. DOI: [10.1038/sj.ki.5002383](https://doi.org/10.1038/sj.ki.5002383)
28. Bays, H. Sodium Glucose co-Transporter Type 2 (SGLT2) Inhibitors: Targeting the Kidney to Improve Glycemic Control in Diabetes Mellitus. *Diabetes Ther.* **2013**, *4* (2), 195–220. DOI: [10.1007/s13300-013-0042-y](https://doi.org/10.1007/s13300-013-0042-y)
29. Santer, R.; Calado, J. Familial Renal Glucosuria and SGLT2: From a Mendelian Trait to a Therapeutic Target. *Clin. J. Am. Soc. Nephrol.* **2010**, *5* (1), 133–141. DOI: [10.2215/CJN.04010609](https://doi.org/10.2215/CJN.04010609)

## REFERENCES

---

30. Vallon, V.; Platt, K. A.; Cunard, R.; Schroth, J.; Whaley, J.; Thomson, S. C.; Koepsell, H.; Rieg, T. SGLT2 Mediates Glucose Reabsorption in the Early Proximal Tubule. *J. Am. Soc. Nephrol.* **2011**, *22* (1), 104–112. DOI: [10.1681/ASN.2010030246](https://doi.org/10.1681/ASN.2010030246)
31. Rahmoune, H.; Thompson, P. W.; Ward, J. M.; Smith, C. D.; Hong, G.; Brown, J. Glucose Transporters in Human Renal Proximal Tubular Cells Isolated from the Urine of Patients with Non–insulin-Dependent Diabetes. *Diabetes* **2005**, *54* (12), 3427–3434. DOI: [10.2337/diabetes.54.12.3427](https://doi.org/10.2337/diabetes.54.12.3427)
32. Wright, E. M.; Turk, E. The Sodium/Glucose Cotransport Family SLC5. *Pflugers Arch.* **2004**, *447* (5), 510–518. DOI: [10.1007/s00424-003-1063-6](https://doi.org/10.1007/s00424-003-1063-6)
33. Bhattacharya, S.; Rathore, A.; Parwani, D.; Mallick, C.; Asati, V.; Agarwal, S.; Rajoriya, V.; Das, R.; Kashaw, S. K. An Exhaustive Perspective on Structural Insights of SGLT2 Inhibitors: A Novel Class of Antidiabetic Agent. *Eur. J. Med. Chem.* **2020**, *204*, 112523. DOI: [10.1016/j.ejmech.2020.112523](https://doi.org/10.1016/j.ejmech.2020.112523)
34. Pałasz, A.; Cież, D.; Trzewik, B.; Miszczak, K.; Tynor, G.; Bazan, B. In the Search of Glycoside-Based Molecules as Antidiabetic Agents. *Top. Curr. Chem. (Cham)* **2019**, *377* (4), 19. DOI: [10.1007/s41061-019-0243-6](https://doi.org/10.1007/s41061-019-0243-6)
35. Aguilón, A. R.; Mascarello, A.; Segretti, N. D.; de Azevedo, H. F. Z.; Guimaraes, C. R. W.; Miranda, L. S. M.; de Souza, R. O. M. A. Synthetic Strategies Toward SGLT2 Inhibitors. *Org. Process Res. Dev.* **2018**, *22* (4), 467–488. DOI: [10.1021/acs.oprd.8b00017](https://doi.org/10.1021/acs.oprd.8b00017)
36. Bonora, B. M.; Avogaro, A.; Fadini, G. P. Extraglycemic Effects of SGLT2 Inhibitors: A Review of the Evidence. *Diabetes Metab. Syndr. Obes.* **2020**, *13*, 161–174. DOI: [10.2147/DMSO.S233538](https://doi.org/10.2147/DMSO.S233538)
37. Scheen, A. J. An Update on the Safety of SGLT2 Inhibitors. *Expert Opin. Drug Saf.* **2019**, *18* (4), 295–311. DOI: [10.1080/14740338.2019.1602116](https://doi.org/10.1080/14740338.2019.1602116)
38. Chao, E. C.; Henry, R. R. SGLT2 Inhibition—A Novel Strategy for Diabetes Treatment. *Nat. Rev. Drug Discov.* **2010**, *9* (7), 551–559. DOI: [10.1038/nrd3180](https://doi.org/10.1038/nrd3180)
39. List, J. F.; Whaley, J. M. Glucose Dynamics and Mechanistic Implications of SGLT2 Inhibitors in Animals and Humans. *Kidney Int. Suppl.* **2011**, *79* (120), S20–S27. DOI: [10.1038/ki.2010.512](https://doi.org/10.1038/ki.2010.512)

## REFERENCES

---

- 40a. Mogensen, C. E. Urinary Albumin Excretion in Early and Long-Term Juvenile Diabetes. *Scand. J. Clin. Lab. Investig.* **1971**, 28 (2), 183–193. DOI: [10.3109/00365517109086899](https://doi.org/10.3109/00365517109086899)
- 40b. Packer, M.; Anker, S. D.; Butler, J.; Filippatos, G.; Ferreira, J. P.; Pocock, S. J.; Sattar, N.; Brueckmann, M.; Jamal, W.; Cotton, D.; Iwata, T.; Zannad, F.; EMPEROR-Reduced Trial Committees and Investigators. Empagliflozin in Patients with Heart Failure, Reduced Ejection Fraction, and Volume Overload: EMPEROR-Reduced Trial. *J. Am. Coll. Cardiol.* **2021b**, 77 (11), 1381–1392. DOI: [10.1016/j.jacc.2021.01.033](https://doi.org/10.1016/j.jacc.2021.01.033)
41. Stenlöf, K.; Cefalu, W. T.; Kim, K. A.; Alba, M.; Usiskin, K.; Tong, C.; Canovatchel, W.; Meininger, G. Efficacy and Safety of Canagliflozin Monotherapy in Subjects with Type 2 Diabetes Mellitus Inadequately Controlled with Diet and Exercise. *Diabetes Obes. Metab.* **2013**, 15 (4), 372–382. DOI: [10.1111/dom.12054](https://doi.org/10.1111/dom.12054)
42. Wang, Z.; Sun, J.; Han, R.; Fan, D.; Dong, X.; Luan, Z.; Xiang, R.; Zhao, M.; Yang, J. Efficacy and Safety of Sodium-Glucose cotransporter-2 Inhibitors Versus Dipeptidyl Peptidase-4 Inhibitors as Monotherapy or Add-On to Metformin in Patients with Type 2 Diabetes Mellitus: A Systematic Review and Meta-analysis. *Diabetes Obes. Metab.* **2018**, 20 (1), 113–120. DOI: [10.1111/dom.13047](https://doi.org/10.1111/dom.13047)
43. Xiang, B.; Zhao, X.; Zhou, X. Cardiovascular Benefits of Sodium-Glucose cotransporter 2 Inhibitors in Diabetic and Nondiabetic Patients. *Cardiovasc. Diabetol.* **2021**, 20 (1), 78. DOI: [10.1186/s12933-021-01266-x](https://doi.org/10.1186/s12933-021-01266-x)
44. Perkovic, V.; Jardine, M. J.; Neal, B.; Bompoint, S.; Heerspink, H. J. L.; Charytan, D. M.; Edwards, R.; Agarwal, R.; Bakris, G.; Bull, S.; Cannon, C. P.; Capuano, G.; Chu, P. L.; de Zeeuw, D.; Greene, T.; Levin, A.; Pollock, C.; Wheeler, D. C.; Yavin, Y.; Zhang, H.; Zinman, B.; Meininger, G.; Brenner, B. M.; Mahaffey, K. W.; CREDENCE Trial Investigators. Canagliflozin and Renal Outcomes in Type 2 Diabetes and Nephropathy. *N. Engl. J. Med.* **2019**, 380 (24), 2295–2306. DOI: [10.1056/NEJMoa1811744](https://doi.org/10.1056/NEJMoa1811744)
45. Wanner, C.; Inzucchi, S. E.; Lachin, J. M.; Fitchett, D.; von Eynatten, M.; Mattheus, M.; Johansen, O. E.; Woerle, H. J.; Broedl, U. C.; Zinman, B.; EMPA-Reg OUTCOME Investigators. Empagliflozin and Progression of Kidney Disease in Type 2 Diabetes. *N. Engl. J. Med.* **2016**, 375 (4), 323–334. DOI: [10.1056/NEJMoa1515920](https://doi.org/10.1056/NEJMoa1515920)

## REFERENCES

---

46. Zelniker, T. A.; Wiviott, S. D.; Raz, I.; Im, K.; Goodrich, E. L.; Bonaca, M. P.; Mosenzon, O.; Kato, E. T.; Cahn, A.; Furtado, R. H. M.; Bhatt, D. L.; Leiter, L. A.; McGuire, D. K.; Wilding, J. P. H.; Sabatine, M. S. SGLT2 Inhibitors for Primary and Secondary Prevention of Cardiovascular and Renal Outcomes in Type 2 Diabetes: A Systematic Review and Meta-analysis of Cardiovascular Outcome Trials. *Lancet* **2019**, 393 (10166), 31–39. DOI: [10.1016/S0140-6736\(18\)32590-X](https://doi.org/10.1016/S0140-6736(18)32590-X)
47. Mosenzon, O.; Wiviott, S. D.; Cahn, A.; Rozenberg, A.; Yanuv, I.; Goodrich, E. L.; Murphy, S. A.; Heerspink, H. J. L.; Zelniker, T. A.; Dwyer, J. P.; Bhatt, D. L.; Leiter, L. A.; McGuire, D. K.; Wilding, J. P. H.; Kato, E. T.; Gause-Nilsson, I. A. M.; Fredriksson, M.; Johansson, P. A.; Langkilde, A. M.; Sabatine, M. S.; Raz, I. Effects of Dapagliflozin on Development and Progression of Kidney Disease in Patients with Type 2 Diabetes: An Analysis from the DECLARE–TIMI 58 Randomised Trial. *Lancet Diabetes Endocrinol.* **2019**, 7 (8), 606–617. DOI: [10.1016/S2213-8587\(19\)30180-9](https://doi.org/10.1016/S2213-8587(19)30180-9)
48. Pinto, L. C.; Rados, D. V.; Remonti, L. R.; Kramer, C. K.; Leitao, C. B.; Gross, J. L. Efficacy of SGLT2 Inhibitors in Glycemic Control, Weight Loss and Blood Pressure Reduction: A Systematic Review and Meta-analysis. *Diabetol. Metab. Syndr.* **2015**, 7 (1), 1–2.
49. Terra, S. G.; Focht, K.; Davies, M.; Frias, J.; Derosa, G.; Darekar, A.; Golm, G.; Johnson, J.; Saur, D.; Lauring, B.; Dagogo-Jack, S. Phase III, Efficacy and Safety Study of Ertugliflozin Monotherapy in People with Type 2 Diabetes Mellitus Inadequately Controlled with Diet and Exercise Alone. *Diabetes Obes. Metab.* **2017**, 19 (5), 721–728. DOI: [10.1111/dom.12888](https://doi.org/10.1111/dom.12888)
50. Vasilakou, D.; Karagiannis, T.; Athanasiadou, E.; Mainou, M.; Liakos, A.; Bekiari, E.; Sarigianni, M.; Matthews, D. R.; Tsapas, A. Sodium–Glucose cotransporter 2 Inhibitors for Type 2 Diabetes: A Systematic Review and Meta-analysis. *Ann. Intern. Med.* **2013**, 159 (4), 262–274. DOI: [10.7326/0003-4819-159-4-201308200-00007](https://doi.org/10.7326/0003-4819-159-4-201308200-00007)
51. Singh, M.; Kumar, A. Risks Associated with SGLT2 Inhibitors: An Overview. *Curr. Drug Saf.* **2018**, 13 (2), 84–91. DOI: [10.2174/1574886313666180226103408](https://doi.org/10.2174/1574886313666180226103408)
52. Inzucchi, S. E.; Iliiev, H.; Pfarr, E.; Zinman, B. Empagliflozin and Assessment of Lower-Limb Amputations in the EMPA-REG OUTCOME Trial. *Diabetes Care* **2018**, 41 (1), e4–e5. DOI: [10.2337/dc17-1551](https://doi.org/10.2337/dc17-1551)

## REFERENCES

---

53. Tang, H.; Dai, Q.; Shi, W.; Zhai, S.; Song, Y.; Han, J. SGLT2 Inhibitors and Risk of Cancer in Type 2 Diabetes: A Systematic Review and Meta-analysis of Randomised Controlled Trials. *Diabetologia* **2017**, *60* (10), 1862–1872. DOI: [10.1007/s00125-017-4370-8](https://doi.org/10.1007/s00125-017-4370-8)
54. Watts, N. B.; Bilezikian, J. P.; Usiskin, K.; Edwards, R.; Desai, M.; Law, G.; Meininger, G. Effects of Canagliflozin on Fracture Risk in Patients with Type 2 Diabetes Mellitus. *J. Clin. Endocrinol. Metab.* **2016**, *101* (1), 157–166. DOI: [10.1210/jc.2015-3167](https://doi.org/10.1210/jc.2015-3167)
55. Neal, B.; Perkovic, V.; Mahaffey, K. W.; De Zeeuw, D.; Fulcher, G.; Erondou, N.; Shaw, W.; Law, G.; Desai, M.; Matthews, D. R.; CANVAS Program Collaborative Group. Canagliflozin and Cardiovascular and Renal Events in Type 2 Diabetes. *N. Engl. J. Med.* **2017**, *377* (7), 644–657. DOI: [10.1056/NEJMoa1611925](https://doi.org/10.1056/NEJMoa1611925)
56. Petersen, C. Analyse Des Phloridzins. *Ann. Pharm.* **1835**, *15* (2), 178–178. DOI: [10.1002/jlac.18350150210](https://doi.org/10.1002/jlac.18350150210)
57. Alvarado, F.; Crane, R. K. Phlorizin as a Competitive Inhibitor of the Active Transport of Sugars by Hamster Small Intestine, In Vitro. *Biochim. Biophys. Acta* **1962**, *56*, 170–172. DOI: [10.1016/0006-3002\(62\)90543-7](https://doi.org/10.1016/0006-3002(62)90543-7)
58. Ohsumi, K.; Matsueda, H.; Hatanaka, T.; Hirama, R.; Umemura, T.; Oonuki, A.; Ishida, N.; Kageyama, Y.; Maezono, K.; Kondo, N. Pyrazole-O-Glucosides as Novel Na<sup>+</sup>-Glucose cotransporter (SGLT) Inhibitors. *Bioorg. Med. Chem. Lett.* **2003**, *13* (14), 2269–2272. DOI: [10.1016/s0960-894x\(03\)00466-9](https://doi.org/10.1016/s0960-894x(03)00466-9)
59. Oku, A.; Ueta, K.; Arakawa, K.; Ishihara, T.; Nawano, M.; Kuronuma, Y.; Matsumoto, M.; Saito, A.; Tsujihara, K.; Anai, M.; Asano, T.; Kanai, Y.; Endou, H. T-1095, an Inhibitor of Renal Na<sup>+</sup>-Glucose cotransporters, May Provide a Novel Approach to Treating Diabetes. *Diabetes* **1999**, *48* (9), 1794–1800. DOI: [10.2337/diabetes.48.9.1794](https://doi.org/10.2337/diabetes.48.9.1794)
60. Oku, A.; Ueta, K.; Nawano, M.; Arakawa, K.; Kano-Ishihara, T.; Matsumoto, M.; Saito, A.; Tsujihara, K.; Anai, M.; Asano, T. Antidiabetic Effect of T-1095, an Inhibitor of Na<sup>+</sup>-Glucose cotransporter, in Neonatally Streptozotocin-Treated Rats. *Eur. J. Pharmacol.* **2000**, *391* (1–2), 183–192. DOI: [10.1016/s0014-2999\(00\)00016-9](https://doi.org/10.1016/s0014-2999(00)00016-9)
61. Katsuno, K.; Fujimori, Y.; Takemura, Y.; Hiratochi, M.; Itoh, F.; Komatsu, Y.; Fujikura, H.; Isaji, M. Sertigliflozin, a Novel Selective Inhibitor of Low-Affinity Sodium Glucose cotransporter (SGLT2), Validates the Critical Role of SGLT2 in Renal Glucose

## REFERENCES

---

- Reabsorption and Modulates Plasma Glucose Level. *J. Pharmacol. Exp. Ther.* **2007**, 320 (1), 323–330. DOI: [10.1124/jpet.106.110296](https://doi.org/10.1124/jpet.106.110296)
62. Ikegai, K.; Imamura, M.; Suzuki, T.; Nakanishi, K.; Murakami, T.; Kurosaki, E.; Noda, A.; Kobayashi, Y.; Yokota, M.; Koide, T.; Kosakai, K.; Ohkura, Y.; Takeuchi, M.; Tomiyama, H.; Ohta, M. Synthesis and Biological Evaluation of C-Glucosides with Azulene Rings as Selective SGLT2 Inhibitors for the Treatment of Type 2 Diabetes Mellitus: Discovery of YM543. *Bioorg. Med. Chem.* **2013**, 21 (13), 3934–3948. DOI: [10.1016/j.bmc.2013.03.067](https://doi.org/10.1016/j.bmc.2013.03.067)
63. Meng, W.; Ellsworth, B. A.; Nirschl, A. A.; McCann, P. J.; Patel, M.; Girotra, R. N.; Wu, G.; Sher, P. M.; Morrison, E. P.; Biller, S. A.; Zahler, R.; Deshpande, P. P.; Pullockaran, A.; Hagan, D. L.; Morgan, N.; Taylor, J. R.; Obermeier, M. T.; Humphreys, W. G.; Khanna, A.; Discenza, L.; Robertson, J. G.; Wang, A.; Han, S.; Wetterau, J. R.; Janovitz, E. B.; Flint, O. P.; Whaley, J. M.; Washburn, W. N. Discovery of Dapagliflozin: A Potent, Selective Renal Sodium-Dependent Glucose cotransporter 2 (SGLT2) Inhibitor for the Treatment of Type 2 Diabetes. *J. Med. Chem.* **2008**, 51 (5), 1145–1149. DOI: [10.1021/jm701272q](https://doi.org/10.1021/jm701272q)
64. Sarnoski-Brocavich, S.; Hilas, O. Canagliflozin (Invokana), a Novel Oral Agent for Type-2 Diabetes. *Pharm. Ther.* **2013**, 38 (11), 656–666.
65. Kumar, S.; Khatik, G. L.; Mittal, A. Recent Developments in Sodium-Glucose co-Transporter 2 (SGLT2) Inhibitors as a Valuable Tool in the Treatment of Type 2 Diabetes Mellitus. *Mini Rev. Med. Chem.* **2020**, 20 (3), 170–182. DOI: [10.2174/1389557519666191009163519](https://doi.org/10.2174/1389557519666191009163519)
66. Miao, Z.; Nucci, G.; Amin, N.; Sharma, R.; Mascitti, V.; Tugnait, M.; Vaz, A. D.; Callegari, E.; Kalgutkar, A. S. Pharmacokinetics, Metabolism, and Excretion of the Antidiabetic Agent Ertugliflozin (PF-04971729) in Healthy Male Subjects. *Drug Metab. Dispos.* **2013**, 41 (2), 445–456. DOI: [10.1124/dmd.112.049551](https://doi.org/10.1124/dmd.112.049551)
67. Mascitti, V.; Maurer, T. S.; Robinson, R. P.; Bian, J.; Boustany-Kari, C. M.; Brandt, T.; Collman, B. M.; Kalgutkar, A. S.; Klenotic, M. K.; Leininger, M. T.; Lowe, A.; Maguire, R. J.; Masterson, V. M.; Miao, Z.; Mukaiyama, E.; Patel, J. D.; Pettersen, J. C.; Prévile, C.; Samas, B.; She, L.; Sobol, Z.; Steppan, C. M.; Stevens, B. D.; Thuma, B. A.; Tugnait, M.; Zeng, D.; Zhu, T. Discovery of a Clinical Candidate from the Structurally Unique Dioxo-Bicyclo[3.2.1]Octane Class of Sodium-Dependent Glucose



## REFERENCES

---

- Cotransporter 2 Inhibitors. *J. Med. Chem.* **2011**, *54* (8), 2952–2960. DOI: [10.1021/jm200049r](https://doi.org/10.1021/jm200049r)
68. Scott, L. J. Empagliflozin: A Review of Its Use in Patients with Type 2 Diabetes Mellitus. *Drugs* **2014**, *74* (15), 1769–1784. DOI: [10.1007/s40265-014-0298-1](https://doi.org/10.1007/s40265-014-0298-1)
69. Markham, A. Remogliflozin Etabonate: First Global Approval. *Drugs* **2019**, *79* (10), 1157–1161. DOI: [10.1007/s40265-019-01150-9](https://doi.org/10.1007/s40265-019-01150-9)
70. Fujimori, Y.; Katsuno, K.; Nakashima, I.; Ishikawa-Takemura, Y.; Fujikura, H.; Isaji, M. Remogliflozin Etabonate, in a Novel Category of Selective Low-Affinity Sodium Glucose cotransporter (SGLT2) Inhibitors, Exhibits Antidiabetic Efficacy in Rodent Models. *J. Pharmacol. Exp. Ther.* **2008**, *327* (1), 268–276. DOI: [10.1124/jpet.108.140210](https://doi.org/10.1124/jpet.108.140210)
71. Markham, A.; Elkinson, S. Luseogliflozin: First Global Approval. *Drugs* **2014**, *74* (8), 945–950. DOI: [10.1007/s40265-014-0230-8](https://doi.org/10.1007/s40265-014-0230-8)
72. Kakinuma, H.; Oi, T.; Hashimoto-Tsuchiya, Y.; Arai, M.; Kawakita, Y.; Fukasawa, Y.; Iida, I.; Hagima, N.; Takeuchi, H.; Chino, Y.; Asami, J.; Okumura-Kitajima, L.; Io, F.; Yamamoto, D.; Miyata, N.; Takahashi, T.; Uchida, S.; Yamamoto, K. (1S)-1,5-anhydro-1-[5-(4-ethoxybenzyl)-2-methoxy-4-methylphenyl]-1-thio-D-glucitol (TS-071) Is a Potent, Selective Sodium-Dependent Glucose cotransporter 2 (SGLT2) Inhibitor for Type 2 Diabetes Treatment. *J. Med. Chem.* **2010**, *53* (8), 3247–3261. DOI: [10.1021/jm901893x](https://doi.org/10.1021/jm901893x).
73. Imamura, M.; Nakanishi, K.; Suzuki, T.; Ikegai, K.; Shiraki, R.; Ogiyama, T.; Murakami, T.; Kurosaki, E.; Noda, A.; Kobayashi, Y.; Yokota, M.; Koide, T.; Kosakai, K.; Ohkura, Y.; Takeuchi, M.; Tomiyama, H.; Ohta, M. Discovery of Ipragliflozin (ASP1941): A Novel C-Glucoside with Benzothiophene Structure as a Potent and Selective Sodium Glucose co-Transporter 2 (SGLT2) Inhibitor for the Treatment of Type 2 Diabetes Mellitus. *Bioorg. Med. Chem.* **2012**, *20* (10), 3263–3279. DOI: [10.1016/j.bmc.2012.03.051](https://doi.org/10.1016/j.bmc.2012.03.051)
74. Poole, R. M.; Prossler, J. E. Tofogliflozin: First Global Approval. *Drugs* **2014**, *74* (8), 939–944. DOI: [10.1007/s40265-014-0229-1](https://doi.org/10.1007/s40265-014-0229-1)
75. Ohtake, Y.; Sato, T.; Kobayashi, T.; Nishimoto, M.; Taka, N.; Takano, K.; Yamamoto, K.; Ohmori, M.; Yamaguchi, M.; Takami, K.; Yeu, S. Y.; Ahn, K. H.; Matsuoka, H.; Morikawa, K.; Suzuki, M.; Hagita, H.; Ozawa, K.; Yamaguchi, K.; Kato, M.; Ikeda, S.

## REFERENCES

---

- Discovery of Tofogliflozin, a Novel C-arylglucoside with an O-spiroketal Ring System, as a Highly Selective Sodium Glucose cotransporter 2 (SGLT2) Inhibitor for the Treatment of Type 2 Diabetes. *J. Med. Chem.* **2012**, *55* (17), 7828–7840. DOI: [10.1021/jm300884k](https://doi.org/10.1021/jm300884k)
76. Lapuerta, P.; Zambrowicz, B.; Strumph, P.; Sands, A. Development of Sotagliflozin, a Dual Sodium-Dependent Glucose Transporter 1/2 Inhibitor. *Diab. Vasc. Dis. Res.* **2015**, *12* (2), 101–110. DOI: [10.1177/1479164114563304](https://doi.org/10.1177/1479164114563304)
77. Yan, P. K.; Zhang, L. N.; Feng, Y.; Qu, H.; Qin, L.; Zhang, L. S.; Leng, Y. SHR3824, a Novel Selective Inhibitor of Renal Sodium Glucose cotransporter 2, Exhibits Antidiabetic Efficacy in Rodent Models. *Acta Pharmacol. Sin.* **2014**, *35* (5), 613–624. DOI: [10.1038/aps.2013.196](https://doi.org/10.1038/aps.2013.196)
78. Zhang, Y. F.; Liu, Y. M.; Yu, C.; Wang, Y. T.; Zhan, Y.; Liu, H. Y.; Zou, J. J.; Jia, J. Y.; Chen, Q.; Zhong, D. F. Tolerability, Pharmacokinetic, and Pharmacodynamic Profiles of Henagliflozin, a Novel Selective Inhibitor of Sodium-Glucose cotransporter 2, in Healthy Subjects Following Single- and Multiple-Dose Administration. *Clin. Ther.* **2021**, *43* (2), 396–409. DOI: [10.1016/j.clinthera.2020.12.012](https://doi.org/10.1016/j.clinthera.2020.12.012)
- 79a. Halvorsen, Y. C.; Walford, G. A.; Massaro, J.; Aftring, R. P.; Freeman, M. W. A. A 96-Week, Multinational, Randomized, Double-Blind, Parallel-Group, Clinical Trial Evaluating the Safety and Effectiveness of Bexagliflozin as a Monotherapy for Adults with Type 2 Diabetes. *Diabetes Obes. Metab.* **2019**, *21* (11), 2496–2504. DOI: [10.1111/dom.13833](https://doi.org/10.1111/dom.13833)
- 79b. Hoy, S. M. Bexagliflozin: First Approval. *Drugs* **2023 April**, *83* (5), 447–453. DOI: [10.1007/s40265-023-01848-x](https://doi.org/10.1007/s40265-023-01848-x)
80. Song, L.; Yao, X.; Liu, Y.; Zhong, W.; Jiang, J.; Liu, H.; Zhou, H.; Shi, C.; Zong, K.; Wang, C.; Ma, C.; Liu, D.; Hu, P. Translational Prediction of First-in-Human Pharmacokinetics and Pharmacodynamics of Janagliflozin, a Selective SGLT2 Inhibitor, Using Allometric Scaling, Dedrick and PK/PD Modeling Methods. *Eur. J. Pharm. Sci.* **2020**, *147*, 105281. DOI: [10.1016/j.ejps.2020.105281](https://doi.org/10.1016/j.ejps.2020.105281)
81. Zhang, L.; Wang, Y.; Xu, H.; Shi, Y.; Liu, B.; Wei, Q.; Xu, W.; Tang, L.; Wang, J.; Zhao, G. Discovery of 6-Deoxydapagliflozin as a Highly Potent Sodium-Dependent Glucose cotransporter 2 (SGLT2) Inhibitor for the Treatment of Type 2 Diabetes. *Med. Chem.* **2014**, *10* (3), 304–317. DOI: [10.2174/15734064113096660051](https://doi.org/10.2174/15734064113096660051)

## REFERENCES

---

82. Bays, H. E.; Kozlovski, P.; Shao, Q.; Proot, P.; Keefe, D. Licogliflozin, a Novel SGLT1 and 2 Inhibitor: Body Weight Effects in a Randomized Trial in Adults with Overweight or Obesity. *Obesity (Silver Spring)* **2020**, *28* (5), 870–881. DOI: [10.1002/oby.22764](https://doi.org/10.1002/oby.22764)
83. Lv, B.; Xu, B.; Feng, Y.; Peng, K.; Xu, G.; Du, J.; Zhang, L.; Zhang, W.; Zhang, T.; Zhu, L.; Ding, H.; Sheng, Z.; Welihinda, A.; Seed, B.; Chen, Y. Exploration of O-spiroketal C-arylglucosides as Novel and Selective Renal Sodium-Dependent Glucose co-Transporter 2 (SGLT2) Inhibitors. *Bioorg. Med. Chem. Lett.* **2009**, *19* (24), 6877–6881. DOI: [10.1016/j.bmcl.2009.10.088](https://doi.org/10.1016/j.bmcl.2009.10.088)
84. Xu, B.; Lv, B.; Feng, Y.; Xu, G.; Du, J.; Welihinda, A.; Sheng, Z.; Seed, B.; Chen, Y. O-Spiro C-Aryl Glucosides as Novel Sodium-Dependent Glucose co-Transporter 2 (SGLT2) Inhibitors. *Bioorg. Med. Chem. Lett.* **2009**, *19* (19), 5632–5635. DOI: [10.1016/j.bmcl.2009.08.030](https://doi.org/10.1016/j.bmcl.2009.08.030)
85. Zhang, X.; Urbanski, M.; Patel, M.; Zeck, R. E.; Cox, G. G.; Bian, H.; Conway, B. R.; Pat Beavers, M. P.; Rybczynski, P. J.; Demarest, K. T. Heteroaryl-O-Glucosides as Novel Sodium Glucose co-Transporter 2 Inhibitors. Part 1. *Bioorg. Med. Chem. Lett.* **2005**, *15* (23), 5202–5206. DOI: [10.1016/j.bmcl.2005.08.067](https://doi.org/10.1016/j.bmcl.2005.08.067)
86. Dudash Jr., J.; Zhang, X.; Zeck, R. E.; Johnson, S. G.; Cox, G. G.; Conway, B. R.; Rybczynski, P. J.; Demarest, K. T. Glycosylated Dihydrochalcones as Potent and Selective Sodium Glucose co-Transporter 2 (SGLT2) Inhibitors. *Bioorg. Med. Chem. Lett.* **2004**, *14* (20), 5121–5125. DOI: [10.1016/j.bmcl.2004.07.082](https://doi.org/10.1016/j.bmcl.2004.07.082)
87. Song, K. S.; Lee, S. H.; Kim, M. J.; Seo, H. J.; Lee, J.; Lee, S. H.; Jung, M. E.; Son, E. J.; Lee, M.; Kim, J.; Lee, J. Synthesis and SAR of Thiazolylmethylphenyl Glucoside as Novel C-Aryl Glucoside SGLT2 Inhibitors. *A.C.S. Med. Chem. Lett.* **2011**, *2* (2), 182–187. DOI: [10.1021/ml100256c](https://doi.org/10.1021/ml100256c)
88. Park, E. J.; Kong, Y.; Lee, J. S.; Lee, S. H.; Lee, J. Exploration of SAR Regarding Glucose Moiety in Novel C-Aryl Glucoside Inhibitors of SGLT2. *Bioorg. Med. Chem. Lett.* **2011**, *21* (2), 742–746. DOI: [10.1016/j.bmcl.2010.11.115](https://doi.org/10.1016/j.bmcl.2010.11.115)
89. Zhou, H.; Danger, D. P.; Dock, S. T.; Hawley, L.; Roller, S. G.; Smith, C. D.; Handlon, A. L. Synthesis and SAR of Benzisothiazole-and Indolizine- $\beta$ -D-glucopyranoside Inhibitors of SGLT2. *A.C.S. Med. Chem. Lett.* **2010**, *1* (1), 19–23. DOI: [10.1021/ml900010b](https://doi.org/10.1021/ml900010b)

## REFERENCES

---

90. Chu, K. F.; Yao, C. H.; Song, J. S.; Chen, C. T.; Yeh, T. K.; Hsieh, T. C.; Huang, C. Y.; Wang, M. H.; Wu, S. H.; Chang, W. E.; Chao, Y. S.; Lee, J. C. N-Indolylglycosides Bearing Modifications at the Glucose C6-Position as Sodium-Dependent Glucose co-Transporter 2 Inhibitors. *Bioorg. Med. Chem.* **2016**, *24* (10), 2242–2250. DOI: [10.1016/j.bmc.2016.03.058](https://doi.org/10.1016/j.bmc.2016.03.058)
91. Jesus, A. R.; Vila-Viçosa, D.; Machuqueiro, M.; Marques, A. P.; Dore, T. M.; Rauter, A. P. Targeting Type 2 Diabetes with C-Glucosyl Dihydrochalcones as Selective Sodium Glucose co-Transporter 2 (SGLT2) Inhibitors: Synthesis and Biological Evaluation. *J. Med. Chem.* **2017**, *60* (2), 568–579. DOI: [10.1021/acs.jmedchem.6b01134](https://doi.org/10.1021/acs.jmedchem.6b01134)
92. Pan, X.; Huan, Y.; Shen, Z.; Liu, Z. Synthesis and Biological Evaluation of Novel Tetrahydroisoquinoline-C-Aryl Glucosides as SGLT2 Inhibitors for the Treatment of Type 2 Diabetes. *Eur. J. Med. Chem.* **2016**, *114*, 89–100. DOI: [10.1016/j.ejmech.2016.02.053](https://doi.org/10.1016/j.ejmech.2016.02.053)
93. Koga, Y.; Sakamaki, S.; Hongu, M.; Kawanishi, E.; Sakamoto, T.; Yamamoto, Y.; Kimata, H.; Nakayama, K.; Kuriyama, C.; Matsushita, Y.; Ueta, K.; Tsuda-Tsukimoto, M.; Nomura, S. C-Glucosides with Heteroaryl Thiophene as Novel Sodium-Dependent Glucose cotransporter 2 Inhibitors. *Bioorg. Med. Chem.* **2013**, *21* (17), 5561–5572. DOI: [10.1016/j.bmc.2013.05.048](https://doi.org/10.1016/j.bmc.2013.05.048)
94. Guo, C.; Hu, M.; DeOrazio, R. J.; Usyatinsky, A.; Fitzpatrick, K.; Zhang, Z.; Maeng, J. H.; Kitchen, D. B.; Tom, S.; Luche, M.; Khmelnsky, Y.; Mhyre, A. J.; Guzzo, P. R.; Liu, S. The Design and Synthesis of Novel SGLT2 Inhibitors: C-Glycosides with Benzyltriazolopyridinone and Phenylhydantoin as the Aglycone Moieties. *Bioorg. Med. Chem.* **2014**, *22* (13), 3414–3422. DOI: [10.1016/j.bmc.2014.04.036](https://doi.org/10.1016/j.bmc.2014.04.036)
95. Ding, Y.; Mao, L.; Xu, D.; Xie, H.; Yang, L.; Xu, H.; Geng, W.; Gao, Y.; Xia, C.; Zhang, X.; Meng, Q.; Wu, D.; Zhao, J.; Hu, W. C-Aryl Glucoside SGLT2 Inhibitors Containing a Biphenyl Motif as Potential Anti-diabetic Agents. *Bioorg. Med. Chem. Lett.* **2015**, *25* (14), 2744–2748. DOI: [10.1016/j.bmcl.2015.05.040](https://doi.org/10.1016/j.bmcl.2015.05.040)
96. Li, Y.; Shi, Z.; Chen, L.; Zheng, S.; Li, S.; Xu, B.; Liu, Z.; Liu, J.; Deng, C.; Ye, F. Discovery of a Potent, Selective Renal Sodium-Dependent Glucose cotransporter 2 (SGLT2) Inhibitor (HSK0935) for the Treatment of Type 2 Diabetes. *J. Med. Chem.* **2017**, *60* (10), 4173–4184. DOI: [10.1021/acs.jmedchem.6b01818](https://doi.org/10.1021/acs.jmedchem.6b01818)

## REFERENCES

---

97. Yuan, M. C.; Yeh, T. K.; Chen, C. T.; Song, J. S.; Huang, Y. C.; Hsieh, T. C.; Huang, C. Y.; Huang, Y. L.; Wang, M. H.; Wu, S. H.; Yao, C. H.; Chao, Y. S.; Lee, J. C. Identification of an Oxime-Containing C-glucosylarene as a Potential Inhibitor of Sodium-Dependent Glucose co-Transporter 2. *Eur. J. Med. Chem.* **2018**, *143*, 611–620. DOI: [10.1016/j.ejmech.2017.11.019](https://doi.org/10.1016/j.ejmech.2017.11.019)
98. Kuo, G. H.; Gaul, M. D.; Liang, Y.; Xu, J. Z.; Du, F.; Hornby, P.; Xu, G.; Qi, J.; Wallace, N.; Lee, S.; Grant, E.; Murray, W. V.; Demarest, K. Synthesis and Biological Evaluation of benzocyclobutane-C-glycosides as Potent and Orally Active SGLT1/SGLT2 Dual Inhibitors. *Bioorg. Med. Chem. Lett.* **2018**, *28* (7), 1182–1187. DOI: [10.1016/j.bmcl.2018.02.057](https://doi.org/10.1016/j.bmcl.2018.02.057)
99. Mukkamala, R.; Kumar, R.; Banerjee, S. K.; Aidhen, I. S. Synthesis of Benzyl C-Analogues of Dapagliflozin as Potential SGLT2 Inhibitors. *Eur. J. Org. Chem.* **2020**, *2020* (12), 1828–1839. DOI: [10.1002/ejoc.202000025](https://doi.org/10.1002/ejoc.202000025)
100. Wang, Y.; Lou, Y.; Wang, J.; Li, D.; Chen, H.; Zheng, T.; Xia, C.; Song, X.; Dong, T.; Li, J.; Li, J.; Liu, H. Design, Synthesis and Biological Evaluation of 6-Deoxy O-spiroketal C-arylglucosides as Novel Renal Sodium-Dependent Glucose cotransporter 2 (SGLT2) Inhibitors for the Treatment of Type 2 Diabetes. *Eur. J. Med. Chem.* **2019**, *180*, 398–416. DOI: [10.1016/j.ejmech.2019.07.032](https://doi.org/10.1016/j.ejmech.2019.07.032)
101. Xu, G.; Du, F.; Kuo, G. H.; Xu, J. Z.; Liang, Y.; Demarest, K.; Gaul, M. D. 5, 5-Difluoro-And 5-Fluoro-5-Methyl-Hexose-Based C-Glucosides as Potent and Orally Bioavailable SGLT1 and SGLT2 Dual Inhibitors. *Bioorg. Med. Chem. Lett.* **2020**, *30* (17), 127387. DOI: [10.1016/j.bmcl.2020.127387](https://doi.org/10.1016/j.bmcl.2020.127387)
102. Lin, T. S.; Liw, Y. W.; Song, J. S.; Hsieh, T. C.; Yeh, H. W.; Hsu, L. C.; Lin, C. J.; Wu, S. H.; Liang, P. H. Synthesis and Biological Evaluation of Novel C-Aryl d-glucofuranosides as Sodium-Dependent Glucose co-Transporter 2 Inhibitors. *Bioorg. Med. Chem.* **2013**, *21* (21), 6282–6291. DOI: [10.1016/j.bmc.2013.08.067](https://doi.org/10.1016/j.bmc.2013.08.067)
103. Yao, C. H.; Song, J. S.; Chen, C. T.; Yeh, T. K.; Hsieh, T. C.; Wu, S. H.; Huang, C. Y.; Huang, Y. L.; Wang, M. H.; Liu, Y. W.; Tsai, C. H.; Kumar, C. R.; Lee, J. C. Synthesis and Biological Evaluation of Novel C-indolylxylosides as Sodium-Dependent Glucose co-Transporter 2 Inhibitors. *Eur. J. Med. Chem.* **2012**, *55*, 32–38. DOI: [10.1016/j.ejmech.2012.06.053](https://doi.org/10.1016/j.ejmech.2012.06.053)

## REFERENCES

---

104. Goodwin, N. C.; Mabon, R.; Harrison, B. A.; Shadoan, M. K.; Almstead, Z. Y.; Xie, Y.; Healy, J.; Buhning, L. M.; DaCosta, C. M.; Bardenhagen, J.; Mseeh, F.; Liu, Q.; Nouraldeen, A.; Wilson, A. G.; Kimball, S. D.; Powell, D. R.; Rawlins, D. B. Novel L-xylose Derivatives as Selective Sodium-Dependent Glucose cotransporter 2 (SGLT2) Inhibitors for the Treatment of Type 2 Diabetes. *J. Med. Chem.* **2009**, *52* (20), 6201–6204. DOI: [10.1021/jm900951n](https://doi.org/10.1021/jm900951n)
105. Yao, C. H.; Song, J. S.; Chen, C. T.; Yeh, T. K.; Hung, M. S.; Chang, C. C.; Liu, Y. W.; Yuan, M. C.; Hsieh, C. J.; Huang, C. Y.; Wang, M. H.; Chiu, C. H.; Hsieh, T. C.; Wu, S. H.; Hsiao, W. C.; Chu, K. F.; Tsai, C. H.; Chao, Y. S.; Lee, J. C. Discovery of Novel N- $\beta$ -D-Xylosylindole Derivatives as Sodium-Dependent Glucose cotransporter 2 (SGLT2) Inhibitors for the Management of Hyperglycemia in Diabetes. *J. Med. Chem.* **2011**, *54* (1), 166–178. DOI: [10.1021/jm101072y](https://doi.org/10.1021/jm101072y)
106. Li, A. R.; Zhang, J.; Greenberg, J.; Lee, T.; Liu, J. Discovery of Non-glucoside SGLT2 Inhibitors. *Bioorg. Med. Chem. Lett.* **2011**, *21* (8), 2472–2475. DOI: [10.1016/j.bmcl.2011.02.056](https://doi.org/10.1016/j.bmcl.2011.02.056)
107. Du, X.; Lizarzaburu, M.; Turcotte, S.; Lee, T.; Greenberg, J.; Shan, B.; Fan, P.; Ling, Y.; Medina, J. C.; Houze, J. Optimization of Triazoles as Novel and Potent Nonphlorizin SGLT2 Inhibitors. *Bioorg. Med. Chem. Lett.* **2011**, *21* (12), 3774–3779. DOI: [10.1016/j.bmcl.2011.04.053](https://doi.org/10.1016/j.bmcl.2011.04.053)
108. Chaurasiya, S.; Kaur, P.; Nayak, S. K.; Khatik, G. L. Virtual Screening for Identification of Novel Potent EGFR Inhibitors Through AutoDock Vina Molecular Modeling Software. *J. Chem. Pharm. Res.* **2016**, *8*, 353–360.
109. Kaur, K.; Kaur, P.; Mittal, A.; Nayak, S. K.; Khatik, G. L. Design and Molecular Docking Studies of Novel Antimicrobial Peptides Using Autodock Molecular Docking Software. *Asian J. Pharm. Clin. Res.* **2017**, *10* (16), 28–31. DOI: [10.22159/ajpcr.2017.v10s4.21332](https://doi.org/10.22159/ajpcr.2017.v10s4.21332)
110. Trott, O.; Olson, A. J.; Vina, A.D. Improving the Speed and Accuracy of Docking with a New Scoring Function, Efficient Optimization, and Multithreading. *J. Comp. Chem.* **2010**, *31* (2), 455–461. DOI: [10.1002/jcc.21334](https://doi.org/10.1002/jcc.21334)
111. Energy Minimizations Were Performed MM2 Interface Program on Chem3D Ultra 16.0, and Structures Were Drawn by ChemDraw Ultra 16.0, Cambridge: Cambridge Soft;. **1985**.

## REFERENCES

---

112. Abramson, J. F.; S.; Cascio, D. Crystal Structure of Sodium/Sugar Symporter with Bound Galactose from *Vibrio parahaemolyticus*. <https://www.rcsb.org/structure/3DH4> (accessed May 7, 2019).
113. Razzaghi-Asl, N.; Sepehri, S.; Ebadi, A.; Miri, R.; Shahabipour, S. Molecular Docking and Quantum Mechanical Studies on Biflavonoid Structures as BACE-1 Inhibitors. *Struct. Chem.* **2015**, *26* (2), 607–621. DOI: [10.1007/s11224-014-0523-2](https://doi.org/10.1007/s11224-014-0523-2)
114. Kumar, S.; Khatik, G. L.; Mittal, A. In Silico Molecular Docking Study to Search New SGLT2 Inhibitor Based on Dioxabicyclo[3.2.1] Octane Scaffold. *Curr. Comput. Aided Drug Des.* **2020**, *16* (2), 145–154. DOI: [10.2174/1573409914666181019165821](https://doi.org/10.2174/1573409914666181019165821)
115. Sharma, S.; Mittal, A. 1,2,4 Triazoles and 1,2,4 Oxadiazoles Scaffold as SGLT2 Inhibitors: Molecular Docking and ADMET Studies. *Lett. Drug Des. Discov.* **2023**, *20* (11), 1799–1811. DOI: [10.2174/1570180819666220610142359](https://doi.org/10.2174/1570180819666220610142359)
116. Yuan, S.; Chan, H. C. S.; Hu, Z. Using PyMOL as a Platform for Computational Drug Design. *WIREs Comput. Mol. Sci.* **2017**, *7* (2), e1298. DOI: [10.1002/wcms.1298](https://doi.org/10.1002/wcms.1298)
117. Design, L. Pharmacophore and Ligand-Based Design with Biovia Discovery Studio®. *BIOVIA* **2014**.
118. Jejurikar, B. L.; Rohane, S. H. *Drug Designing in Discovery Studio*, 2021.
119. Lazar Toxicity Prediction. <https://lazar.in-silico.ch/predict> (accessed January 21, 2023)
120. Swiss ADME Prediction. <http://www.swissadme.ch/index.php> (accessed January 21, 2023)
121. Balamash, K. S.; Alkreathy, H. M.; Al Gahdali, E. H.; Khoja, S. O.; Ahmad, A. ComparAtive Biochemical and Histopathological Studies on the Efficacy of Metformin and Virgin Olive Oil Against Streptozotocin-Induced Diabetes in Sprague-Dawley Rats. *J. Diabetes Res.* **2018**, 2018, 4692197. DOI: [10.1155/2018/4692197](https://doi.org/10.1155/2018/4692197)
122. Sharma, S.; Mittal, A.; Khurana, N. Utilization of Computational Tool for the Discovery of Schiff Base Based 1, 4-thiadiazole scaffold as SGLT2 inhibitors. *Curr. Signal Transduct. Ther.* **2023**, *3*, 18 (3), 26-44. DOI: [10.2174/0115743624247062230926110428](https://doi.org/10.2174/0115743624247062230926110428)

## List of Appendix

### I. Letter of Candidacy



Centre for  
Research Degree Programmes

*LPU/CRDP/EC/20190727/0037*

Dated: 08 Mar 2019

Shivani Sharma  
Registration Number: 41700187  
Programme Name: Doctor of Philosophy (Pharmaceutical Chemistry)

**Subject: Letter of Candidacy for Ph.D.**

Dear Candidate,

We are very pleased to inform you that the Department Doctoral Board has approved your candidacy for the Ph.D. Programme on 08 Mar 2019 by accepting your research proposal entitled: "DESIGN, SYNTHESIS AND EVALUATION OF SGLT-2 INHIBITORS"

As a Ph.D. candidate you are required to abide by the conditions, rules and regulations laid down for Ph.D. Programme of the University, and amendments, if any, made from time to time.

We wish you the very best!!

In case you have any query related to your programme, please contact Centre of Research Degree Programmes.

Head  
Centre for Research Degree Programmes

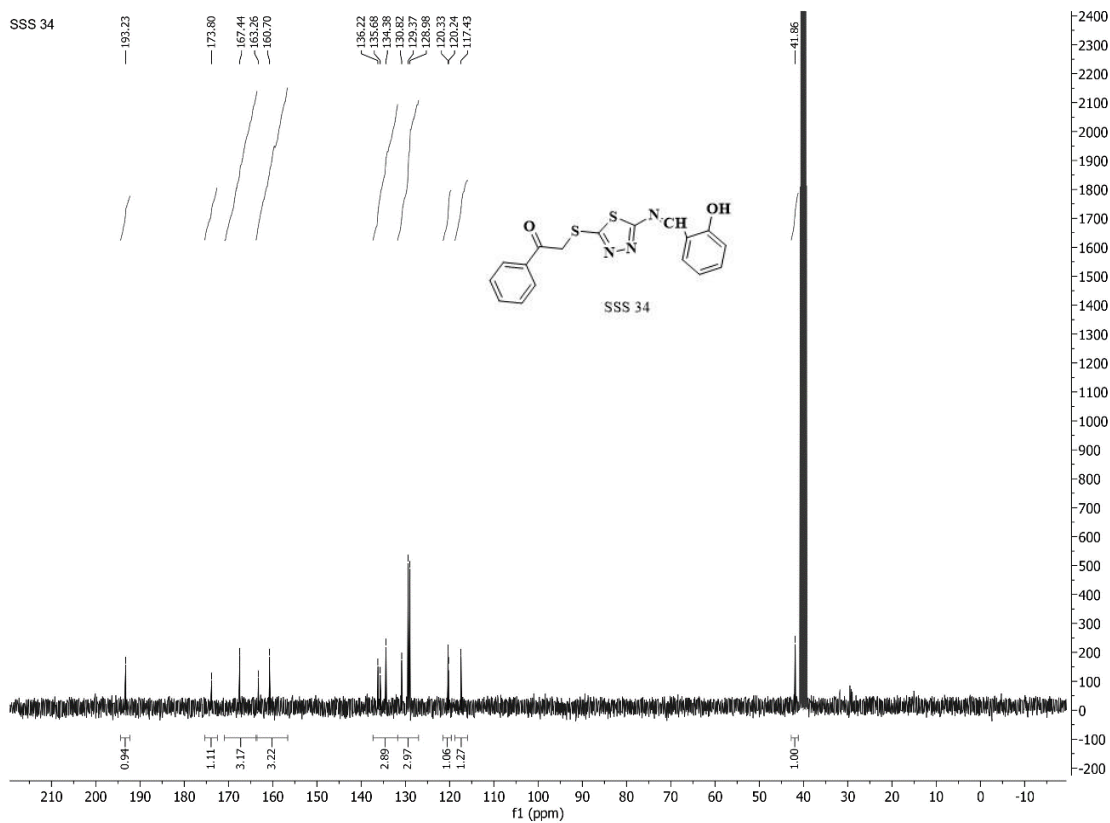
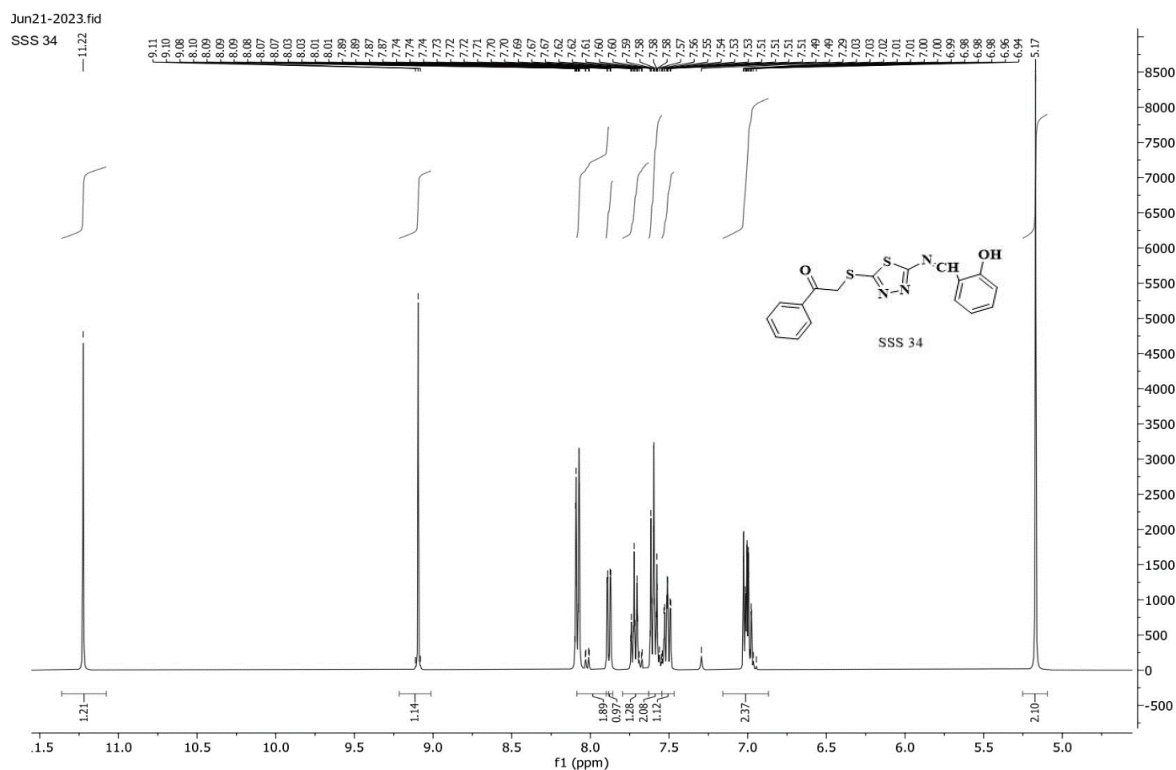
Note:-This is a computer generated certificate and no signature is required. Please use the reference number generated on this certificate for future conversations.

---

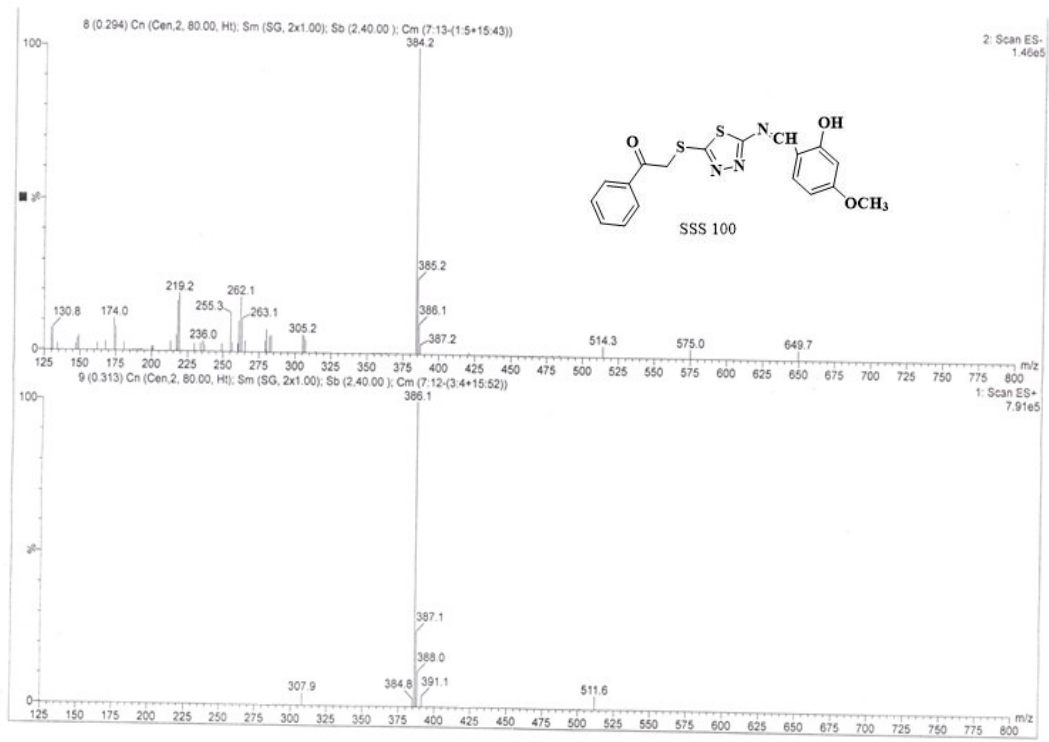
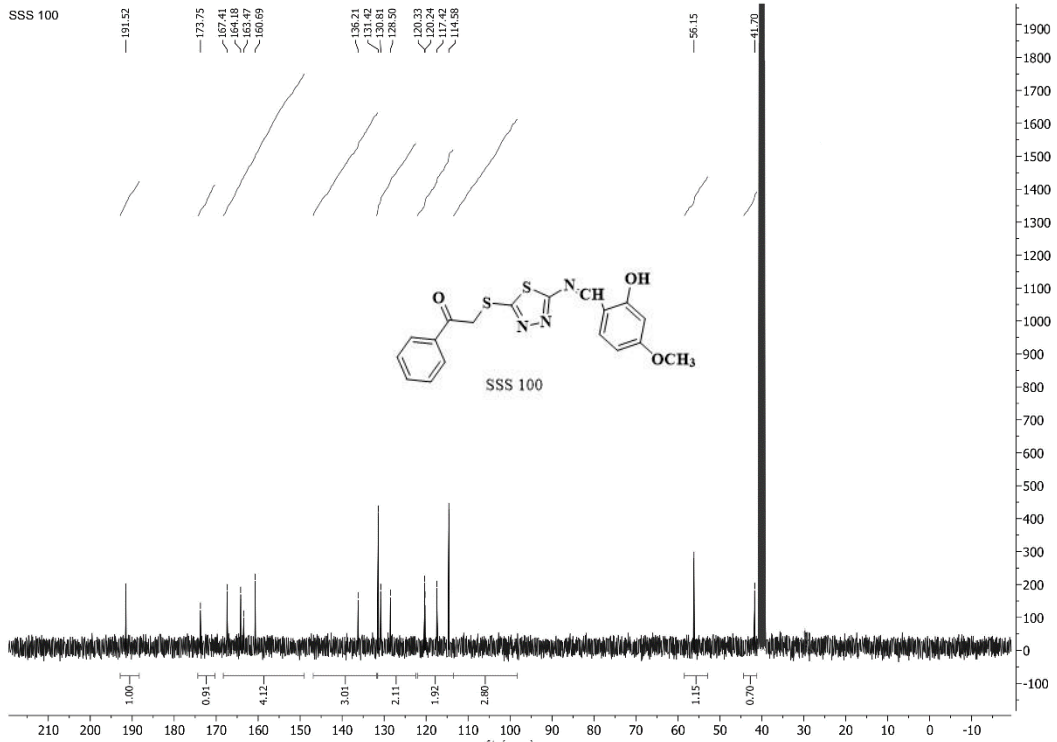
Jalandhar-Delhi G.T.Road, Phagwara, Punjab (India) - 144411  
Ph : +91-1824-444594 E-mail : drp@lpu.co.in website : www.lpu.in



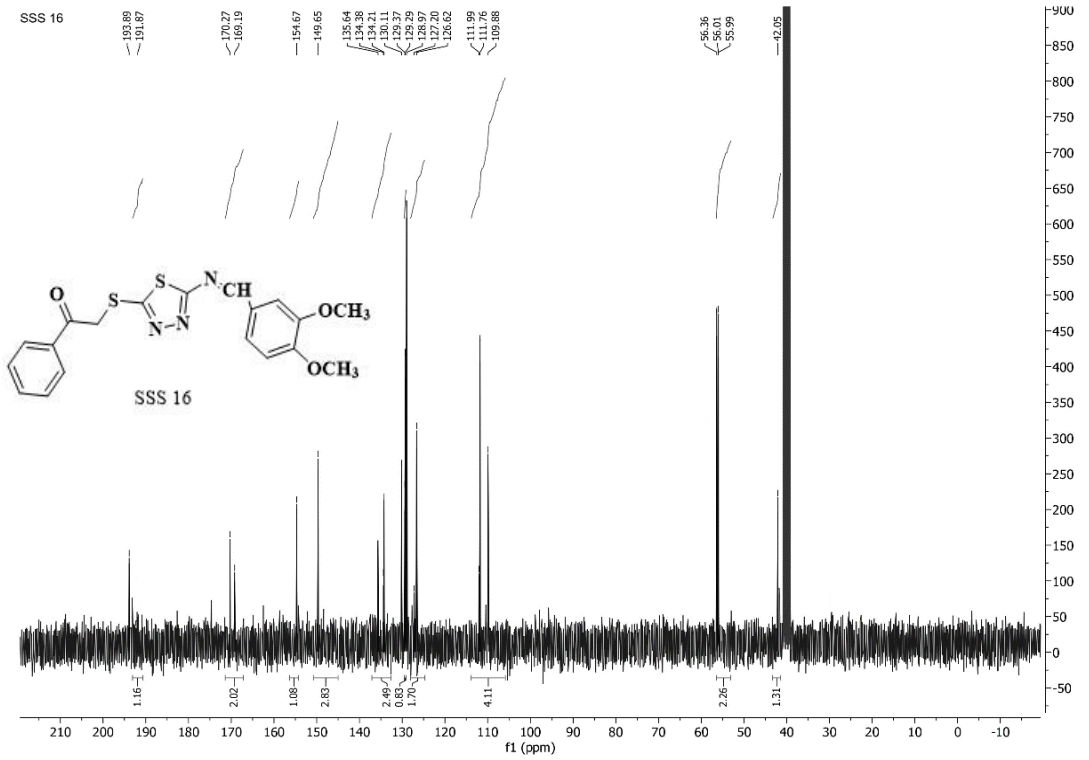
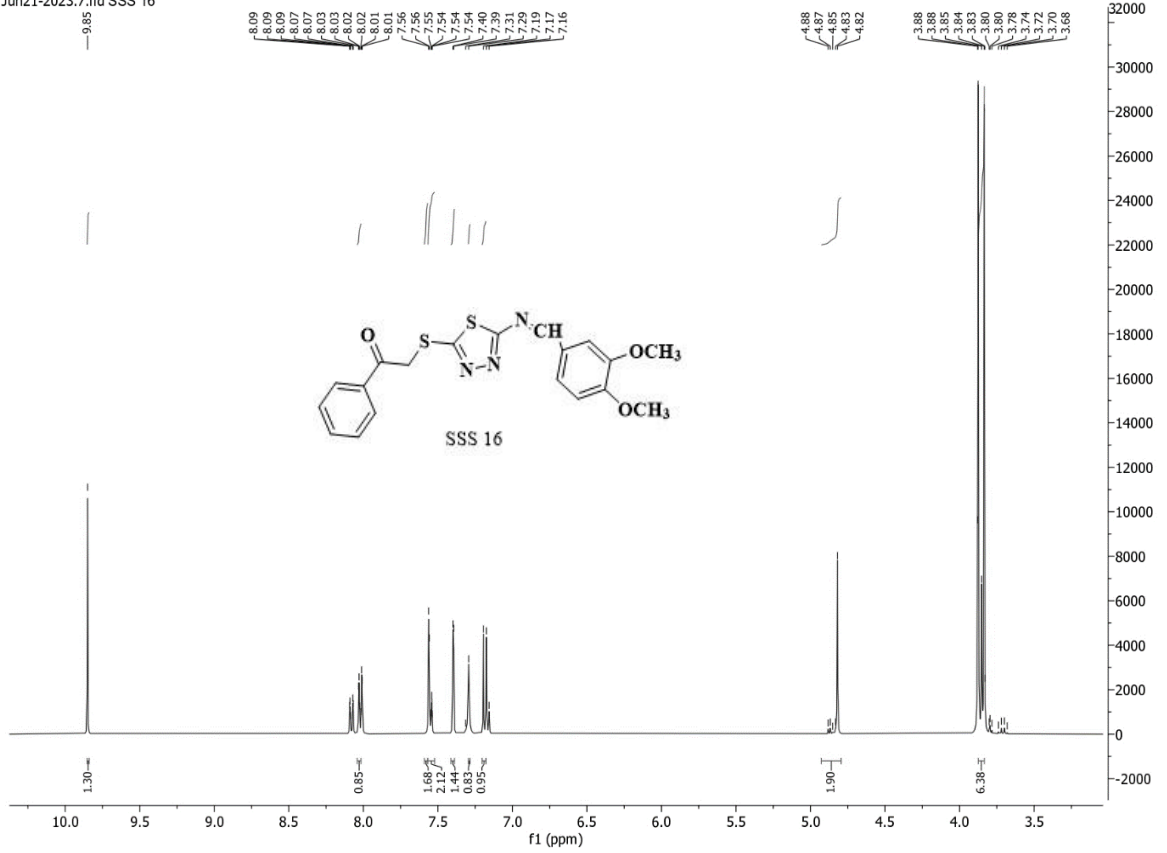
## II NMR and Mass spectra for (SSS 1-SSS 12)

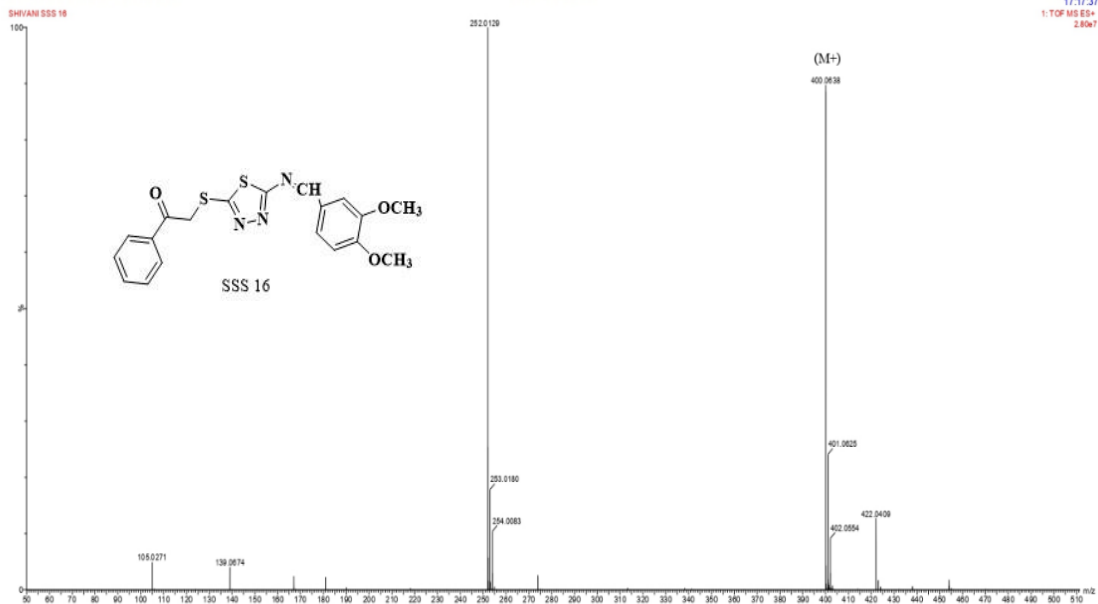




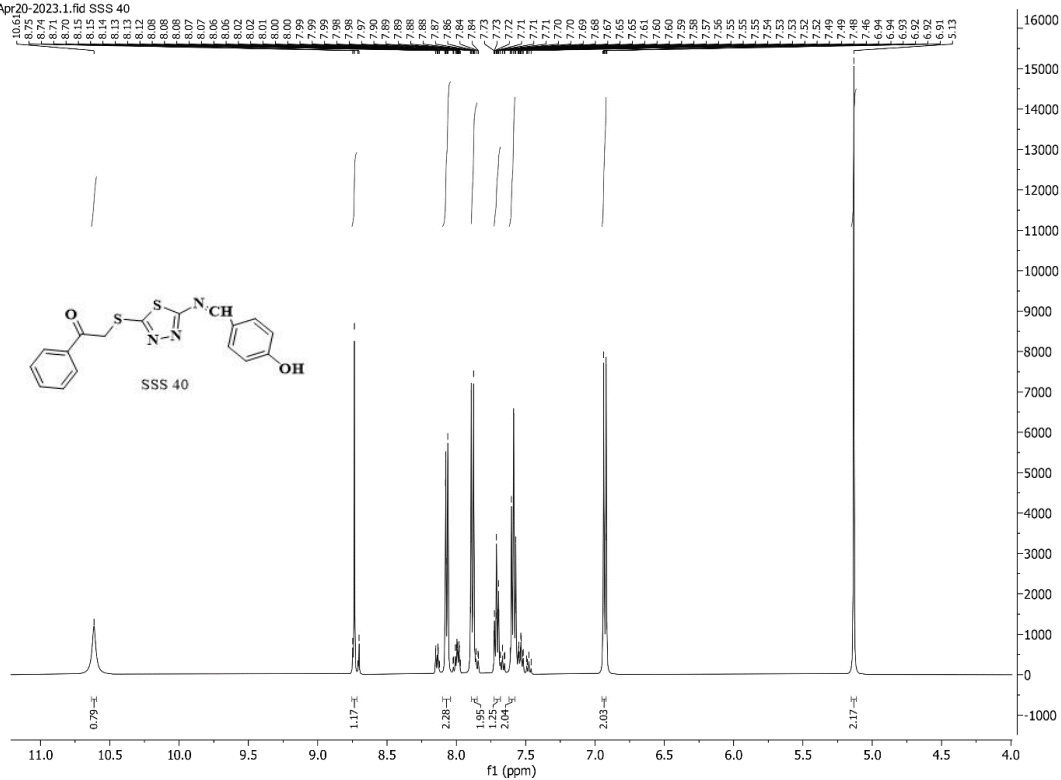


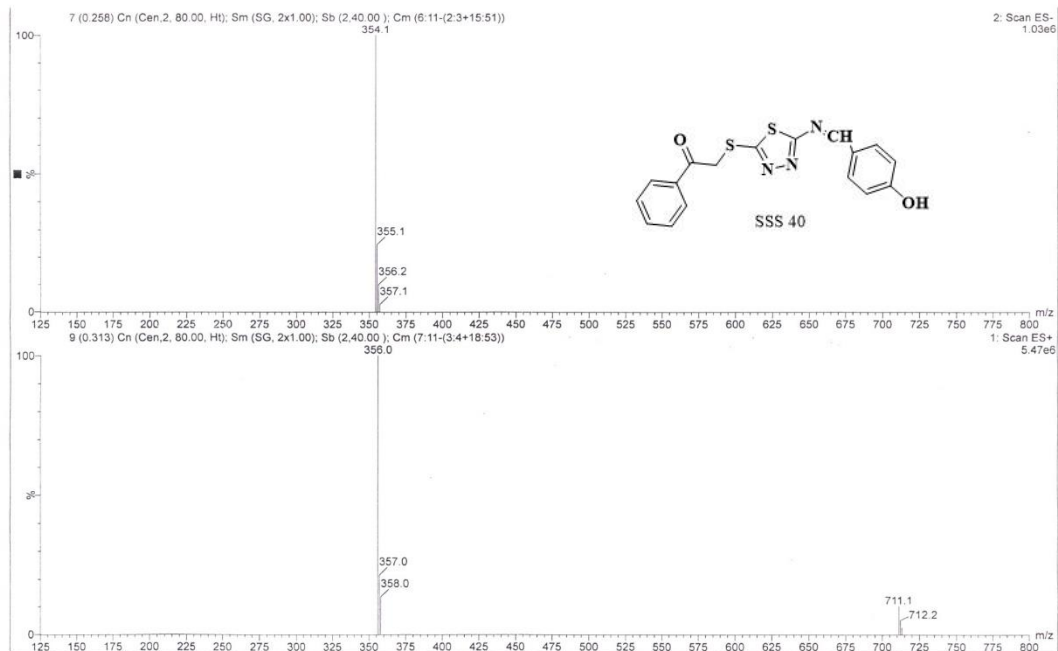
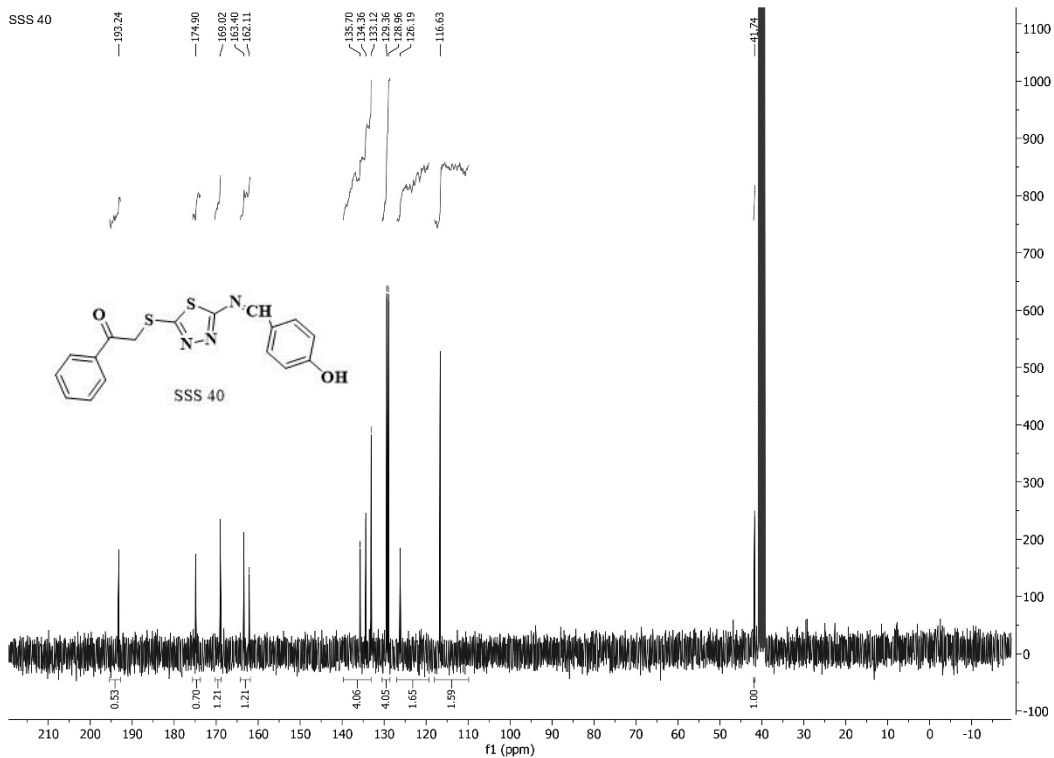
Jun21-2023.7.fid SSS 16



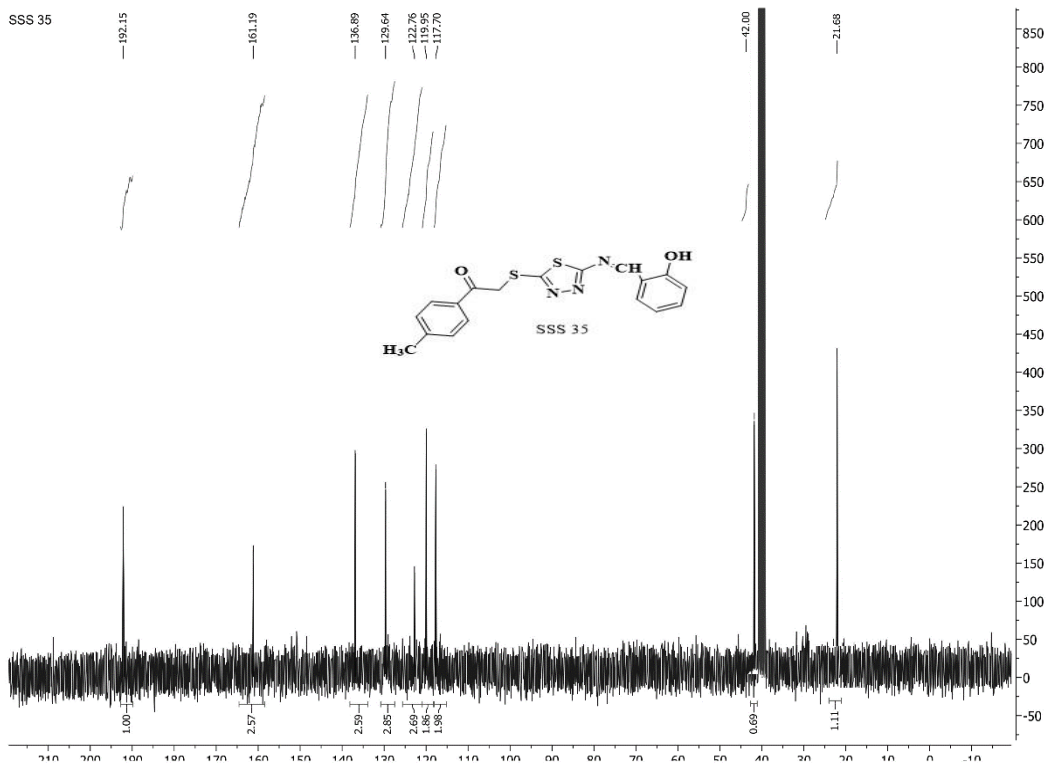
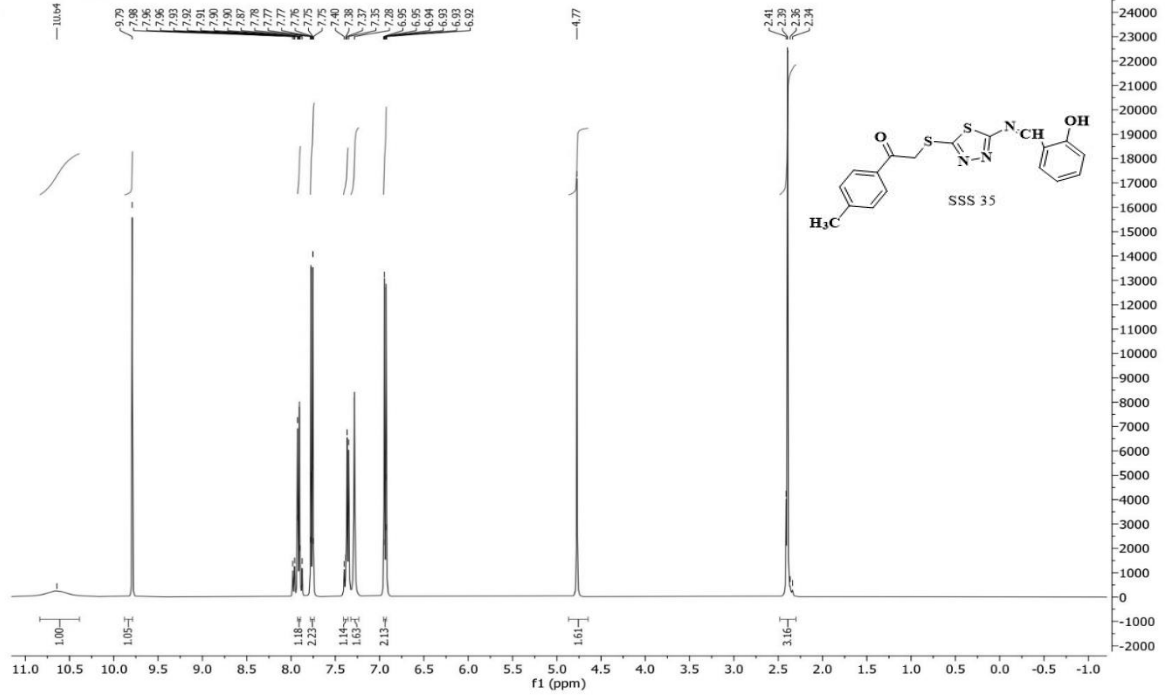


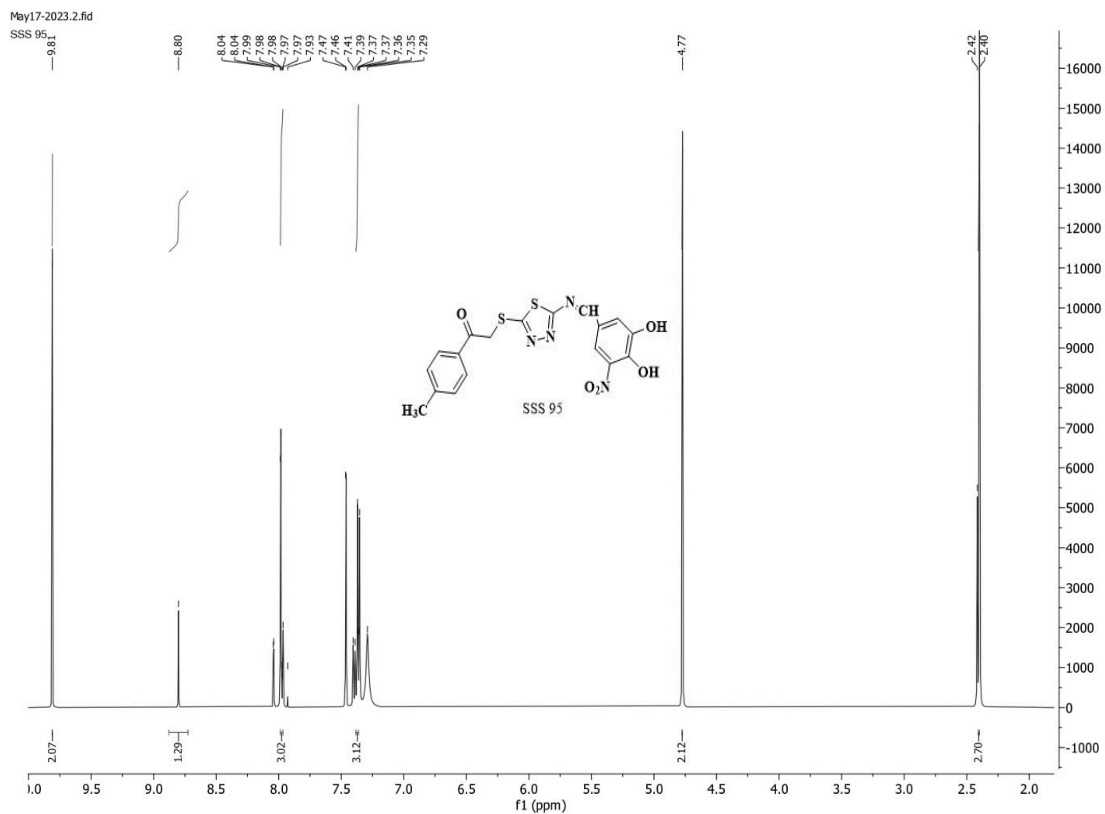
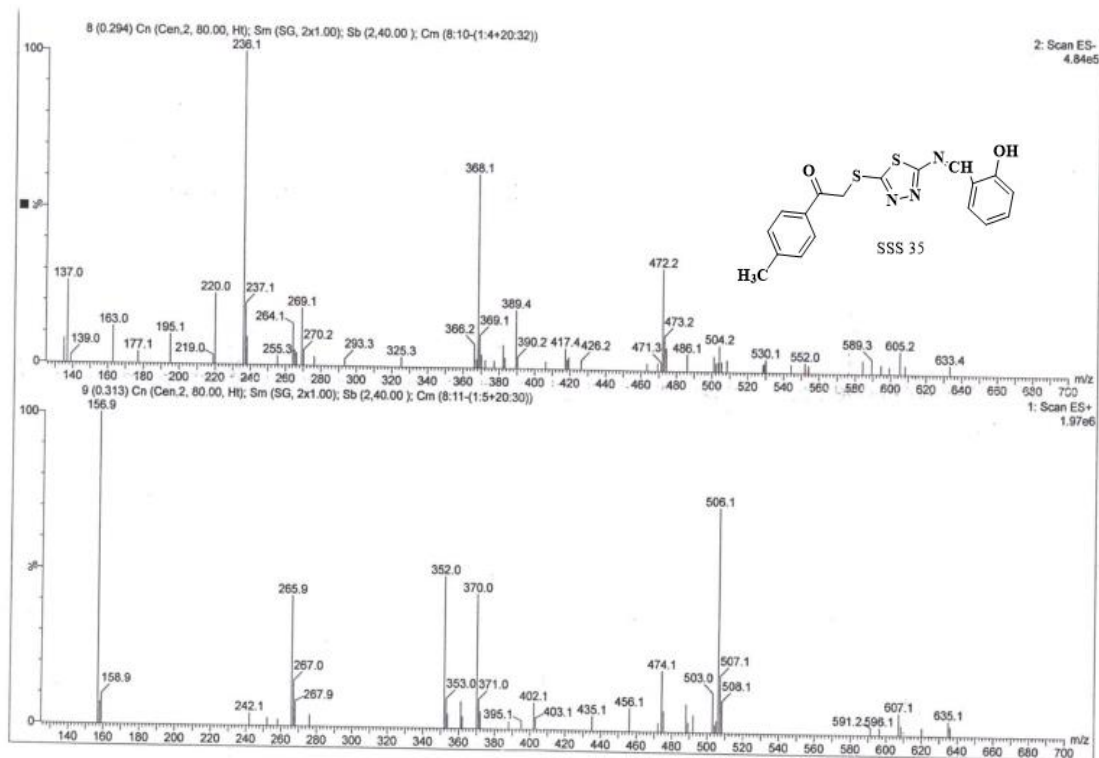
Apr20-2023.1.fid SSS 40



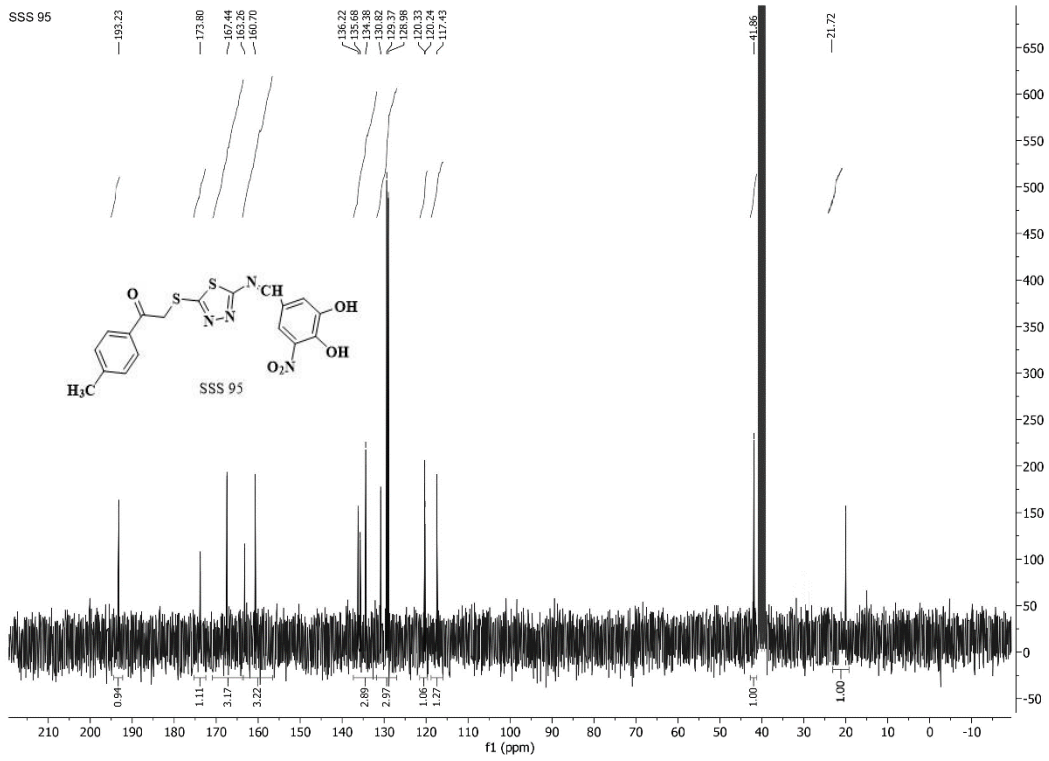


Jun21-2023 SSS 35





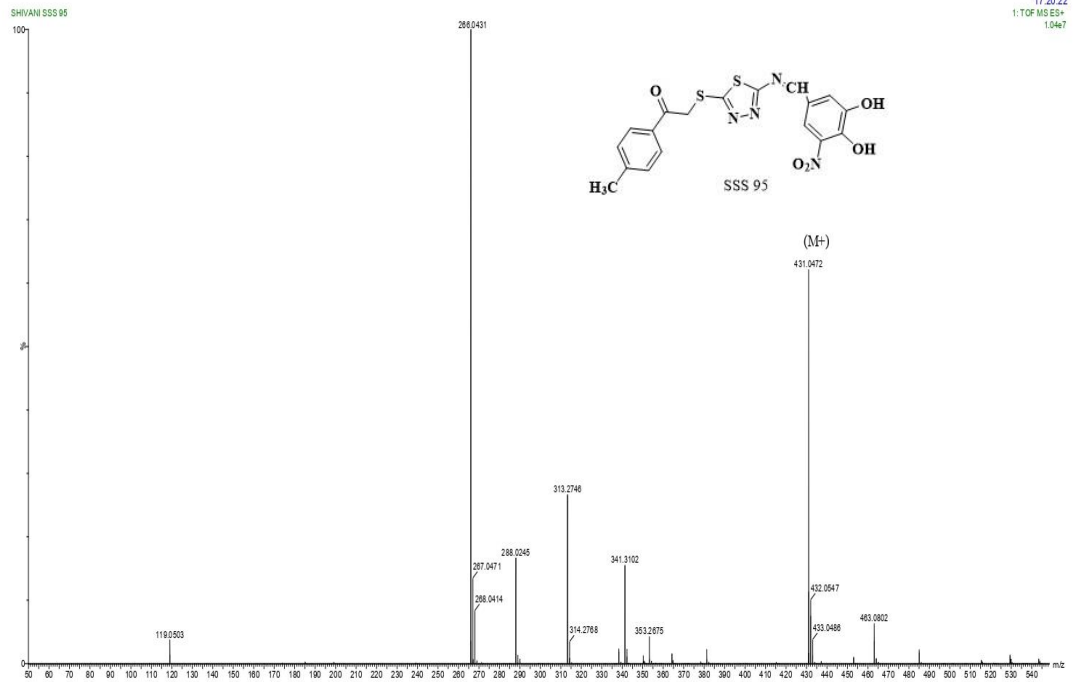




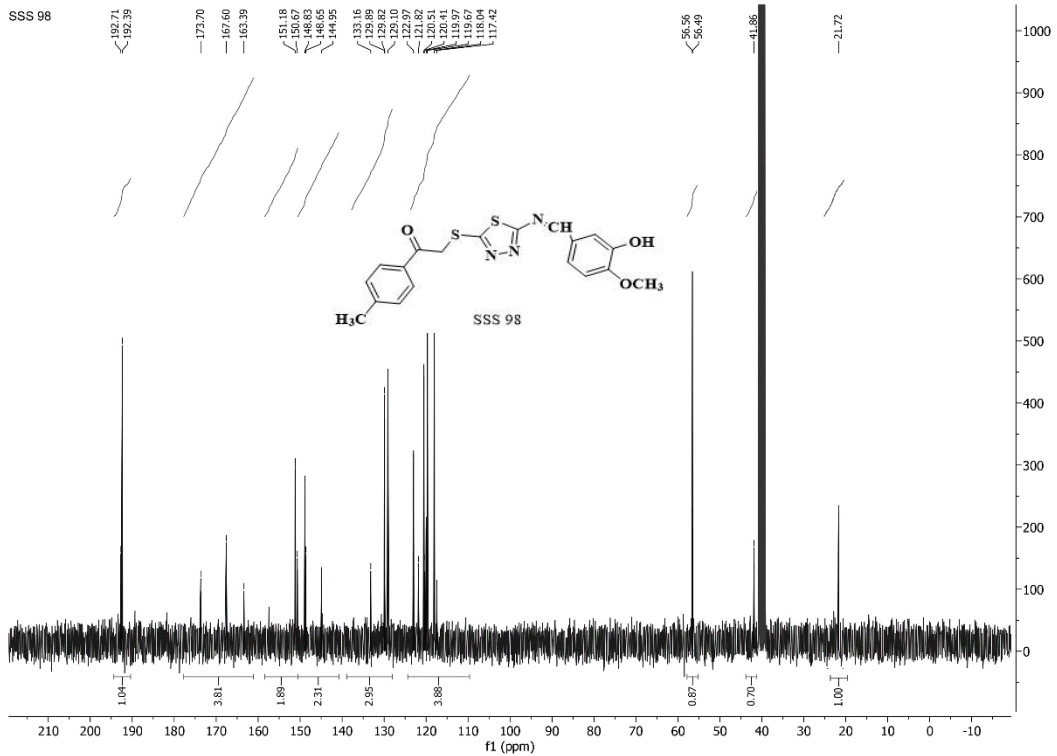
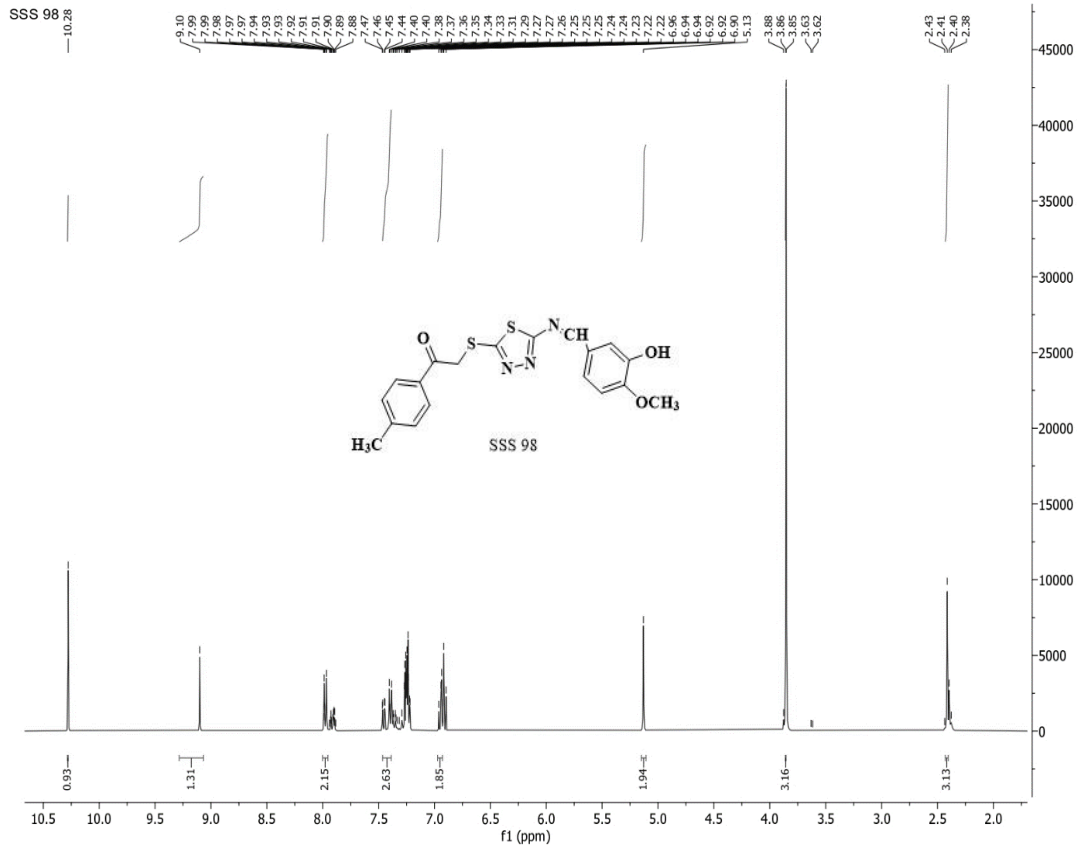
SAIF, PANJAB UNIVERSITY, CHANDIGARH

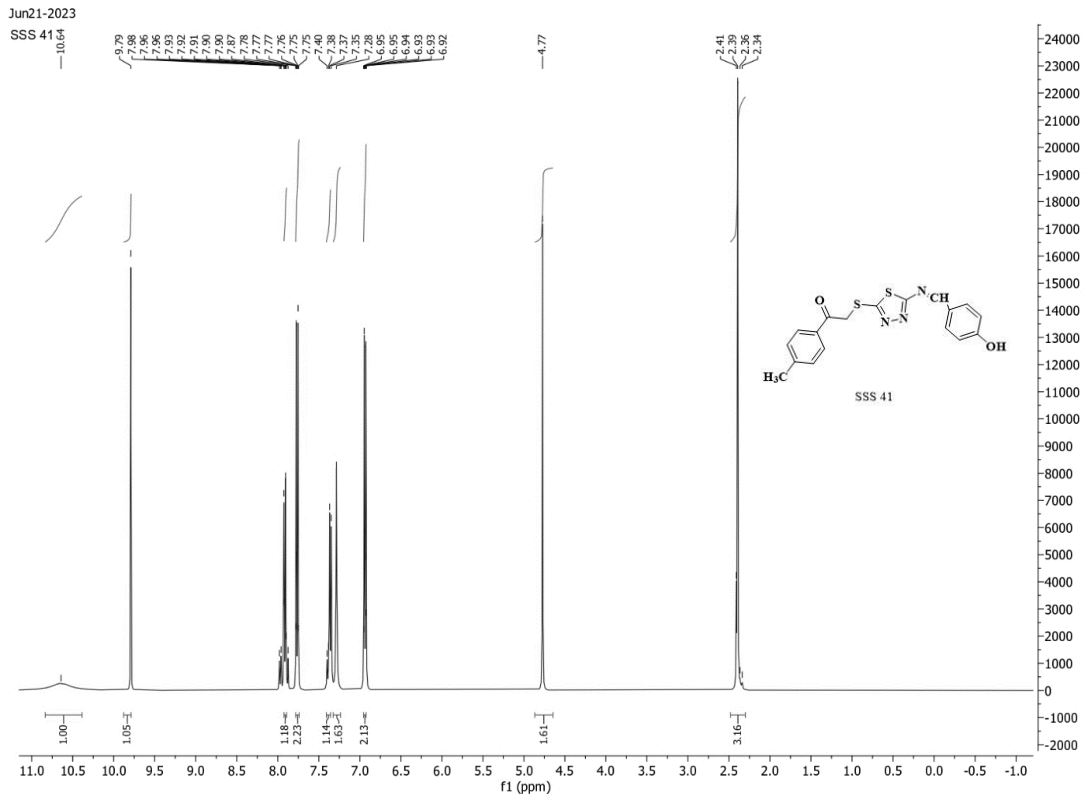
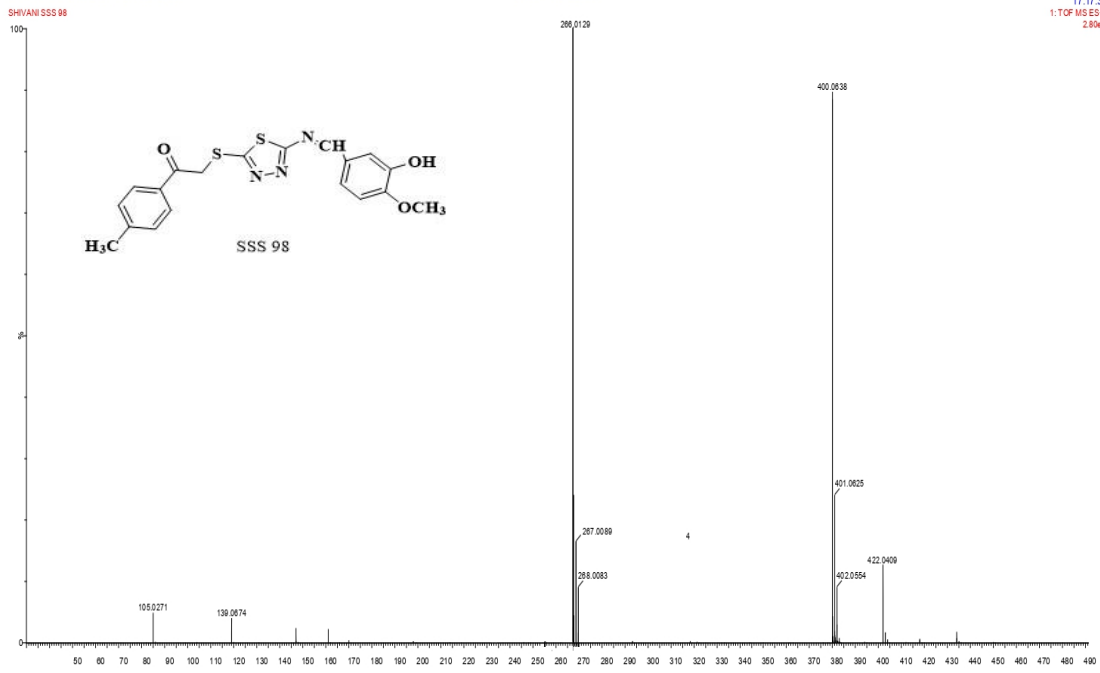
SYNAPT-XS#DBA064

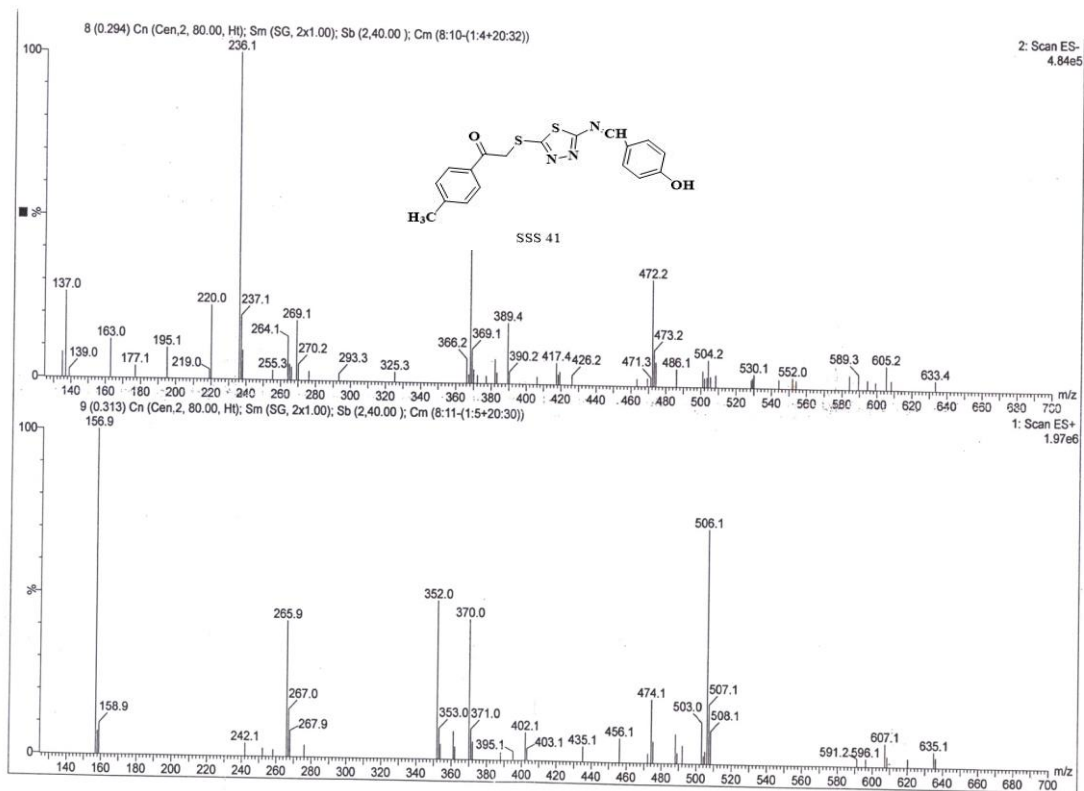
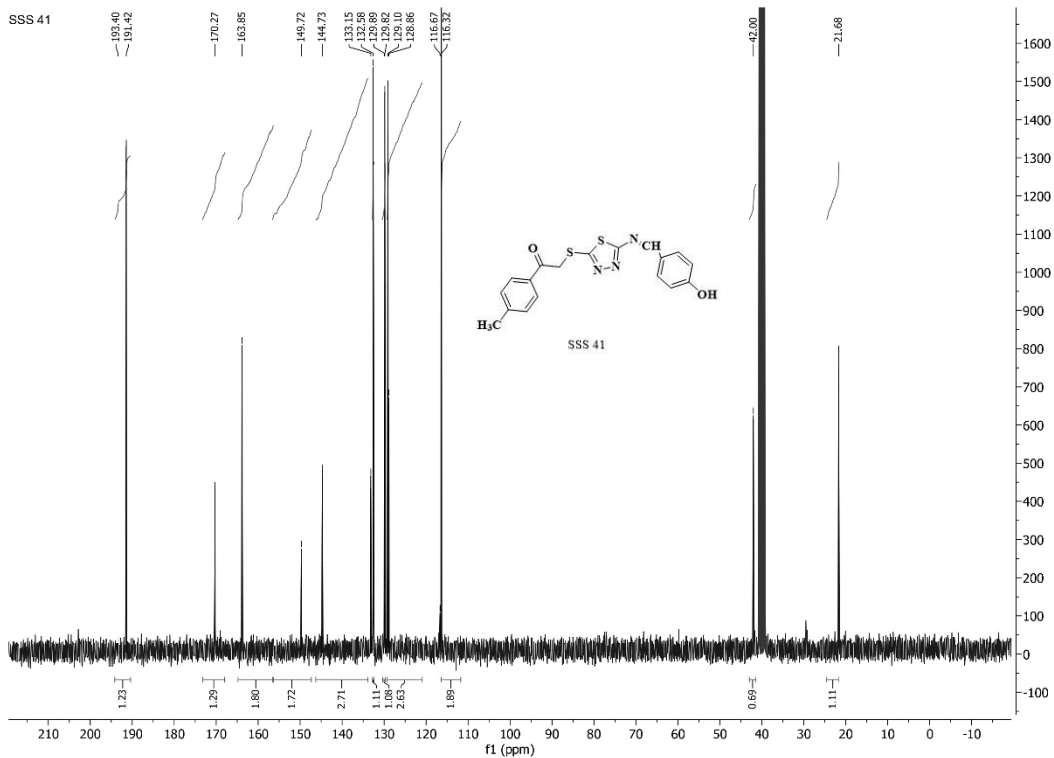
13-Jul-2023  
17:20:22  
1: TOF MS ES+  
1.0467



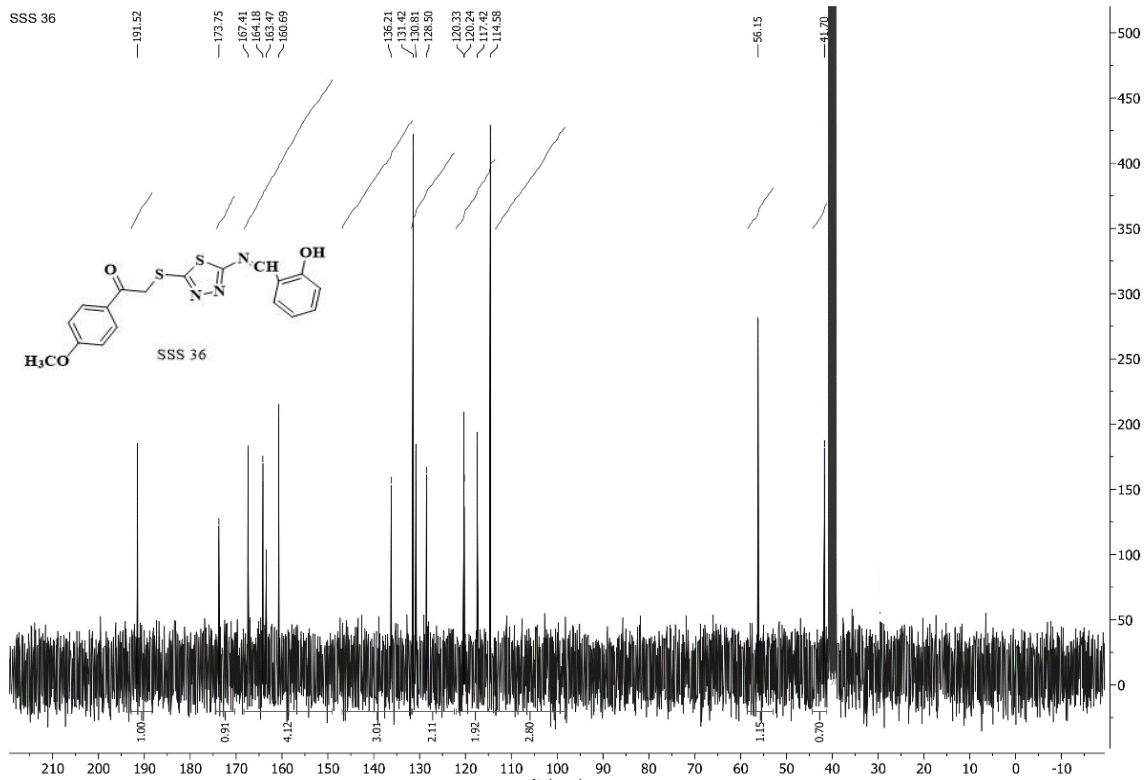
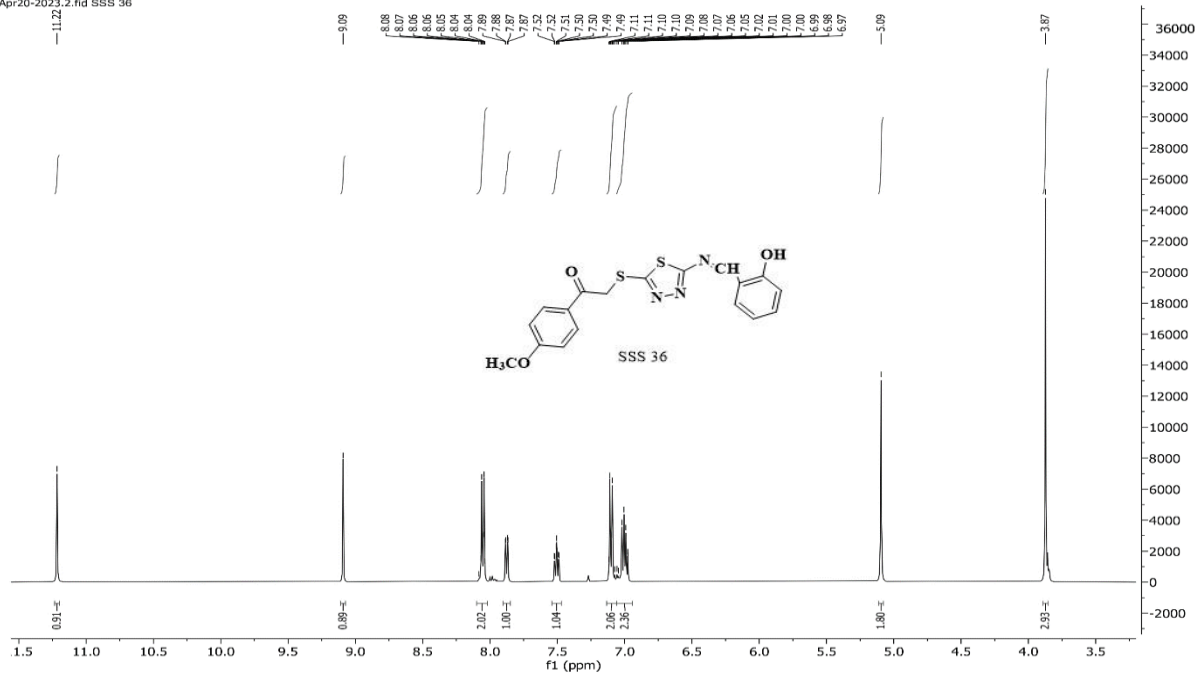
Jun21-2023.9.fid

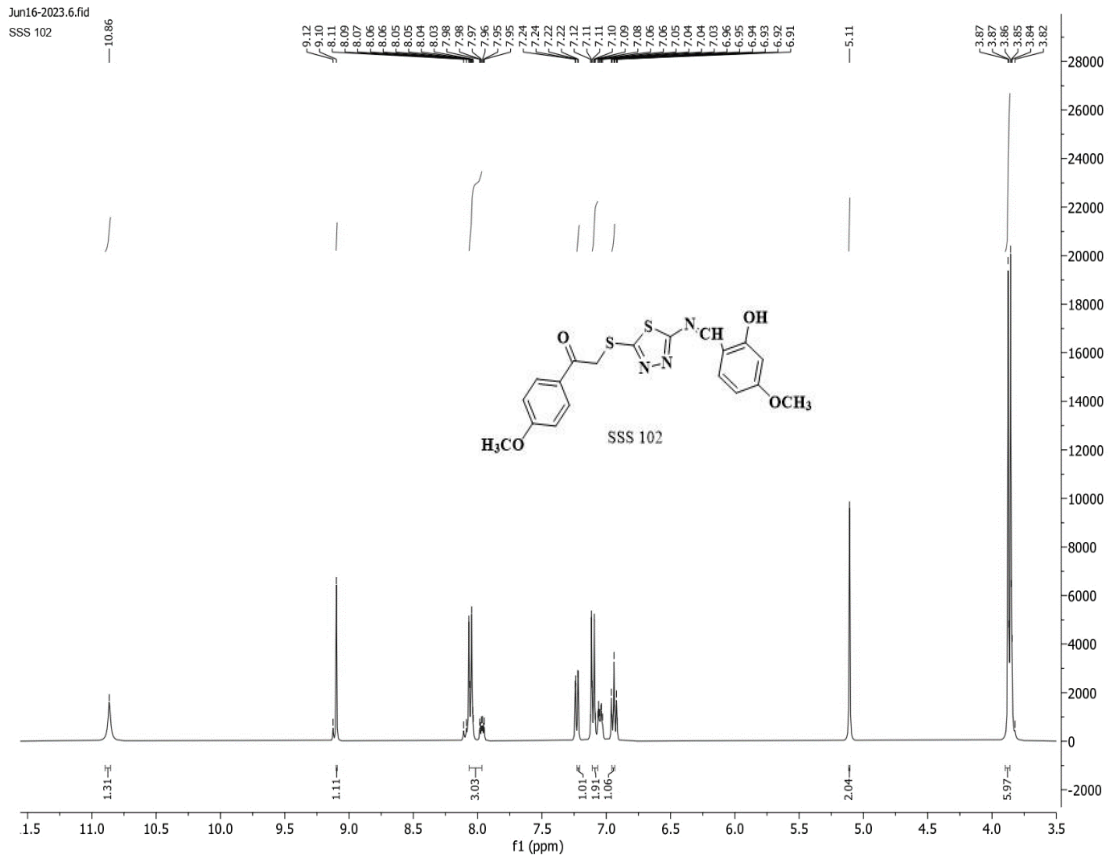
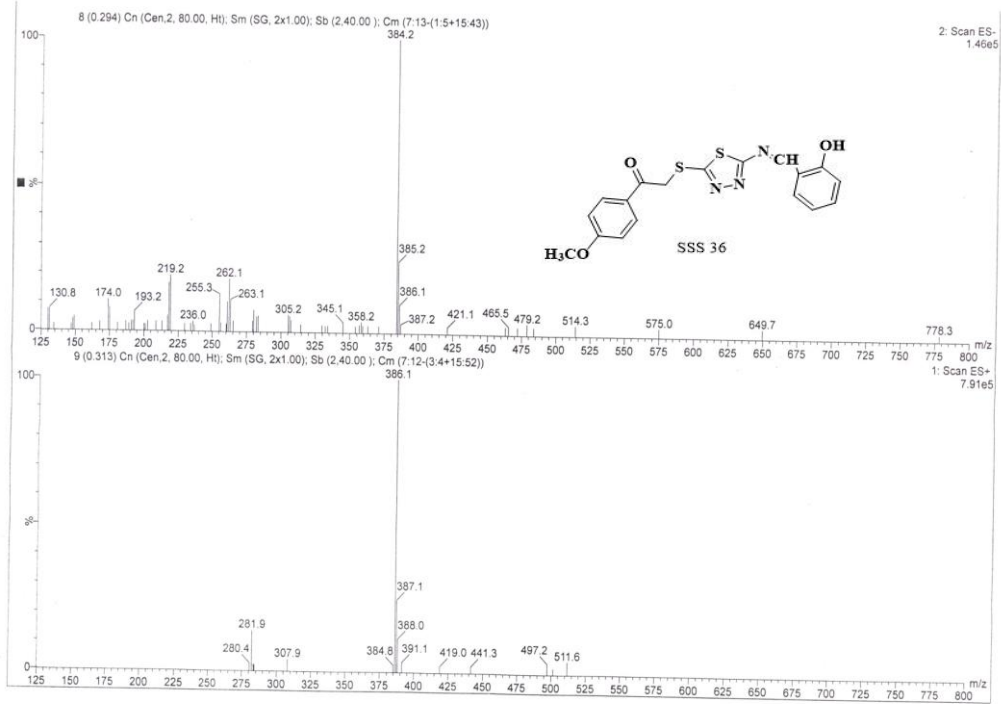


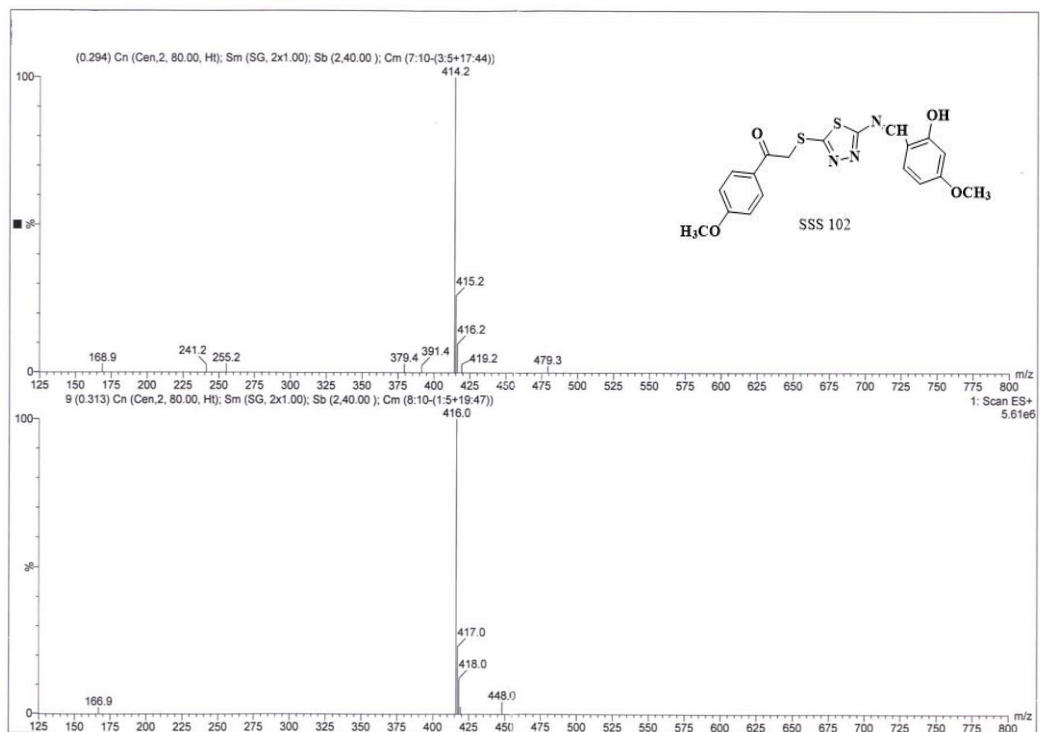
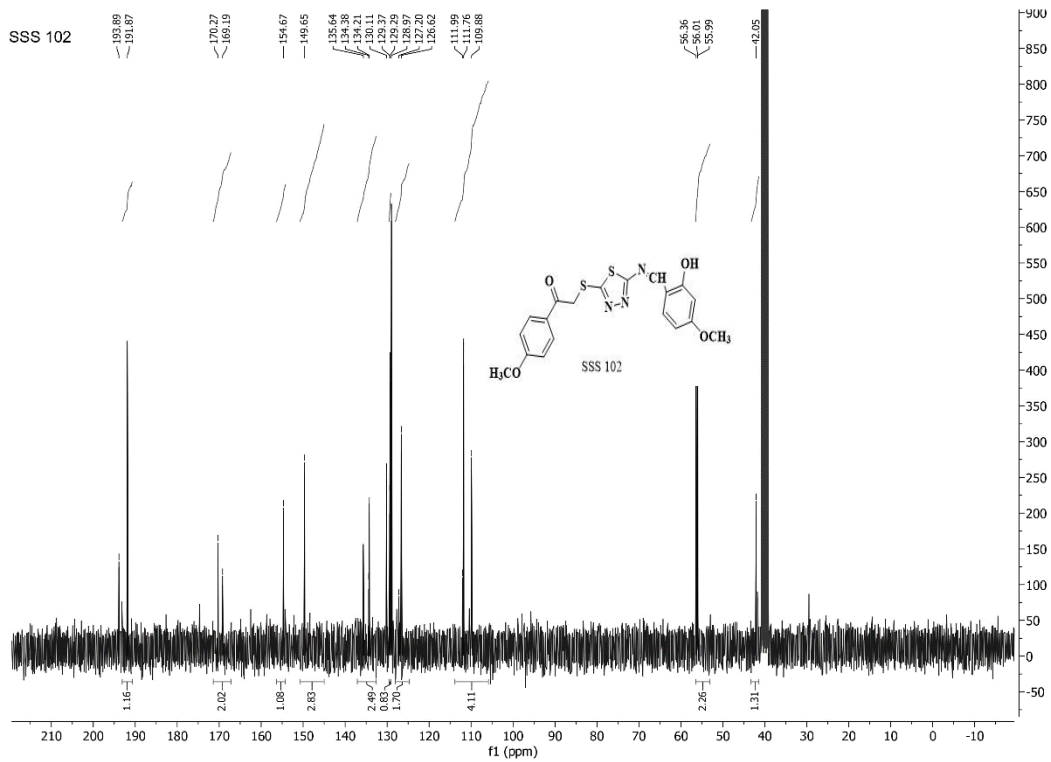


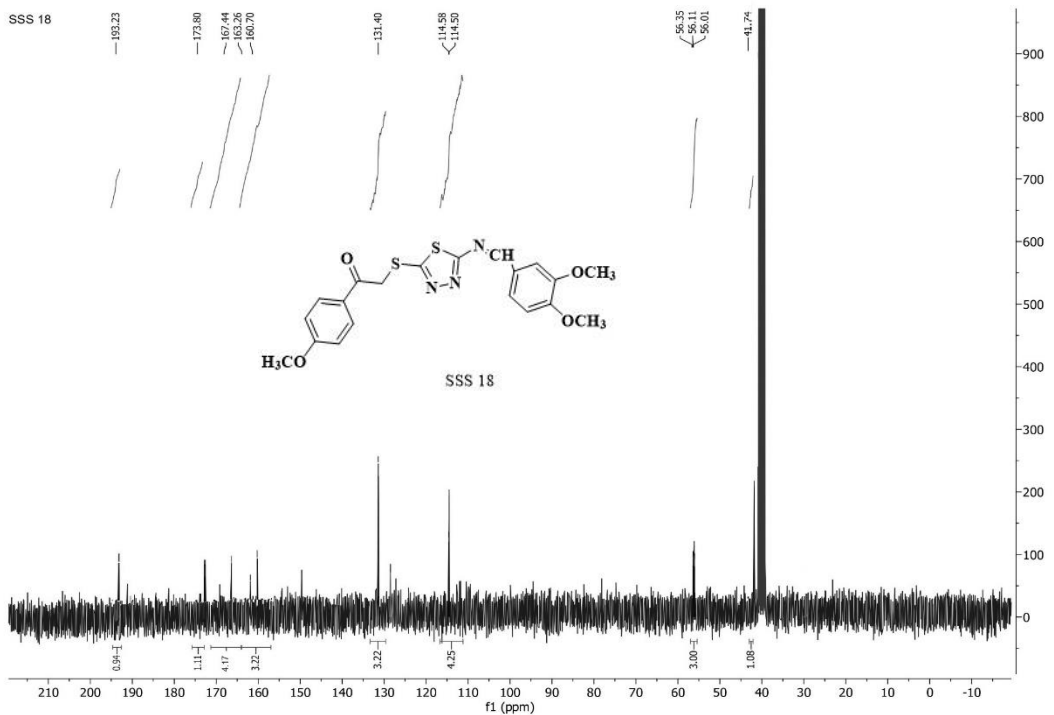
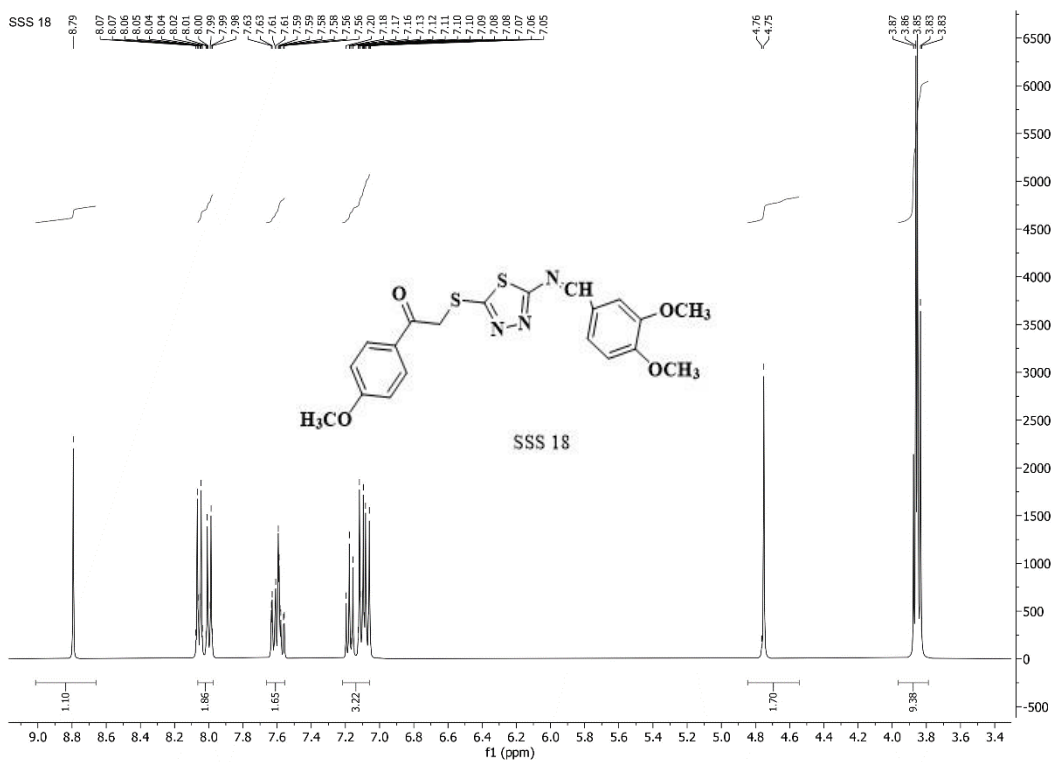


Apr20-2023.2.fid SSS 36

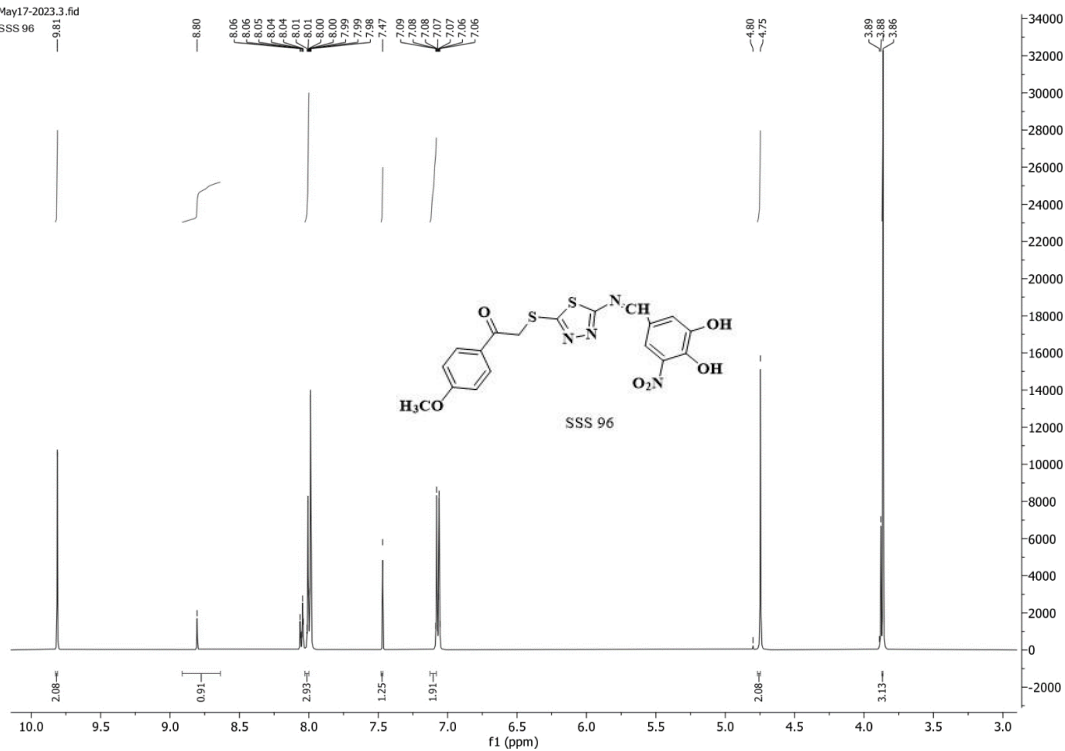
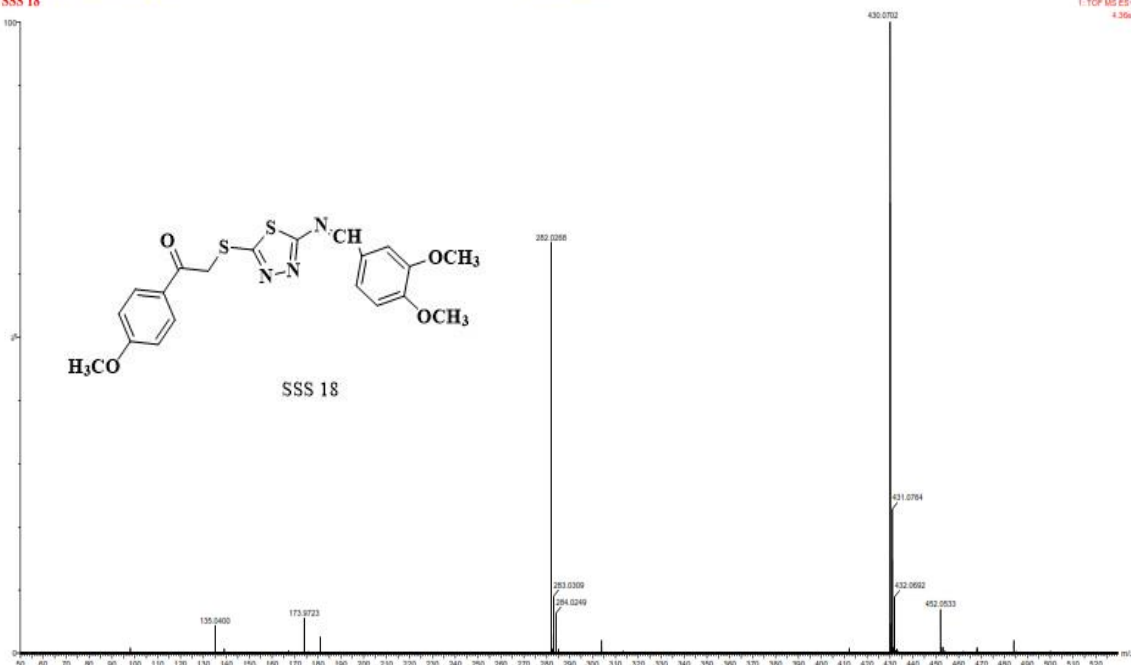


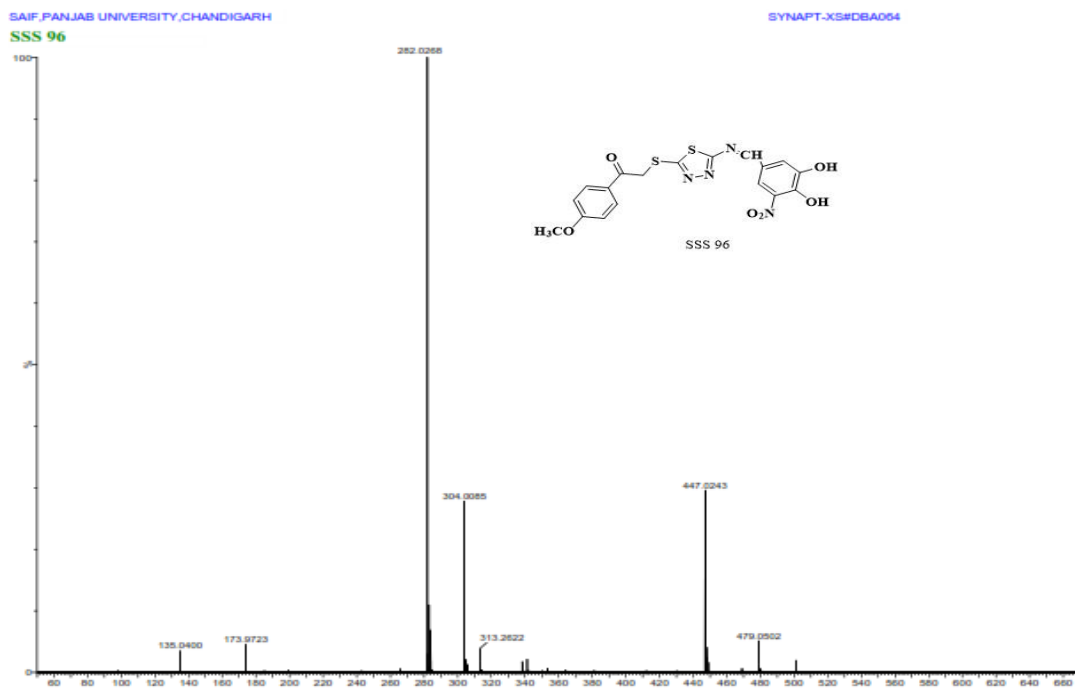
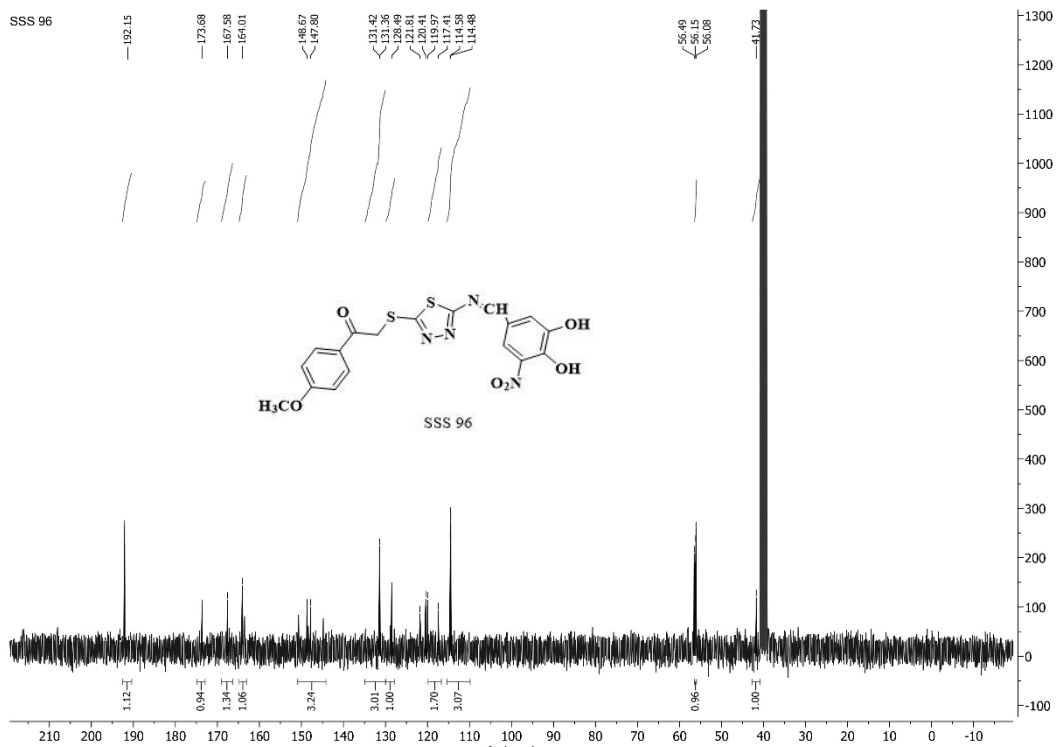












### III. List of Publications

#### Research Article from Current Research Work

Sharma, Shivani; Mittal, Amit\*; Khurana, Navneet. Utilization of Computational Tool for the Discovery of Schiff Base Based 1, 3, 4-thiadiazole scaffold as SGLT2 inhibitors. *Current Signal Transduction Therapy*, 2023, 18 (3), 26-44. DOI: [10.2174/0115743624247062230926110428](https://doi.org/10.2174/0115743624247062230926110428)

Send Orders for Reprints to [reprints@benthamscience.net](mailto:reprints@benthamscience.net)

Current Signal Transduction Therapy, XXXX, XX, 0-0

1

#### RESEARCH ARTICLE

### Utilization of Computational Tools for the Discovery of Schiff Base-based 1, 3, 4-thiadiazole Scaffold as SGLT2 Inhibitors

Shivani Sharma<sup>1</sup>, Amit Mittal<sup>1,2,\*</sup> and Navneet Khurana<sup>1</sup>

<sup>1</sup>School of Pharmaceutical Sciences, Lovely Professional University, Jalandhar-Delhi G.T. Road, Phagwara, Punjab, 144411, India; <sup>2</sup>Faculty of Pharmaceutical Sciences, Desh Bhagat University, Amloh Road, Mandi Gobindgarh, Punjab, 147301, India

**Abstract: Background:** High or abnormal blood sugar levels are the hallmark of diabetes mellitus (DM), a metabolic disorder that will be one of the major causes of mortality in 2021. SGLT2 inhibitors have recently shown beneficial effects in the treatment of diabetes by reducing hyperglycemia and glucosuria.

**Objective:** Molecular docking and ADMET studies of Schiff base-based 1, 3, 4-thiadiazole scaffold as SGLT2 inhibitors.

**Methods:** Chem draw Ultra 16.0 software was used to draw the structures of newly designed molecules of Schiff base-based 1, 3, 4-thiadiazole, which were then translated into 3D structures. For the molecular docking study, AutoDock Vina 1.5.6 software was employed. Lazar *in silico* and Swiss ADME predictors were used to calculate *in silico* ADMET characteristics.

**Results:** We have designed 111 novel Schiff base-based 1, 3, 4-thiadiazole derivatives as SGLT2 inhibitors. A total of 10 compounds from the thiadiazole series were found to have higher binding affinity to the SGLT2 protein than dapagliflozin. SSS 56 had the best docking scores and binding affinities, with -10.4 Kcal/mol, respectively. *In silico* ADMET parameters demonstrated that the best binding compounds were found to be non-carcinogenic with LogP = 2.53-4.02.

**Conclusion:** Novel Schiff base-based 1, 3, 4-thiadiazole were designed and binding affinity was assessed against SGLT2 protein, which resulted in a new lead molecule with a maximal binding affinity and estimated to be noncarcinogenic with an optimal partition coefficient (iLogP = 2.53-4.02).

**Keywords:** SGLT2 inhibitors, 3DH4, ADMET, type-2 diabetes mellitus, molecular docking, auto dock vina.

#### 1. INTRODUCTION

Type-2 diabetes mellitus (T2DM) is the metabolic disorder that has the highest mortality rate and has a significant influence on contemporary society. T2DM prevalence was estimated at 537 million in 2021, and it is anticipated that this figure will increase to 643 million by 2030 and 783 million by 2045 [1]. Diabetes cannot be cured and effectively treated with either insulin therapy or oral medications [2, 3]. In actuality, it's a result of bad lifestyle choices, increased urbanisation and inadequate nutrition. Recently, SGLT (Sodium-Glucose Cotransporter) has been explored as a possible therapeutic target for diabetes [4, 5]. There are numerous SGLT isoforms, and SGLT2 principally accounts for 90% of the reabsorption of glucose in the kidney's proximal tube, whereas SGLT1 reabsorbs the remaining 10% [6-9]. Due to

their insulin-independent activities, which they trigger at various points during the development of T2DM, SGLT2 inhibitors are renowned for being potent. The use of SGLT2 inhibitors in the treatment of T2DM improves blood sugar control, lowers the A1C, may cause a modest drop in blood pressure due to sodium loss, and increases the risk of moderate hypoglycemia and excessive weight loss [10, 11].

The US FDA has approved SGLT2 inhibitors such as Dapagliflozin (Farxiga) [12], Canagliflozin (Invokana) [13], Ertugliflozin (Steglatro) [14], and Empagliflozin (Jardiance) [15]. Remogliflozin (RemoTM, RemozenTM) [16] is currently approved in India. Other SGLT2 inhibitors have also received approval in Japan, including Ipragliflozin (Suglat) [17], Luseogliflozin (Lusefi) [18], and Tofogliflozin (Apleway, Deberza) [19]. While Henagliflozin [20] and Bexagliflozin [21] are undergoing late-stage clinical trials to validate their effectiveness in the treatment of diabetes (Fig. 1).

Our research focuses on the interaction between SGLT2 protein (3DH4) and newly designed 1, 3, 4 thiadiazole molecules

\*Address correspondence to this author at the Faculty of Pharmaceutical Sciences, Desh Bhagat University, Amloh Road, Mandi Gobindgarh, Punjab, 147301, India; Tel: +91-9023900379; E-mail: [amitmittal77@yahoo.com](mailto:amitmittal77@yahoo.com)

Sharma, Shivani; Mittal, Amit.\* 1, 2, 4 Triazoles and 1, 2, 4 Oxadiazoles Scaffold as SGLT2 Inhibitors: Molecular Docking and ADMET Studies. *Letters in Drug Design, Discovery*, 2023, 20(11), 1799–1811. DOI: [10.2174/1570180819666220610142359](https://doi.org/10.2174/1570180819666220610142359)

Send Orders for Reprints to [reprints@benthamscience.net](mailto:reprints@benthamscience.net)

*Letters in Drug Design & Discovery*, 2023, 20, 1799-1811

1799

RESEARCH ARTICLE

## 1,2,4 Triazoles and 1,2,4 Oxadiazoles Scaffold as SGLT2 Inhibitors: Molecular Docking and ADMET Studies

Shivani Sharma<sup>1,2</sup> and Amit Mittal<sup>1,\*</sup>

<sup>1</sup>Department of Pharmaceutical Chemistry, School of Pharmaceutical Sciences, Lovely Professional University, Jalandhar-Delhi G.T. Road (NH-1), Phagwara (Punjab) 144411, India; <sup>2</sup>Faculty of Pharmaceutical Sciences, PCTE Group of Institutes, Campus-2, Near Baddowal Cantt, Ferozepur Road, Ludhiana-142021, India

**Abstract: Background:** Diabetes mellitus (DM) is a metabolic disorder in which blood sugar levels are elevated over a prolonged period of time. SGLT2 inhibitors have recently demonstrated positive effects on diabetes care by minimizing hyperglycemia through decreased glucosuria.

**Objective:** The aim was to carry out molecular docking and ADMET studies of 1,2,4 triazole and 1,2,4 oxadiazole scaffolds as SGLT2 inhibitors.

**Methods:** Structures of newer molecules of two series of 1,2,4 triazoles and 1,2,4 oxadiazoles were drawn by using Chem Draw Ultra 8.0 software. The AutoDock Vina 1.5.6 software was used for the molecular docking studies. *In silico* ADMET properties were calculated online using admetSAR and pkCSM predictors.

**Results:** We have designed 1563 different 1,2,4 triazoles and 1,2,4 oxadiazoles as SGLT2 inhibitors. A total of 14 compounds from both the triazole and oxadiazole series were shown to have better binding affinity to the SGLT2 protein than canagliflozin. Among them, SSN 10 and SSON 7 showed the highest docking score and binding affinity of -10.7 kcal/mol and -10.5 kcal/mol, respectively. *In silico* ADMET properties were also calculated in order to determine physicochemical properties, pharmacokinetics and toxicity of best binding molecules. In addition, these molecules were predicted to be non-carcinogens, showing good oral bioavailability and physicochemical characteristics safer with optimal partition coefficient (LogP = 2.07-5.24).

**Conclusion:** Novel SGLT2 inhibitors were designed based on the scaffold of 1,2,4 triazoles and 1,2,4 oxadiazoles resulting in a new lead molecule with a maximum binding affinity; these molecules were also estimated to be noncarcinogenic with low LogP.

**Keywords:** Type-2 diabetes mellitus, 3DH4, ADMET, SGLT2 inhibitors, molecular docking, auto dock vina.

### 1. INTRODUCTION

Metabolic disorders have a major impact on modern society, and among them, Type-2 diabetes Mellitus (T2DM) causes the highest mortality rate. In 2019, the prevalence of T2DM was estimated at 463 million people and this number is projected to reach 578 million by 2030, and 700 million by 2045 [1]. There is no cure for diabetes, neither insulin therapy nor oral medication is effective in treating it [2, 3]. In fact, its effect comes from rapid urbanization, inadequate nutrition, and an unhealthy lifestyle continuum. SGLT (Sodium-Glucose Cotransporter) has recently been investigated as a potential drug target in diabetes [4, 5]. SGLT exists in several isoforms, with SGLT2 accounting for 90% of sugar

reabsorption in the PCT of the kidney and SGLT1 accounting for the remainder [6-9]. SGLT2 inhibitors provide enhanced glucose regulation by increasing insulin sensitivity and incorporation into muscle cells, reducing gluconeogenesis and enhancing early insulin release in beta cells. SGLT2 inhibitors are known to be robust because of their insulin-independent actions, which they activate at different times during T2DM development. Treating T2DM with SGLT2 inhibitors results in better glycemia, A1C decrease and a slight decrease in blood pressure that may result from sodium loss, risk mild hypoglycemia, and excessive weight loss [10, 11].

SGLT2 inhibitors such as Dapagliflozin (Farxiga) [12], Canagliflozin (Invokana) [13], Ertugliflozin (Steglatro) [14], and Empagliflozin (Jardiance) [15] have been approved by the US FDA. At present, Remogliflozin (Remo™, Remozen™) [16] has been approved in India. Other SGLT2 inhibitors such as Ipragliflozin (Suglat) [17], Luseogliflozin

\*Address correspondence to this author at the Department of Pharmaceutical Chemistry, School of Pharmaceutical Sciences, Lovely Professional University, Jalandhar-Delhi G.T. Road (NH-1), Phagwara (Punjab) 144411, India; Tel: +91-9023900379, E-mail: [amit.13145@lpu.co.in](mailto:amit.13145@lpu.co.in)

## Review Article from Project Work

Sharma Shivani, Mittal Amit\*, Kumar Shubham, Mittal Anu. Structural Perspectives and Advancement of SGLT2 Inhibitors for the Treatment of Type 2 Diabetes.

Current Diabetes Reviews. 2022 Jul 1;18 (6):12-34. DOI:

[10.2174/1573399817666210917122745](https://doi.org/10.2174/1573399817666210917122745)



REVIEW ARTICLE

### Structural Perspectives and Advancement of SGLT2 Inhibitors for the Treatment of Type 2 Diabetes

Current Diabetes Reviews, 2022, 18, e170921196601

Shivani Sharma<sup>1,2</sup>, Amit Mittal<sup>1,\*</sup>, Shubham Kumar<sup>1,2</sup> and Anu Mittal<sup>3</sup>

<sup>1</sup>Department of Pharmaceutical Chemistry, School of Pharmaceutical Sciences, Lovely Professional University, Jalandhar-Delhi G.T. Road (NH-1), Phagwara (Punjab) 144411, India; <sup>2</sup>Faculty of Pharmaceutical Sciences, PCTE Group of Institutes, Campus-2, Near Baddowal Cantt. Ferozepur Road, Ludhiana-142021, India; <sup>3</sup>Department of Chemistry, Guru Nanak Dev University College, Patti, Distt. Tarn Taran, India

#### ARTICLE HISTORY

Received: April 26, 2021  
Revised: August 12, 2021  
Accepted: August 14, 2021

DOI:  
[10.2174/1573399817666210917122745](https://doi.org/10.2174/1573399817666210917122745)



**Abstract:** Diabetes mellitus is an ailment that affects a large number of individuals worldwide and its pervasiveness has been predicted to increase later on. Every year, billions of dollars are spent globally on diabetes-related health care practices. Contemporary hyperglycemic therapies to rationalize Type 2 Diabetes Mellitus (T2DM) mostly involve pathways that are insulin-dependent and lack effectiveness as the pancreas'  $\beta$ -cell function declines more significantly. Homeostasis *via* kidneys emerges as a new and future strategy to minimize T2DM complications. This article covers the reabsorption of glucose mechanism in the kidneys, the functional mechanism of various Sodium-Glucose Cotransporter 2 (SGLT2) inhibitors, their structure and driving profile, and a few SGLT2 inhibitors now accessible in the market as well as those in different periods of advancement. The advantages of SGLT2 inhibitors are dose-dependent glycemic regulation changes with a significant reduction both in the concentration of HbA1c and body weight clinically and statistically. A considerable number of SGLT2 inhibitors have been approved by the FDA, while a few others, still in preliminaries, have shown interesting effects.

**Keywords:** SGLT2 Inhibitors, diabetes mellitus, dapagliflozin, glucose, hypoglycemia, phlorizin.

#### 1. INTRODUCTION

Type 2 diabetes has become a source of concern because it is one of the leading causes of death and morbidity. Due to diabetes and its related complications, the mortality rate increased to approximately 4.2 million deaths on a global scale in 2019 [1]. The prevalence of type 2 diabetes mellitus affected 463 million individuals worldwide in 2019 and, if the current trend continues, it will reach 700 million by 2045 [2]. In 2019, the WHO evaluated that 9.3% of adults between the ages of 20-79 years had diabetes and about one-half of cases of type 2 diabetes, *i.e.* 50.1%, were undiagnosed [2]. In developed countries, 87-91% of all diabetes patients have type 2 diabetes. 79.4% of adults are estimated to have type 2 diabetes, especially those living in developing and middle-income countries. The proportion of diabetes in women aged 20-79 years was estimated to be slightly lower than in men (9.0% vs. 9.6%). Diabetes accounted for at least \$760 billion global healthcare expenditures in 2019, with the figure expected to rise to \$845 billion by 2045, accounting for approximately 10% of total adult health spending. [3, 4]. The progression of type 2 diabetes mellitus (T2DM) is influenced by activities such as the consumption of unhealthy food and lack of exercise commonly associated with urba-

nization [5]. Lifestyle modifications like intervention in nutrition and physical activity are usually recommended as starting treatment for patients with T2DM, and then a switch to diabetes-management pharmacotherapy [6]. The diagnostic criteria for diabetes have been modified by WHO and it is diagnosed by detecting elevated blood glucose levels, as shown in Table 1. The American Diabetes Association (ADA) recommends levels of glycated hemoglobin (HbA1c) between 6.5%-7.0% [7-9]. Conventional oral anti-diabetic agents such as thiazolidinediones [10-12], sulphonylureas [13], meglitinides, biguanides, and alpha-glucoside inhibitors are limited by severe adverse effects *i.e.* hypoglycemia as shown in Table 2 and their structures are given in (Fig. 1). There is a growing demand for a new approach to counteract the effect of insulin release. Renal gluconeogenesis, blood-stream insulin use, and glucose reabsorption from glomerular filtrate are known to be critical in regulating glucose [14].

#### 2. SODIUM GLUCOSE COTRANSPORTER 2 (SGLT2) INHIBITORS

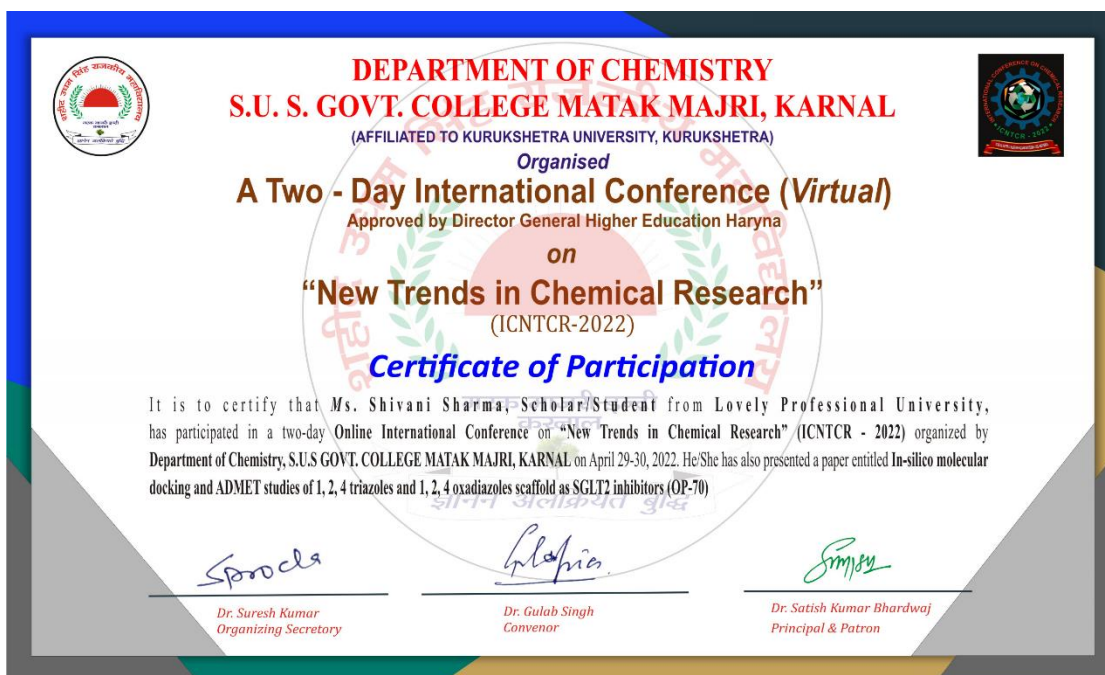
Cotransporters of sodium/glucose are a class of drugs that restrain glucose reabsorption in the kidneys and improve the discharge of urinary glucose, leading to low glucose levels. The two sodium/glucose cotransporter types are SGLT1 and SGLT2, which are cloned from the rodent kidney on the Proximal Convoluted tubule (PCT) apical membrane and encoded by SLC5A1 and SLC5A2 [15-17].

\*Address correspondence to this author at the 1Department of Pharmaceutical Chemistry, School of Pharmaceutical Sciences, Lovely Professional University, Jalandhar-Delhi G.T. Road (NH-1), Phagwara (Punjab) 144411, India; E-mail: amitmittal77@yahoo.com

#### IV. Other Allied Publications

1. **Sharma, Shivani**; Mittal, A.; Mehra, A. Oral Insulin Delivery: A Patent Review. *Pharm. Pat. Anal.* 2022 November, 11 (6), 199–212. DOI: 10.4155/ppa-2022-0017
2. Sharma, **Shivani**; Joshi, S.; Anuradha, S.; Kaur, S.; Mittal, A. Kisquali (Ribociclib): A Promising Therapeutic Candidate against Breast Cancer. *A.I.P. Conf. Proc.* 2023, 2800, 020221. DOI: 10.1063/5.0169010
3. Mehra, A.; Sangwan, R.; Mehra, A.; Sharma, **Shivani**; Wadhwa, P.; Mittal, A. Therapeutic Charisma of Imidazo [2, 1-b][1, 3, 4]-Thiadiazole Analogues: A Patent Review. *Pharm. Pat. Anal.* 2023 July, 12 (4), 177–191. DOI: 10.4155/ppa-2023-0006
4. Mohil, D.; Kumar, S.; Mittal, A.; **Sharma, Shivani**; Sharma, P. K.; Mittal, A. Recent Advancement in DPP-4 Inhibitors for the Treatment of T2DM. *THINK INDIA JOURNAL* December 2019, Vol-22-NO–30. Special Issue.
5. Anuradha, A. M.; Mittal, A.; **Sharma, Shivani**. Indole as an Emerging Scaffold in Anticancer Drug Design. *A.I.P. Conf. Proc.* 2023, 2800, 020198. DOI: 10.1063/5.0169005
6. Anuradha, A. M.; Mittal, A.; **Sharma, Shivani**. Diabetes Mellitus Type-2: The Panoramic View of Potential Therapeutic Targets. *A.I.P. Conf. Proc.* 2023, 2800, 020205. DOI: 10.1063/5.0169009

## V Conferences Attended



**A-139**  
**Canagliflozin: A Novel SglT-2 Inhibitor As An Antidiabetic Agent**  
Shivani Sharma\*<sup>1,2</sup> and Amit Mittal<sup>1</sup>

<sup>1</sup>Department of Pharmaceutical Chemistry, School of Pharmaceutical Sciences,  
Lovely Professional University, Phagwara (Punjab) 144411, India

<sup>2</sup> Faculty of Pharmaceutical Sciences, PCTE Group of Institutes  
Baddowal Cantt., Ferozpur Road, Ludhiana-142021

Tel: 9915735203

Email address: [sharma.shivani665@gmail.com](mailto:sharma.shivani665@gmail.com)

Diabetes is undeniably a big problem in today's world because it is the leading mortality and morbidity factor and is expected to hit 642 million by 2040. It is a metabolic disorder with hyperglycemia. Using new agents with a favorable risk-benefit profile could theoretically help clinicians and patients gain sufficient management of diabetes. Canagliflozin, the first regulator of the sodium-glucose co-transporter 2 (SGLT-2), provides a novel mechanism of action *via* blocking the renal reabsorption of glucose, thus increasing the excretion of urinary glucose. Canagliflozin approved by the USFDA in 2013 and launched by Janssen Pharmaceuticals as "Invokana". Canagliflozin lowers HbA1C by about 0.37%-1.16 % in combination with

 <b>L</b> OVELY <b>P</b> ROFESSIONAL <b>U</b> NIVERSITY <i>Transforming Education Transforming India</i>	<b>Certificate No. 245187</b> 
<h2 style="margin: 0;">Certificate of Participation</h2>	
<p>Presented to <b>Ms. Shivani Sharma</b> of <b>Lovely Professional University</b> in recognition of his/her participation in <b>"International Conference on Innovation and Intellectual Property Rights"</b> held on <b>18-19<sup>th</sup> April, 2022</b> organized by Division of Research and Development, Lovely Professional University, Punjab.</p>	
<small>Date of Issue: 13-05-2022 Place: Phagwara (Punjab), India</small>	<small>Prepared by (Administrative Officer-Records)</small>
 <small>Convener Dr. Runjhun Tondon (IAIPR 2022)</small>	 <small>Dr. Chander Prakash CD, Division of Research and Development</small>



# DIVISION OF RESEARCH AND DEVELOPMENT

[Under the Aegis of Lovely Professional University, Jalandhar-Delhi G.T. Road, Phagwara (Punjab)]

Certificate No.240483


## Certificate of Participation

This is to certify that **Ms. Shivani Sharma** of **Lovely Professional University, Phagwara, Punjab, India** has presented paper on **Kisquali (Ribociclib): A promising therapeutic candidate against breast Cancer** in the **International Conference on Materials for Emerging Technologies (ICMET-21)** held on February 18-19, 2022, organized by Department of Research Impact and Outcome, Division of Research and Development, Lovely Professional University, Punjab.

Date of Issue: 16-03-2022  
Place: Phagwara (Punjab), India



Prepared by  
(Administrative Officer-Records)



Dr. Vipul Srivastava  
Convener  
(ICMET-21)




Dr. Manish Vyas  
Organizing Secretary  
(ICMET-21)




Dr. Chander Prakash  
Co-Chairperson  
(ICMET-21)

## VI COPYRIGHTS




**Copyright Office**  
Government of India




सत्यमेव जयते

### Extracts from the Register of Copyrights

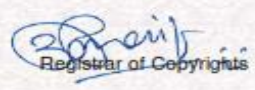
Dated : 21/12/2022



1. Registration Number	: <b>L-119943/2022</b>
2. Name, address and nationality of the applicant	: LOVELY PROFESSIONAL UNIVERSITY , LOVELY PROFESSIONAL UNIVERSITY JALANDHAR DELHI GT ROAD PHAGWARA PUNJAB-144411 INDIAN
3. Nature of the applicant's interest in the copyright of the work	: OWNER
4. Class and description of the work	: LITERARY/ DRAMATIC WORK IN THE PRESENT WORK A GRAPHICAL ABSTRACT RELATED TO THE MECHANISM OF ACTION OF SGLT2 INHIBITORS HAS BEEN REPRESENTED.
5. Title of the work	: MECHANISM OF ACTION OF SGLT-2 INHIBITORS.
6. Language of the work	: ENGLISH
7. Name, address and nationality of the author and if the author is deceased, date of his decease	: SHIVANI SHARMA , LOVELY PROFESSIONAL UNIVERSITY JALANDHAR DELHI GT ROAD PHAGWARA PUNJAB-144411 INDIAN  ANURADHA , LOVELY PROFESSIONAL UNIVERSITY JALANDHAR DELHI GT ROAD PHAGWARA PUNJAB-144411 INDIAN  AMIT MITTAL , LOVELY PROFESSIONAL UNIVERSITY JALANDHAR DELHI GT ROAD PHAGWARA PUNJAB-144411 INDIAN
8. Whether the work is published or unpublished	: UNPUBLISHED
9. Year and country of first publication and name, address and nationality of the publisher	: N.A.
10. Years and countries of subsequent publications, if any, and names, addresses and nationalities of the publishers	: N.A.
11. Names, addresses and nationalities of the owners of various rights comprising the copyright in the work and the extent of rights held by each, together with particulars of assignments and licences, if any	: LOVELY PROFESSIONAL UNIVERSITY , LOVELY PROFESSIONAL UNIVERSITY JALANDHAR DELHI GT ROAD PHAGWARA PUNJAB-144411 INDIAN
12. Names, addresses and nationalities of other persons, if any, authorised to assign or licence of rights comprising the copyright	: N.A.
13. If the work is an 'Artistic work', the location of the original work, including name, address and nationality of the person in possession of the work. (In the case of an architectural work, the year of completion of the work should also be shown).	: N.A.
14. If the work is an 'Artistic work' which is used or capable of being used in relation to any goods or services, the application should include a certification from the Registrar of Trade Marks in terms of the provision to Sub-Section (i) of Section 45 of the Copyright Act, 1957.	: N.A.
15. If the work is an 'Artistic work', whether it is registered under the Designs Act 2000 if yes give details.	: N.A.
16. If the work is an 'Artistic work', capable of being registered as a design under the Designs Act 2000, whether it has been applied to an article through an industrial process and ,if yes ,the number of times it is registered.	: N.A.
17. If the work is a computer program, whether it is registered under the Copyright Act, 1957.	: THE WORK IS ORIGINAL AND CREATED BY THE STUDENTS, FACULTY, AND STAFF OF THE UNIVERSITY.



14848/2022-CO/L  
11/07/2022  
11/07/2022



Registrar of Copyrights



Dated : 04/10/2022

1. Registration Number	:	<b>L-118041/2022</b>
2. Name, address and nationality of the applicant	:	LOVELY PROFESSIONAL UNIVERSITY, LOVELY PROFESSIONAL UNIVERSITY JALANDHAR DELHI GT ROAD PHAGWARA PUNJAB-144411 INDIAN
3. Nature of the applicant's interest in the copyright of the work	:	OWNER
4. Class and description of the work	:	LITERARY/ DRAMATIC WORK THE PRESENT WORK DEPICTS THE MECHANISM INVOLVED IN THE NEPHROPROTECTIVE AND CARDIOPROTECTIVE ACTIONS OF SGLT2 UPON ITS INHIBITION.
5. Title of the work	:	THE MOMENTOUS NEPHROPROTECTIVE CARDIOPROTECTIVE ACTIONS OF SGLT2 INHIBITION.
6. Language of the work	:	ENGLISH
7. Name, address and nationality of the author and if the author is deceased, date of his decease	:	ANURADHA, LOVELY PROFESSIONAL UNIVERSITY JALANDHAR DELHI GT ROAD PHAGWARA PUNJAB-144411 INDIAN AMIT MITTAL, LOVELY PROFESSIONAL UNIVERSITY JALANDHAR DELHI GT ROAD PHAGWARA PUNJAB-144411 INDIAN SHIVANI SHARMA, LOVELY PROFESSIONAL UNIVERSITY JALANDHAR DELHI GT ROAD PHAGWARA PUNJAB-144411 INDIAN
8. Whether the work is published or unpublished	:	UNPUBLISHED
9. Year and country of first publication and name, address and nationality of the publisher	:	N.A.
10. Years and countries of subsequent publications, if any, and names, addresses and nationalities of the publishers	:	N.A.
11. Names, addresses and nationalities of the owners of various rights comprising the copyright in the work and the extent of rights held by each, together with particulars of assignments and licences, if any	:	LOVELY PROFESSIONAL UNIVERSITY, LOVELY PROFESSIONAL UNIVERSITY JALANDHAR DELHI GT ROAD PHAGWARA PUNJAB-144411 INDIAN
12. Names, addresses and nationalities of other persons, if any, authorised to assign or licence of rights comprising the copyright	:	N.A.
13. If the work is an 'Artistic work', the location of the original work, including name, address and nationality of the person in possession of the work. (In the case of an architectural work, the year of completion of the work should also be shown).	:	N.A.
14. If the work is an 'Artistic work' which is used or capable of being used in relation to any goods or services, the application should include a certification from the Registrar of Trade Marks in terms of the provision to Sub-Section (i) of Section 45 of the Copyright Act, 1957.	:	N.A.
15. If the work is an 'Artistic work', whether it is registered under the Designs Act 2000 if yes give details.	:	N.A.
16. If the work is an 'Artistic work', capable of being registered as a design under the Designs Act 2000, whether it has been applied to an article or to an industrial process and, if yes, the number of times it is applied.	:	N.A.
17.	:	THE WORK IS ORIGINAL AND CREATED BY THE STUDENTS, FACULTY, AND STAFF OF THE UNIVERSITY.



11782/2022-CO/L

03/06/2022

03/06/2022

*(Signature)*  
Registrar of Copyrights

## VII Animal House Certificate

### CENTRAL ANIMAL HOUSE FACILITY (CAHF)

Lovely Institute of Technology (Pharmacy), Lovely Professional University

Ludhiana- Jalandhar G.T. Road, Phagwara (Punjab), 144411

Registration Number -954/PO/ReRcBiBt/S/06/CPCSEA

### CERTIFICATE

This is to certify that the project titled "*Form B title: Pharmacological evaluation of SGLT2 Inhibitors as Antidiabetic agents. Thesis Title: Design, Synthesis and Evaluation of SGLT2 Inhibitors*" has been approved by the IAEC.

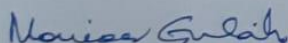
Name of Principal Investigator: Dr. Navneet Khurana

IAEC approval number: LPU/IAEC/2023/24

Date of Approval: 29<sup>th</sup> April 2022

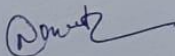
Animals approved: 72 Rats

Remarks if any: - NA



Dr. Monica Gulati

Biological Scientist,  
Chairperson IAEC



Dr. Navneet Khurana

Scientist from different discipline



Dr. Bimlesh Kumar

Scientist In-Charge of Animal House,  
Member Secretary IAEC

## VIII HISTOPATHOLOGY RESULTS

### LABORATORY REPORT



# SYNERGY LAB

Compassion | Quality | Trust  
An ISO 9001:2008 Certified Co.  
Certification No.: 192/05/2/09



IAS-ANZ  
M6551144X®



24 Hrs  
LABORATORY  
AVAILABLE

Address :663, Guru Teg Bahadur Nagar,  
Near Guru Ravidass Chowk, Jalandhar - 144003  
Lab :0181-2463300  
Mobile+91-76961-65796, +91-98766-44073  
E-mail:synergylab2010@gmail.com  
Website:www.synergypathlab.com


Ms.Shivani Sharma, Lovely Professional University, Phagwara (Punjab)-144411

### Histopathology of Kidney

Group No.	Group Name	Results
Group 1	Vehicle control	Sections show unremarkable histology.
Group 2	Synthesized molecule-SSS 95 <i>per se</i>	Sections show unremarkable histology.
Group 3	Synthesized molecule-SSS 100 <i>per se</i>	Sections show unremarkable histology.
Group 4	Negative control	Sections from both the kidneys show thickening of basement membrane, mesangial expansion and tubular atrophy. Hyalinization of vessels also seen.
Group 5	Positive control	Sections show almost normal histology.
Group 6	Synthesized molecule-SSS 95 low dose	Sections show focal sclerosis of glomeruli. Rest of the renal parenchyma is unremarkable.
Group 7	Synthesized molecule- SSS 95 high dose	Sections show focal tubular atrophy. Rest of the renal parenchyma is unremarkable.
Group 8	Synthesized molecule- SSS 100 low dose	Sections show unremarkable histology.
Group 9	Synthesized molecule- SSS 100 high dose	Sections show unremarkable histology.

  
 Dr. DEEKSHA CHOWDHARY  
 M.D. (Pathology)  
 Director  
 SYNERGY LAB


**LABORATORY REPORT**



**SYNERGY  
LAB**


Compassion | Quality | Trust  
An ISO 9001:2008 Certified Co.  
Certification No.: ISO/9112/100

**IAS-ANZ**



MS0211149/0

Address :663, Guru Teg Bahadur Nagar,  
Near Guru Ravidass Chowk, Jalandhar - 144003  
Lab :0181-2463300  
Mobile+91-76961-65796, +91-98766-44073  
E-mail:synergylab2010@gmail.com  
Website:www.synergypathlab.com



**Histopathology of Pancreas**

Group No.	Group Name	Results
Group 1	Vehicle control	Sections show normal acinar parenchyma of pancreas along with ducts and islets of Langerhans.
Group 2	Synthesized molecule-SSS 95 <i>per se</i>	Sections show normal acinar parenchyma of pancreas along with ducts and islets of Langerhans.
Group 3	Synthesized molecule-SSS 100 <i>per se</i>	Sections show normal acinar parenchyma of pancreas along with ducts and islets of Langerhans.
Group 4	Negative control	Sections show swelling and degeneration of acinar cells along with depletion of Islets of Langerhans.
Group 5	Positive control	Sections show almost normal histology.
Group 6	Synthesized molecule-SSS 95 low dose	Sections show normal looking acinar cells along with mild depletion of beta cells in Islets of Langerhans.
Group 7	Synthesized molecule- SSS 95 high dose	Sections show normal acinar parenchyma of pancreas along with ducts and islets of Langerhans.
Group 8	Synthesized molecule- SSS 100 low dose	Sections show normal acinar parenchyma of pancreas along with ducts and islets of Langerhans.
Group 9	Synthesized molecule- SSS 100 high dose	Sections show normal acinar parenchyma of pancreas along with ducts and islets of Langerhans.

  
**Dr. DEEKSHA CHOWDHARY**  
 M.D. (Pathology)  
 Director  
 SYNERGY LAB